

BA  
31



PCT

WORLD INTELLECTUAL PROPERTY ORGANIZATION  
International Bureau

INTERNATIONAL APPLICATION PUBLISHED UNDER THE PATENT COOPERATION TREATY (PCT)

(51) International Patent Classification <sup>6</sup> : C07K 1/00, 14/00, G01N 33/53, 33/567		A1	(11) International Publication Number: <b>WO 98/30576</b>
			(43) International Publication Date: 16 July 1998 (16.07.98)
(21) International Application Number: PCT/US97/15753 (22) International Filing Date: 7 October 1997 (07.10.97) (30) Priority Data: 08/729,743                      7 October 1996 (07.10.96)      US 60/061,323                      2 October 1997 (02.10.97)      US (63) Related by Continuation (CON) or Continuation-in-Part (CIP) to Earlier Application US                                      08/729,743 (CIP) Filed on                              7 October 1996 (07.10.96) (71) Applicant (for all designated States except US): THE JOHNS HOPKINS UNIVERSITY SCHOOL OF MEDICINE [US/US]; 720 Rutland Avenue, Baltimore, MD 21205 (US). (72) Inventors; and (75) Inventors/Applicants (for US only): BEACHY, Philip, A. [US/US]; 5703 Chilham Road, Baltimore, MD 21209 (US). PORTER, Jeffrey, A. [US/US]; Apartment 510, 1E University Parkway, Baltimore, MD 21218 (US). (74) Agent: HAILE, Lisa, A.; Fish & Richardson P.C., Suite 1400, 4225 Executive Square, La Jolla, CA 92037 (US).		(81) Designated States: AL, AM, AT, AU, AZ, BA, BB, BG, BR, BY, CA, CH, CN, CU, CZ, DE, DK, EE, ES, FI, GB, GE, HU, ID, IL, IS, JP, KE, KG, KP, KR, KZ, LC, LK, LR, LS, LT, LU, LV, MD, MG, MK, MN, MW, MX, NO, NZ, PL, PT, RO, RU, SD, SE, SG, SI, SK, SL, TJ, TM, TR, TT, UA, UG, US, UZ, VN, ZW, ARIPO patent (GH, KE, LS, MW, SD, SZ, UG, ZW), Eurasian patent (AM, AZ, BY, KG, KZ, MD, RU, TJ, TM), European patent (AT, BE, CH, DE, DK, ES, FI, FR, GB, GR, IE, IT, LU, MC, NL, PT, SE), OAPI patent (BF, BJ, CF, CG, CI, CM, GA, GN, ML, MR, NE, SN, TD, TG).  Published With international search report.	
(54) Title: NOVEL HEDGEHOG-DERIVED POLYPEPTIDES			
(57) Abstract			
<p>The present invention provides two novel polypeptides, referred to as the "N" and "C" fragments of hedgehog, or N-terminal and C-terminal fragments, respectively, which are derived after specific cleavage at a G↓CF site recognized by the autoproteolytic domain in the native protein. Also included are sterol-modified hedgehog polypeptides and functional fragments thereof. Methods of identifying compositions which affect hedgehog activity based on inhibition of cholesterol modification of hedgehog protein are described.</p>			
BEST AVAILABLE COPY			

**FOR THE PURPOSES OF INFORMATION ONLY**

Codes used to identify States party to the PCT on the front pages of pamphlets publishing international applications under the PCT.

AL	Albania	ES	Spain	LS	Lesotho	SI	Slovenia
AM	Armenia	FI	Finland	LT	Lithuania	SK	Slovakia
AT	Austria	FR	France	LU	Luxembourg	SN	Senegal
AU	Australia	GA	Gabon	LV	Latvia	SZ	Swaziland
AZ	Azerbaijan	GB	United Kingdom	MC	Monaco	TD	Chad
BA	Bosnia and Herzegovina	GE	Georgia	MD	Republic of Moldova	TG	Togo
BB	Barbados	GH	Ghana	MG	Madagascar	TJ	Tajikistan
BE	Belgium	GN	Guinea	MK	The former Yugoslav Republic of Macedonia	TM	Turkmenistan
BF	Burkina Faso	GR	Greece	ML	Mali	TR	Turkey
BG	Bulgaria	HU	Hungary	MN	Mongolia	TT	Trinidad and Tobago
BJ	Benin	IE	Ireland	MR	Mauritania	UA	Ukraine
BR	Brazil	IL	Israel	MW	Malawi	UG	Uganda
BY	Belarus	IS	Iceland	MX	Mexico	US	United States of America
CA	Canada	IT	Italy	NE	Niger	UZ	Uzbekistan
CF	Central African Republic	JP	Japan	NL	Netherlands	VN	Viet Nam
CG	Congo	KE	Kenya	NO	Norway	YU	Yugoslavia
CH	Switzerland	KG	Kyrgyzstan	NZ	New Zealand	ZW	Zimbabwe
CI	Côte d'Ivoire	KP	Democratic People's Republic of Korea	PL	Poland		
CM	Cameroon	KR	Republic of Korea	PT	Portugal		
CN	China	KZ	Kazakstan	RO	Romania		
CU	Cuba	LC	Saint Lucia	RU	Russian Federation		
CZ	Czech Republic	LI	Liechtenstein	SD	Sudan		
DE	Germany	LK	Sri Lanka	SE	Sweden		
DK	Denmark	LR	Liberia	SG	Singapore		
EE	Estonia						

- 1 -

## NOVEL HEDGEHOG-DERIVED POLYPEPTIDES

### BACKGROUND OF THE INVENTION

#### 1. *Field of the Invention*

This invention relates generally to the field of protein processing and protein signalling pathways and specifically to two novel proteins having distinct activities, which are derived from a common hedgehog protein precursor.

#### 2. *Description of the Related Art*

Embryologists have long performed experimental manipulations that reveal the striking abilities of certain structures in vertebrate embryos to impose pattern upon surrounding tissues. Speculation on the mechanisms underlying these patterning effects usually centers on the secretion of signaling molecule that elicits an appropriate response from the tissues begin patterned. More recent work aimed at the identification of such signaling molecules implicates secreted proteins encoded by individual members of a small number of gene families. One such family of proteins which may have an influential effect upon patterning activities are those proteins encoded by the *hedgehog* gene family.

The *hedgehog* (*hh*) gene was initially identified based on its requirement for normal segmental patterning in *Drosophila* (Nüsslein-Volhard, C. & Wieschaus, E, *Nature* 287:795-801, 1980). Its functions include local signaling to coordinate the identities of adjacent cells within early embryonic segments (Hooper, J.E., & Scott, M.P. *Early Embryonic Development of Animals*, pp.1-48, 1992) and a later function in cuticle patterning that extends across many cell diameters (Heernskerk, J. & DiNardo, S., *Cell*, 76:449-460, 1994). The *hh* gene also functions in the patterning of imaginal precursors of adult structures, including the appendages and the eye (Mohler, J. *Genetics*, 120:1061-1072, 1988; Ma, *et al.*, *Cell*, 75:927-938, 1993; Heberlein, *et al.*, *Cell*, 75:913-926, 1993; Tabata, T. & Kornberg, T.D., *Cell*, 76:89-102, 1992; Basler, K. & Struhl, G., *Nature*,

- 2 -

368:208-214, 1994). Genetic and molecular evidence indicates that *hedgehog* proteins are secreted and function in extracellular signaling (Mohler, J., *supra*; Lee, *et al.*, *Cell*, 71:33-50, 1992; Taylor, *et al.*, *Mech. Dev.*, 42:89-96, 1993).

In vertebrates activities encoded by *hh* homologues have been implicated in anterior/posterior patterning of the limb (Riddle, *et al.*, *Cell*, 75:1401-1416, 1993; Chang, *et al.*, *Development*, 120:3339, 1994), and in dorsal/ventral patterning of the neural tube (Echelard, *et al.*, *Cell*, 75:1417-1430, 1993; Krauss, *et al.*, *Cell*, 75:1431-1444, 1993; Roelink, *et al.*, *Cell*, 76:761-775, 1994).

The vertebrate ventral midbrain contains neurons whose degeneration or abnormal function are linked to a number of diseases, including Parkinson's disease and schizophrenia. It is known that motor neurons develop in close proximity to the floor plate in the ventral midbrain. Midbrain projections to the striatum are involved in the control of voluntary movement (Bjorklund and Lindvall, In: *Handbook of Chemical Neuroanatomy*, eds., Borklund, *et al.*, Amsterdam: Elsevier, pp55-122, 1984) and loss of these neurons results in the motor disorders of Parkinson's disease (Hirsch, *et al.*, *Nature*, 334:345, 1988). Midbrain dopaminergic neurons that innervate limbic structures and the cortex influence emotional and cognitive behavior, respectively, and abnormal function of these neurons has been associated with schizophrenia and drug addiction (Seeman, *et al.*, *Nature*, 365:441, 1993).

While the molecular nature of the factors that specify neuronal cell fate have not been established, members of the transforming growth factor- $\beta$  (TGF- $\beta$ ) (Lyons, *et al.*, *Trends in Genetics*, 7:408, 1991) or the hedgehog protein family (Smith, J.C., *Cell*, 76:193, 1994) may possess the characteristics expected from such factors as they participate in specification of cell fate, mediate inductive interactions between tissues, and in many cases act at a distance of only a few cell diameters.

- 3 -

The present invention establishes that *hh* activities encoded by these genes play a crucial role in early patterning of the developing eye and in patterning of the brain. For the first time, the invention shows that internal cleavage of hedgehog protein product is critical for full function, and that the two novel products of this auto-proteolytic cleavage display 5 distinguishable activities, thus demonstrating that *hh* signaling activity is a composite effect of two separate signaling proteins that derive from a common *hh* protein precursor. In so doing, the invention provides the means for specific patterning and proliferation of desired neuronal cell types for addressing disorders which arise from neuronal degeneration or abnormal function.

## 10 SUMMARY OF THE INVENTION

The present invention is based on the seminal discovery that hedgehog proteins undergo auto-proteolytic cleavage which results in two separate proteins having distinct functional and structural characteristics. The two polypeptides, referred to as the "N" and "C" fragments of hedgehog, or N-terminal and C-terminal fragments, respectively, are 15 produced after specific cleavage at a G<sup>1</sup>CF site recognized by the autoproteolytic domain in the native protein. The "C" fragment functions as a cholesterol transferase during autoproteolysis thus allowing cholesterol modification of the "N" fragment.

Thus, in one embodiment, the invention provides a substantially pure polypeptide characterized by having an amino acid sequence derived from amino terminal amino 20 acids of a hedgehog protein and having at its carboxy terminus, a G<sup>1</sup>CF cleavage site specifically recognized by a proteolytic activity of the carboxy terminal fragment of the native hedgehog polypeptide. The invention also provides a substantially pure polypeptide characterized by having an amino acid sequence of a hedgehog polypeptide or a fragment derived from amino terminal amino acids of a hedgehog polypeptide, wherein 25 the polypeptide or fragment thereof comprises a sterol moiety. Fragments derived from a native hedgehog polypeptide are included and preferably include extracellular amino

- 4 -

acid residues, such as those derived from the N fragment. In one embodiment of the invention, the sterol moiety is cholesterol.

In another embodiment, the invention provides a substantially pure polypeptide characterized by having an amino acid sequence derived from carboxy terminal amino acids of a hedgehog protein and having at its amino terminus, a GICF cleavage site specifically recognized by a proteolytic activity of the carboxy terminal fragment of the native hedgehog polypeptide.

The invention also provides a method for modulating proliferation or differentiation of neuronal cells, comprising contacting the cells with a hedgehog polypeptide. The native hedgehog polypeptide, the N, or the C fragment, or functional fragments derived therefrom, are most useful for the induction of proliferation or differentiation of neuronal cells substantially derived from floor plate neuronal cells.

In yet another embodiment, the invention provides a method for identifying a compound which affects hedgehog activity comprising incubating the compound with hedgehog polypeptide, or with biologically active fragments thereof, or with a recombinant cell expressing hedgehog, under conditions sufficient to allow the components to interact; and determining the effect of the compound on hedgehog activity or expression. For example, cholesterol level (*e.g.*, biosynthesis or transport) is measured as an indicator of hedgehog activity. In one aspect of the invention, the method provides a means for affecting cholesterol biosynthesis or transport in a cell comprising contacting a cell with an effective amount of a compound that affects hedgehog, thereby affecting cholesterol biosynthesis or transport. The effect may be inhibition or stimulation of cholesterol biosynthesis or transport.

- 5 -

**BRIEF DESCRIPTION OF THE DRAWINGS**

FIGURE 1 shows processing of the hh protein by immunoblots (A,C) with antibodies against amino (Ab1) and carboxy-terminal (Ab2) epitopes. FIGURE 1B and D are blots of samples immunoprecipitated with Ab1 (B, lanes 7-9), Ab2 (D, lanes 19-21), or pre-immune serum (B, lanes 10-12, and D, lanes 22-24).

FIGURES 1E and 1F show a schematic illustration of the hedgehog cleavage mechanism.

FIGURE 2 shows sequence similarity between hh proteins and serine proteases. hh protein sequences are aligned to residues 323 to 329 of the *D. melanogaster* protein and numbered as positions 1 to 7 (group A). The catalytic histidines of mammalian serine proteinases (group B) are aligned to the invariant histidine at position 7 in hh proteins.

FIGURE 3 shows autoproteolysis of the hh protein. 3A shows a coomassie blue stained polyacrylamide gel showing production and purification of His<sub>6</sub>-U and His<sub>6</sub>-U<sub>H329A</sub> proteins from *E. coli*. Samples were molecular weight markers (lanes 1 and 2); lysates of *E. coli* cells carrying the His<sub>6</sub>-U expression construct without (lane 3) and with (lane 4) induction by IPTG; purified His<sub>6</sub>-U protein (lane 5); lysates of *E. coli* cells that carry the His<sub>6</sub>-U<sub>H329A</sub> expression construct without (lane 6) and with (lane 7) induction by IPTG; purified His<sub>6</sub>-U<sub>H329A</sub> protein (lane 8). FIGURE 3(B) is an immunoblot detected with Ab2 showing transfected S2 cells induced to express *hh* (lane 1); His<sub>6</sub>-U and His<sub>6</sub>-U<sub>H329A</sub> proteins incubated in cleavage reaction buffer for 0 hours (lanes 2 and 5), for 20 hours (lanes 3 and 6), and for 20 hours in the presence of 20 mM TAME (a serine protease inhibitor) (lanes 4 and 7).

FIGURE 4 shows autoproteolytic functions of *Drosophila* (4A-C) and zebrafish (D) hh proteins map to the carboxy terminal fragments by in vitro translations of wild-type and mutant hh proteins. The locations of mutations and cleavage sites (arrows) in these proteins are illustrated schematically in 4E.

- 6 -

FIGURE 5 shows immunoblots showing heat shock induced expression of wild type and H329A mutant hh proteins in *Drosophila* embryos (A) and (B) are immunoblots developed using Ab1 and Ab2 antibodies, respectively. Lanes 1 and 6, induced untransfected S2 cells; lanes 2 and 7, transfected S2 cells induced to express hh; lanes 3 and 8, heat shocked wild-type embryos; lanes 4 and 9, heat shocked hshh embryos; lanes 5 and 10, heat shocked hshh H329A embryos.

FIGURE 6 shows *in situ* hybridization showing the embryonic effects of ubiquitously expressed wild type and H329A hh proteins. FIGURE 6 shows the embryonic distribution of *wingless* (*wg*) RNA as revealed by *in situ* hybridization is shown in (A) wild-type (homozygous  $y^1 w^{118}$ ), (B) *hshh*, and (C) *hshh* H329A embryos that were exposed to two 10 minute heat shocks separated by a 90-minute recovery period (33). Wild-type embryos showed little change in *wg* expression, whereas the wild-type protein and, to a lesser extent, the H329A protein each induced ectopic *wg* expression (Table 1). Panels (D), (E), and (F) show the dorsal surfaces of  $y^1 w^{118}$ , *hshh*, and *hshh* H329A larvae, respectively, at the level of the fourth abdominal segment. These larvae were shocked for 30 minutes as embryos and allowed to complete embryogenesis. Cuticle cell types (1°, 2°, 3°, and 4°) are labeled as described (J. Heemskerk and S. DiNardo, *Cell* 76, 449, 1994). Note the expansion of 2° cell types (naked cuticle) at the expense of 3° and some 4° types in the *hshh* embryo (E) under conditions where the phenotype of *hshh* H329A embryos (F) is identical to that of control embryos (D).

FIGURE 7 shows X-gal staining to show imaginal disc effects of ubiquitous wild type and H329 hh proteins. X-gal staining was used to follow expression of *wg* (A-C) or *dpp* (D-O) in imaginal discs of late third-instar larvae that carry *wg-lacZ* or *dpp-lacZ* reporter genes. Leg (A-F), wing (G-I) and eye-antennal discs (J-L) from control larvae (A, D, G, J), larvae carrying the *hshh* transgene (B, E, H, K) and larvae carrying the *hshh* H329A transgene (C, F, I, L) are displayed. In all panels anterior is to the left.

- 7 -

FIGURE 8 (A) and (B) are immunoblots of cell pellets (lane 1) or supernatants (lane 2) from transfected S2 cell cultures expressing HH protein, developed with Ab1 (A) and Ab2 (B). Samples in each lane were from the same volume of resuspended total culture. Whereas N remained mostly associated with the cell pellet (compare lanes 1 and 2 in A), C was nearly quantitatively released into the supernatant (compare lanes 1 and 2 in B). U displayed partitioning properties in between those of N and C (A and B). (C) demonstrates the heparin binding activity of various HH protein species generated by in vitro translations with microsomes (38). Samples were: total translation mix (lane 1); supernatant after incubation with heparin agarose or agarose (control) beads (lanes 2 and 4); and material eluted from heparin agarose or agarose beads after washing (lanes 3 and 5). F, U, N<sub>SS</sub> and N fragments are depleted from reactions incubated with heparin agarose but not agarose beads (compare lanes 2 and 4 to 1), and the same species subsequently can be eluted from the heparin agarose but not the agarose beads (compare lanes 3 and 5 with lane 1).

FIGURE 9 shows the differential localizations of N and C in embryos by in situ localization of the *hh* transcript. Fig. 9 (A) is shown in comparison to the distribution of N and C epitopes detected with Ab1 and Ab2 in panels (B) and (C), respectively. Note that the distribution of N and C epitopes span approximately one-third and one-half of each segmental unit respectively, while the transcript is limited to approximately one-quarter of each unit. In (D), the localization of C epitopes in embryos homozygous for the *hh*<sup>13E</sup> allele is detected with the use of Ab2. C epitopes in this mutant, which displays impaired auto-proteolytic activity (see text), are more restricted, and resemble the wild-type localization of N. Homozygous *hh*<sup>13E</sup> embryos were identified by loss of a marked balancer from a heterozygous parent stock. All embryos are at mid to late stage 9 (extended germ-band).

FIGURE 10 shows a signal relay versus dual function models for hh protein action. In Fig. 10 (A), the long-range effects of hh signaling are achieved indirectly through short-range induction of a second signaling molecule (X). Based on its biochemical properties

- 8 -

and its restricted tissue localization, N is presumed to represent the active short-range signal while the role of C would be limited to supplying the catalytic machinery required for biogenesis of N. In (B), the long- and short-range signaling functions of hh are supplied by the N and C proteins derived by internal auto-proteolysis of the U precursor.

5 N is implicated in short-range signaling by retention near its cellular site of synthesis, while C is less restricted in its distribution and would execute long-range signaling functions. In both models, auto-proteolysis is required to generate fully active signaling proteins.

FIGURES 10 C and D show an immunoblot of the N fragment synthesized from a wild type construct (C) or a construct lacking the C domain (D).

10

FIGURES 11 A and B show the nucleotide and deduced amino acid sequences for partial human *hh* clones.

FIGURE 12 A and B show *in vitro* cleavage reactions of a *Drosophila hh* protein produced in *E. coli* and purified to homogeneity. FIGURE 12, Panel A shows a time course of cleavage after initiation by addition of DTT. Panel B shows incubations of concentrations ranging over three order of magnitude for a fixed time period (four hours), with no difference in the extent of conversion to the cleaved form. Panel C shows the sequence around the cleavage site as determined by amino-terminal sequence of the cleaved fragment C. The cleavage site is denoted by the arrow, and the actual residues sequenced by Edman degradation of the C fragment are underlined. Panel C also shows an alignment of all published vertebrate *hh* sequences plus some of unpublished sequences from fish and *Xenopus*. The sequences shown correspond to the region of *Drosophila hh* where the cleavage occurs, and demonstrates the absolute conservation of the Gly-Cys-Phe sequence at the site of cleavage. Panel D shows a SDS-PAGE gel loaded with *in vitro* transcription/translation reactions as described in the previous Examples, using various *hh* genes as templates. *dhh* is *Drosophila*, *twhh* and *zfs hh* are the *twiggy-winkle* and *sonic hh* genes of the zebrafish, and *mshh* is the *shh/Hgh-1/vhh-1*

15

20

25

- 9 -

gene of the mouse. Panel E shows that Edman degradation of the C fragments releases <sup>35</sup>S counts on the first but not subsequent rounds for all these proteins, indicating that the site of autoproteolytic cleavage for all of these *hh* proteins is the amide bond to the amino-terminal side of the Cys residue that forms the center of the conserved Gly-Cys-Phe sequence highlighted in panel C.

FIGURE 13 shows the predicted amino acid sequences are shown in single letter code. 13(a) shows sequences common to five distinct *hh*-like genes are shown with a dot indicating identity with the corresponding residue of zebrafish *twiggy-winkle*. 13(b) shows amino acid sequences of *twhh* and *shh* are aligned to those of the *soniclvhh-1* class from chick and mouse. The amino-terminal hydrophobic stretch common to all four *hh* genes is shaded. The asterisk (\*) denotes invariant amino acid residues associated with the proteolytic domain of C fragment from various species. 13(c) shows percent identity of residues carboxy-terminal to the hydrophobic region.

FIGURES 14A-S show a comparative expression of *twhh*, *shh*, and *pax-2* during zebrafish embryogenesis.

FIGURE 15, panels 15A-15I, show the effects of ectopic *hh* on zebrafish development. Wild type zebrafish, *Danio rerio*, (Eckwill Waterlife Resources) were maintained at 28.5°C, some embryos were then cultured overnight at RT. Zebrafish embryos were injected at the 1-8 cell stage with *twhh*, *shh*, or *lacZ*RNA and examined at 28 h of development. (a-c) Dorsal view of the midbrain-hindbrain region; anterior is left. (a) *lacZ*. (b) *twhh*. (c) *shh*. (d-f) Frontal optical section of the forebrain region; anterior is up. (d) *lacZ*. (e) *twhh*. (f) *shh*. (g-i) Lateral view of the eye region; anterior is left. (g) *lacZ*. (h) *twhh*. (i) *twhh*.

FIGURE 16 is a table showing the effects of ectopic expression of *shh*, *twhh* and *twhh* mutants on zebrafish embryonic development.

- 10 -

FIGURE 17 shows zebrafish *twiggy-winkle hedgehog* derivatives. FIGURE 17A shows cartoons of various *twhh* open reading frames. SS (shaded) is the predicted N-terminal signal sequence for secretion of these proteins and encompasses the first 27 amino acids of each open reading frame. The arrow indicates the predicted internal site of auto-proteolytic cleavage. Amino acid residue numbers are according to Figure 13b. The filled triangle denotes the normal termination codon for the *twhh* open reading frame. Construct U<sub>HA</sub> contains a mutation that blocks auto-proteolysis (the histidine at residue 273 is changed to an alanine; see Lee, J.J., *et al.*, supra). Construct U356<sub>HA</sub> contains a stop codon in place of amino acid residue 357 as well as the H273A mutation in U<sub>HA</sub>. Construct N encodes just the first 200 amino acids of *twhh*. Construct C has had the codons for residues 31-197 deleted.

FIGURE 17B shows *in vitro* translation of the expression constructs shown schematically in part a. Constructs were translated *in vitro* in the presence of <sup>35</sup>S methionine and analyzed by autoradiography after SDS-PAGE.

FIGURES 18A and 18B show Northern blot analysis of the effect of hedgehog on expression of various neural markers.

FIGURES 19A and 19B show *hh* synergy with naturally occurring neural markers or agents (*e.g.*, XAG-1, XANF-2, Otx-A, En-2, Krox-20, Xlh box-6, NCAM, and EF-1 $\alpha$ ).

FIGURE 20A shows *hh* constructs including delta N-C.

FIGURE 20B shows a Northern blot analysis of the effect of hedgehog N or C on various neural markers.

FIGURE 21 shows  $\Delta$ N-C interferes with X-*bhh* and N-activity in animal cap explants as shown by RT-PCR analysis.

- 11 -

FIGURE 22A is an illustration of lipid stimulation of hedgehog autoprocessing.

FIGURE 22B shows a Coomassie blue stained SDS-PAGE of autocleavage reactions in bacterially expressed His<sub>6</sub>Hh-C protein.

FIGURE 23A is a thin layer chromatography (TLC) plate coated with silica gel G (Merck) showing the fractionation of bulk S2 cell lipids using a heptane:ether:formic acid solvent (80:20:2).

FIGURE 23B is a Coomassie blue-stained SDS-polyacrylamide gel showing in vitro autocleavage reactions of the bacterially expressed His<sub>6</sub>Hh-C protein incubated with 1 mM DTT plus either unfractionated S2 cell lipids (lane 1), or spots A through F (lanes 2-7, respectively).

FIGURE 23C is TLC of S2 cell lipids (lane 1) along with selected lipid standards: phosphatidylcholine (lane 2), a diacylglycerol (lane 3), cholesterol (lane 4), stearic acid (lane 5), a triacylglycerol (lane 6), and cholesteryl ester (lane 7). Lipid spot B comigrates with cholesterol, as also demonstrated by mixing radio-labeled cholesterol with S2 lipids before TLC fractionation.

FIGURE 23D is a Coomassie blue stained SDS-polyacrylamide gel showing that relative to 1 mM DTT alone (lane 1) cholesterol (0.35 mM) + 1 mM DTT (lane 2) stimulates His<sub>2</sub>Hh-C autocleavage in vitro.

FIGURE 23E is an autoradiogram of electrophoretically-resolved products of His<sub>6</sub>Hh-C autocleavage reactions driven by 20 mM DTT (lane 1) or 1 mM DTT+0.35 mM cholesterol (lane 2).

- 12 -

FIGURE 24A shows Coomassie stained gels of His6Hh-C autocleavage reactions carried out in the presence of 20 mM DTT (lane 1), or 1 mM DTT+0.35 mM cholesterol (lane 2). Lane 3 contains a mixture of the samples loaded in lanes 1 and 2.

FIGURE 24B is Coomassie stained gels showing protein products of His6Hh-C autocleavage reactions carried out in the presence of 1 mM DTT+0.35 mM cholesterol (lanes 1 and 2) or with 20 mM DTT (lane 3).

FIGURE 24C is an autoradiogram of immunoblotted Hh amino-terminal domains purified from cultured S2 cells.

FIGURE 25A is an autoradiogram of a gel loaded with total cell proteins from S2 cells containing a stably integrated Cu<sup>++</sup>-inducible hedgehog gene.

FIGURE 25B is an HPLC profile of sterols separated on a C18 column by isocratic elution with a solvent containing methanol:ethanol:water (86:10:4).

FIGURE 25C shows HPLC analysis as in (B) of the adduct released by base treatment of Hh-Np metabolically labeled with [3H]cholesterol (A).

FIGURE 25D shows metabolic labeling of vertebrate Sonic hedgehog protein with [3H]cholesterol. Autoradiogram of a gel loaded with total cell proteins from COS-7 cells transfected with a wild-type Sonic hedgehog expression construct (Shh, lane 1) or a construct that generates an unprocessed amino-terminal protein truncated after the conserved glycine at the site of autocleavage (Shh-N, lane 2).

FIGURE 26A is a schematic drawing of a two-step mechanism for Hh autoprocessing. Aided by deprotonation by either solvent or a base (B1), the thiol group of Cys-258 initiates a nucleophilic attack on the carbonyl carbon of the preceding residue, Gly-257. This attack results in replacement of the peptide bond between Gly-257 and Cys-258 by

- 13 -

a thioester linkage (step 1). The emerging  $\alpha$ -amino group of Cys-258 likely becomes protonated, and an acid (A) is shown donating a proton. The Thioester is subject to a second nucleophilic attack from the  $3\beta$ -hydroxyl group of a cholesterol molecule, shown here facilitated by a second base (B2), resulting in a cholesterol-modified amino-terminal domain and a free carboxy-terminal domain. In vitro cleavage reactions may also be stimulated by addition of small nucleophiles including DTT, glutathione, and hydroxylamine.

Figure 26B is a schematic drawing of a mechanism for intein self-splicing. A base (B1') or solvent deprotonates a cysteine or serine residue at the N-extein/intein junction (shown here as a cysteine residue) for attack on the carbonyl group of the preceding amino-acid residue resulting in the formation of a thioester/ester intermediate. An acid (A') may protonate the  $\alpha$ -amino group of the cysteine/serine residue promoting its release. The thioester/ester is then subject to a second nucleophilic attack from a cysteine, serine, or threonine residue at the intein/C-extein junction (shown here as a cysteine residue). A second base (B2') is shown facilitating deprotonation of the second nucleophile, although this function may also be carried out by B1'. This reaction produces a branched protein intermediate that ultimately resolves to a free intein and ligated exteins.

Figure 27 is a Coomassie Brilliant Blue-stained SDS-polyacrylamide gel showing in vitro autocleavage reactions of bacterially-expressed His<sub>6</sub>Hh-C<sub>25</sub> (lanes 1-3) and His<sub>6</sub>Hh-C<sub>17</sub> (lanes 4-6) proteins. Proteins were incubated with 1 mM DTT (lanes 1 and 4), 50 mM DTT (lanes 2 and 5) or 350  $\mu$ M cholesterol/1 mM DTT (lanes 3 and 6). The uncleaved His<sub>6</sub>Hh-C<sub>25</sub> protein migrates as a ~29-kDa species, and the carboxy-terminal cleavage product of this protein migrates as a ~25-kDa species (Porter et al., 1996). The uncleaved His<sub>6</sub>Hh-C<sub>17</sub> protein migrates as a ~21-kDa species, and the carboxy-terminal product of this truncated protein migrates as a ~14-kDa species. The amino-terminal product of the His<sub>6</sub>Hh-C<sub>25</sub> and His<sub>6</sub>Hh-C<sub>17</sub> proteins migrates as a ~7-kDa species when DTT-modified or as a ~5-kDa species when cholesterol-modified. His<sub>6</sub>Hh-C<sub>17</sub> was also incubated with 46  $\mu$ M [<sup>3</sup>H]cholesterol/1 mM DTT, and no cholesterol-modified product

- 14 -

was detected by autoradiography. A cholesterol-transfer activity 1% of wildtype could have been detected by this radioassay.

Figure 28A is a ribbon diagram of Hh-C<sub>17</sub>. The amino- (N) and carboxy- (C) termini are labeled. This panel was prepared with MOLSCRIPT (Kraulis, 1991).

- 5 Figure 28B is a topology diagram of Hh-C<sub>17</sub>. Residues in  $\beta$  strands are in boxes with amino-acid type and number indicated. Residues in turns of  $3_{10}$  helix are ovals with amino-acid type and number indicated. Other residues in the structure are in boxes with amino-acid number indicated. Hydrogen bonds between  $\beta$  strands are indicated with arrows. A pseudo two-fold axis of symmetry is indicated with a diamond. This panel  
10 was prepared using the output of the program PROMOTIF.

FIGURE 29A is a pseudo two-fold symmetry in Hh-C<sub>17</sub>. A stereodiagram of a trace of the  $\alpha$ -carbon backbone of residues 258-393 of Hh-C17 viewed along the pseudo-twofold symmetry axis is shown. Equivalent loops are colored identically. Residues 258-276 and 324-347 are colored yellow, residues 276-301 and 347-373 are colored magenta, and  
15 residues 312-320 and 381-389 are colored cyan. The pseudo two-fold axis is indicated with a closed circle.

FIGURE 29B is a stereodiagram of a backbone trace of Hh-C17 is shown with residues 258-323 colored green and residues 324-395 colored yellow. The extended loops that make up the Hh-C<sub>17</sub> structure are labeled in the order in which they appear in the amino-  
20 acid sequence, A1-A2-A3-B1-B2-B3. Two structurally cohesive subdomains are apparent, one comprising loops A1, A2, and B3 and another comprising loops B1, B2, and A3. Hh-C<sub>17</sub> appears to have arisen from a tandem duplication of a primordial gene to produce the 'A' and 'B' sequence regions coupled with exchange of the homologous A3 (residues 310-323) and B3 (residues 379-395) loops to form structural subdomains  
25 that are hybrids of 'A' and 'B' sequences. A pivot about which exchange of these loops appears to have occurred is indicated by an arrow.

- 15 -

FIGURE 29C is a stereodiagram of backbone traces of the regions of Hh-C17 corresponding to the sequence duplication (residues 259-320 colored green and residues 325-389 colored yellow) following superposition is shown. The structures were aligned with the program QUANTA (Polygen). The r.m.s. deviation in  $\alpha$ -carbon position for 50 matched residues in the subdomains is 1.38 Å. Conserved  $\beta$  turns (see below) are colored red. Panels A, B and C were prepared with MOLSCRIPT (Kraulis, 1991, supra).

FIGURE 29D is a structure-based alignment of the amino-acid sequences of the two subdomains of Hh-C<sub>17</sub>. Conserved amino acids are highlighted with yellow. Active site residues are in red.  $\beta$  strands are indicated with arrows.  $\beta$ 1b and  $\beta$ 2b are slightly longer than  $\beta$ 1a and  $\beta$ 2a, respectively, and are indicated with lighter green coloring. Fractional solvent accessibility (FSA) is shown in blue for each residue in the Hh-C<sub>17</sub> structure. The FSA is the ratio of the solvent accessible surface area of residue X in a Gly-X-Gly tripeptide vs. in the Hh-C17 structure. A value of 0 represents a value from 0.00 to 0.09, 1 represents 0.10 to 0.19, and so on. Type I  $\beta$  turns are conserved at homologous positions in both Hh-C<sub>17</sub> subdomains at residues 260-263 (homologous to residues 326-329) and residues 317-320 (homologous to residues 386-389). A type II  $\beta$  turn is conserved between both subdomains at residues 279-282 (homologous to residues 350-353), and a type IV  $\beta$  turn is conserved between both subdomains at residues 288-291 (homologous to residues 359-362).  $\beta$  bulges are found at homologous positions in both Hh-C<sub>17</sub> subdomains at residues 282 (homologous to residue 353) and 300 (homologous to 372).

FIGURE 30A is a stereodiagram of the nucleophilic residue, Cys-258, and nearby residues. Distances (Å) between atoms are indicated.

FIGURE 30B is a ribbon diagram of Hh-C<sub>17</sub> with the side chains of Cys-258 and other putative active site residues indicated. Panels A and B were prepared with MOLSCRIPT (Kraulis, 1991, supra).

- 16 -

FIGURE 30C shows a Coomassie Brilliant Blue-stained SDS-polyacrylamide gel showing in vitro autocleavage reactions of bacterially-expressed His<sub>6</sub>HhC wildtype (lanes 1-3) and mutant proteins, H329A (lanes 4-6), T326A (lanes 7-9), and D303A (lanes 10-12). Proteins were incubated with 1 mM DTT (lanes 1, 4, 7, and 10), 50 mM DTT (lanes 2, 5, 8, and 11) or 350  $\mu$ M cholesterol/1 mM DTT (lanes 3, 6, 9, and 12). The uncleaved protein migrates as a ~29 kDa species. The carboxy-terminal cleavage product migrates as a ~25-kDa species and the amino-terminal product migrates as a ~7-kDa species when DTT-modified or as a ~5-kDa species when cholesterol-modified. The significant level of apparent cleavage seen with the D303A protein with 1 mM DTT results from preexisting cleavage products in the preparation; however, addition of 50 mM DTT greatly increases the amount of cleavage products and addition of cholesterol does not produce a cholesterol-modified product (~5-kDa species). D303A was also incubated with 46  $\mu$ M [<sup>3</sup>H]cholesterol/1 mM DTT, and no cholesterol-modified product was detected by autoradiography (data not shown). A cholesterol-transfer activity 1% of wildtype could have been detected by this radioassay.

FIGURE 31A is an alignment of the Hh-C<sub>17</sub> amino-acid sequence (residues 258-402) with other Hh sequences, with nematode sequences homologous to Hh-C, and intein sequences. The alignment was constructed by superimposing the Hh-C and intein alignments produced by the CLUSTALW program using the results of the PSI-BLAST analysis as a guide (Thompson et al., 1994). Additionally, the alignment was verified by analyzing a subset of the sequences containing fifteen diverse intein sequences and three Hh-C sequences with the MACAW program (Schuler et al., 1991, supra). In this analysis the alignment of the blocks containing the cysteine and histidine residues implicated in catalysis was significant with  $p < 10^{-8}$ , and the block including  $\beta$ 2b of Hh-C with

$p < 10^{-4}$ . The exact counterpart of  $\beta$ 4a in the intein sequences remained uncertain; the respective region is replaced by the number of amino-acid residues. The position of the endonuclease domain (ENDO - domain II according to Duan et al., 1997) inserted in the intein sequences is shown and the number of amino acid residues in these domains is

- 17 -

indicated. A second inserted domain in the PI-SceI/YEAST intein thought to be involved in DNA recognition (DRR) is located between  $\beta 1b$  and  $\beta 2b$ . Three inteins, GYRA/MYCXE, DNAB/PORPU, and KLBA/METJA, contain a short insert replacing the endonuclease domain. The yeast HO endonuclease does not undergo self-splicing, but contains a vestigial, inactive intein domain. The KLBA/METJA intein homologue in which the amino-terminal nucleophile is replaced by alanine is likely inactive as well. A consensus sequence is shown above the aligned sequences and shows amino acid residues conserved in at least one half of the sequences in each of the two aligned sets. 'U' indicates a bulky hydrophobic residue (I, L, V, M, F, Y, W), and "-" indicates a negatively-charged residue (D or E). Catalytic site residues are highlighted with red; hydrophobic residues are highlighted with yellow; other residues that conform with the consensus are highlighted with blue. The secondary structure elements and for Hh-C<sub>17</sub> are shown. Every tenth residue in the Hh-C<sub>17</sub> sequence is indicated with a dot. The leftmost column shows abbreviated protein and species names, and the second column shows the gene identification number in the NCBI protein database. Protein name abbreviations: CE(R084B4.1), F46B3 (F46B3.C), M75 (ZK678.5), M89 (C29F3.d), ZK (ZK1290.5), ZK377 (ZK377.1), M110 (T05C12.10) - uncharacterized nematode proteins containing Hh carboxy-terminal domain homologues; HH - hedgehog; EHH - Echinidna hedgehog; CHH - Cephalic hedgehog; DHH - Desert hedgehog; IHH - Indian hedgehog; BHH - Banded hedgehog; TWHH - Tiggy-winkle hedgehog; XHH - Xenopus hedgehog; SHH - Sonic hedgehog; PI-SceI, PI-Ctrl - yeast intein endonucleases; GYRA, GYRB - DNA gyrase A and B subunits; RECA - recombinase; DNAB - replicative DNA helicase; POLC - DNA polymerase III a subunit; CLPP - endopeptidase; IF-2 - translation initiation factor 2; HELI - putative helicase; RFC - replication factor C; ORF - uncharacterized open reading frame product; G6PT - glucose-6-phosphate transaminase; RPO-A', PRO-A" - DNA-dependent RNA -polymerase subunits; RGYR - reverse gyrase; PEPS - phosphoenolpyruvate synthase; UDGD - uridine diphosphate glucose dehydrogenase; RNR - ribonucleotide reductase; DPOL - DNA polymerase, B family; TFIIB - transcription factor IIB; KLBA - predicted ATPase; HO - homothallic endonuclease. Species abbreviations: CAEEL - Caenorhabditis elegans; DANRE -

- 18 -

Danio rerio; XENLA - *Xenopus laevis*; Cynpy - *Cynops pyrrhogaster*; DROHY - *Drosophila hydei*; DROME - *Drosophila melanogaster*; CANTR - *Candida tropicalis*; MYCLE - *Mycobacterium leprae*; MYCXE - *Mycobacterium xenopi*; MYCTU - *Mycobacterium tuberculosis*; PORPU - *Porphyra purpurea*; SYNSP - *Synechocystis* sp;  
5 CHLEU - *Chlamydomonas*; METJA - *Methanococcus jannaschii*; PYRFU - *Pyrococcus furiosus*; PYRSP - *Pyrococcus* sp.; THELI - *Thermococcus litoralis*. Several Hh and intein sequences closely related to those included were omitted.

FIGURE 31B is a stereo ribbon diagram of Hh-C<sub>17</sub>, showing where the endonuclease domain and additional DNA recognition region of PI-SceI are inserted. The loop where  
10 the endonuclease domain is inserted is colored red and the loop where the additional DNA recognition region ("the arm of the self-splicing domain" is inserted is colored blue. The orientation of the Hh-C<sub>17</sub> in this view is the same as the orientation of the PI-SceI intein in Figure 2 of Duan, et al., 1997, supra. This panel was prepared with MOLSCRIPT.

15 FIGURE 32 is a schematic drawing illustrating the duplication and insertion events that appear to have occurred during the evolution of Hh proteins and inteins. The insertion of the intein into a host protein is not shown. The order of some of these events is speculative. For example, dimerization through loop swapping may have preceded the gene duplication that produced an Hh-C<sub>17</sub>-like protein. Abbreviations: Hh-C - Hh  
20 carboxy-endonuclease domain, DRR - DNA recognition region.

FIGURE 33 shows inhibition of cholesterol biosynthesis by the plant steroidal alkaloid, jervine.

## DETAILED DESCRIPTION OF THE INVENTION

The present invention provides two novel polypeptides originally derived from a single precursor protein, both of which have distinct structural and functional characteristics. The proteins are derived from a hedgehog protein and can be naturally produced by auto-proteolytic cleavage of the full-length hedgehog protein. Based on evidence provided  
5 herein, which indicates that hedgehog precursor protein and the auto-proteolytic products of hedgehog precursor protein are expressed in the floorplate of the ventral midline of the neural tube and notochord, the invention now provides a method for the induction of proliferation or differentiation of neuronal cells associated with or in close proximity to  
10 the floorplate and notochord. The invention also provides cholesterol modified hedgehog polypeptides and function fragments thereof.

In a first embodiment, the invention provides a substantially pure polypeptide characterized by having an amino acid sequence derived from amino terminal amino acids of a hedgehog protein and having at its carboxy terminus, a glycine-cysteine-phenylalanine (G↓CF) cleavage site specifically recognized by a proteolytic activity of  
15 the carboxy terminal fragment of the native hedgehog polypeptide. This fragment is denoted the N-terminal fragment or polypeptide or "N", herein. For example, in the case of the *Drosophila* hedgehog, the N fragment includes amino acids 1-257 of hedgehog protein, wherein amino acids 85-257 have a molecular weight of about 19 kD by non-reducing SDS-PAGE (Amino acid residue numbers 1-257 include non-structural features  
20 such as signal sequences.). The G↓CF cleavage site in *Drosophila* hedgehog precursor protein occurs at amino acid residues 257-259. Those of skill in the art will be able to identify the G↓CF cleavage site in other hedgehog genes, as the amino acid location will be similar and the site will be specifically recognized by the autoproteolytic activity of  
25 the corresponding C fragment.

The N-terminal polypeptide is also characterized by being cell-associated in cells expressing the polypeptide *in vitro*, and being specifically localized in vertebrate or

- 20 -

*Drosophila* cells or embryos, for example. In other words, this N-terminal fragment of hedgehog, remains close to the site of cellular synthesis. The association of N with the cell is a result of the processing event which involves lipophilic modification of the amino terminal domain. (See Figure 1E and Example 19) This modification is initiated  
5 by the action of the carboxy terminal domain, generating a thioester intermediate; the carboxy-terminal domain thus does not act simply as a protease, although cleavage of a peptide bond does ultimately result from its action. Specifically, the lipid modification is a cholesterol moiety. In addition, the N fragment binds to heparin agarose *in vitro*.

The N polypeptide of the invention is characterized by having an amino acid sequence  
10 derived from amino terminal amino acids of hedgehog protein, *e.g.*, 1-257 in *Drosophila*, wherein amino acids 1-257 have a molecular weight of about 19 kD by non-reducing SDS-PAGE. The N polypeptide includes smaller fragments which retain the functional characteristics of full length N, *e.g.*, bind to heparin. The hedgehog protein from which N is derived includes, but is not limited to *Drosophila*, *Xenopus*, chicken, zebrafish,  
15 mouse, and human. Crystallographic analysis shows the structure of SHH-N includes the presence of a zinc ion. While not wanting to be bound by a particular theory, the presence of the zinc ion is suggestive of zinc hydrolase activity. Zinc hydrolases include proteases such as carboxypeptidase A and thermolysin, lipases such as phospholipase C, and other enzymes such as carbonic anhydrase. Alterations in the zinc hydrolase site of  
20 the amino terminal signaling domain may be useful for modulating the range of diffusion of a hedgehog protein or to alter the signaling characteristics of the amino terminal signaling domain. For example, a mutation in the zinc hydrolase site may result in a tethered protein where ordinarily the protein is secreted at a distance. The result would be induction of a cell type not typically induced. Alteration in the zinc site may result in  
25 a molecule capable of inducing motor neurons and not floor plate, and vice versa.

The identification of a cell-surface, or extracellular matrix localization of N and its expression in notochord and floor plate-associated cells, provides a means for isolation or specific selection of cells expressing N, *e.g.*, to isolate a notochord sample or to isolate

- 21 -

floor plate cells. In addition, antibodies directed to N are useful for histological analysis of tissues suspected of expressing N protein.

The invention also provides a substantially pure polypeptide characterized by having an amino acid sequence derived from carboxy terminal amino acids of a hedgehog protein and having at its amino terminus a G↓CF cleavage site specifically recognized by a proteolytic activity of the carboxy terminal fragment of the native hedgehog polypeptide. This fragment is denoted the C-terminal fragment or polypeptide or "C", herein. For example, in *Drosophila* this "C" polypeptide derives from the C-terminal domain of hedgehog precursor protein beginning at amino acid residue 258, wherein the full length C-terminal domain has a molecular weight of about 25 kD by non-reducing SDS-PAGE, a histidine residue at position 72, and has protease activity. The G↓CF cleavage site specifically recognized by the proteolytic activity of the carboxy terminal fragment of the native hedgehog polypeptide is located at amino acid residues 257-259. As described above for the N fragment, now that the present invention has shown the precise cleavage recognition site for the autoproteolytic domain of hedgehog, those of skill in the art can readily discern the cleavage site in other hedgehog proteins thereby allowing the ready identification of any N or C polypeptide of any hedgehog precursor protein.

The "C" polypeptide of the invention is derived from the C-terminus of a hedgehog precursor protein, beginning at the autoproteolytic cleavage site identified at the GCF amino acid sequence, which in *Drosophila* corresponds to amino acids 257-259. In *Drosophila* the histidine residue found invariably at amino acid residue 329 of the native hedgehog protein, and at amino acid residue 72 of the C polypeptide, is essential for auto-proteolytic cleavage between amino acids 257 and 258 (G and C). Corresponding C-polypeptides of the invention will likewise contain a similarly located histidine residue which can be readily identified, such as by comparison to the *Drosophila* C-polypeptide. Among various species, the proteolytic domain can be characterized by the amino acid sequence -XTXXHLXX-.

- 22 -

The C polypeptide of the invention, unlike N, does not significantly bind to heparin agarose. C is characterized by being released into the culture supernatant of cells expressing C polypeptide *in vitro* and by being localized diffusely in cells and embryos. Because C polypeptide diffuses freely, it would be detectable in various body fluids and  
5 tissues in a subject. Identification of C polypeptide expression near the midline of the neural tube, as described herein, provides a useful assay for neural tube closure in an embryo/fetus, for example. The presence of C polypeptide in amniotic fluid would be diagnostic of a disorder in which the neural tube may be malformed.

Altered levels of C polypeptide in cerebrospinal fluid may be indicative of neuro-  
10 degenerative disorders, for example. Because C polypeptide is released from the cell after synthesis and autoproteolysis of native hedgehog precursor polypeptide, tumors synthesizing and releasing high levels of C polypeptide would be detectable without prior knowledge of the exact location of the tumor.

C fragment is effective in inducing genes of the pituitary and anterior brain as well. In  
15 particular, induction is increased by the addition of a member of the TGF- $\beta$  family of growth factors. For example, human activin in combination with C fragment may be effective in enhancing pituitary cell growth and activity or development. C fragment possesses cholesterol transferase activity thereby effecting precursor cleavage and transfer of a cholesterol moiety to N fragment, resulting in a biologically active N  
20 fragment.

C fragment is effective in inducing posterior markers of the brain by inhibiting N. Such a fragment is exemplified in Example 18 as  $\Delta$ N-C. Therefore in another embodiment, the invention includes a polypeptide deleting amino acid residues 28-194 of X-*bhh*. (Autoproteolysis gives a C domain of 198-409 as well as a seven amino acid peptide,  
25 representing aa 24-27 and 195-197). This polypeptide blocks the activity of X-*bhh* and N in explants and reduces dorsoanterior structures in embryos. Also included are polynucleotide sequences encoding  $\Delta$ N-C.  $\Delta$ N-C is useful for increasing expression of

- 23 -

posterior neural markers (*e.g.*, En-2, Krox-20, Xlftbox-6) and decreasing expression of anterior neural markers (*e.g.*, XANF-2, XAG-1, Otx-A) when desirable to do so to modulate neural patterning.

The term "substantially pure" as used herein refers to hedgehog N or C polypeptide  
5 which is substantially free of other proteins, lipids, carbohydrates, nucleic acids or other materials with which it is naturally associated. One skilled in the art can purify hedgehog N or C polypeptide using standard techniques for protein purification. The substantially pure polypeptide will yield a single major band on a non-reducing polyacrylamide gel. The purity of the hedgehog N or C polypeptide can also be determined by amino-  
10 terminal amino acid sequence analysis.

The invention includes a functional N or C polypeptide, and functional fragments thereof. As used herein, the term "functional polypeptide" or "functional fragment" refers to a polypeptide which possesses a biological function or activity which is identified through a defined functional assay and which is associated with a particular  
15 biologic, morphologic, or phenotypic alteration in the cell. Functional fragments of the hedgehog N or C polypeptide include fragments of N or C polypeptide as long as the activity, *e.g.*, proteolytic activity or cholesterol transferase activity of C polypeptide remains. Smaller peptides containing the biological activity of N or C polypeptide are therefore included in the invention. The biological function, for example, can vary from  
20 a polypeptide fragment as small as an epitope to which an antibody molecule can bind to a large polypeptide which is capable of participating in the characteristic induction or programming of phenotypic changes within a cell. A "functional polynucleotide" denotes a polynucleotide which encodes a functional polypeptide as described herein.

Biologically active or functional fragments of hedgehog, as described herein, are  
25 included in the invention and can be identified as such by functional assays. For example, fragments of hedgehog are identified as inducing differentiation of neuronal cells; regulating differentiation of chondrocytes; able to complement a loss of function

- 24 -

mutation of hedgehog, for example in a transgenic *Drosophila*; binding to Patched (Ptc); or having cholesterol transferase activity (e.g., C fragment). Fragments of the invention may be from about 30 to 450 amino acids in length; from about 50 to 300 amino acids in length; from about 75 to 250 amino acids in length; or from about 100 to 200 amino acids in length, as long as a biological activity of hedgehog is retained therein.

Minor modifications of the N or C polypeptide primary amino acid sequence may result in polypeptides which have substantially equivalent activity as compared to the N or C polypeptide described herein. Such modifications may be deliberate, as by site-directed mutagenesis, or may be spontaneous. All of the polypeptides produced by these modifications are included herein as long as the proteolytic activity of C polypeptide, for example, is present. Further, deletion of one or more amino acids can also result in a modification of the structure of the resultant molecule without significantly altering its activity. This can lead to the development of a smaller active molecule which would have broader utility. For example, it is possible to remove amino or carboxy terminal amino acids which may not be required for N or C polypeptide activity.

The N or C polypeptide of the invention also includes conservative variations of the polypeptide sequence. The term "conservative variation" as used herein denotes the replacement of an amino acid residue by another biologically similar residue. Examples of conservative variations include the substitution of one hydrophobic residue such as isoleucine, valine, leucine or methionine for another, or the substitution of one polar residue for another, such as the substitution of arginine for lysine, glutamic for aspartic acids, or glutamine for asparagine, and the like. The term "conservative variation" also includes the use of a substituted amino acid in place of an unsubstituted parent amino acid provided that antibodies raised to the substituted polypeptide also immunoreact with the unsubstituted polypeptide.

The N fragment of the invention includes both the active form of the polypeptide and the N fragment including the uncleaved signal sequence. For example, in *Drosophila* where

- 25 -

the signal sequence is internal (at about amino acids 60-80), the entire uncleaved N fragment beginning at the initiating methionine is included in the invention. Those of skill in the art can readily ascertain the nature and location of the signal sequence by using, for example, the algorithm described in von Heijne, G., *Nucl. Acids Res.* 14:4683, 5 (1986).

Hedgehog polypeptides of the invention include polypeptides having at least about 50%-100% homology with the hedgehog polypeptides provided herein, for example 52%, 64%, 68%, 70%, 75%, 80%, 85%, 90%, 95% and up to 100% homology. Preferably homologous polypeptides are derived from vertebrate species, most preferably 10 mammalian species, such as humans.

The invention also provides an isolated polynucleotide sequence encoding a polypeptide having the amino acid sequence of N or C polypeptide of the invention. The term "isolated" as used herein includes polynucleotides substantially free of other nucleic acids, proteins, lipids, carbohydrates or other materials with which it is naturally 15 associated. Polynucleotide sequences of the invention include DNA, cDNA and RNA sequences which encode N or C polypeptide. It is understood that all polynucleotides encoding all or a portion of N or C polypeptide are also included herein, as long as they encode a polypeptide with N or C polypeptide activity. Such polynucleotides include naturally occurring, synthetic, and intentionally manipulated polynucleotides. For 20 example, N or C polypeptide polynucleotide may be subjected to site-directed mutagenesis. The polynucleotide sequence for N or C polypeptide also includes antisense sequences. The polynucleotides of the invention include sequences that are degenerate as a result of the genetic code. There are 20 natural amino acids, most of which are specified by more than one codon. Therefore, all degenerate nucleotide 25 sequences are included in the invention as long as the amino acid sequence of N or C polypeptide polypeptide encoded by the nucleotide sequence is functionally unchanged. In addition, the invention also includes a polynucleotide consisting essentially of a polynucleotide sequence encoding a polypeptide having an amino acid sequence of N or

- 26 -

C and having at least one epitope for an antibody immunoreactive with N or C polypeptide.

The polynucleotide encoding N or C polypeptide includes the entire polypeptide or fragments thereof, as well as nucleic acid sequences complementary to that sequence.

- 5 A complementary sequence may include an antisense nucleotide. When the sequence is RNA, the deoxynucleotides A, G, C, and T are replaced by ribonucleotides A, G, C, and U, respectively. Also included in the invention are fragments of the above-described nucleic acid sequences that are at least 15 bases in length, which is sufficient to permit the fragment to selectively hybridize to DNA that encodes the protein under physiologi-  
10 cal conditions.

- Hedgehog encoding polynucleotides of the invention include nucleic acid sequences identified by hybridization to a hedgehog nucleic acid described herein. In nucleic acid hybridization reactions, the conditions used to achieve a particular level of stringency will vary, depending on the nature of the nucleic acids being hybridized. For example,  
15 the length, degree of complementarity, nucleotide sequence composition (*e.g.*, GC v. AT content), and nucleic acid type (*e.g.*, RNA v. DNA) of the hybridizing regions of the nucleic acids can be considered in selecting hybridization conditions. An additional consideration is whether one of the nucleic acids is immobilized, for example, on a filter.

- An example of progressively higher stringency conditions is as follows: 2 x SSC/0.1%  
20 SDS at about room temperature (hybridization conditions); 0.2 x SSC/0.1% SDS at about room temperature (low stringency conditions); 0.2 x SSC/0.1% SDS at about 42°C (moderate stringency conditions); and 0.1 x SSC at about 68°C (high stringency conditions). Washing can be carried out using only one of these conditions, *e.g.*, high stringency conditions, or each of the conditions can be used, *e.g.*, for 10-15 minutes each,  
25 in the order listed above, repeating any or all of the steps listed. However, as mentioned above, optimal conditions will vary, depending on the particular hybridization reaction involved, and can be determined empirically.

- 27 -

DNA sequences of the invention can be obtained by several methods. For example, the DNA can be isolated using hybridization techniques which are well known in the art. These include, but are not limited to: 1) hybridization of genomic or cDNA libraries with probes to detect homologous nucleotide sequences; 2) antibody screening of expression  
5 libraries to detect cloned DNA fragments with shared structural features; and 3) PCR amplification of a desired nucleotide sequence using oligonucleotide primers.

Preferably the hedgehog, N, or C polynucleotide of the invention is derived from a vertebrate organism, and most preferably from human. Screening procedures which rely on nucleic acid hybridization make it possible to isolate any gene sequence from any  
10 organism, provided the appropriate probe is available. Oligonucleotide probes, which correspond to a part of the sequence encoding the protein in question, can be synthesized chemically. This requires that short, oligopeptide stretches of amino acid sequence must be known. The DNA sequence encoding the protein can be deduced from the genetic code, however, the degeneracy of the code must be taken into account. It is possible to  
15 perform a mixed addition reaction when the sequence is degenerate. This includes a heterogeneous mixture of denatured double-stranded DNA. For such screening, hybridization is preferably performed on either single-stranded DNA or denatured double-stranded DNA. Hybridization is particularly useful in the detection of cDNA clones derived from sources where an extremely low amount of mRNA sequences  
20 relating to the polypeptide of interest are present. In other words, by using stringent hybridization conditions directed to avoid non-specific binding, it is possible, for example, to allow the autoradiographic visualization of a specific cDNA clone by the hybridization of the target DNA to that single probe in the mixture which is its complete complement (Wallace, *et al.*, *Nucl. Acid Res.*, 9:879, 1981).

25 The development of specific DNA sequences encoding hedgehog can also be obtained by: 1) isolation of double-stranded DNA sequences from the genomic DNA; 2) chemical manufacture of a DNA sequence to provide the necessary codons for the polypeptide of interest; and 3) *in vitro* synthesis of a double-stranded DNA sequence by reverse

- 28 -

transcription of mRNA isolated from a eukaryotic donor cell. In the latter case, a double-stranded DNA complement of mRNA is eventually formed which is generally referred to as cDNA.

Of the three above-noted methods for developing specific DNA sequences for use in recombinant procedures, the isolation of genomic DNA isolates is the least common. This is especially true when it is desirable to obtain the microbial expression of mammalian polypeptides due to the presence of introns.

The synthesis of DNA sequences is frequently the method of choice when the entire sequence of amino acid residues of the desired polypeptide product is known. When the entire sequence of amino acid residues of the desired polypeptide is not known, the direct synthesis of DNA sequences is not possible and the method of choice is the synthesis of cDNA sequences. Among the standard procedures for isolating cDNA sequences of interest is the formation of plasmid- or phage-carrying cDNA libraries which are derived from reverse transcription of mRNA which is abundant in donor cells that have a high level of genetic expression. When used in combination with polymerase chain reaction technology, even rare expression products can be cloned. In those cases where significant portions of the amino acid sequence of the polypeptide are known, the production of labeled single or double-stranded DNA or RNA probe sequences duplicating a sequence putatively present in the target cDNA may be employed in DNA/DNA hybridization procedures which are carried out on cloned copies of the cDNA which have been denatured into a single-stranded form (Jay, *et al.*, *Nucl. Acid Res.*, 11:2325, 1983).

A preferred method for obtaining genomic DNA, for example, is Polymerase Chain Reaction (PCR), which relies on an *in vitro* method of nucleic acid synthesis by which a particular segment of DNA is specifically replicated. Two oligonucleotide primers that flank the DNA fragment to be amplified are utilized in repeated cycles of heat denaturation of the DNA, annealing of the primers to their complementary sequences,

- 29 -

and extension of the annealed primers with DNA polymerase. These primers hybridize to opposite strands of the target sequence and are oriented so that DNA synthesis by the polymerase proceeds across the region between the primers. Since the extension products themselves are also complementary to and capable of binding primers, successive cycles of amplification essentially double the amount of the target DNA synthesized in the previous cycle. The result is an exponential accumulation of the specific target fragment, approximately  $2^n$ , where  $n$  is the number of cycles of amplification performed (see PCR Protocols, Eds. Innis, *et al.*, Academic Press, Inc., 1990, incorporated herein by reference).

- 10 A cDNA expression library, such as  $\lambda$ gt11, can be screened indirectly for hedgehog, N, or C polypeptides having at least one epitope, using antibodies specific for hedgehog, N, or C. Such antibodies can be either polyclonally or monoclonally derived and used to detect expression product indicative of the presence of the desired hedgehog cDNA.

The polynucleotide sequence for hedgehog, N, or C, also includes sequences complementary to the polynucleotide encoding hedgehog, N or C (antisense sequences). Antisense nucleic acids are DNA or RNA molecules that are complementary to at least a portion of a specific mRNA molecule (Weintraub, *Scientific American*, 262:40, 1990). The invention embraces all antisense polynucleotides capable of inhibiting production of hedgehog, N, or C polypeptide. In the cell, the antisense nucleic acids hybridize to the corresponding mRNA, forming a double-stranded molecule. The antisense nucleic acids interfere with the translation of the mRNA since the cell will not translate a mRNA that is double-stranded. Antisense oligomers of about 15 nucleotides are preferred, since they are easily synthesized and are less likely to cause problems than larger molecules when introduced into the target hedgehog, N, or C-producing cell. The use of antisense methods to inhibit the translation of genes is well known in the art (Marcus-Sakura, *Anal. Biochem.*, 172:289, 1988). Inhibition of target nucleotide would be desirable, for example, in inhibiting cell-proliferative disorders, such as certain tumors, which are mediated by hedgehog, N or C.

- 30 -

In addition, ribozyme nucleotide sequences for hedgehog, N or C are included in the invention. Ribozymes are RNA molecules possessing the ability to specifically cleave other single-stranded RNA in a manner analogous to DNA restriction endonucleases. Through the modification of nucleotide sequences which encode these RNAs, it is possible to engineer molecules that recognize specific nucleotide sequences in an RNA molecule and cleave it (Cech, *J. Amer. Med. Assn.*, 260:3030, 1988). A major advantage of this approach is that, because they are sequence-specific, only mRNAs with particular sequences are inactivated.

There are two basic types of ribozymes namely, *tetrahymena*-type (Hasselhoff, *Nature*, 334:585, 1988) and "hammerhead"-type. *Tetrahymena*-type ribozymes recognize sequences which are four bases in length, while "hammerhead"-type ribozymes recognize base sequences 11-18 bases in length. The longer the recognition sequence, the greater the likelihood that sequence will occur exclusively in the target mRNA species. Consequently, hammerhead-type ribozymes are preferable to *tetrahymena*-type ribozymes for inactivating a specific mRNA species and 18-based recognition sequences are preferable to shorter recognition sequences.

DNA sequences encoding hedgehog, N or C can be expressed *in vitro* by DNA transfer into a suitable host cell. "Host cells" are cells in which a vector can be propagated and its DNA expressed. The term also includes any progeny of the subject host cell. It is understood that all progeny may not be identical to the parental cell since there may be mutations that occur during replication. However, such progeny are included when the term "host cell" is used. Methods of stable transfer, meaning that the foreign DNA is continuously maintained in the host, are known in the art.

In the present invention, the hedgehog, N or C polynucleotide sequences may be inserted into a recombinant expression vector. The term "recombinant expression vector" refers to a plasmid, virus or other vehicle known in the art that has been manipulated by insertion or incorporation of the hedgehog, N or C genetic sequences. Such expression

- 31 -

vectors contain a promoter sequence which facilitates the efficient transcription of the inserted genetic sequence of the host. The expression vector typically contains an origin of replication, a promoter, as well as specific genes which allow phenotypic selection of the transformed cells. Vectors suitable for use in the present invention include, but are not limited to the T7-based expression vector for expression in bacteria (Rosenberg, *et al.*, *Gene*, 56:125, 1987), the pMSXND expression vector for expression in mammalian cells (Lee and Nathans, *J. Biol. Chem.*, 263:3521, 1988) and baculovirus-derived vectors for expression in insect cells. The DNA segment can be present in the vector operably linked to regulatory elements, for example, a promoter (e.g., T7, metallothionein I, or polyhedrin promoters).

Polynucleotide sequences encoding hedgehog, N or C can be expressed in either prokaryotes or eukaryotes, although post-translational modification of eukaryotically derived polypeptides, such as carboxylation, would occur in a eukaryotic host. Hosts can include microbial, yeast, insect and mammalian organisms. Methods of expressing DNA sequences having eukaryotic or viral sequences in prokaryotes are well known in the art. Biologically functional viral and plasmid DNA vectors capable of expression and replication in a host are known in the art. Such vectors are used to incorporate DNA sequences of the invention.

Methods which are well known to those skilled in the art can be used to construct expression vectors containing the hedgehog, N or C coding sequence and appropriate transcriptional/translational control signals. These methods include *in vitro* recombinant DNA techniques, synthetic techniques, and *in vivo* recombination/genetic techniques. See, for example, the techniques described in Maniatis, *et al.*, 1989 Molecular Cloning A Laboratory Manual, Cold Spring Harbor Laboratory, N.Y.

A variety of host-expression vector systems may be utilized to express the hedgehog, N or C coding sequence. These include but are not limited to microorganisms such as bacteria transformed with recombinant bacteriophage DNA, plasmid DNA or cosmid

- 32 -

DNA expression vectors containing the hedgehog, N or C coding sequence; yeast transformed with recombinant yeast expression vectors containing the hedgehog, N or C coding sequence; plant cell systems infected with recombinant virus expression vectors (e.g., cauliflower mosaic virus, CaMV; tobacco mosaic virus, TMV) or transformed with  
5 recombinant plasmid expression vectors (e.g., Ti plasmid) containing the Hedgehog, N or C coding sequence; insect cell systems infected with recombinant virus expression vectors (e.g., baculovirus) containing the hedgehog, N or C coding sequence; or animal cell systems infected with recombinant virus expression vectors (e.g., retroviruses, adenovirus, vaccinia virus) containing the hedgehog, N or C coding sequence, or  
10 transformed animal cell systems engineered for stable expression.

Depending on the host/vector system utilized, any of a number of suitable transcription and translation elements, including constitutive and inducible promoters, transcription enhancer elements, transcription terminators, etc., may be used in the expression vector (see e.g., Bitter, *et al.*, 1987, *Methods in Enzymology*, 153:516-544). For example, when  
15 cloning in bacterial systems, inducible promoters such as pL of bacteriophage  $\gamma$ , plac, ptrp, ptac (ptrp-lac hybrid promoter) and the like may be used. When cloning in mammalian cell systems, promoters derived from the genome of mammalian cells (e.g., metallothionein promoter) or from mammalian viruses (e.g., the retrovirus long terminal repeat; the adenovirus late promoter; the vaccinia virus 7.5K promoter) may be used.  
20 Promoters produced by recombinant DNA or synthetic techniques may also be used to provide for transcription of the inserted hedgehog, N or C coding sequence.

In bacterial systems a number of expression vectors may be advantageously selected depending upon the use intended for the expressed. For example, when large quantities of hedgehog, N or C are to be produced, vectors which direct the expression of high  
25 levels of fusion protein products that are readily purified may be desirable. Those which are engineered to contain a cleavage site to aid in recovering are preferred. Such vectors include but are not limited to the *E. coli* expression vector pUR278 (Ruther, *et al.*, *EMBO J.*, 2:1791, 1983), in which the Hedgehog, N or C coding sequence may be ligated into

- 33 -

the vector in frame with the lac Z coding region so that a hybrid -lac Z protein is produced; pIN vectors (Inouye and Inouye, *Nucleic Acids Res.*, 13:3101, 1985; Van Heeke and Schuster, *J. Biol. Chem.* 264:5503, 1989) and the like.

In yeast, a number of vectors containing constitutive or inducible promoters may be used.

- 5 For a review see, Current Protocols in Molecular Biology, Vol. 2, 1988, Ed. Ausubel, *et al.*, Greene Publish. Assoc. & Wiley Interscience, Ch. 13; Grant, *et al.*, 1987, Expression and Secretion Vectors for Yeast, *in* Methods in Enzymology, Eds. Wu and Grossman, 31987, Acad. Press, N.Y., Vol. 153, pp.516-544; Glover, 1986, DNA Cloning, Vol. II, IRL Press, Wash., D.C., Ch. 3; and Bitter, 1987, Heterologous Gene
- 10 Expression in Yeast, Methods in Enzymology, Eds. Berger and Kimmel, Acad. Press, N.Y., Vol. 152, pp. 673-684; and The Molecular Biology of the Yeast *Saccharomyces*, 1982, Eds. Strathern, *et al.*, Cold Spring Harbor Press, Vols. I and II. A constitutive yeast promoter such as ADH or LEU2 or an inducible promoter such as GAL may be used (Cloning in Yeast, Ch. 3, R. Rothstein *In*: DNA Cloning Vol.11, A Practical
- 15 Approach, Ed. DM Glover, 1986, IRL Press, Wash., D.C.). Alternatively, vectors may be used which promote integration of foreign DNA sequences into the yeast chromosome.

- In cases where plant expression vectors are used, the expression of the hedgehog, N or C coding sequence may be driven by any of a number of promoters. For example, viral
- 20 promoters such as the 35S RNA and 19S RNA promoters of CaMV (Brisson, *et al.*, *Nature*, 310:511, 1984), or the coat protein promoter to TMV (Takamatsu, *et al.*, *EMBO J.*, 6:307, 1987) may be used; alternatively, plant promoters such as the small subunit of RUBISCO (Coruzzi, *et al.*, *EMBO J.*, 3:1671-1680, 1984; Broglie, *et al.*, *Science*, 224:838, 1984); or heat shock promoters, *e.g.*, soybean hsp17.5-E or hsp17.3-B (Gurley,
- 25 *et al.*, *Mol. Cell. Biol.*, 6:559, 1986) may be used. These constructs can be introduced into plant cells using Ti plasmids, Ri plasmids, plant virus vectors, direct DNA transformation, microinjection, electroporation, etc. For reviews of such techniques see, for example, Weissbach and Weissbach, 1988, Methods for Plant Molecular Biology,

- 34 -

Academic Press, NY, Section VIII, pp. 421-463; and Grierson and Corey, 1988, Plant Molecular Biology, 2d Ed., Blackie, London, Ch. 7-9.

An alternative expression system which could be used to express is an insect system. In one such system, *Autographa californica* nuclear polyhedrosis virus (AcNPV) is used  
5 as a vector to express foreign genes. The virus grows in *Spodoptera frugiperda* cells. The hedgehog, N or C coding sequence may be cloned into non-essential regions (for example the polyhedrin gene) of the virus and placed under control of an AcNPV promoter (for example the polyhedrin promoter). Successful insertion of the hedgehog, N or C coding sequence will result in inactivation of the polyhedrin gene and production  
10 of non-occluded recombinant virus (*i.e.*, virus lacking the proteinaceous coat coded for by the polyhedrin gene). These recombinant viruses are then used to infect *Spodoptera frugiperda* cells in which the inserted gene is expressed. (*e.g.*, see Smith, *et al.*, *J. Viol.*, 46:584, 1983; Smith, U.S. Patent No. 4,215,051).

Eukaryotic systems, and preferably mammalian expression systems, allow for proper  
15 post-translational modifications of expressed mammalian proteins to occur. Eukaryotic cells which possess the cellular machinery for proper processing of the primary transcript, glycosylation, phosphorylation, and advantageously, secretion of the gene product may be used as host cells for the expression of hedgehog, N or C. Mammalian cell lines may be preferable. Such host cell lines may include but are not limited to  
20 CHO, VERO, BHK, HeLa, COS, MDCK, -293, and WI38.

Mammalian cell systems which utilize recombinant viruses or viral elements to direct expression may be engineered. For example, when using adenovirus expression vectors, the hedgehog, N or C coding sequence may be ligated to an adenovirus transcription/-translation control complex, *e.g.*, the late promoter and tripartite leader sequence. This  
25 chimeric gene may then be inserted in the adenovirus genome by *in vitro* or *in vivo* recombination. Insertion in a non-essential region of the viral genome (*e.g.*, region E1 or E3) will result in a recombinant virus that is viable and capable of expressing the

- 35 -

protein in infected hosts (e.g., see Logan and Shenk, *Proc. Natl. Acad. Sci. USA*, 81:3655, 1984). Alternatively, the vaccinia virus 7.5K promoter may be used. (e.g., see, Mackett, *et al.*, *Proc. Natl. Acad. Sci. USA*, 79:7415, 1982; Mackett, *et al.*, *J. Virol.*, 49: 857, 1984; Panicali, *et al.*, *Proc. Natl. Acad. Sci. USA*, 79:4927, 1982). Of particular  
5 interest are vectors based on bovine papilloma virus which have the ability to replicate as extrachromosomal elements (Sarver, *et al.*, *Mol. Cell. Biol.*, 1:486, 1981). Shortly after entry of this DNA into mouse cells, the plasmid replicates to about 100 to 200 copies per cell. Transcription of the inserted cDNA does not require integration of the plasmid into the host's chromosome, thereby yielding a high level of expression. These  
10 vectors can be used for stable expression by including a selectable marker in the plasmid, such as, for example, the neo gene. Alternatively, the retroviral genome can be modified for use as a vector capable of introducing and directing the expression of the hedgehog, N or C gene in host cells (Cone and Mulligan, *Proc. Natl. Acad. Sci. USA*, 81:6349, 1984). High level expression may also be achieved using inducible promoters, including,  
15 but not limited to, the metallothionine IIA promoter and heat shock promoters.

For long-term, high-yield production of recombinant proteins, stable expression is preferred. Rather than using expression vectors which contain viral origins of replication, host cells can be transformed with the hedgehog, N or C cDNA controlled by appropriate expression control elements (e.g., promoter, enhancer, sequences,  
20 transcription terminators, polyadenylation sites, etc.), and a selectable marker. The selectable marker in the recombinant plasmid confers resistance to the selection and allows cells to stably integrate the plasmid into their chromosomes and grow to form foci which in turn can be cloned and expanded into cell lines. For example, following the introduction of foreign DNA, engineered cells may be allowed to grow for 1-2 days in  
25 an enriched media, and then are switched to a selective media. A number of selection systems may be used, including but not limited to the herpes simplex virus thymidine kinase (Wigler, *et al.*, *Cell*, 11: 223, 1977), hypoxanthine-guanine phosphoribosyltransferase (Szybalska and Szybalski, *Proc. Natl. Acad. Sci. USA*, 48:2026, 1962), and adenine phosphoribosyltransferase (Lowy, *et al.*, *Cell*, 22: 817,

- 36 -

1980) genes can be employed in tk<sup>-</sup>, hgp<sup>r</sup>t<sup>-</sup> or apr<sup>r</sup>t<sup>-</sup> cells respectively. Also, antimetabolite resistance can be used as the basis of selection for dhfr, which confers resistance to methotrexate (Wigler, *et al.*, *Natl. Acad. Sci. USA*, 77: 3567, 1980; O'Hare, *et al.*, *Proc. Natl. Acad. Sci. USA*, 78: 1527, 1981); gpt, which confers resistance to mycophenolic acid (Mulligan and Berg, *Proc. Natl. Acad. Sci. USA*, 78: 2072, 1981; neo, which confers resistance to the aminoglycoside G-418 (Colberre-Garapin, *et al.*, *J. Mol. Biol.*, 150:1, 1981); and hyg<sup>r</sup>, which confers resistance to hygromycin (Santerre, *et al.*, *Gene*, 30:147, 1984) genes. Recently, additional selectable genes have been described, namely trpB, which allows cells to utilize indole in place of tryptophan; hisD, which allows cells to  
5 utilize histinol in place of histidine (Hartman and Mulligan, *Proc. Natl. Acad. Sci. USA*, 85:8047, 1988); and ODC (ornithine decarboxylase) which confers resistance to the ornithine decarboxylase inhibitor, 2-(difluoromethyl)-DL-ornithine, DFMO (McConlogue L., 1987, In: Current Communications in Molecular Biology, Cold Spring Harbor Laboratory ed.).

15 Transformation of a host cell with recombinant DNA may be carried out by conventional techniques as are well known to those skilled in the art. Where the host is prokaryotic, such as *E. coli*, competent cells which are capable of DNA uptake can be prepared from cells harvested after exponential growth phase and subsequently treated by the CaCl<sub>2</sub> method using procedures well known in the art. Alternatively, MgCl<sub>2</sub> or RbCl can be  
20 used. Transformation can also be performed after forming a protoplast of the host cell if desired.

When the host is a eukaryote, such methods of transfection of DNA as calcium phosphate co-precipitates, conventional mechanical procedures such as microinjection, electroporation, insertion of a plasmid encased in liposomes, or virus vectors may be used.  
25 Eukaryotic cells can also be cotransformed with DNA sequences encoding the hedgehog, N or C of the invention, and a second foreign DNA molecule encoding a selectable phenotype, such as the herpes simplex thymidine kinase gene. Another method is to use a eukaryotic viral vector, such as simian virus 40 (SV40) or bovine papilloma virus, to

- 37 -

transiently infect or transform eukaryotic cells and express the protein. (see for example, *Eukaryotic Viral Vectors*, Cold Spring Harbor Laboratory, Gluzman ed., 1982).

Isolation and purification of microbial expressed polypeptide, or fragments thereof, provided by the invention, may be carried out by conventional means including  
5 preparative chromatography and immunological separations involving monoclonal or polyclonal antibodies.

The invention includes antibodies immunoreactive with or which bind to hedgehog, N or C polypeptide or functional fragments thereof. Antibody which consists essentially of pooled monoclonal antibodies with different epitopic specificities, as well as distinct  
10 monoclonal antibody preparations are provided. Monoclonal antibodies are made from antigen containing fragments of the protein by methods well known to those skilled in the art (Kohler, *et al.*, *Nature*, 256:495, 1975). The term antibody as used in this invention is meant to include intact molecules as well as fragments thereof, such as Fab and F(ab')<sub>2</sub>, which are capable of binding an epitopic determinant on hedgehog, N or C.  
15 The antibodies of the invention include antibodies which bind to the N or C polypeptide and which bind with immunoreactive fragments N or C.

The term "antibody" as used in this invention includes intact molecules as well as fragments thereof, such as Fab, F(ab')<sub>2</sub>, and Fv which are capable of binding the epitopic determinant. These antibody fragments retain some ability to selectively bind with its  
20 antigen or receptor and are defined as follows:

- (1) Fab, the fragment which contains a monovalent antigen-binding fragment of an antibody molecule can be produced by digestion of whole antibody with the enzyme papain to yield an intact light chain and a portion of one heavy chain;

- 38 -

- (2) Fab', the fragment of an antibody molecule can be obtained by treating whole antibody with pepsin, followed by reduction, to yield an intact light chain and a portion of the heavy chain; two Fab' fragments are obtained per antibody molecule;
- 5 (3) (Fab')<sub>2</sub>, the fragment of the antibody that can be obtained by treating whole antibody with the enzyme pepsin without subsequent reduction; F(ab')<sub>2</sub> is a dimer of two Fab' fragments held together by two disulfide bonds;
- (4) Fv, defined as a genetically engineered fragment containing the variable genetically fused single chain molecule.
- 10 Methods of making these fragments are known in the art. (See for example, Harlow and Lane, *Antibodies: A Laboratory Manual*, Cold Spring Harbor Laboratory, New York (1988), incorporated herein by reference).

As used in this invention, the term "epitope" means any antigenic determinant on an antigen to which the paratope of an antibody binds. Epitopic determinants usually  
15 consist of chemically active surface groupings of molecules such as amino acids or sugar side chains and usually have specific three dimensional structural characteristics, as well as specific charge characteristics.

Antibodies which bind to the hedgehog, N or C polypeptide of the invention can be prepared using an intact polypeptide or fragments containing small peptides of interest  
20 as the immunizing antigen. The polypeptide such as N or C, or fragments thereof used to immunize an animal can be derived from translated cDNA or chemical synthesis which can be conjugated to a carrier protein, if desired. Such commonly used carriers which are chemically coupled to the peptide include keyhole limpet hemocyanin (KLH), thyroglobulin, bovine serum albumin (BSA), and tetanus toxoid. The coupled peptide  
25 is then used to immunize the animal (e.g., a mouse, a rat, or a rabbit).

- 39 -

If desired, polyclonal or monoclonal antibodies can be further purified, for example, by binding to and elution from a matrix to which the polypeptide or a peptide to which the antibodies were raised is bound. Those of skill in the art will know of various techniques common in the immunology arts for purification and/or concentration of polyclonal  
5 antibodies, as well as monoclonal antibodies (See for example, Coligan, *et al.*, Unit 9, *Current Protocols in Immunology*, Wiley Interscience, 1991, incorporated by reference). It is also possible to use the anti-idiotypic technology to produce monoclonal antibodies which mimic an epitope. For example, an anti-idiotypic monoclonal antibody made to a first monoclonal antibody will have a binding domain in the hypervariable region  
10 which is the "image" of the epitope bound by the first monoclonal antibody.

Antibodies as described herein as having specificity for N polypeptide, *e.g.*, Ab1 (residues 83-160), are useful for specific identification of cells or tissues expressing the N fragment of hedgehog. Similarly, antibodies described herein as having specificity for C polypeptide, *e.g.*, Ab2 (residues 300-391), are useful for specific identification of cells  
15 or tissues expressing the C fragment of hedgehog. Both antibodies, naturally, will also detect native hedgehog polypeptide.

The N and C-specific antibodies of the invention are useful for purification of N and C polypeptide, respectively, especially using the antibodies immobilized on solid phase. By contacting a sample with anti-N antibody, both N and native hedgehog polypeptides  
20 can be isolated. By next contacting the sample removed by anti-N antibodies, with anti-C antibodies, the native hedgehog polypeptide is removed, thus allowing purification of N polypeptide. In a similar manner, C polypeptide can be antibody purified from a sample.

Monoclonal antibodies of the invention are suited for use, for example, in immunoassays  
25 in which they can be utilized in liquid phase or bound to a solid phase carrier. In addition, the monoclonal antibodies in these immunoassays can be detectably labeled in various ways. Examples of types of immunoassays which can utilize monoclonal

- 40 -

antibodies of the invention are competitive and non-competitive immunoassays in either a direct or indirect format. Examples of such immunoassays are the radioimmunoassay (RIA) and the sandwich (immunometric) assay. Detection of the antigens using the monoclonal antibodies of the invention can be done utilizing immunoassays which are  
5 run in either the forward, reverse, or simultaneous modes, including immunohistochemical assays on physiological samples. Those of skill in the art will know, or can readily discern, other immunoassay formats without undue experimentation.

The term "immunometric assay" or "sandwich immunoassay", includes simultaneous sandwich, forward sandwich and reverse sandwich immunoassays. These terms are well  
10 understood by those skilled in the art. Those of skill will also appreciate that antibodies according to the present invention will be useful in other variations and forms of assays which are presently known or which may be developed in the future. These are intended to be included within the scope of the present invention.

Monoclonal antibodies can be bound to many different carriers and used to detect the  
15 presence of N or C polypeptide. Examples of well-known carriers include glass, polystyrene, polypropylene, polyethylene, dextran, nylon, amylases, natural and modified celluloses, polyacrylamides, agaroses and magnetite. The nature of the carrier can be either soluble or insoluble for purposes of the invention. Those skilled in the art will know of other suitable carriers for binding monoclonal antibodies, or will be able to  
20 ascertain such using routine experimentation.

For purposes of the invention, N or C polypeptide may be detected by the monoclonal antibodies when present in biological fluids and tissues. Any sample containing a detectable amount of N or C can be used. A sample can be a liquid such as urine, saliva, cerebrospinal fluid, blood, serum and the like, or a solid or semi-solid such as tissues,  
25 feces, and the like, or, alternatively, a solid tissue such as those commonly used in histological diagnosis. C polypeptide in particular is detectable in biological samples, since it tends to diffuse more readily than N polypeptide.

- 41 -

In performing the assays it may be desirable to include certain "blockers" in the incubation medium (usually added with the labeled soluble antibody). The "blockers" are added to assure that non-specific proteins, proteases, or anti-heterophilic immunoglobulins to anti-C or N immunoglobulins present in the experimental sample do not  
5 cross-link or destroy the antibodies on the solid phase support, or the radiolabeled indicator antibody, to yield false positive or false negative results. The selection of "blockers" therefore may add substantially to the specificity of the assays described in the present invention.

The invention also provides a method for modulating proliferation or differentiation of  
10 neuronal cells comprising contacting the cells with a hedgehog polypeptide. The hedgehog polypeptide may be a native hedgehog polypeptide, or a N or C polypeptide, or functional fragments thereof. Preferably, the modulation is induction of proliferation or differentiation of a particular cell type. This can involve either synergistic positive induction of neuronal cells by N, or negative modulation by delta N-C for example (Lai,  
15 *et al.*, *Development* 121:2349, 1995). Delta N-C enhances expression of posterior relative to anterior neural genes and does so through inhibition of N (see EXAMPLE 18 and Figure 18D). In addition to hedgehog polypeptide, a TGF- $\beta$  factor may also be utilized in the method of the invention.

Previous studies with the rat hedgehog gene showed that co-culture of cells expressing  
20 rat hedgehog precursor gene, with explant from neural tube, was sufficient to induce formation of motor neurons and floor plate from the explant (Jessesl, T., and Dodd, J., In *Cell-Cell Signaling in Vertebrate Development* (ed. E.J. Robertson, *et al.*, pp 139-155, San Diego, Ca.), 1993). Therefore, based on the Examples herein showing that hedgehog is expressed near the floorplate of the ventral midline of the neural tube and notochord,  
25 neuronal cells substantially derived from floor plate neuronal cells can be induced by contacting the cells with hedgehog, N or C polypeptide. As used herein, the term "substantially derived", refers to those cells from the floor plate or proximate to the floor plate. For example, such cells include motor neurons and dopaminergic neurons. Those

- 42 -

of skill in the art will be able to identify other neuronal cells substantially derived from the floor plate. Preferably the cells are vertebrate cells and most preferably, human cells.

In addition, as described herein in the Examples, hedgehog, and particularly C fragment, induces the expression of pituitary genes. Hedgehog is also effective in inducing anterior  
5 brain gene expression as exemplified by the OTX-A marker. Further, the addition of a TGF- $\beta$  family member, for example activin, may be used to further induce expression of such genes. Other TGF- $\beta$  family members will be known to those of skill in the art. This apparent synergy of *hh* fragments with TGF- $\beta$  family members occurs through the  
10 TGF- $\beta$  protein inducing expression of neural inducers such as noggin and follistatin. The *hh* fragment then synergizes with these inducers to pattern neural gene expression.

*hh* fragments may also be useful as nerve-sparing agents or in restoring or promoting appropriate patterning during the healing of major limb trauma. In addition, the N and C fragments may be useful in the area of genetic counseling. Specifically, familial  
15 midline defects such as cyclopia, polydactyly or neural tube defects may be diagnosed by mapping close to *hh*. Since autoproteolytic defects may be responsible for the disorders, N or C therapy could be provided.

The invention also provides an autoproteolytic fusion protein comprising a first polypeptide including the proteolytic domain of the C polypeptide of the invention, a  
20 cleavage site recognized by the first polypeptide, and a second polypeptide. (It is understood that the first and second polypeptides can be reversed.) The auto-proteolytic activity of the native hedgehog protein is found entirely within the C polypeptide, therefore, the C polypeptide is useful for producing a fusion polypeptide which can then be cleaved at the junction of the C polypeptide and the second polypeptide. The fusion  
25 protein may optionally have a purification tag, such as a poly-histidine tag for isolation on a nickel column, or an antibody epitope tag, preferably on the C fragment. The cleavage site includes the sequence "GCF", which is recognized by the proteolytic

- 43 -

domain of the C polypeptide and is utilized to cleave the second polypeptide from the C fragment. Also included in the invention is a polynucleotide encoding the fusion protein of the invention.

The invention also provides a method for producing an autoproteolytic fusion protein comprising operably linking a first polynucleotide, wherein the first polynucleotide encodes a first polypeptide including the proteolytic domain of the C polypeptide of the invention and the cleavage site recognized by the proteolytic domain, and a second polynucleotide encoding a second polypeptide. As described above, the fusion protein may also include a carrier peptide and/or a purification tag.

- 10 The C polypeptide or functional fragment thereof is useful as a fusion partner to cause lipophilic modification and tethering of other proteins *in vivo* or *in vitro*. Such fusion proteins may be desirable for factors whose activity is required in a localized manner, either by targeting DNA constructs to specific cells or by introducing cells transfected with specific DNA constructs, for example. It may be desirable to lipid-modify a normally secreted protein in order to produce a cell-associated protein. For example, it may be desirable to produce a viral antigen that remains cell associated. Specifically, cholesterol is covalently attached to the N-terminal protein during autoprocessing and the C polypeptide acts as an intramolecular cholesterol transferase.

Alternatively, the C polypeptide or functional fragments thereof can be used as a fusion partner with a protein of interest (*e.g.*, Protein X fused to hh-C domain). Such fusions form thioesters at the junction between Protein X and hh-C (via an S to N shift). The thioesters are then available as substrates for a peptide ligation reaction in which any peptide or protein having an amino terminal cysteine (Peptide Y) is added and undergoes spontaneous rearrangement (S to N shift) that generates a stable peptide bond between Protein X and Peptide Y (Protein X-peptide bond-Peptide Y). For example, a protein that is toxic when produced *in vivo* could be produced *in vitro* using the hh-C domain fusion protein method.

- 44 -

The fusion polypeptide may also include an optional carrier peptide. The "carrier peptide", or signal sequence, is located at the amino terminal end of the fusion peptide sequence. In the case of eukaryotes, the carrier peptide is believed to function to transport the fusion polypeptide across the endoplasmic reticulum. The secretory protein  
5 is then transported through the Golgi apparatus, into secretory vesicles and into the extracellular space or, preferably, the external environment. Carrier peptides which can be utilized according to the invention include pre-pro peptides which contain a proteolytic enzyme recognition site. Acceptable carrier peptides include the amino terminal pro-region of calcitonin or other hormones, which undergo cleavage at the  
10 flanking dibasic sites. However, it should be noted that the invention is not limited to the use of any particular peptide as a carrier. Other carrier peptides are known to those skilled in the art or can be readily ascertained without undue experimentation.

In one embodiment of the invention, a carrier peptide which is a signal sequence is included in the expression vector, specifically located adjacent to the N-terminal end of  
15 the fusion polypeptide. This signal sequence allows the fusion protein to be directed toward the endoplasmic reticulum. Typically, the signal sequence consists of a leader of from about 16 to about 29 amino acids, starting with two or three polar residues and continuing with a high content of hydrophobic amino acids; there is otherwise no detectable conservation of sequence known. Such signal sequences are known to those  
20 of skill in the art, and include the naturally occurring signal sequence derived from a hedgehog protein.

The fusion polypeptide of the invention includes a polypeptide encoded by a structural gene, preferably at the amino-terminus of the fusion polypeptide. Any structural gene is expressed in conjunction with the C-polypeptide (polynucleotide) and optionally a  
25 carrier peptide. The structural gene is operably linked with the carrier in an expression vector so that the fusion polypeptide is expressed as a single unit.

- 45 -

The identification of the autoproteolysis of hedgehog into the N and C domains is useful in a screening method to identify compounds or compositions which affect this processing activity. Thus, in another embodiment, the invention provides a method for identifying a composition which affects hh processing, which can be determined by  
5 activity or gene expression, comprising incubating the components, which include the composition to be tested (*e.g.*, a drug, a small molecule, a protein) and a hh polypeptide or a recombinant cell expressing hedgehog or a gene encoding a C domain or functional fragment thereof operably linked to an N domain or functional fragment thereof, under conditions sufficient to allow the components to interact, then subsequently measuring  
10 the effect the composition has on hedgehog activity or expression. Fragments of hedgehog polypeptide or polynucleotide can be used in the method of the invention as long as autoproteolytic activity remains (*e.g.*, the construct exemplified in Figure 12a and 12b, Example 10). The observed effect on hh may be either inhibitory or stimulatory. For example, one can determine whether the N domain is associated with the cell, or  
15 whether the N domain is secreted into the medium, in other words, whether incomplete processing has occurred. Such methods for determining the effect of the compound or composition on hh processing include those described herein (see Example 10, Figure 12a and 12b) such as time course of autoproteolytic cleavage or course of cleavage based on concentration ranges. Alternatively, the effect of the composition on hh can be  
20 determined by the expression of anterior or posterior neural markers. Other methods for determining the effect of a composition on processing of N and C will be known to those of skill in the art. Various labels can be used to detect the N and C domains, for example, a radioisotope, a fluorescent compound, a bioluminescent compound, a chemiluminescent compound, a metal chelator or an enzyme could be used. Those of  
25 ordinary skill in the art will know of other suitable labels or will be able to ascertain such, using routine experimentation.

The identification of the lipid modification of the N domain of hedgehog by the C domain, resulting in a biologically active N domain, is useful in a screening method to identify compounds or compositions which affect the cholesterol transferase/processing

- 46 -

activity of hedgehog. In a broader aspect, the modification may be a general sterol or lipid modification, and not limited to cholesterol. Thus, in another embodiment, the invention provides a method for identifying a composition which affects hh biological activity, which can be determined by activity or lipid modification (*e.g.*, cholesterol),  
5 comprising incubating the components, which include the composition to be tested (*e.g.*, a drug, a small molecule, a protein) and a hh polypeptide or a recombinant cell expressing hedgehog or a gene encoding a C domain or functional fragment thereof operably linked to an N domain or functional fragment thereof, under conditions sufficient to allow the components to interact, then subsequently measuring the effect the  
10 composition has on hedgehog activity. Fragments of hedgehog polypeptide or polynucleotide can be used in the method of the invention as long as cholesterol transferase activity remains, for example. The effect on hh may be either inhibitory or stimulatory. For example, one can determine whether the N domain is associated with the cell, or whether the N domain is secreted into the medium, in other words, whether  
15 incomplete processing and modification has occurred. Such methods for determining the effect of the compound or composition on hh processing include those described herein (see Example 10, Figure 12a and 12b) such as time course of autoproteolytic cleavage or course of cleavage based on concentration ranges. Alternatively, the effect of the composition on hh can be determined by the level of cholesterol modification as  
20 determined by thin layer chromatography (*e.g.*, Example 19, Figure 23) or incorporation of labeled cholesterol into hh protein (*e.g.*, Example 19, Figure 25) or into a fragment appended to the transferase (c) domain.. Other methods for determining the effect of a composition on processing and cholesterol modification of N and C will be known to those of skill in the art. Various labels can be used to detect the N and C domains, for  
25 example, a radioisotope, a fluorescent compound, a bioluminescent compound, a chemiluminescent compound, a metal chelator or an enzyme could be used. Those of ordinary skill in the art will know of other suitable labels or will be able to ascertain such, using routine experimentation.

- 47 -

As used herein, "hh activity" as described in the screening method refers preferably to autoproteolytic activity. However, it is understood, that one of skill in the art could use the above-described screening assay to identify a composition having an affect on other hh activities, for example, zinc hydrolase activity or cholesterol transferase activity; or  
5 induction or regulation of differentiation of neuronal cells or chondrocytes. Appropriate assays for determining the effect on such activities will be known to those of skill in the art. Example 19 provides lipophilic modification assays useful in the described screening methods above.

Now that the present invention describes the cholesterol modification of N by C, it is  
10 possible to design various diagnostic and therapeutic approaches for treatment of hh associated disorders due to defective or altered sterol modification. For example, Smith-Lemli-Optiz syndrome (SLOS) is characterized by a loss of hh function and a sterol profile indicating a cholesterol deficiency. Therefore, SLOS may be diagnosed and/or treated based on the cholesterol profile. Further, a defect in Desert hh in the testes is  
15 associated with male sterility (M.Bitgood, L.Shen, A.P. McMahon, *Current Biology* 6, 298, 1996; A. Vortkamp et al., *Science* 273, 613, 1996), consequently, it may be possible to design male contraceptives based on defective cholesterol modification of hh. On the other hand, if sterility or decreased fertility was desirable, hh cholesterol transferase activity could be altered to reduce cholesterol modification. Processing of the C and N  
20 fragments of hh is required for hh activity, therefore alterations in cholesterol modification of the amino terminal fragment may also be related to developmental defects in vertebrate embryos.

Another aspect of the present invention concerns three-dimensional molecular models of the subject hedgehog proteins, and their use as templates for the design of agents able  
25 to inhibit or potentiate at least one biological activity of the hedgehog, particularly the autoproteolytic. An integral step to our approach to designing inhibitors of the subject hedgehog proteins, for example, involves construction of computer graphics models of the hedgehog protein which can be used to design pharmacophores by rational drug design.

- 48 -

For instance, for an inhibitor to interact optimally with the subject proteolytic domain of hedgehog, it will generally be desirable that it have a shape which is at least partly complimentary to that of a particular binding site of the enzyme, as for example those portions of the human hedgehog protein which are involved in the autoproteolytic activity.

- 5 Additionally, other factors, including electrostatic interactions, hydrogen bonding, hydrophobic interactions, desolvation effects, and cooperative motions of ligand and enzyme, all influence the binding effect and should be taken into account in attempts to design bioactive inhibitors.

A computer-generated molecular model of the subject hedgehog proteins can be created.

- 10 In preferred embodiments, at least the  $\alpha$ -carbon positions of the hedgehog sequence of interest are mapped to a particular coordinate pattern, such as the coordinates for hedgehog determined by x-ray crystallography, by homology modeling, and the structure of the protein and velocities of each atom are calculated at a simulation temperature ( $T_0$ ) at which the docking simulation is to be determined. Typically, such a protocol involves
- 15 primarily the prediction of side-chain conformations in the modeled protein, while assuming a main-chain trace taken from a tertiary structure such as provided in x-crystallographic model described herein. Computer programs for performing energy minimization routines are commonly used to generate molecular models. For example, both the CHARMM (Brooks et al. (1983) *J Comput Chem* 4:187-217) and AMBER
- 20 (Weiner et al (1981) *J. Comput. Chem.* 106: 765) algorithms handle all of the molecular system setup, force field calculation, and analysis (see also, Eisenfield et al. (1991) *Am J Physiol* 261:C376-386; Lybrand (1991) *J Pharm Belg* 46:49-54; Froimowitz (1990) *Biotechniques* 8:640-644; Burbam et al. (1990) *Proteins* 7:99-111; Pedersen (1985) *Environ Health Perspect* 61:185-190; and Kini et al. (1991) *J Biomol Struct Dyn* 9:475-
- 25 488). At the heart of these programs is a set of subroutines that, given the position of every atom in the model, calculate the total potential energy of the system and the force on each atom. These programs may utilize a starting set of atomic coordinates, such as the model coordinates provided in crystallographic-derived models, the parameters for the various terms of the potential energy function, and a description of the molecular

- 49 -

topology (the covalent structure). Common features of such molecular modeling methods include: provisions for handling hydrogen bonds and other constraint forces; the use of periodic boundary conditions; and provisions for occasionally adjusting positions, velocities, or other parameters in order to maintain or change temperature, pressure,  
5 volume, forces of constraint, or other externally controlled conditions.

Most conventional energy minimization methods use the input data described above and the fact that the potential energy function is an explicit, differentiable function of Cartesian coordinates, to calculate the potential energy and its gradient (which gives the force on each atom) for any set of atomic positions. This information can be used to  
10 generate a new set of coordinates in an effort to reduce the total potential energy and, by repeating this process over and over, to optimize the molecular structure under a given set of external conditions. These energy minimization methods are routinely applied to molecules similar to the subject hedgehog proteins as well as nucleic acids, polymers and zeolites.

15 In general, energy minimization methods can be carried out for a given temperature,  $T_i$ , which may be different than the docking simulation temperature,  $T_o$ . Upon energy minimization of the molecule at  $T_i$ , coordinates and velocities of all the atoms in the system are computed. Additionally, the normal modes of the system are calculated. It will be appreciated by those skilled in the art that each normal mode is a collective,  
20 periodic motion, with all parts of the system moving in phase with each other, and that the motion of the molecule is the superposition of all normal modes. For a given temperature, the mean square amplitude of motion in a particular mode is inversely proportional to the effective force constant for that mode, so that the motion of the molecule will often be dominated by the low frequency vibrations.

25 After the molecular model has been energy minimized at  $T_i$ , the system is "heated" or "cooled" to the simulation temperature,  $T_o$ , by carrying out an equilibration run where the velocities of the atoms are scaled in a step-wise manner until the desired temperature,

- 50 -

$T_0$ , is reached. The system is further equilibrated for a specified period of time until certain properties of the system, such as average kinetic energy, remain constant. The coordinates and velocities of each atom are then obtained from the equilibrated system.

Further energy minimization routines can also be carried out. For example, a second class of methods involves calculating approximate solutions to the constrained EOM for the protein. These methods use an iterative approach to solve for the Lagrange multipliers and, typically, only need a few iterations if the corrections required are small. The most popular method of this type, SHAKE (Ryckaert et al. (1977) *J Comput Phys* 23:327; and Van Gunsteren et al. (1977) *Mol Phys* 34:1311) is easy to implement and scales as  $O(N)$  as the number of constraints increases. Therefore, the method is applicable to macromolecules such as the Hedgehog proteins of the present invention. An alternative method, RATTLE (Anderson (1983) *J Comput Phys* 52:24) is based on the velocity version of the Verlet algorithm. Like SHAKE, RATTLE is an iterative algorithm and can be used to energy minimize the model of the subject hedgehog protein.

The increasing availability of biomacromolecule structures of potential pharmacophoric molecules that have been solved crystallographically has prompted the development of a variety of direct computational methods for molecular design, in which the steric and electronic properties of catalytic and substrate recognition sites are used to guide the design of potential inhibitors (Cohen et al. (1990) *J. Med. Chem.* 33: 883-894; Kuntz et al. (1982) *J. Mol. Biol* 161: 269-288; DesJarlais (1988) *J. Med. Chem.* 31: 722-729; Bartlett et al. (1989) (*Spec. Publ., Roy. Soc. Chem.*) 78: 182-196; Goodford et al. (1985) *J. Med. Chem.* 28: 849-857; DesJarlais et al. *J. Med. Chem.* 29: 2149-2153). Directed methods generally fall into two categories: (1) design by analogy in which 3-D structures of known molecules (such as from a crystallographic database) are docked to the enzyme structure and scored for goodness-of-fit; and (2) *de novo* design, in which the ligand model is constructed piece-wise in the enzyme. The latter approach, in particular, can facilitate the development of novel molecules, uniquely designed to bind to, and, e.g., inhibit the proteolytic activity of a hedgehog protein.

- 51 -

In an illustrative embodiment, the design of potential hedgehog inhibitors begins from the general perspective of shape complimentary for the active site and substrate specificity subsites of the enzyme, and a search algorithm is employed which is capable of scanning a database of small molecules of known three-dimensional structure for candidates which fit geometrically into the target protein site. It is not expected that the molecules found in the shape search will necessarily be leads themselves, since no evaluation of chemical interaction necessarily be made during the initial search. Rather, it is anticipated that such candidates might act as the framework for further design, providing molecular skeletons to which appropriate atomic replacements can be made.

Of course, the chemical complimentary of these molecules can be evaluated, but it is expected that atom types will be changed to maximize the electrostatic, hydrogen bonding, and hydrophobic interactions with the enzyme. Most algorithms of this type provide a method for finding a wide assortment of chemical structures that are complementary to the shape of a binding site of the subject enzyme. Each of a set of small molecules from a particular data-base, such as the Cambridge Crystallographic Data Bank (CCDB) (Allen et al. (1973) *J. Chem. Doc.* 13: 119), is individually docked to the binding site of the hedgehog proteolytic domain in a number of geometrically permissible orientations with use of a docking algorithm. In a preferred embodiment, a set of computer algorithms called DOCK, can be used to characterize the shape of invaginations and grooves that form the active sites and recognition surfaces of the subject protein (Kuntz et al. (1982) *J. Mol. Biol* 161: 269-288). The program can also search a database of small molecules for templates whose shapes are complementary to particular binding sites of the enzyme (DesJarlais et al. (1988) *J Med Chem* 31: 722-729). These templates normally require modification to achieve good chemical and electrostatic interactions (DesJarlais et al. (1989) *ACS Symp Ser* 413: 60-69). However, the program has been shown to position accurately known cofactors for inhibitors based on shape constraints alone.

The orientations are evaluated for goodness-of-fit and the best are kept for further examination using molecular mechanics programs, such as AMBER or CHARMM.

- 52 -

Such algorithms have previously proven successful in finding a variety of molecules that are complementary in shape to a given binding site of a receptor-enzyme, and have been shown to have several attractive features. First, such algorithms can retrieve a remarkable diversity of molecular architectures. Second, the best structures have, in  
5 previous applications to other proteins, demonstrated impressive shape complementarity over an extended surface area. Third, the overall approach appears to be quite robust with respect to small uncertainties in positioning of the candidate atoms.

Goodford (1985, *J Med Chem* 28:849-857) and Boobbyer et al. (1989, *J Med Chem* 32:1083-1094) have produced a computer program (GRID) which seeks to determine  
10 regions of high affinity for different chemical groups (termed probes) on the molecular surface of the binding site. GRID hence provides a tool for suggesting modifications to known ligands that might enhance binding. It may be anticipated that some of the sites discerned by GRID as regions of high affinity correspond to "pharmacophoric patterns" determined inferentially from a series of known ligands. As used herein, a  
15 pharmacophoric pattern is a geometric arrangement of features of the anticipated ligand that is believed to be important for binding. Attempts have been made to use pharmacophoric patterns as a search screen for novel ligands (Jakes et al. (1987) *J Mol Graph* 5:41-48; Brint et al. (1987) *J Mol Graph* 5:49-56; Jakes et al. (1986) *J Mol Graph* 4:12-20); however, the constraint of steric and "chemical" fit in the putative (and  
20 possibly unknown) receptor binding site is ignored. Goodsell and Olson (1990, *Proteins: Struct Funct Genet* 8:195-202) have used the Metropolis (simulated annealing) algorithm to dock a single known ligand into a target protein. They allow torsional flexibility in the ligand and use GRID interaction energy maps as rapid lookup tables for computing approximate interaction energies. Given the large number of degrees of freedom  
25 available to the ligand, the Metropolis algorithm is time-consuming and is unsuited to searching a candidate database of a few thousand small molecules.

Yet a further embodiment of the present invention utilizes a computer algorithm such as CLIX which searches such databases as CCDB for small molecules which can be

- 53 -

oriented in the receptor binding site in a way that is both sterically acceptable and has a high likelihood of achieving favorable chemical interactions between the candidate molecule and the surrounding amino acid residues. The method is based on characterizing the receptor site in terms of an ensemble of favorable binding positions for different chemical groups and then searching for orientations of the candidate molecules that cause maximum spatial coincidence of individual candidate chemical groups with members of the ensemble. The current availability of computer power dictates that a computer-based search for novel ligands follows a breadth-first strategy. A breadth-first strategy aims to reduce progressively the size of the potential candidate search space by the application of increasingly stringent criteria, as opposed to a depth-first strategy wherein a maximally detailed analysis of one candidate is performed before proceeding to the next. CLIX conforms to this strategy in that its analysis of binding is rudimentary -it seeks to satisfy the necessary conditions of steric fit and of having individual groups in "correct" places for bonding, without imposing the sufficient condition that favorable bonding interactions actually occur. A ranked "shortlist" of molecules, in their favored orientations, is produced which can then be examined on a molecule-by-molecule basis, using computer graphics and more sophisticated molecular modeling techniques. CLIX is also capable of suggesting changes to the substituent chemical groups of the candidate molecules that might enhance binding.

The algorithmic details of CLIX is described in Lawrence et al. (1992) *Proteins* 12:31-41, and the CLIX algorithm can be summarized as follows. The GRID program is used to determine discrete favorable interaction positions (termed target sites) in the binding site of the protein for a wide variety of representative chemical groups. For each candidate ligand in the CCDB an exhaustive attempt is made to make coincident, in a spatial sense in the binding site of the protein, a pair of the candidate's substituent chemical groups with a pair of corresponding favorable interaction sites proposed by GRID. All possible combinations of pairs of ligand groups with pairs of GRID sites are considered during this procedure. Upon locating such coincidence, the program rotates the candidate ligand about the two pairs of groups and checks for steric hindrance and

- 54 -

coincidence of other candidate atomic groups with appropriate target sites. Particular candidate/orientation combinations that are good geometric fits in the binding site and show sufficient coincidence of atomic groups with GRID sites are retained.

Consistent with the breadth-first strategy, this approach involves simplifying assumptions. Rigid protein and small molecule geometry is maintained throughout. As a first approximation rigid geometry is acceptable as the energy minimized coordinates of the hedgehog deduced structure, describe an energy minimum for the molecule, albeit a local one. If the surface residues of the site of interest are not involved in crystal contacts then the crystal configuration of those residues. We believe that the deduced crystal structure described in herein should reasonably mimic the mean solution configuration. Moreover, the equivalent models of of hedgehog isoforms (Ihh, Dhh, etc) can be derived by the same method.

A further assumption implicit in CLIX is that the potential ligand, when introduced into the active site of hedgehog protein, does not induce change in the protein's stereochemistry or partial charge distribution and so alter the basis on which the GRID interaction energy maps were computed. It must also be stressed that the interaction sites predicted by GRID are used in a positional and type sense only, i.e., when a candidate atomic group is placed at a site predicted as favorable by GRID, no check is made to ensure that the bond geometry, the state of protonation, or the partial charge distribution favors a strong interaction between the protein and that group. Such detailed analysis should form part of more advanced modeling of candidates identified in the CLIX shortlist.

Yet another embodiment of a computer-assisted molecular design method for identifying inhibitors of the subject hedgehog protein comprises the *de novo* synthesis of potential inhibitors by algorithmic connection of small molecular fragments that will exhibit the desired structural and electrostatic complementarity with the active site of the enzyme. The methodology employs a large template set of small molecules with are iteratively pieced together in a model of the hedgehog active site. Each stage of ligand growth is

- 55 -

evaluated according to a molecular mechanics-based energy function, which considers van der Waals and coulombic interactions, internal strain energy of the lengthening ligand, and desolvation of both ligand and enzyme. The search space can be managed by use of a data tree which is kept under control by pruning according to the binding  
5 criteria.

In an illustrative embodiment, the search space is limited to consider only amino acids and amino acid analogs as the molecular building blocks. Such a methodology generally employs a large template set of amino acid conformations, though need not be restricted to just the 20 natural amino acids, as it can easily be extended to include other related  
10 fragments of interest to the medicinal chemist, e.g. amino acid analogs. The putative ligands that result from this construction method are peptides and peptide-like compounds rather than the small organic molecules that are typically the goal of drug design research. The appeal of the peptide building approach is not that peptides are preferable to organics as potential pharmaceutical agents, but rather that: (1) they can be  
15 generated relatively rapidly *de novo*; (2) their energetics can be studied by well-parameterized force field methods; (3) they are much easier to synthesize than are most organics; and (4) they can be used in a variety of ways, for peptidomimetic inhibitor design, protein-protein binding studies, and even as shape templates in the more commonly used 3D organic database search approach described above.

20 Such a *de novo* peptide design method has been incorporated in a software package called GROW (Moon et al. (1991) *Proteins* 11:314-328). In a typical design session, standard interactive graphical modeling methods are employed to define the structural environment in which GROW is to operate. For instance, environment could be the active site cleft of hedgehog, or it could be a set of features on the protein's surface to  
25 which the user wishes to bind a peptide-like molecule, a peptide sequence based on the cleavage site of hedgehog itself (e.g., to represent the autoproteolytic event). The GROW program then operates to generate a set of potential ligand molecules. Interactive

- 56 -

modeling methods then come into play again, for examination of the resulting molecules, and for selection of one or more of them for further refinement.

To illustrate, GROW operates on an atomic coordinate file generated by the user in the interactive modeling session, such as the coordinates provided in the crystallographic-  
5 derived models, plus a small fragment (e.g., an acetyl group) positioned in the active site to provide a starting point for peptide growth. These are referred to as "site" atoms and "seed" atoms, respectively. A second file provided by the user contains a number of control parameters to guide the peptide growth (Moon et al. (1991) *Proteins* 11:314-328).

The operation of the GROW algorithm is conceptually fairly simple. GROW proceeds  
10 in an iterative fashion, to systematically attach to the seed fragment each amino acid template in a large preconstructed library of amino acid conformations. When a template has been attached, it is scored for goodness-of-fit to the receptor site, and then the next template in the library is attached to the seed. After all the templates have been tested, only the highest scoring ones are retained for the next level of growth. This procedure  
15 is repeated for the second growth level; each library template is attached in turn to each of the bonded seed/amino acid molecules that were retained from the first step, and is then scored. Again, only the best of the bonded seed/dipeptide molecules that result are retained for the third level of growth. The growth of peptides can proceed in the N-to-C direction only, the reverse direction only, or in alternating directions, depending on the  
20 initial control specifications supplied by the user. Successive growth levels therefore generate peptides that are lengthened by one residue. The procedure terminates when the user-defined peptide length has been reached, at which point the user can select from the constructed peptides those to be studied further. The resulting data provided by the GROW procedure include not only residue sequences and scores, but also atomic  
25 coordinates of the peptides, related directly to the coordinate system of the receptor site atoms.

In yet another embodiment, potential pharmacophoric compounds can be determined using a method based on an energy minimization-quenched molecular dynamics

- 57 -

algorithm for determining energetically favorable positions of functional groups in the binding sites of the subject hedgehog protein. The method can aid in the design of molecules that incorporate such functional groups by modification of known ligands or *de novo* construction.

- 5 For example, the multiple copy simultaneous search method (MCSS) described by Miranker et al. (1991) *Proteins* 11: 29-34. To determine and characterize a local minima of a functional group in the forcefield of the protein, multiple copies of selected functional groups are first distributed in a binding site of interest on the hedgehog protein. Energy minimization of these copies by molecular mechanics or quenched  
10 dynamics yields the distinct local minima. The neighborhood of these minima can then be explored by a grid search or by constrained minimization. In one embodiment, the MCSS method uses the classical time dependent Hartree (TDH) approximation to simultaneously minimize or quench many identical groups in the forcefield of the protein.
- 15 Implementation of the MCSS algorithm requires a choice of functional groups and a molecular mechanics model for each of them. Groups must be simple enough to be easily characterized and manipulated (3-6 atoms, few or no dihedral degrees of freedom), yet complex enough to approximate the steric and electrostatic interactions that the functional group would have in binding to the site of interest in the hedgehog protein.
- 20 A preferred set is, for example, one in which most organic molecules can be described as a collection of such groups (*Patai's Guide to the Chemistry of Functional Groups*, ed. S. Patai (New York: John Wiley, and Sons, (1989)). This includes fragments such as acetonitrile, methanol, acetate, methyl ammonium, dimethyl ether, methane, and acetaldehyde.
- 25 Determination of the local energy minima in the binding site requires that many starting positions be sampled. This can be achieved by distributing, for example, 1,000-5,000 groups at random inside a sphere centered on the binding site; only the space not

- 58 -

occupied by the protein needs to be considered. If the interaction energy of a particular group at a certain location with the protein is more positive than a given cut-off (e.g. 5.0 kcal/mole) the group is discarded from that site. Given the set of starting positions, all the fragments are minimized simultaneously by use of the TDH approximation (Elber et al. (1990) *J Am Chem Soc* 112: 9161-9175). In this method, the forces on each fragment consist of its internal forces and those due to the protein. The essential element of this method is that the interactions between the fragments are omitted and the forces on the protein are normalized to those due to a single fragment. In this way simultaneous minimization or dynamics of any number of functional groups in the field of a single protein can be performed.

Minimization is performed successively on subsets of, e.g. 100, of the randomly placed groups. After a certain number of step intervals, such as 1,000 intervals, the results can be examined to eliminate groups converging to the same minimum. This process is repeated until minimization is complete (e.g. RMS gradient of 0.01 kcal/mole/Å). Thus the resulting energy minimized set of molecules comprises what amounts to a set of disconnected fragments in three dimensions representing potential pharmacophores.

The next step then is to connect the pharmacophoric pieces with spacers assembled from small chemical entities (atoms, chains, or ring moieties). In a preferred embodiment, each of the disconnected can be linked in space to generate a single molecule using such computer programs as, for example, NEWLEAD (Tschinke et al. (1993) *J Med Chem* 36: 3863,3870). The procedure adopted by NEWLEAD executes the following sequence of commands (1) connect two isolated moieties, (2) retain the intermediate solutions for further processing, (3) repeat the above steps for each of the intermediate solutions until no disconnected units are found, and (4) output the final solutions, each of which is single molecule. Such a program can use for example, three types of spacers: library spacers, single-atom spacers, and fuse-ring spacers. The library spacers are optimized structures of small molecules such as ethylene, benzene and methylamide. The output produced by programs such as NEWLEAD consist of a set of molecules containing the

- 59 -

original fragments now connected by spacers. The atoms belonging to the input fragments maintain their original orientations in space. The molecules are chemically plausible because of the simple makeup of the spacers and functional groups, and energetically acceptable because of the rejection of solutions with van-der Waals radii violations.

The three-dimensional structure of hedgehog is useful to aid in screening and development of diagnostic and therapeutic protein fragments as in rational drug design, to search for structural analogs of known protein structures, or to aid in an analysis of biological function and activity. Also, the method may be used to predict protein secondary structures and protein subsecondary structures from amino acid sequences alone, and to predict those regions of a protein molecule that are on the outside and those that are on the inside.

Compounds can also be prepared using the three-dimensional structure provided herein and tested using assays known to those of skill in the art. For example, compounds can be synthesized and screened for hedgehog autoprolytic activity by cleavage assays (see for example, Porter *et al.*, Cell 86:21, 1996; WO96/17924, herein incorporated by reference).

Compounds of the invention include drugs, small molecules, peptides, peptidomimetics, polypeptides, chemical compounds and biologic agents. For example, peptidomimetics are synthetic compounds having a three-dimensional structure (*i.e.*, a "peptide motif") based upon the three-dimensional structure of a selected peptide. The peptide motif provides the peptidomimetic compound with Hedgehog agonist or antagonist activity that is substantially the same as, or greater than, the Hedgehog agonist or antagonist activity of the peptide from which the peptidomimetic was derived. Peptidomimetic compounds can have additional characteristics that enhance their therapeutic application, *e.g.*, enhanced cell permeability, increased receptor or polypeptide binding affinity and/or avidity, and prolonged biological half-life. The design of peptidomimetic compounds

- 60 -

having agonist or antagonist activity can be aided through computer modeling techniques well known in the art. Other methods for the design, as well as the preparation of, p-eptidomimetic compounds are well known in the art.

Atomic coordinates and structure factors have been deposited in the Brookhaven Protein  
5 Data Bank. Applicant assures complete access and disclosure of these coordinates and factors upon issuance of a patent.

The following examples are intended to illustrate but not limit the invention. While they are typical of those that might be used, other procedures known to those skilled in the art may alternatively be used.

10

#### EXAMPLE 1

#### HEDGEHOG PROTEIN PROCESSING

The full length form of the *hh* protein (F) migrates with a mobility corresponding to a relative molecular mass of 46 kD. FIGURES 1 (A) and (C) are immunoblots with antibodies against amino- (Ab1) and carboxy-terminal (Ab2) epitopes. GST fusion  
15 proteins containing either residues 83 to 160 or 300 to 391 from HH protein were expressed in *Escherichia coli*, purified as recommended [F. M. Ausubel, *et al.*, *Current Protocols in Molecular Biology* (Greene and Wiley-Interscience, New York, 1991)], and used to immunize rabbits by standard methods. The antibodies were affinity purified on a column of His<sub>6</sub>-U protein [E. Harlow and D. Lane, *Antibodies: A Laboratory Manual*  
20 (Cold Spring Harbor Laboratory, Cold Spring Harbor, NY, 1988)] linked to Affi-Gel 10 beads (Bio-Rad). The purification was performed as described (Harlow and Lane, *supra*) except that the acid and base elutions contained 10 percent dioxane. Biotinylated *hh* antibodies were prepared by purifying the rabbit antisera over a protein A column, followed by biotinylation with the use of the Immunoprobe biotinylation kit (Sigma).  
25 Immunoprecipitations were performed as described [Harlow and Lane] with the use of cold RIPA lysis buffer containing 0.25 mM phenylmethylsulfonyl fluoride (PMSF) and

- 61 -

5 mM EDTA for tissue homogenization. Lysates were precleared twice with pre-immune rabbit serum plus protein A beads (Gibco-BRL). Affinity-purified antibodies or preimmune serum was then added, and the immunoprecipitation was performed with protein A beads, with the use of NP-40 lysis buffer for the washes.

- 5 Immunoblots were performed with affinity purified Ab1 or Ab2 by either of two chemiluminescence based protocols. In the first protocol (used in Figures 1, 3, and 5) samples were resolved on 15 percent or 12 percent SDS-polyacrylamide gels (F. M. Ausubel et al., *supra*) and transferred to Magnagraph nylon membranes (MSI) by electroblotting. Blots were developed with the use of an alkaline phosphatase conjugated
- 10 donkey anti-rabbit IgG secondary antibody and Lumi-Phos 530 (Boehringer Mannheim) under recommended conditions. In the second protocol (used in FIGURE 8), samples were transferred to nitrocellulose filters (Schleicher and Schuell), and blots were developed using ECL reagents (Amersham) as recommended. The secondary antibody in this case was horseradish peroxidase conjugated goat anti-rabbit IgG (Jackson I-
- 15 mmunoResearch). Lanes contain protein from induced untransfected S2 cells (lanes 1 and 13), transfected S2 cells induced to express *hh* (lanes 2 and 14), imaginal discs (lanes 3 and 15), wild type embryos (lanes 6 and 18), and *in vitro* translations of synthetic *h* mRNA both in the presence (lanes 5 and 17) and absence of microsomes (lanes 4 and 16).
- 20 cDNAs encoding various *hh* protein species were cloned into the pMK33 vector, which allows for inducible expression under metallothionein promoter control (M. R. Koelle et al., *Cell* 67:59,1991). Stable S2 cell lines were made by transfection of the *hh*/pMK33 plasmids with constant selection for hygromycin resistance. Proteins were expressed by plating a log phase culture of cells diluted to 0.1 A<sub>595</sub> units, waiting 48 hours, inducing
- 25 with CuSO<sub>4</sub> at 0.2 mM final concentration, and harvesting the cells and/or supernatant 24 hours later. Cell samples for immunoblotting were made by adding 10 volumes of 1X SDS PAGE loading buffer to pelleted cells.

- 62 -

*In vitro* translations were performed with the use of the TNT coupled transcription-translation system (Promega). <sup>35</sup>S methionine (DuPont NEN) was used for detection by autoradiography. In the heparin binding experiment *in vitro* translation lysate with microsomes that produce wild-type *hh* protein was added to heparin agarose (Sigma) or  
 5 Sepharose CL-4B (Pharmacia) beads pre-equilibrated with heparin binding buffer (HBB; 20 mM Tris (7.4), 150 mM NaCl, 0.1 percent Triton X-100). Samples were incubated at 4° C for four hours with gentle rocking. After pelleting the beads, supernatants in some samples were analyzed (lanes 2 and 4). The beads were then washed 5 times with chilled HBB and samples (lanes 3 and 5) were subsequently eluted at 80° C for 10 minutes in  
 10 SDS PAGE loading buffer (F. M. Ausubel et al., *supra*).

Embryos from the wild-type Canton-S line and from the matings, *hshh/hshh* or *hshh* H329A/*hshh* H329A X *y*; *Sco/CyO*, *enlacZ11::wg* (Kassis, et al., *Proc. Natl. Acad. Sci. U.S.A.* 89: 1919, 1992), were collected 0 to 16 hours after egg laying (AEL) at 25° C. They were heat shocked for 30 minutes at 37° C and allowed to recover for 1 hour at 25°  
 15 C. Embryos in FIGURE 1 (Canton-S) were collected 4 to 8 hours AEL at 25° C. In preparation for immunoblotting, all embryos were dechorionated in 2.6 percent sodium hypochlorite and homogenized in 10 volumes of 1X SDS PAGE loading buffer.

Multiple species were detected and minor cross reactive bands are seen in most samples including extracts of induced untransfected S2 cells (lanes 1 and 13). One of these bands  
 20 (occurring in both panels) co-migrates with U (at 39 kD) and is particularly abundant in lane 6 of FIGURE 1 (A).

FIGURES 1 (B) and (D) are blots of samples immunoprecipitated with Ab1 (B, lanes 7-9), Ab2 (D, lanes 19-21), or pre-immune serum (B, lanes 10-12 and D, lanes 22-24). Detection was with biotinylated derivatives of Ab1 (B) and Ab2 (D). Samples used were:  
 25 induced untransfected S2 cells, lanes 7, 10, 19 and 22; transfected S2 cells induced to express *hh*, lanes 8, 11, 20 and 23; and embryos, lanes 9, 12, 21 and 24. For either antibody, *hh* protein fragments were specifically immunoprecipitated from *hh* expressing

- 63 -

cells and embryos, but not from untransfected cells. (E) In the schematic diagram, cleavage sites are denoted by arrows. The cleavage site marked by the asterisk is inferred by identification of only one cleavage product and may therefore occur at another location within the C fragment. The first two columns to the right of the diagram indicate the reactivity of Ab1 and Ab2 to each *hh* fragment. The other columns indicate the presence (+) or absence (-) of each *hh* fragment in the various samples. Parentheses around F and N<sub>SS</sub> indicate that these species are detected in *in vitro* translation reactions but not *in vivo*.

The 46kD species was detected from *in vitro* translation extracts by Ab1 and Ab2 (FIGURE 1, lanes 4 and 16), and was partially converted to a species of 39 kD (U) when translation occurred in the presence of microsomes (FIGURE 1, lanes 5 and 17). A 39 kD species co-migrating with U is also present in extracts from all *in vivo* sources, but none of these extracts contain detectable levels of F. U represents the signal-cleaved form of F; signal cleavage thus appears to be relatively inefficient *in vitro*, as reported previously, (J. J. Lee, *et al.*, *Cell*, 71:33, 1992), but is highly efficient *in vivo*. To confirm that signal cleavage indeed is occurring at this unusual internal location, a mutation that changes residue S<sub>84</sub> to N at the predicted signal cleavage site was introduced. This mutation prevented conversion by microsomes of F to U and also produced a species that comigrated with F upon transfection into cultured S2 cells. The effects of independently mutating the two methionine codons present upstream of the signal sequence were also examined. *In vitro* translation of the sequence in which the first methionine is removed produces a protein species intermediate in mobility between F and U, and this species is converted to a species that comigrates with U in the presence of microsomes or when produced *in vivo*. Alteration of the second methionine codon caused no change in the electrophoretic mobility of *Hh* protein produced *in vivo* or *in vitro*.

Smaller species of *Hh* proteins from *in vivo* sources have been reported previously (T. Tabata and T. B. Kornberg, *Cell* 76: 89, 1994). The latter study examined not endogenous proteins, but proteins induced to express at high levels from exogenously

- 64 -

introduced constructs. The antibody used did not distinguish epitopes from distinct portions of the molecule.

In addition to signal cleavage, a further cleavage of the U precursor is responsible for generating other forms of *hh* protein observed *in vivo*. This was deduced from the observation that Ab1 and Ab2 both detected the U (uncleaved) species, but also interacted individually with smaller protein species expressed endogenously in embryos and imaginal discs or with species expressed upon introduction of the *hh* gene into S2 cells. Ab1 thus interacts with a 19kD species from all of these tissues (FIGURE 1, lanes 2, 3, 6, 8, 9), while Ab2 interacts with a 25 kD species and a 16 kD species (FIGURE 1, lanes 14, 15, 18, 20, 21). The 19 kD species hereafter is referred to as N (N-terminal fragment), the 25 kD species as C (C-terminal fragment) and the 16 kD species as C<sup>\*</sup>; these species represent the major forms of endogenous *hh* protein present *in vivo*.

The proposed cleavages by which these species arise are shown schematically in the bottom portion of FIGURE 1. The N and C species are uniquely detected by Ab1 and Ab2, respectively, and the sum of the relative masses of the two smaller species is roughly equivalent to the relative mass of U. The electrophoretic mobilities of the F and U species are somewhat at variance with their predicted relative masses (52.1 kD and 43.3 kD, respectively). The identities of these species were confirmed by *in vitro* translation of a variety of *hedgehog* open reading frames modified to contain different extents of sequence at the NH<sub>2</sub>- or COOH- terminus, and by insertion of epitope tags. The migration anomalies appear to be associated with protein species in which sequences from both the NH<sub>2</sub>- and COOH-terminal fragments are simultaneously present. The mobilities of the NH<sub>2</sub>- and COOH-terminal fragments, in contrast, correspond to relative masses (19 kD and 25 kD, respectively) that sum to yield 44 kD, roughly equivalent to the expected relative mass of U.

A simple mechanism that could account for the derivation of the two smaller species therefore would be a single internal cleavage of the U precursor. Processing of the *hh*

- 65 -

protein when translated *in vitro* also yields a 25 kD species (C; lanes 16 and 17) and either a 29 kD or 19 kD (N) species (lanes 4 and 5). The 19 kD species comigrates with N, and its formation depends upon the presence of microsomes, consistent with the proposal that N derives from F by signal cleavage and a further internal cleavage. The overall pathway for formation of the predominant forms of *hh* protein observed *in vivo* thus appears to involve signal cleavage of F to generate U. U is then cleaved internally to form N and C, which are the predominant forms found *in vivo*. Further processing of the 25 kD C species might then generate the 16 kD C\* species, but whether this processing is a single cleavage event or not is not clear since Ab2 does not recognize the smaller 9 kD fragment that would result. The processing of C to generate C\* appears to occur with greater efficiency in imaginal discs as compared to embryos (compare lanes 15 and 18); this may be caused by the more extended mass isolation procedure of imaginal discs (O. M. Eugene, *et al.*, *Tissue Culture Assn. Man.*, 5: 1055, 1979).

## EXAMPLE 2

### AUTO-PROTEOLYSIS OF THE HEDGEHOG PROTEIN

The comigration of endogenous and *in vitro*-generated *hh* protein species suggested that *in vitro* processing is similar to that observed *in vivo*. FIGURE 2 shows limited sequence similarity between *hh* proteins and serine proteinases. *hh* protein sequences are aligned to residues 323 to 329 of the *D. melanogaster* protein and numbered as positions 1 to 7 (group A). Conserved *hh* residues are in bold letters. The catalytic histidines (A. J. Barrett, in *Proteinase inhibitors* A. J. Barrett, G. Salvesen, Eds. (Elsevier, Amsterdam, 1986) pp. 3-22) of mammalian serine proteinases (group B) are aligned to the invariant histidine at position 7 in *Hh* proteins. Abbreviations are as follows: C-*Shh*, chicken *Sonic hh* (R. D. Riddle, *et al.*, *Cell* 75: 1401, 1993); M-*Shh*, mouse *Sonic hh* (Y. Echelard *et al.*, *Cell* 75: 1417, 1993) (identical to *Hhg*-1; R *vhh*-1, rat *vhh*-1 (H. Roelink *et al.*, *Cell* 76: 761, 1994); Z-*Shh*, zebrafish *Sonic hh* (S. Krauss, *et al.*, *Cell* 75: 1431, 1993) (identical to *shh*) and zebrafish *vhh*-1, (H. Roelink *et al.*, *supra*); *twhh*, no other abbreviation; M-*Dhh*, mouse *Desert hh* (Y. Echelard *et al.*, *Cell* 75: 1417, 1993); M-*Ihh*,

- 66 -

mouse *Indian hh* (Y. Echelard et al., *supra*); CHT, bovine chymotrypsin; TRP, bovine trypsin; ELA, porcine elastase; UKH, human urokinase; C1R, human complement factor 1R; C1S, human complement factor 1S; MCP, rat mast cell protease; FAX, human blood clotting factor X; TPA, human tissue plasminogen activator.

- 5 Figure 2 shows that a seven residue region of *hh* coding sequence (residues 323 to 329 in the *Drosophila* protein) displays some similarity to the sequences of serine proteases. This region lies approximately two thirds of the distance from the signal cleavage site to the carboxy-terminus, and includes Thr and His, residues (positions 4 and 7 in FIGURE 2) that are invariant among all *hh* sequences from all species. In the serine proteases, this  
10 conserved sequence contains an invariant His that acts as a general base in catalysis (A. J. Barrett, in *Proteinase inhibitors* A. J. Barrett, G. Salvesen, Eds. Elsevier, Amsterdam, 1986, pp. 3-22).

To determine whether this invariant His residue in the *hh* protein indeed plays a role in auto-proteolysis, two proteins from *E. coli* were purified: one carried the wild type  
15 sequence and the other a substitution of an Ala codon for the His codon at position 329 (H329A). Both of these proteins were engineered to contain a hexa-histidine tag at the amino terminus fused to *Drosophila* sequences extending from a residue just before the signal cleavage site to the carboxy-terminus (residues 83 to 471; the wild type form of this protein is referred to as His<sub>6</sub>-U). Both proteins were extensively purified under  
20 denaturing conditions using a Ni<sup>++</sup>-chelating matrix. FIGURE 3(A) is a coomassie blue stained polyacrylamide gel that shows the production and purification of His<sub>6</sub>-U and His<sub>6</sub>-U<sub>H329A</sub> proteins from *E. coli*. Samples were molecular weight markers (lanes 1 and 2); lysates of *E. coli* cells carrying the His<sub>6</sub>-U expression construct without (lane 3) and with (lane 4) induction by IPTG; purified His<sub>6</sub>-U protein (lane 5); lysates of *E. coli* cells  
25 that carry the His<sub>6</sub>-U<sub>H329A</sub> expression construct without (lane 6) and with (lane 7) induction by IPTG; purified His<sub>6</sub>-U<sub>H329A</sub> protein (lane 8). Purified proteins were essentially homogeneous except for several minor species of lower relative mass; these species are endogenous breakdown products of the full-length proteins since they were

- 67 -

absent in uninduced extracts and were detectable with *hh* antibodies. FIGURE 3 (B) is an immunoblot detected with Ab2 showing transfected S2 cells induced to express *hh* (lane 1); His<sub>6</sub>-U and His<sub>6</sub>-U<sub>H329A</sub> proteins incubated in cleavage reaction buffer for 0 hours (lanes 2 and 5), for 20 hours (lanes 3 and 6), and for 20 hours in the presence of 20 mM TAME (a serine protease inhibitor) (lanes 4 and 7). Upon incubation the His<sub>6</sub>-U, but not the His<sub>6</sub>-U<sub>H329A</sub> protein, released a fragment presumed to be C on the basis of reactivity with Ab2 and co-migration with C produced in S2 cells. Release of C (lane 3) was only partially inhibited by TAME.

Preliminary proteinase inhibitor studies have been performed on *in vitro* translated *Hh* protein by adding various inhibitors at the start of the translation reaction. These studies have been complicated by the fact that numerous protease inhibitors lower or block translation efficiency. In some cases the effectiveness of an inhibitor was assayed by determining if addition of an inhibitor to a completed translation reaction will inhibit the self-processing that normally continues to occur. At this time we can only state the following with certainty: (i) the serine protease inhibitor TAME (-p-toluenesulfonyl-L-arginine methyl ester) inhibits auto-proteolysis of *in-vitro* translated *Hh* protein; (ii) soybean trypsin inhibitor, a<sub>1</sub> anti-trypsin, aprotinin, leupeptin, and E-64 do not block auto-proteolysis of translated *Hh* protein; and (iii) TAME partially inhibits auto-proteolysis of purified His<sub>6</sub>-U protein (FIGURE 3, panel B).

As seen in FIGURE 3B, upon dilution of denaturant the wild type protein but not the H329A mutant protein released a 25 kD species detectable by Ab2 and identical in mobility with the C species produced from *in vitro* translations and various *in vivo* sources. This cleavage was also observed when the wild type protein was purified and renatured by other protocols and cleaved under distinct conditions. Plasmids encoding the His<sub>6</sub>-U and His<sub>6</sub>-U<sub>H329A</sub> proteins were generated by inserting sequences corresponding to residues 83 to 471 from the wild-type or *hh* H329A ORF into the pRSETB expression vector (Invitrogen). Proteins were induced in BL21(DE3)/pLysS *E. coli* cells as described (F. M. Ausubel et al., *supra*). The basic purification was performed on

- 68 -

Ni-NTA agarose beads (Qiagen) by a denaturing protocol with the use of 6 M guanidinium HCl and 8 M urea essentially as recommended (a detailed protocol of exact conditions used is available upon request). Washes contained 0.2 percent Tween 20 and 5 mM b-mercaptoethanol. The final wash buffer was: 6 M urea, 100 mM Tris, 500 mM NaCl, 20 percent glycerol, (pH 7.4). Elutions were with the final wash buffer containing 250 mM imidazole. In vitro cleavage reactions were performed by incubating the purified protein (diluted 1:30 in the final mix) in cleavage buffer [50 mM Tris, 500 mM NaCl, 5 percent glycerol, 0.2% Triton X-100, 50 mM DTT, (pH 7.4)]. To isolate soluble full-length His<sub>6</sub>-U protein free from denaturants or detergents, additional steps were taken (this refers to the other renaturation protocols mentioned in the text). Full-length protein from the eluate described above was further purified from breakdown products by precipitation, by urea removal through dialysis. The precipitate was then re-solubilized in a buffer containing guanidinium HCl and loaded onto another Ni-NTA agarose column. After washing as described, the protein was re-folded (while attached to the beads) by gradual dilution of urea (from 6M to 0.5M) with dilution buffer [(100 mM Tris, 500 mM NaCl, 20 percent glycerol, (pH 7.4)] over an 8 hour period at 4° C. The protein was eluted with dilution buffer containing 250 mM imidazole and 0.5M urea. The eluate was dialyzed in 100 mM Tris, 150 mM NaCl, 10 percent glycerol, (pH 7.4) at 4° C and stored at -70° C.

20

### EXAMPLE 3

#### MAPPING THE AUTO-PROTEOLYTIC FUNCTIONS OF *hh*

To more precisely define the domain of the *hh* protein responsible for this auto-proteolytic event, the effects of several distinct types of mutations upon *in vitro* processing were examined. The most informative mutation was a deletion that removes residues 89 to 254 ( $\Delta 89-254$ ), which together constitute most of the amino acids within the portion of the molecule presumed to form the N fragment. *In vitro* translations of wild-type and mutant *Hh* proteins from *Drosophila* (FIGURES 4 A-C) and zebrafish

- 69 -

(FIGURE 4D) are shown. The locations of mutations and cleavage sites (arrows) in these proteins are schematically illustrated (FIGURE 4E). In the *Drosophila* protein (FIGURES 4A, B, and C), auto-proteolysis is blocked or severely inhibited by several mutations in the COOH-terminus (H329A, 294 trunc, 410 trunc, flu408 and 456 trunc),  
5 but is unaffected by a large deletion ( $\Delta$ 89-254) or insertion of a flu-tag epitope trimer (flu227) in the NH<sub>2</sub>-terminus. Auto-proteolysis thus depends primarily on residues within the C fragment (sequences to the right of the cleavage site in the diagram below; see FIGURE 1). Furthermore, the H329A/flu227 double mutant is not cleaved by wild-type protein in a mixing experiment (lane 11), suggesting an intramolecular mechanism for  
10 auto-proteolysis. *Hh* proteins encoded by the zebrafish genes *twhh* and *shh* display a pattern of processing (D) similar to that of the *Drosophila* protein although the NH<sub>2</sub>-terminal fragment of each zebrafish protein (23 kD for *twhh* and 22 kD for *shh*) has a lower apparent mass than the COOH-terminal fragment (25 kD for *twhh* and *shh*). This is the result of a shorter stretch of residues that precedes the signal sequences as  
15 compared to the *Drosophila* protein. Processing is blocked by H273A and H270A mutations in *twhh* and *shh* proteins respectively (analogous to the H329A mutation in the *Drosophila* protein), which suggests an auto-proteolytic processing mechanism is used similar to that observed for the *Drosophila* protein.

*In vitro* translations were performed with the use of the TNT coupled  
20 transcription-translation system (Promega). <sup>35</sup>S methionine (DuPont NEN) was used for detection by autoradiography. In the heparin binding experiment (FIGURE 8C), *in vitro* translation lysate with microsomes that produce wild-type *Hh* protein was added to heparin agarose (Sigma) or Sepharose CL-4B (Pharmacia) beads pre-equilibrated with heparin binding buffer (HBB; 20 mM Tris (7.4), 150 mM NaCl, 0.1 percent Triton  
25 X-100). Samples were incubated at 4° C for four hours with gentle rocking. After pelleting the beads, supernatants in some samples were analyzed (lanes 2 and 4). The beads were then washed 5 times with chilled HBB and samples (lanes 3 and 5) were subsequently eluted at 80° C for 10 minutes in SDS PAGE loading buffer (F. M. Ausubel et al., *supra*).

- 70 -

All mutations in the *hh* gene were generated in the plasmid pF1 (J. J. Lee, *et al.*, *supra*). Mutations in the zebrafish *twhh* and *shh* genes were generated with the original cDNA clones as described (Ekker, *et al.*, *Current Biology*, 5(8): 944,1995). All point mutations were generated with the use of recombinant circle PCR (D. H. Jones and S. C. Winistorfer, *Biotechniques* 12: 528, 1992). The flu408 and flu227 mutations were generated by inserting a trimer of the influenza hemagglutinin antigen (42 residues for flu408 and 43 residues for flu227) into the AlwN I and Bgl I sites present in the *hh* ORF (nucleotide positions 1604 and 1058 respectively) (J. J. Lee, *et al.*, *supra*). The  $\Delta 89-254$  mutation was generated by removing sequences between the EcoN I site (644) and the Pml I site (1145). The 294 trunc mutation was generated by removing sequences between the Acc I site (1265) and the Xcm I site (1792). The 410 trunc mutation was previously generated and identified as *Hh*<sub>410</sub> (J. J. Lee, *et al.*, *supra*). To map the mutation in the *hh*<sup>13E</sup> allele (base change C<sub>1756</sub> to A; coding change Ty<sub>557</sub> to STOP), DNA isolated from *hh*<sup>13E</sup>/TM3 was used to seed PCR reactions generating regions of the *hh* ORF and flanking sequences, which were subcloned into Bluescript KSM (Stratagene). Six clones each, derived from two different PCR amplifications were sequenced.

As seen in lanes 1 and 2 of FIGURE 4A, this construct generates a full length species of a mobility corresponding to the expected relative mass of 33 kD, and two cleaved products whose apparent relative masses (25 and 9 kD) sum to give the relative mass of the larger species. The smaller of the cleaved products will occasionally migrate as two bands as seen in Fig 4A. We have chosen the lower of the two bands between the 14.3-kD and 6.2-kD markers for our molecular weight measurement. The larger of the two cleaved products comigrates with the C species produced from the wild type protein, suggesting that the  $\Delta 89-254$  *hh* protein contains the residues normally present in C and all of the determinants required for auto-proteolysis, including the normal cleavage site; most of the residues within N are dispensable for auto-proteolytic activity.

In contrast, lesions affecting residues presumed to lie within C block auto-proteolysis *in vitro*. All mutations tested by *in vitro* translation were also examined in S2 cells by

- 71 -

immunoblotting. In all cases the patterns of cleavage in S2 cells were identical to those observed in translations except that C\* was always present whenever C was formed. The former fragment was not observed in translations. These include the H329A mutation described above, a mutation that inserts an influenza virus epitope between residues 408  
5 and 409 (flu408), and three mutations that cause premature termination of the protein at the carboxy terminus. The two most severe truncations, 294 trunc and 410 trunc, are mutations generated *in vitro*. They cause a loss of 177 and 61 residues, respectively, from the carboxyl-terminus of the protein, and neither undergoes proteolysis. The 456 trunc *hh* protein is like that encoded by the EMS-induced *hh*<sup>13E</sup> mutant allele, which  
10 results in the loss of 15 residues from the carboxy-terminus of the protein. This protein undergoes auto-proteolysis, as demonstrated by the appearance of a 24 kD band in place of C, but the efficiency of the reaction is much impaired *in vitro* (FIGURE 4B). Auto-proteolysis of the *hh* protein relies mainly upon residues within C; deletion or alteration of residues within this domain is associated with reduced efficiency of processing, and  
15 one such deletion appears to be the cause of the *hh*<sup>13E</sup> mutation.

The sequence homology and auto-proteolytic function of the full length *hh* protein suggested the possibility that F or the C fragment is a sequence-specific protease. As a first step in clarifying the mechanism of auto-proteolysis, an influenza virus epitope tag was introduced into the N-terminus of a *hh* open reading frame that also carried a H329A  
20 mutation. FIGURE 4C shows that the insertion of the epitope tag alone does not interfere with auto-proteolysis (lane 9), and yields a normal C fragment and an N fragment of increased relative mass (compare to wild type in lane 12). The protein carrying both mutations does not undergo proteolysis (lane 10), and since the epitope-tagged N fragment migrates differently from N, this double mutant provides an ideal substrate to  
25 look for intermolecular cleavage upon mixture with a wild type sequence. Lane 11 shows that in such a mixture, although normal N is formed, no tagged N can be detected. Thus, in this experiment, no appreciable intermolecular cleavage occurs. We also failed to detect intermolecular cleavage in the following two experiments: (i) co-transfection of wild type and 410 trunc sequences into S2 cells (the cleaved 410 trunc protein would

- 72 -

yield a smaller and therefore identifiable form of C); (ii) mixing of excess unlabelled, purified His<sub>6</sub>-U protein with labelled, *in vitro* translated H329A mutant protein. Thus, although an intermolecular mechanism for regulation of auto-proteolysis or for cleavage of other proteins can not be ruled out, the current evidence suggests that cleavage of the  
5 *hh* protein occurs predominantly by an intramolecular mechanism.

The *hh* gene has been broadly conserved in evolution, with single homologues unidentified in a wide variety of invertebrate species and multiple distinct homologues in each of several vertebrate species (Y. Echelard et al., *Cell* 75: 1417, 1993; S. Krauss, et al., *Cell* 75: 1431, 1993; H. Roelink et al., *Cell*, *supra*). As seen in FIGURE 2, all of  
10 these coding sequences contain an invariant histidine and other conserved residues at a position corresponding to H329 in the *Drosophila* protein. In addition, the protein encoded by at least one of the mouse genes appears to be processed *in vivo* to yield two smaller species in a manner resembling the *in vivo* processing of the *Drosophila* protein. To determine whether auto-proteolysis may also play a role in vertebrates we examined  
15 the behavior of proteins encoded by two distinct *hh* homologues from the zebrafish, *twhh* and *shh*. FIGURE 4D demonstrates that when these sequences are translated *in vitro*, smaller species are generated whose relative masses sum to yield approximately the relative mass of the full length protein (lanes 1 and 3). As seen in lanes 2 and 4, this cleavage reaction is blocked by substitution of Ala codons for the His codons at positions  
20 corresponding to H329 in *Drosophila* (see FIGURE 2). Vertebrate *hh* proteins thus appear to be processed by a similar mechanism as the *Drosophila* protein.

#### EXAMPLE 4

#### ROLE OF AUTO-PROTEOLYSIS IN EMBRYOS

Numerous functions for the *hh* gene have been described in *Drosophila*. At the  
25 morphological level these include a role in patterning of larval cuticular structures and adult structures such as the eye and appendages (C. Nüsslein-Volhard and E. Wieschaus,

- 73 -

*Nature* 287: 795, 1980; and J. Mohler, *Genetics* 120: 1061, 1988).; the mechanistic basis for these morphological effects involves signaling for maintenance or induction of gene expression in embryos and imaginal discs (J. J. Lee, *supra*; T. Tabata and T. B. Kornberg, *Cell* 76: 89, 1994; and K. Basler and G. Struhl, *Nature* 368: 208, 1994). To

5 ascertain the importance of auto-proteolysis for these functions, the H329A mutant gene under control of the hsp 70 promoter was introduced by P element-mediated transformation into the *Drosophila* germline. The *hshh* H329A construct was made identically to the *hshh* construct with the use of a *hh* ORF fragment containing the H329A mutation. Transgenic flies were generated from a  $y^1 w^{1118}$  parental strain using standard methods of

10 P element mediated transformation (A. C. Spradling and G. M. Rubin, *Science* 218: 341 1982). A line, HA3, carrying the *hshh* H329A P element on the second chromosome was maintained as a homozygous stock. To assay for expansion of *wg* stripes, embryos collected at 4 to 6 hours after egg laying (AEL) at 25° C were subjected to the following heat shock protocols prior to fixation. Embryos receiving single shocks (10 or 30 minutes

15 at 37° C) were allowed to recover for 1 hour at 25° C. Embryos receiving double shocks (two 10 minute or two 30 minute shocks at 37° C) were allowed to recover 90 minutes after the first shock and 40 minutes after the second (Both recoveries were at 25° C. The double 30 minute protocol was as previously described, (S. Krauss, *supra*). *In situ* hybridizations were performed as described (D. Tautz, *Chromosoma* 98: 81, 1989) using

20 a *wg* specific probe (D. T. Chang et al., *supra*). Embryos assayed for cuticle phenotype were heat shocked 6 to 8 hours AEL for 30 minutes at 37° C, allowed to develop at 25° C for 36 hours and then processed and mounted as described (M. Ashburner, *Drosophila: A Laboratory Manual*, Cold Spring Harbor Laboratory Press, New York, 1989). Immunolocalizations (single or double stains) were performed as described. With the use

25 of affinity purified Ab1 or Ab2 for the primary antibody and alkaline phosphatase (AP) or horseradish peroxidase (HRP) conjugated anti rabbit or mouse IgG (Jackson Immuno-research) for the secondary. Embryos from a *hh*<sup>13E</sup>/TM3 *ftz-lacZ* (the balancer chromosome was from the Bloomington Stock Center, strain 3218) stock homozygous for the *hh*<sup>13E</sup> allele were identified by the lack of staining with an anti b-galactosidase

30 antibody (Promega) in a double stain with Ab2 (FIGURE 9, panel D). Staining in

- 74 -

FIGURE 9, panels B and C were performed formaldehyde fixed Canton-S embryos with the use of an AP conjugated anti-rabbit IgG secondary. Although standard formaldehyde fixation was generally used, heat and acid-formaldehyde fixation also gave similar results. GST fusion proteins containing either residues 83 to 160 or 300 to 391 from the

5 *Hh* protein were expressed in *E. coli*, purified as recommended (F. M. Ausubel et al., *supra*), and used to immunize rabbits by standard methods. The antibodies were affinity purified on a column of His<sub>6</sub>-U protein (Harlow and Lane, *supra*) linked to Affi-Gel 10 beads (Bio-Rad). The purification was performed as described (Harlow and Lane, *supra*) except that the acid and base elutions contained 10 percent dioxane. Biotinylated *hh*

10 antibodies were prepared by purifying the rabbit antisera over a protein A column, followed by biotinylation with the use of the Immunoprobe biotinylation kit (Sigma). Immunoprecipitations were performed as described (Harlow and Lane, *supra*) with the use of cold RIPA lysis buffer containing 0.25 mM PMSF and 5 mM EDTA for tissue homogenization. Lysates were precleared twice with pre-immune rabbit serum plus

15 protein A beads (Gibco BRL). Affinity purified antibodies or pre-immune serum was then added, and the immunoprecipitation was performed with protein A beads, with the use of NP-40 lysis buffer for the washes.

FIGURE 5 (A) and (B) are immunoblots developed with the use of Ab1 and Ab2 antibodies respectively. Lanes 1 and 6, induced untransfected S2 cells; lanes 2 and 7,

20 transfected S2 cells induced to express *hh*; lanes 3 and 8, heat shocked wild-type embryos; lanes 4 and 9, heat shocked *hshh* embryos; lanes 5 and 10, heat shocked *hshh* H329A embryos. In heat shocked *hshh* embryos, the wild-type *Hh* protein is both induced and properly processed to generate the U, N, C and C\* species seen in other expression contexts. In contrast, the H329A is induced but not appreciably processed in

25 *hshh* H329A embryos (the low levels of processed species in lanes 5 and 10 are probably from endogenous *hh* expression since they are seen at identical levels in heat shocked wild-type embryos in lanes 3 and 8).

- 75 -

FIGURE 5 shows that heat shock induction results in the formation of an abundant species that corresponds to U based on its mobility and its interaction with Ab1 and Ab2 (lanes 5 and 10). In contrast, induction of wild type *hh* protein using a similar construct resulted in similar levels of the N and C processed products (lanes 4 and 9), with very little uncleaved U. Thus, as observed *in vitro* and in S2 cells, the H329A mutation in embryos appears to greatly reduce the efficiency of auto-proteolytic cleavage of the *hh* protein.

In FIGURE 6, the embryonic distribution of *wingless* (*wg*) RNA as revealed by in situ hybridization is shown in FIGURE 6 (A) wild-type (homozygous *y<sup>1</sup> w<sup>1118</sup>*), (B) *hshh*, and (C) *hshh* H329A embryos that were exposed to two 10 minute heat shocks separated by a 90-minute recovery period. Wild-type embryos showed little change in *wg* expression, whereas the wild-type protein and, to a lesser extent, the H329A protein each induced ectopic *wg* expression (Table 1). Panels (D), (E), and (F) show the dorsal surfaces of *y<sup>1</sup> w<sup>1118</sup>*, *hshh*, and *hshh* H329A larvae, respectively, at the level of the fourth abdominal segment. These larvae were shocked for 30 minutes as embryos and allowed to complete embryogenesis. Cuticle cell types (1°, 2°, 3°, and 4°) are labeled as described (J. Heemskerk and S. DiNardo, *Cell* 76: 449, 1994). Note the expansion of 2° cell types (naked cuticle) at the expense of 3° and some 4° types in the *hshh* embryo (E) under conditions where the phenotype of *hshh* H329A embryos (F) is identical to that of control embryos (D).

Perhaps the earliest known requirement for *Hh* protein is in maintenance of an adjacent stripe of *wingless* (*wg*) gene expression in each embryonic segment (A. Martinez Arias, *et al.*, *Development* 103: 157, 1988; and S. DiNardo, *et al.*, *Nature* 332: 604, 1988). This requirement is deduced from the loss of *wg* expression when *hh* function is absent; in addition, the ubiquitous expression of wild-type *Hh* protein induces expansion of the domain of *wg* gene expression (P. W. Ingham, *Nature* 366: 560, 1993). The effects of the H329A mutation upon *wg* expansion were examined by heat shocking embryos carrying the H329A mutant construct in parallel with embryos containing the wild-type construct.

- 76 -

Although the H329A mutant protein is able to induce some expansion of the *wg* domain, the efficiency of this activity is impaired relative to that of the wild-type protein (FIGURE 6, B and C; Table 1). The difference in efficiency ranges nearly as high as threefold depending upon the heat shock regime, and these results suggest that a  
 5   uto-proteolysis of the *Hh* protein is important for optimal activity in embryonic signaling to induce *wg* expression.

**TABLE 1****Wild-type and mutant *hh* activity in embryonic induction of *wg* expression\***

	minutes of heat shock			
	10	30	10/10	30/30
<i>hshh</i>	1.0 ± 0.3 (93)	1.5 ± 0.6 (120)	2.9 ± 0.3 (41)	2.8 ± 0.4 (54)
<i>hshh</i> H329A	0.7 ± 0.5 (190)	0.9 ± 0.4 (111)	1.1 ± 0.4 (145)	1.9 ± 0.5 (93)

\* Expansion of *wg* expression beyond wild-type controls is given as average number of  
 15   cell diameters ± standard deviation with number of embryos scored in parentheses.

The effects of *Hh* protein on the patterning of cuticular structures are most clearly visible on the dorsal surface of the larva, where four distinctive cell types can be identified in each parasegment. These cell types have been designated 1°, 2°, 3°, and 4°, from anterior to posterior, with *hh* transcription occurring in precursors of the 1° cells (J.  
 20   Heemskerk and S. DiNardo, *supra*). Differentiation of the first three cell types was shown to be dependent upon *hh* gene function, and it has been proposed that the fates of these cells are determined by the concentration of *Hh* protein, with highest concentra-

- 77 -

tions producing the 1° fate, intermediate concentrations producing the 2° fate, and the lowest concentrations producing the 3° fate (J. Heemskerk and S. DiNardo, *supra*). This proposal was supported by observations that the most anterior cell types display the greatest sensitivity to a reduction of *hh* expression, and that all of the 3° and some of the 4° bristles are replaced by naked cuticle characteristic of the more anterior 2° cell type when *hh* is expressed ubiquitously at high levels. We have reproduced suppression 3° and some 4° fates by heat shock induction of embryos that carry our wild-type construct (FIGURE 6E), but find that the H329A mutant is unable to alter cell fates in the dorsal cuticle of the larva (FIGURE 6F). Auto-proteolysis, or perhaps some other function blocked by the H329A mutation, thus appears to be essential for the patterning influence of *Hh* protein upon the dorsal cuticle.

#### EXAMPLE 5

##### EFFECTS OF THE H329A MUTATION UPON SIGNALING IN IMAGINAL DISCS

Studies of H329A mutant protein were extended to the function to the patterning of adult structures and signaling within imaginal discs. In the eye imaginal disc *hh* function is required for appropriate development of pattern (J. Mohler, *Genetics* 120: 1061, 1988; J. J. Lee, *supra*; and J. Mohler and K. Vani, *supra*) and more recently has been shown to control progression of a wave of differentiation via induction of *decapentaplegic* (*dpp*) gene expression in the morphogenetic furrow of the eye (U. Heberlein, *et al.*, *Cell* 75: 913, 1993; and C. Ma, *et al.*, *Cell* 75: 927, 1993). In leg and wing discs, ectopic expression of *hh* has also been shown to yield pattern duplications and defects and is associated with induction of ectopic expression of other signaling molecules normally expressed in a zone along the anterior/posterior compartment boundary (T. Tabata and T. B. Kornberg, *Cell* 76: 89, 1994; and K. Basler and G. Struhl, *Nature* 368: 208, 1994).

- 78 -

For studies of signaling in imaginal discs, a thermal cycler was utilized to subject larvae carrying heat shock-inducible *hh* constructs to successive rounds of heat shock and recovery. The effects of temperature cycling upon expression of *dpp* and *wg* in imaginal discs was examined by monitoring  $\beta$ -galactosidase expression from a reporter gene

5 carrying *dpp* promoter sequences or from an enhancer detector P element inserted in the *wg* gene. In FIGURE 7, X-gal staining was used to follow expression of *wg* FIGURE 7 (A-C) or *dpp* FIGURE 7 (D-L) in imaginal discs of late third-instar larvae that carry *wg-lacZ* or *dpp-lacZ* reporter genes. Leg (A-F), wing (G-I) and eye-antennal discs (J-L) from control larvae (A, D, G, J), larvae carrying the *hshh* transgene (B, E, H, K) and

10 larvae carrying the *hshh* H329A transgene (C, F, I, L) are displayed. In all panels anterior is to the left. Arrows highlight the following features: an ectopic patch of *dpp* expression in the anterior compartment of wing discs in *hshh* H329A larvae (I); and an ectopic band of *dpp* expression in eye portion of the eye-antennal disc anterior to the morphogenetic furrow (marked by the other band of *dpp* expression more posteriorly) in *hshh* larvae (K).

15 Expansion into the anterior compartment of *wg* expression in leg discs, and *dpp* expression in leg and wing discs in *hshh* larvae is similar to that described for the ectopic expression of *hh*. Morphological changes in the anterior compartment of leg (B and E) and wing discs (H) were also as described (K. Basler and G. Struhl, *supra*). In contrast, discs from *hshh* H329A and control larvae showed very little change in *wg* and *dpp*

20 expression, even under prolonged heat shock conditions and morphological changes were never observed. (M-O) The eye phenotypes of adult control (M), *hshh* (N) and *hshh* H329A (O) flies that were shocked during larval development in a manner similar to that of the imaginal disc experiments above. Duplicated eye structures were observed in *hshh* flies, but never in *hshh* H329A flies. The arrow in (N) points to a thin strip of cuticle

25 between the two eye structures. Other deformities were also seen in *hshh* flies (for example, compare the thorax in N to M) .

Virgin female flies from the homozygous lines *hshh* (D. T. Chang et al., *Development*, 1994, in press), *hshh* H329A, and *y<sup>1</sup> w<sup>1118</sup>* were crossed to males from the homozygous BS3.0 line (bearing a P element *dpp* reporter construct on the 2nd chromosome, referred

- 79 -

- to as *dpp-lacZ*) (R. K. Blackman, *et al.*, *Development* 111: 657, 1991) or the line *y; Sco/CyO, enlacZ11::wg* (bearing a *wg* reporter P element enhancer trap on a second chromosome balancer; called *wg-lacZ*) (J. A. Kassis, *et al.*, *Proc. Natl. Acad. Sci. U.S.A.* 89: 1919, 1992). Progeny were grown at 25°C in aerated 0.5-ml microcentrifuge tubes
- 5 containing yeast paste until the late second instar or early third instar stage of larval development. The larvae were then cycled continuously at 37° C for 30 minutes followed by 25° C for 90 minutes in a Perkin-Elmer thermal cycler until they reached the late third instar stage. They were subsequently dissected and stained with X-gal as described (M. Ashburner, *supra*) or allowed to grow to adulthood for phenotypic analysis.
- 10 As shown in FIGURE 7A, *wg* expression normally occurs in a ventral sector of the leg disc along the anterior/posterior compartment boundary while *dpp* is expressed in the dorsal portion of the disc along this boundary (FIGURE 7D). Although thermal cycling of larvae carrying the wild-type *hh* gene produced abnormal leg disc morphology and extensive ectopic expression of both target genes, as previously reported for ectopic *hh*
- 15 expression (FIGURE 7B and E), the H329A construct produced little if any detectable difference in these patterns of expression (FIGURE 7, C and F). Ectopic *hh* expression in the wing disc also leads to morphological changes and expanded expression of *dpp* (compare FIGURE 7, G and H), but the H329A construct produced only an occasional small patch of anterior ectopic expression (FIGURE 7I).
- 20 Ubiquitous expression of wild-type *hh* also leads to ectopic expression of *dpp* in the eye-antennal disc (compare FIGURE 7, J and K). In the antennal portion of this disc the expansion of *dpp* expression resembles that observed in leg discs. In the eye portion of the disc *dpp* expression is observed at its normal location in the furrow; however, ectopic expression also occurs in the form of a second dorso-ventral band at a location somewhat
- 25 anterior to the furrow, thus giving the appearance of an eye disc with two morphogenetic furrows (FIGURE 7K). Indeed, in adults derived from temperature-cycled larvae that carry the wild-type *hh* construct, an apparently duplicated eye structure such as that in FIGURE 7N can be observed, with two eye structures separated by a thin strip of cuticle

- 80 -

(arrow). The H329A mutant protein, in contrast, did not induce expansion of *dpp* expression in either portion of the eye-antennal disc (FIGURE 7L), and does not induce eye duplications or cuticle defects in the adult (FIGURE 7O).

The experiments described thus far comprise multiple series of larvae subjected to two  
5 days of thermal cycling followed by immediate dissection for analysis of imaginal  
structures or further incubation at constant temperature for analysis of adult structures.  
Although the H329A protein appeared to have little activity in these experiments, the  
small patch of ectopic *dpp* expression induced in the wing disc (FIGURE 7I, arrow)  
suggested that some residual activity remained. This suggestion was borne out in a  
10 similar experiment involving three days of cycling prior to dissection: the H329A protein  
clearly displayed some *dpp*-inducing activity in this experiment, presumably as a result  
of the higher amounts of protein that accumulated during the longer cycling period. The  
wing in particular, but also other imaginal discs, displayed low and variable amounts of  
ectopic *dpp* expression. This expression in all cases was far less extensive than that  
15 observed for the wild-type construct examined in parallel; furthermore, morphological  
deformations of the imaginal discs, although quite common with the wild-type protein,  
were extremely rare with the H329A protein. Although its potency is greatly reduced  
relative to wild-type, the H329A protein retained at least some activity in early  
embryonic and imaginal disc induction of *wg* and *dpp* expression; in contrast, even under  
20 heat shock conditions far more severe than those required for effects by the wild-type  
protein, the H329A mutant remained completely inert with respect to the re-specification  
of cell fates in the dorsal cuticle of the larva.

- 81 -

**EXAMPLE 6**  
**DIFFERENTIAL RELEASE OF N AND C**  
**INTO CULTURED CELL SUPERNATANTS**

A puzzling feature of *hh* function is its apparent short-range action in settings such as embryonic and imaginal disc signaling to *wg* and *dpp*, and longer-range action in other settings, such as patterning of the dorsal larval cuticle. These observations and the existence of two major protein products *in vivo* prompted us to look for differences in the solubility or diffusibility of N and C expressed in S2 cultured cells. FIGURES 8 (A) and (B) are immunoblots of cell pellets (lane 1) or supernatants (lane 2) from transfected S2 cell cultures expressing *Hh* protein, developed with Ab1 (A) and Ab2 (B). Samples in each lane were from the same volume of resuspended total culture. Whereas N remained mostly associated with the cell pellet (compare lanes 1 and 2 in A), C was nearly quantitatively released into the supernatant (compare lanes 1 and 2 in B). U displayed partitioning properties in between those of N and C (A and B). (8C) demonstrates the heparin binding activity of various *Hh* protein species generated by *in vitro* translations with microsomes. Samples were: total translation mix (lane 1); supernatant after incubation with heparin agarose or agarose (control) beads (lanes 2 and 4); and material eluted from heparin agarose or agarose beads after washing (lanes 3 and 5). F, U, N<sub>SS</sub> and N fragments are depleted from reactions incubated with heparin agarose but not agarose beads (compare lanes 2 and 4 to 1), and the same species subsequently can be eluted from the heparin agarose but not the agarose beads (compare lanes 3 and 5 with lane 1). FIGURES 8, A and B indeed show that these proteins behave differently, with most of the N fragment remaining cell-associated and all, or nearly all, of C being released into the culture supernatant.

One possible explanation for this differential behavior might be association of the N fragment with extracellular matrix proteins on the surfaces of the S2 cells. Accordingly, the relative affinity of these two proteins for heparin agarose was examined, since heparin binding is a common property of proteins that associate with the extracellular

- 82 -

matrix. Given the obvious difficulty in obtaining soluble N from cultured cells, in vitro translation in the presence of microsomes was used to generate soluble, labelled N and C. As shown in FIGURE 8C, N but not C is depleted from these translation extracts by treatment with heparin agarose beads, while treatment with unmodified agarose beads  
5 did not deplete either fragment. Furthermore, N but not C was retained upon the heparin agarose beads upon extensive washing with a solution that contains 0.1% Triton X-100 and 150 mM NaCl; in contrast, neither fragment was retained by unmodified agarose. N, but not C, binds tightly to heparin, and this behavior suggests that the low concentration of N released into culture supernatants may be the result of binding to the extracellular  
10 matrix. Another mechanism that might contribute to the differential release of N and C into culture supernatant would be the expression in S2 cells of a receptor for N but not for C. Our current data can not distinguish these possibilities.

#### EXAMPLE 7

#### DISTINCT EMBRYONIC LOCALIZATIONS OF N AND C

15 The differential release of N and C into cultured cell supernatants suggested the possibility that these fragments might also be differentially localized in embryos. Previously reported *hh* protein localizations utilized either antibodies specific for N epitopes or antibodies unable to distinguish between N and C. FIGURE 9 shows the differential localizations of N and C in embryos by in situ localization of the *hh*  
20 transcript. FIGURE 9 (A) is shown in comparison to the distribution of N and C epitopes detected with Ab1 and Ab2 in panels (9B) and (9C), respectively. Note that the distribution of N and C epitopes span approximately one-third and one-half of each segmental unit respectively, while the transcript is limited to approximately one-quarter of each unit. In (9D), the localization of C epitopes in embryos homozygous for the *hh*<sup>13E</sup>  
25 allele is detected with the use of Ab2. C epitopes in this mutant, which displays impaired auto-proteolytic activity are more restricted, and resemble the wild-type localization of N. Homozygous *hh*<sup>13E</sup> embryos were identified by loss of a marked balancer from a heterozygous parent stock. All embryos are at mid to late stage 9 (extended germ-band).

- 83 -

FIGURE 9B shows in accordance with these reports, Ab1, which is specific for N epitopes, reveals a segmentally localized distribution that is slightly broader than that of the *hh* transcript at the same stage (FIGURE 9A). Also consistent with these reports, we observed that N epitopes at later stages accumulate in large punctate structures. Our analysis here concentrates on the earlier stage, when antibody staining is weaker but before formation of the invaginations and grooves that later crease the epidermis and thereby complicate the interpretation. Ab2 was also utilized to detect C-specific epitopes with a variety of fixation and staining procedures. Although detection of C epitopes above background is more difficult than for N, we consistently observed a segmentally modulated pattern, albeit with a broader distribution than N (FIGURE 9C). This localization is also distinctive in that C epitopes at early or late stages are not found in the punctate structures characteristic of N.

The *hh*<sup>13E</sup> mutation encodes a prematurely truncated protein that is missing 15 residues normally present at the COOH-terminus. Because this protein displays a much reduced efficiency in auto-proteolysis the distribution of C in this mutant background was examined. FIGURE 9D shows that C epitopes in a homozygous *hh*<sup>13E</sup> embryo (identified by absence of a marked balancer) are distributed in a much tighter segmental pattern than in wild-type. This localization resembles that of N, and we thus conclude that the broad distribution of C epitopes normally seen is altered in *hh*<sup>13E</sup> by retention of the uncleaved precursor near the site of synthesis.

### EXAMPLE 8

#### THE ROLE OF AUTO-PROTEOLYSIS IN BIOGENESIS OF ACTIVE HEDGEHOG PROTEIN

In addition to signal cleavage, the *hh* protein undergoes auto-proteolysis at an internal site to generate the predominant protein species observed *in vivo*. All or most of the amino acid residues required for this auto-proteolysis function map to C, the carboxy-terminal product of this internal cleavage. In an effort to determine the

- 84 -

importance of auto-proteolysis for function, we introduced a single residue mutation (H329A) that blocks auto-proteolysis of the *hh* protein *in vitro* and demonstrated that both processing and function of this protein is impaired *in vivo*. Since similar levels of induced protein were detected from a strain carrying the wild-type construct or from  
5 several strains carrying independent insertions of the mutant construct (FIGURE 5), the impaired function of the H329A protein relative to wild-type is not the result of reduced levels of expression. Further evidence in support of a role for auto-proteolysis derives from the effect of the *hh*<sup>13E</sup> mutation, which reduces but does not eliminate auto-proteolysis of the *hh* protein *in vitro* (FIGURE 4). Correspondingly, the *hh*<sup>13E</sup>  
10 mutation is associated with a phenotype of intermediate strength *in vivo* (J. Mohler, *supra*).

Curiously, the H329A *Hh* protein appears to retain weak activity in embryonic signaling to induce ectopic *wg* expression and, to a lesser degree, can function in imaginal disc signaling for induction of ectopic *wg* and *dpp* expression. In contrast to its retention of  
15 at least some signaling functions in embryonic and imaginal tissues, the H329 protein is completely inert when assayed for the ability to reprogram cell fates in the dorsal cuticle of the larva.

The assays in which the H329A protein is active or partially active involve short-range signaling that normally occurs across one or at most several cell diameters; in contrast,  
20 the H329A protein fails to exert any effect upon patterning of the dorsal cuticle, a long-range activity that normally operates across most of the segment. Previous proposals to account for long-range patterning activities have suggested that *hh* expression induces other signaling molecules which are then responsible for executing the patterning functions (the signal relay model; see FIGURE 10A). FIGURE 10 shows  
25 a signal relay versus dual function models for *hh* protein action. In FIGURE 10 (A), the long-range effects of *hh* signaling are achieved indirectly through short-range induction of a second signaling molecule (X). Based on its biochemical properties and its restricted tissue localization, N is presumed to represent the active short-range signal

- 85 -

while the role of C would be limited to supplying the catalytic machinery required for biogenesis of N. In (10B), the long- and short-range signaling functions of *hh* are supplied by the N and C proteins derived by internal auto-proteolysis of the U precursor. N is implicated in short-range signaling by retention near its cellular site of synthesis, while C is less restricted in its distribution and would execute long-range signaling functions. In both models, auto-proteolysis is required to generate fully active signaling proteins. See text for further discussion.

These proposals seek to maintain a consistent mode of *hedgehog* action by rationalizing the apparent long-range activities of *hh* products as indirect consequences of short-range signaling. Based on the distribution observed, the active molecule in this model might be N and the role of C would then be limited to supplying the catalytic machinery required for biogenesis of N.

Our evidence suggests an alternative model, the dual function model (FIGURE 10B), in which long- and short-range activities of the *hh* protein might be executed by N and C, the two predominant forms of the molecule observed *in vivo*. The nearly quantitative release of C fragment into the culture medium of *hh*-expressing S2 cells and its broad, though segmentally modulated distribution within embryos suggests that C might execute or contribute to long-range signaling functions. The N fragment, on the other hand, predominantly remains associated with the expressing S2 cells and also binds to heparin, which suggests a possible association with the extracellular matrix. These properties and the segmentally restricted embryonic distribution of N are suggestive of a role in the execution of short-range *hh* signaling activities. Since the vertebrate *Hh* proteins we tested also appear to be auto-processed and also carry predicted heparin binding sites just carboxy-terminal to their signal sequences (H. Roelink et al., *supra*), many aspects of the dual function model discussed here in the context of *Drosophila* development may also apply to *hh* protein function in vertebrate development.

- 86 -

Execution of short-range functions by N would be consistent with the observation that the H329A mutant protein has at least partial function in signaling for the induction of *wg* and *dpp*, since this mutation does not alter residues located in the amino-terminal portion of the protein that normally would give rise to N. The uncleaved H329A protein thus would carry all the residues that normally interact with a presumed receptor for N, although there might be some effect on the affinity of the interaction due to the presence of carboxy-terminal sequences, thus accounting for the decreased potency of the H329A protein. Alternatively, the partial function of H329A protein may derive from an extremely small fraction of protein that appears to be cleaved, a very faint band with identical mobility to C appears in *in vitro* translations with the H329A protein (FIGURE 4, lane 3). Execution of long-range functions by C is also consistent with our observations because long-range signaling might require the release of the C fragment or otherwise require the H329 residue for some function other than for cleavage.

When N is synthesized from a native construct (wild type hh), it remains primarily cell-associated (FIGURE 10C), however, N generated from a truncated construct in cultured cells predominantly enters the culture medium (FIGURE 10D) (For constructs, see Porter, *et al.*, *Nature*, 374:363, 1995). These results further confirm that autoprocessing by fragment C may regulate the degree of N association with the cell surface and therefore its range of action.

20

### EXAMPLE 9

#### ISOLATION OF HEDGEHOG HOMOLOGUES

The mouse and human *hh*-like sequences were isolated by polymerase chain reaction (PCR) using primers degenerate for all possible coding combinations of the sequences underlined in FIGURE 1 of Chang, *et al.*, (*Development*, 120: 1994). PCR amplifications contained from 100 ng to 2  $\mu$ g genomic DNA (depending upon the genome size of the species), 2  $\mu$ M of each primer, 200  $\mu$ M dNTPs (Pharmacia), 1X reaction buffer (Boehringer-Mannheim) and 2.5 units Taq polymerase (Boehringer-Mannheim) in 50  $\mu$ l

- 87 -

reactions. Amplification was as follows: 94°C 5 min, addition of Taq polymerase at 75°C, followed by 94°C 1 min, 52°C 1.5 min and 72°C 1 min for 30 cycles and a final extension of 72°C for 5 min. All PCR products were cloned into pBluescript (Stratagene) prior to sequence determination.

- 5 Mouse clones obtained in this manner contained 144 bases of sequence between the primer ends and were labelled with [ $\alpha$ -<sup>32</sup>P]dATP and used for high stringency screens of mouse cDNA libraries made from whole 8.5 dpc embryonic RNA and from 14.5 dpc embryonic brain in the  $\lambda$ ZAP vector (a gift from A. Lanahan). Several clones corresponding to *Hhg-1* were isolated and the largest, 2629 bp in length (pDTC8.0), was  
10 chosen for sequence analysis using dideoxy chain termination (Sanger, *et al.*, 1977) and Sequenase v2.0 (US Biochemicals). Compressions were resolved by using 7-deaza-guanosine (US Biochemicals). Sequence analysis made use of the Geneworks 2.0 (IntelliGenetics) and MacVector 3.5 (IBI) software packages.

One of the three mouse clones, *Hhg-1*, when used as a probe, yielded a 2.0 kb clone from  
15 a 8.5 dpc mouse embryonic cDNA library and a 2.7 kb clone from a 14.5 dpc embryonic cDNA library. The 2.7 kb cDNA appears to represent a nearly full length mRNA because it corresponds to a 2.7 kb band detected by hybridization on a Northern blot. The largest methionine-initiated open reading frame within this cDNA encompasses 437 codons, and is preceded by one in frame upstream stop codon. Sequence comparisons  
20 indicate that the protein encoded by *Hhg-1* is identical to the independently characterized mouse *Shh* (Echelard, *et al.*, *Cell*, 75:1417-1430, 1993) except for an arginine to lysine difference at residue 122. *Hhg-1* also corresponds closely to the rat *vhh-1* gene (97% amino acid identity; Roelink, *et al.*, *Cell*, 76:761-775, 1994), the chicken Sonic hedgehog (81% identity; Riddle, *et al.*, *Cell*, 75:1401-1416, 1993) and *Shh* from the zebrafish (68%  
25 identity; Krauss, *et al.*, *Cell*, 75:1431-1444, 1993; Roelink, *et al.*, *Cell*, 76:761-775, 1994). The PCR-generated fragments *Hhg-2* and *Hhg-3* appear to correspond to the Indian and Desert classes of mouse hedgehog genes, respectively (Echelard, *et al.*, *Cell*, 75:1417-1430, 1993).

- 88 -

- Alignment of the *Hhg-1* open reading frame with the two *Drosophila hh* sequences showed that all three proteins contain hydrophobic amino acid sequences near their amino-termini; the hydrophobic stretches within the *D. melanogaster* protein (residues 64 to 83) and within the mouse protein are known to act efficiently as signal sequences for cleavage (Lee, *et al*, *Cell*, 71:33-50, 1992). Both *Drosophila* signal sequences are unusual in their internal locations, while the hydrophobic stretch of the mouse gene occurs at the extreme amino-terminus, a more conventional location for cleaved signal sequences. Although portions of sequence N-terminal to the *Drosophila* signal sequences are conserved, suggesting a functional role, the mouse gene lacks this region.
- 10 The overall level of amino acid identity between *Hhg-1* and *hh* carboxy-terminal to the signal sequences is 46%. A closer examination shows that the amino terminal portion, from residues 25 to 187, displays 69% identity, while remaining residues in the carboxy-terminal portion display a much lower 31% identity. Like *hh*, the *Hhg-1* coding sequence is divided into three exons, and the boundaries of these exons are at the same
- 15 positions within coding sequence as those of the three *Drosophila hh* exons. Curiously, the boundary between coding sequences of the second and third exons occurs near the transition from high to low levels of overall sequence conservation. The coincidence of these two boundaries suggests a possible demarcation of functional domains within these proteins. This location within *Hhg-1* coding sequence also coincides approximately with
- 20 the site of a presumed proteolytic cleavage.

#### EXAMPLE 10

#### HUMAN CLONING OF *hh* GENES

- Partial sequence for two human *hh* genes has been obtained by DNA sequencing of clones derived by PCR amplification from genomic DNA with *hh*-specific degenerate
- 25 primers as outlined in Chang, *et al.*, (*Development*, 120:3339, 1994) and EXAMPLE 9 (FIGURE 11A and B). More extensive screening by the same approach, either with the

- 89 -

same primers or with other primers from the *hh* coding region or with the human *hh* fragments seen in FIGURES 11A and B, is expected to yield at the least a third gene, and possibly more, since at least three genes are found in the mouse. These segments of human *hh* genes can be used to obtain full coding sequences for human proteins by the following cloning method commonly used by those of skill in the art and which are extensively described in the literature.

For example, ready-made cDNA libraries or RNAs from a variety of human sources, including various fetal stages and organs (from abortuses) and specific infant or adult organs (from pathological or autopsy specimens), are being tested for the presence of *hh* sequences by PCR or RT-PCR using the primers described in Chang, *et al.*, *supra*, and other primers derived directly from the sequence of the human fragments. Ready-made libraries containing *hh* sequences are being screened directly and, where necessary, new libraries are being constructed by standard methods from RNA sources containing *hh* sequences. The probe for these screens is a mixture of all the distinct human *hh* fragments. Sequences of cDNA clones can then be determined. Most clones containing the probe sequences, which are located in the N region, will also include a full C coding region since standard methods of library construction result in cDNA clones that are most complete at their 3' ends. All full length *hh*-coding sequences obtained previously in vertebrates and invertebrates contain N and C sequences encoded in a single RNA. Screening is continued until complete open reading frames that correspond to all of the fragments of human *hh* genes are obtained. Specifically,  $1.2 \times 10^6$  clones from a human fetal brain library (Stratagene, La Jolla, CA) was screened using a mixture of the two human *hh* fragments (FIGURE 11A and B) as probes. Twenty-nine clones were identified as specifically hybridizing with these probes.

Second, the RNA sources identified as containing *hh* sequences can be used as templates from anchored PCR (also referred to in the literature as RACE, for rapid amplification of cDNA ends). Briefly, this method provides a means to isolate further mRNA

- 90 -

sequence in either the 5' or 3' direction provided that sequence is known from an internal starting point. Anchored PCR can also be used to isolate sequences from cDNA library.

Third, genomic libraries can be screened with the probes described in the first technique. Where necessary, human *hh* exons and coding sequences are being identified by  
5 hybridization to previously isolated human and mouse coding sequences by sequence determination, and by exon-trapping methods to identify all *hh* coding sequences within genomic clones; these coding sequences can be "stitched" together by standard recombinant DNA methods to generate complete *hh* open reading frames.

FIGURE 12 A and B show *in vitro* cleavage reactions of a *Drosophila hh* protein  
10 produced in *E. coli* and purified to homogeneity. This protein has residues 89-254 deleted, rendering it more soluble and easier to purify. It also contains a His<sub>6</sub> purification tag appended to the N-terminus. Autoproteolysis of this protein is triggered by the addition of reducing agents (DTT), and the resulting product corresponds to the C fragment identified *in vivo*. FIGURE 12, Panel A shows a time course of cleavage after  
15 initiation by addition of DTT. Panel B shows incubations of concentrations ranging over three order of magnitude for a fixed time period (four hours), with no difference in the extent of conversion to the cleaved form. This concentration-independent rate of cleavage indicates an intramolecular mechanism of cleavage. Panel C shows the sequence around the cleavage site as determined by amino-terminal sequence of the  
20 cleaved fragment C. The cleavage site is denoted by the arrow, and the actual residues sequenced by Edman degradation of the C fragment are underlined. Panel C also shows an alignment of all published vertebrate *hh* sequences plus some of unpublished sequences from fish and *Xenopus*. The sequences shown correspond to the region of *Drosophila hh* where the cleavage occurs, and demonstrates the absolute conservation  
25 of the Gly-Cys-Phe sequence at the site of cleavage. Panel D shows a SDS-PAGE gel loaded with *in vitro* transcription/translation reactions as described in the previous Examples, using various *hh* genes as templates. *dhh* is *Drosophila*, *twhh* and *zfshh* are the *twiggy-winkle* and *sonic hh* genes of the zebrafish, and *mshh* is the *shh/Hgh-1/vhh-1*

- 91 -

gene of the mouse. The translation mix included  $^{35}\text{S}$ -labelled cysteine, used to visualize the resulting products by autoradiography. Note that each gene give a larger product (the precursor or U) and two smaller products of cleavage (N and C). The larger species is C for each of the vertebrate genes, whereas the *Drosophila* N is larger than C due to the presence of -60 residues occurring amino-terminal to the signal sequence that are present in the vertebrate open reading frame. This panel shows that vertebrate *hh* proteins are processed similarly to the *Drosophila* protein. Panel E shows that Edman degradation of the C fragments releases  $^{35}\text{S}$  counts on the first but not subsequent rounds for all these proteins, indicating that the site of autoproteolytic cleavage for all of these *hh* proteins is the amide bond to the amino-terminal side of the Cys residue that forms the center of the conserved Gly-Cys-Phe sequence highlighted in panel C. This is a generalizable approach to establish the composition of protein fragments from any other *hh* family members.

#### EXAMPLE 11

#### DIFFERENTIAL EXPRESSION OF TWO *hh* GENES IN AXIAL MESODERM AND IN NEURAL PROGENITORS.

Partial sequences corresponding to five distinct zebrafish *hh*-like genes were isolated and the complete coding sequences for two of these genes were obtained from an embryonic cDNA library. One of these two sequences is identical to that of the zebrafish *nhh-1* gene (Roelink, *et al.*, *Cell*, 76:761, 1994), and appears to correspond to the *shh* gene reported by Krauss, *et al.*, (*Cell*, 75:1431, 1993) (See FIGURE 13 description); the other gene, *tiggy-winkle* (Potter, B., The Tale of Mrs. Tiggy-Winkle, *The Penguin Group*, London, 1905), represents a novel vertebrate *hh*. Coding sequences for both are shown in alignment to mouse and chicken sequences of the *sonic/vhh-1* class (FIGURE 13b). Like other vertebrate *hh* homologues, the *twhh* and *shh* proteins contain an amino-terminal stretch of hydrophobic residues. These residues function as signal sequences since cleavage is observed when coding sequences are translated in the presence of micro-

- 92 -

somoses; vertebrate *hh* genes thus appear to encode secreted proteins, as previously reported for *Drosophila hh* (Kimmel C.B. & Warga, R.M., *Developmental Biology*, 124:269-280, 1987; Warge, R.M., & Kimmel, C.B., *Development*, 108:569-580, 1990).

- The first four sequences were isolated from zebrafish genomic DNA (a gift from J. Pellegrino) using degenerate primers in polymerase chain reactions as described (Chang, *et al.*, *supra*). *twhh* and *shh* clones were isolated from a 20-28 hour cDNA library (a gift from R. Riggelman, K. Helde, D. Grunwald and J. Pellegrino) using the first three sequences as probes. The translational reading frames for *twhh* and *shh* were closed 12 and 16 codons, respectively, upstream of the putative initiating methionine.
- 10 Figure 13 shows the predicted amino acid sequences are shown in single letter code. 13(a) shows sequences common to five distinct *hh*-like genes are shown with a dot indicating identity with the corresponding residue of zebrafish *twiggy-winkle* (*twhh*; Potter 1905; *supra*), *hh*[zfB] and *hh*[zfC] is more diverged and appears to represent a novel class. 13(b) shows amino acid sequences of *twhh* and *shh* are aligned to those of
- 15 the *sonicvhh-1* class from chick and mouse (Riddle, *et al.*, *Cell*, 75:1401-1416, 1993; Chang, D.T., *et al.*, *Development*, *supra*; Echelard, Y., *et al.*, *Cell*, 75:1431-1444, 1993). Zebrafish *sonic hedgehog* (*shh*) is identical in sequence to *z-vhh-1* reported by Roelink, *et al.*, *Cell*, 76:761-775, 1994. Based on expression and extensive sequence identity throughout most of the coding region, *vhh-1* and the *sonic* sequence reported here
- 20 probably correspond to *shh* of Krauss, *et al.*, *Cell*, 75:1431-1444, 1993, diverges dramatically throughout a 26 residue stretch near the carboxy-terminus. Rat *vhh-1/sonic hh* (Roelink, *et al.*, *supra*.) was excluded in this alignment because of its 97% sequence identity to the predicted mouse protein. Residues identical in all four sequences are boxed, and a dash indicates a gap in the alignment. The arrow indicates the predicted
- 25 signal sequence cleavage site (von Heijine, G., *Nucleic Acids Res.*, 14, 4683-4690, 1986) for *twhh*. The amino-terminal hydrophobic stretch common to all four *hh* genes is shaded. 13(c) shows percent identity of residues carboxy-terminal to the hydrophobic region.

- 93 -

Figure 14 shows a comparative expression of *twhh*, *shh*, and *pax-2* during zebrafish embryogenesis. Whole mount *in situ* hybridizations on 0-36 hour embryos were performed using a modification of the procedure of Tautz and Pfeifle, *Chronosoma*, 98:81-85, 1989, with antisense probes. Transcript localization is revealed by the purple product of an alkaline phosphatase enzymatic reaction. Staging of the embryos is according to Westerfield, M., (*The Zebrafish Book*, University of Oregon Press, Eugene, 1993). Transcripts were visualized by *in situ* hybridization to whole embryos. (a, b) *twhh* expression in a single late shield stage embryo. (a) Dorsal view, animal pole is to the top. The triangular shape of expression is characteristic of axial mesoderm-forming cells of the hypoblast (Statchel, S.E., *et al.*, *Development*, 117:1261-1274, 1993). (b) Lateral view: the thicker layer of cells on the left (dorsal) side of the embryo is the embryonic shield; the two arrows indicate the *twhh*-expressing hypoblast cells and the non-expressing epiblast. Anterior is to the left in all subsequent embryos. Dorsal is to the top in all lateral views. (c, d) A single embryo at the end of gastrulation (100% epiboly) with *twhh*-expressing cells. (d) Caudal-dorsal view. Note the wide patch of stain in the presumptive tailbud which narrows anteriorly. (e, j) Early somitogenesis (11.5 hour, 3-4 somite) embryos; optic vesicles have not begun to evaginate from the wall of the diencephalon. (e, h, k) Lateral views of developing brain. (f, i, l) Dorsal views of developing brain. (e, f, g) Localization of *twhh*-expressing in a single row of cells that will form the floor plate. The arrowhead marks a patch of *twhh*-expressing cells lateral to the tailbud. (h, i, j) Localization of *shh*. *shh* is also expressed strongly in the protuberance. (j) Lateral view of the developing tail. *shh* is also expressed strongly in the protuberance. (j) Lateral view of developing tail. *shh* is expressed in cells that will form both floor plate and notochord. (k, l, m) Localization of *pax-2* during early optic vesicle formation; (m) also shows *twhh* expression. (k) 12 hour (4-5 somites) embryo. (l) 12.5 hour (5-6 somites) embryo. Expression of *pax-2* in the developing optic vesicle is in a gradient away from the protuberance. Note the expression of *pax-2* (asterisk) at the future midbrain-hindbrain border. (m) *twhh* (arrow) and *pax-2* expression in a 6-7 somite (13 hour) stage embryo. Note differential expression of *twhh* in ventral neural keel (corresponding to neural tube in other vertebrates). (n-s) Embryos

- 94 -

at end of somitogenesis (22-24 hours). (n, o, p) Localization of *twhh*. (n, o) Developing brain. Note isolated groups of cells staining in the diencephalon (filled triangles) and the protuberance (arrowhead), and floor plate expression underlying the midbrain and hindbrain. The floor plate expression is contiguous caudally along the axis. (n) Lateral  
 5 view. (o) Dorsal view. (p) Lateral view of tail. Expression is restricted to the floor plate. (q, r, s) Localization of *shh*. (q, r) Developing brain (q) Lateral view. *pax-2* expression in the otic vesicle is indicated. (r) Dorsal view. Expression in the protuberance (arrowhead) and in the neural keel. (s) Lateral view of tail. Expression is strongest in the floor plate, but contrary to the report of Krauss, *et al.*, supra, is still also  
 10 in the notochord. Abbreviations: white e - epiblast; h - hypoblast; tb - tailbud; p - protuberance; c - eye; ov - optic vesicle; ot - otic vesicle; fp - floor plate; nc - notochord; asterisk - midbrain-hindbrain boundary or *pax-2*-labeled prospective midbrain-hindbrain boundary; t - telencephalon.

Comparison of *twhh* and *shh* expression patterns (Krauss, *et al.*, *supra*), reveals that both  
 15 gene are predominantly expressed in midline structures, albeit with notable differences in regard to timing, rostra-caudal extent, and tissue restriction. Expression of *twhh* is first detected during gastrulation in the dorsal mesoderm (FIGURE 14a, b); this expression occurs in a band corresponding to a subset of the embryonic shield, a structure, analogous to Spemann's organizer in *Xenopus* (Stachel, *et al.*, *Dev.*, 117:1261-  
 20 1274, 1993, and reference therein; Ho., R., *Seminars in Developmental Biology*, pg.3, 1992). In concert with the movements of convergence and extension, this band of *twhh* expression shortens along the equatorial plane and extends along the incipient embryonic axis until, by the end of gastrulation, expression occurs throughout the entire axis (FIGURE 14c,d). Early in somitogenesis, *twhh* RNA is found restricted to presumptive  
 25 ventral neural tissue along the entire body (FIGURE 14e, f, g), the only exception being cells in and near the tailbud (FIGURE 14g). In contrast to the neural restriction of *twhh*, *shh* is localized both to presumptive neural and notochordal cells (FIGURE 14j).

- 95 -

As somitogenesis proceeds, ventral midline expression of *shh* and *twhh* is reduced in most of the prospective forebrain, but remains strong in an anterior patch of midline cells within the floor of the prospective diencephalon (FIGURES 14e, f, for *twhh*; FIGURES h, i for *shh*). This patch later will give rise to the protuberance (Schmitt, E.A. and Dowling, J.D., *J. Comp. Neur.*, 344:532-542, 1994), an anterior extension of the diencephalon. This structure, which is medial and just rostral to the developing optic stalks, is the site we propose as the focus of early patterning activity for the developing eyes (see below). By the end of somitogenesis, both *twhh* and *shh* are strongly expressed in the floor plate (FIGURES 14p, s), although *shh* transcripts remain detectable in the notochord at this stage and at 36 hours of development (FIGURES 14s; later stage not shown). At 28 hours, *twhh* transcripts are also found in a small cluster of cells within the first gill arch (not shown), as also reported for *shh* at 33 hours of development (Krauss, *et al.*, *supra*).

Differences between *twhh* and *shh* expression are apparent from the beginning of gastrulation, since *twhh* RNA can be detected as early as the shield stage while *shh* is first detected later, at about 60% epiboly (not shown; (Krauss, *et al.*, *supra*). In addition, *twhh* transcripts are restricted to neural tissues early in development, and are never detected in the notochord (compare FIGURE 14g to FIGURE 14j). Later differences in expression include differential rostra-caudal restriction within the diencephalon and midbrain and weaker and more restricted expression of *twhh* in the protuberance (compare FIGURES 14n and 14q), such that the later domain of *twhh* expression in the brain appears to constitute a subset of the *shh* domain. In addition, *shh* but not *twhh* is expressed in the developing fin bud (Krauss, *et al.*, *supra*). Comparison of *shh* and *twhh* expression patterns to this previously reported for *hh* homologues in zebrafish and other vertebrate species indicates that *shh* is the zebrafish homologue of the *sonic/vhh-I* class while *twhh* represents a novel class of vertebrate *hh*.

- 96 -

**EXAMPLE 12****DEVELOPMENTAL CONSEQUENCES OF ECTOPIC *hh* EXPRESSION DURING ZEBRAFISH EMBRYOGENESIS**

To gain insight into the potential roles of *hh* products in development, synthetic *twhh* and *shh* mRNA was injected into 1-8 cell embryos. This technique yields a mosaic but fairly uniform pattern of expression, as determined for the control mRNA encoding  $\beta$ -galactosidase (not shown). Uniformity of expression is in good agreement with fate mapping studies of the early zebrafish embryo (Kimmel & Warga, *supra*; Warga & Kimmel, *supra*; Heide, *et al.*, *Science*, 265:517-520, 1994), which indicate that blastomeres undergo extensive cell mixing during the cleavages prior to gastrulation. We note that mosaicism of expression caused surprisingly little variation in the phenotypes of the *hh* injected embryos, possibly due to secretion of *hh* gene products.

Embryos injected with synthetic *twhh* or *shh* mRNA (*hh* RNA) exhibited numerous yet highly reproducible abnormalities in comparison to control embryos injected with *lacZ* mRNA. These abnormalities, discussed below, are primarily defects in the brain and eyes. Although the effects of ectopic *twhh* and *shh* expression were qualitatively similar, the incidence and severity were greater with *twhh* RNA (see text below, FIGURE 15 and FIGURE 16). The proteins encoded by these two genes have qualitatively similar biological activities, but apparent differences in potency.

FIGURE 15 shows the effects of ectopic *hh* on zebrafish development. Wild type zebrafish, *Danio rerio*, (Eckwill Waterlife Resources) were maintained at 28.5°C, some embryos were then cultured overnight at RT. Zebrafish embryos were injected at the 1-8 cell stage with *twhh*, *shh*, or *lacZ*RNA and examined at 28 h of development. (a-c) Dorsal view of the midbrain-hindbrain region; anterior is left. (a) *lacZ*. (b) *twhh*. (c) *shh*. (d-f) Frontal optical section of the forebrain region; anterior is up. (d) *lacZ*. (e) *twhh*. (f) *shh*. (g-i) Lateral view of the eye region; anterior is left. (g) *lacZ*. (h) *twhh*. (i) *twhh*. At levels caudal to the prospective brain, the notochord, somites, and neural keel formed

- 97 -

by most *hh*-injected embryos appeared grossly normal except for an overall shortening and dorsal curvature of the axis. A minority of *hh*-injected embryos (15% are not shown) displayed partially bifurcated axes, containing duplicated axial mesoderm and parallel neural keels, each neural keel comprising ventral midline cells and some bilaterally symmetric lateral cells (not shown). Although we have not determined the primary cause of these axial defects, analysis of late gastrulation stage embryos suggests that the bifurcation may result from difficulties in epiboly and convergence. Abbreviations: mv - mesencephalic ventricle; rv - rhombencephalic ventricle; asterisk - midbrain-hindbrain boundary; ot - otic vesicle; tv - third (diencephalic) ventricle; r - retina or retina-like structure; l - lens or lens-like structure; pe - pigmented retinal epithelium.

Morphological defects in the brain and other rostral neural derivatives occur at high frequency in *hh*-injected embryos. The three ventricles of the fish brain normally apparent at 28 hours of development - the rhombencephalic, mesencephalic (FIGURE 15a), and diencephalic (third ventricle; FIGURE 15d) - are not formed in the brains of *hh* injectees (FIGURES 15b, c; FIGURES 15e, f), despite the obvious presence of a lumen. The prominent constriction normally present at the midbrain-hindbrain boundary also is absent (compare FIGURE 15a to FIGURES 15b, c). Formation of this constriction requires function of *pax-2* (Krauss, *et al.*, *Nature*, 353:267-270, 1991; Krauss, *et al.*, *Nature*, 360:87-89, 1992), which normally is expressed in a band at the midbrain-hindbrain boundary (Krauss, *et al.*, *supra*; Krauss, *et al.*, *Development*, 113:1193-1206, 1991) *pax2* expression at this boundary is not disrupted by *hh* RNA injection, however, indicating that this phenotype does not result from disruption of rostra-caudal information.

Defects in eye development also occur at high frequency in embryos injected with *hh* RNA. Thus, while at 28 hours the normal zebrafish eye has a lens and a retina with pigmented epithelium (FIGURE 15d, g), *hh*-injected embryos usually fail to develop lenses and retinal pigmentation (FIGURE 15e, h). Eye duplications are also observed at low frequencies (FIGURE 15i). The poorly developed eyes do not appear to result

- 98 -

from a simple delay in development since pigmentation elsewhere in injected embryos appears in its normal time course. Examined at three days of development, the consequences of *hh* RNA injection include defects that range from complete absence of eyes to partially formed eyes lacking a ventral portion of the retina.

- 5 The eye phenotypes caused by *hh* RNA injection resemble those produced by treatment of zebrafish and *Xenopus laevis* embryos with retinoic acid. In *Xenopus*, phenotypes range from reduction of the eye and absence of the lens to eyes with retinal folds (resembling duplicated eyes) and multiple small lenses (Manns, M. & Fritsch, B., *Neurosci. Lett.*, 127:150-154, 1991). In zebrafish, exposure to retinoic acid during  
10 gastrulation interferes with the formation of the eye (Holder, N. & Hill, J., *Development*, 113:1159-1170, 1991), while exposure during formation of the optic primordia induces formation of duplicated retinas and extra lenses (Hyatt, *et al.*, *Proc. Natl. Acad. Sci. USA*, 89:8293-8297, 1992). Patterning effects of retinoic acid upon the developing chick limb appear to be mediated through ectopic activation of the endogenous *sonic hh* gene  
15 (Riddle, *et al.*, *supra*), these results with ectopic *hh* expression suggest the possibility of a similar mechanism underlying the patterning effects of retinoid acid treatment in the vertebrate eye.

### EXAMPLE 13

#### *hh* EXPRESSION IN THE OPTIC VESICLE SPECIFIES

#### 20 PROXIMAL FATES AT THE EXPENSE OF DISTAL FATES

- To further elucidate the role of *hh* in eye development we utilized *pax-2* and *pax-6* (Krauss, *et al.*, *EMBO J.*, 10:3609-3619, 1991; Pitischel, *et al.*, *Development*, 114:643-651, 1992) were utilized as positional markers to examine the effects of ectopic *hh* expression on the optic vesicle. As the optic vesicle evaginates from the lateral walls of  
25 the zebrafish forebrain (Schmitt, E.A. & Dowling, J.D., *J. Comp. Neur.*, 344:532-542, 1994), *pax-2* is expressed in a gradient, with highest RNA levels in the anterior and

- 99 -

ventral regions of the optic vesicle (Krauss, *et al.*, *supra*; FIGURE 14k, l, m). Immediately adjacent to the maximum of this *pax-2* expression gradient is the region of the diencephalon termed the protuberance (Schmitt & Dowling, *supra*), where both *twhh* and *shh* but not *pax-2* are strongly expressed (FIGURES 14e, f, h, i, m). The concentration gradient of *pax-2* expression in the optic vesicle thus appears to incline downward from its maximum at a location adjacent to the site of *twhh* and *shh* expression in the protuberance. Superposition of developmental fate within the optic vesicle (Schmitt, *et al.*, *supra*), upon the pattern of *pax-2* expression suggests that the gradient of *pax-2* RNA prefigures the future proximal/distal axis of the eye.

10 Ectopic *hh* alters the expression of *pax-2*, *pax-6*, and *F-spondin*. Zebrafish embryos were injected at the 1-8 cell stage with *twhh* or *shh* RNA and the pattern of *pax-2*, *pax-6*, or *F-spondin* expression was examined by whole mount *in situ* hybridization. Control embryos injected with *lacZ* RNA were performed in every case and displayed wild-type expression patterns. At embryo stage, the anterior-posterior axis of the optic vesicle corresponds to the future proximal-distal axis of the eye. During the next hour of development, the posterior edge of the optic vesicle will separate from the diencephalon (Schmitt and Dowling, *Comp. Neur.*, 344:532-542, 1994).

Injection of either *hh* RNA causes uniform initiation of *pax-2* expression along both the proximal-distal and dorsal-ventral axes of the optic vesicle as it begins to evaginate. The ectopic *pax-2* expression appears at the same time as normal *pax-2* expression is initiated in the eye, and in some cases, is also seen in the diencephalon between the optic vesicles. At the end of somitogenesis, a time when *pax-2* would normally be restricted to the optic stalk, *pax-2* RNA in *hh* injected embryos is detected in all but the most distal portion of the optic vesicle.

25 The effects of ectopic *hh* on expression of *pax-6*, which encodes a transcription factor critical for eye development was also studied. At 22 hours of zebrafish development, *pax-6* is normally expressed in the lens and in most of the distal part of the optic cup

- 100 -

(Krauss, *et al.*, *supra*; Puschel, *et al.*, *Development*, 114:643-651, 1992). In *hh*-injected embryos, *pax-6* is repressed in the optic vesicle, although many embryos retain *pax-6* expression in the most distal cells. With regard to *pax-2* and *pax-6* as markers of positional identity, *hh* expression in the optic vesicle can be characterized as inducing  
5 proximal fates and repressing distal fates.

The distal part of the optic vesicle is the most refractory to *hh*-induced changes in both *pax-2* and *pax-6* gene expression. Due to a later rotation, this distal portion of the optic vesicle will give rise to the dorsal portion of the mature eye (Schmitt, *et al.*, *supra*); interestingly, this is the portion of the eye that remains in 3-day old injected embryos  
10 with intermediate phenotypes (see above).

Lesions in the *pax-6* gene have been assigned as the basis for the *Aniridia* (Ton, *et al.*, *Cell*, 67:1059-1074, 1991; Glaser, *et al.*, *Nat. Genetics*, 2:232-239, 1992), *Small eye* (Hill, *et al.*, *Nature*, 354:522-525, 1992), and *eyeless* mutations (Quiring, *et al.*, *Science* 265:785-789, 1994), in humans, mice and *Drosophila*, respectively; *pax-6* function thus  
15 appears to be critically required for eye development in *Drosophila* and mammals. As we argue here, *hh*-encoded activities also appear to play a role in vertebrate eye development, and this suggests a further molecular parallel between vertebrates and insects, since the role of *hh* in *Drosophila* eye development is well established (Mohler, *et al.*, *supra*; Ma, *et al.*, *supra*; Heberlein, *et al.*, *supra*; Lee, *et al.*, *supra*). The reciprocal  
20 and non-overlapping patterns of *hh* and *pax-6* expression in the developing *Drosophila* eye (Ma, *et al.*, *supra*; Quiring, *et al.*, *Science*, 265:785-789, 1994), suggest the possibility of *pax-6* repression by *hh*, but whether *hh* functions by similar mechanisms in vertebrate and *Drosophila* eye development is a questions that requires further investigation.

25 In mice, the dosage of *pax-6* protein is crucial for normal eye development (Hill, *et al.*, *supra*). *Small eye* heterozygotes develop an abnormally small lens (Hogan, *et al.*, *J. Embryol. Exp. Morph.*, 97:95-110, 1986; Hogan, *et al.*, *Development*, 103 Suppl., 115-

- 101 -

119, 1988), as do *hh*-injected embryos with weaker phenotypes (FIGURE 14f). *Small* eye homozygotes lacking lenses eventually generate and the animals lack eyes at birth (Hogan, *et al.*, *supra*; Hogan, *et al.*, *supra*), as do many of the *hh*-injected embryos at three days of development. These parallels suggest that many of the later eye defects  
5 observed in *hh*-injected zebrafish may be caused by partial or complete repression of *pax-6* during eye development.

#### **EXAMPLE 14**

##### **GENETIC ABLATION OF *hh* FOREBRAIN EXPRESSION CAUSES LOSS OF PROXIMAL FATES IN THE OPTIC VESICLE**

10 The patterns of *twhh* and *shh* expression (FIGURE 14) and the effects of ectopic *hh* expression (FIGURE 15) are consistent with a normal role for *shh* and *twhh* in eye development. If *hh* activities indeed play a normal role in promoting proximal fates within the developing eye, removal of *hh* activities would be expected to result in a loss of proximal fates. In embryos homozygous for the *cyclops* mutation ventral neural  
15 structures fail to form and the developing eyes fuse at the midline,, yielding an embryo with a single eye (Hatta, *et al.*, *Nature*, 350:339-341, 1991). The missing ventral structures in *cyclops* mutants include the regions where we observe expression of *twhh* and *shh*, and we therefore examined the effects of the *cyclops* mutation on *hh* expression.

*cyc*<sup>b16</sup> (Hatta, *et al.*, *Nature*, 350:339-341, 1991), heterozygous adults (a kind gift of R.  
20 Riggleman) were spawned and their offspring analyzed by whole mount *in situ* hybridization. Detection of *pax-2* and either *twhh* or *shh* RNAs in embryos homozygous for the *cyc* mutation or their wild-type siblings. *twhh* RNA is only expressed in the presumptive tailbud (caret) of *cyc* embryos. As reported by Krauss, *et al.*, *Cell*, *supra*, neural expression of *shh* is abolished in *cyc* embryos. Strong *pax-2* expression was  
25 observed in the optic vesicles of wild-type embryos which is significantly reduced in *cyc* mutant embryos.

- 102 -

*twhh* RNA in *cyclops* embryos is found only in a small patch of cells at the presumptive tailbud and neural expression was not detected at any later stage examined. Neural expression of *shh* is also lost in *eye* mutants, although expression in the notochord is reunited (Krauss, *et al.*, *supra*; data not shown).

- 5 Since the *eye* mutation appears to ablate *hh*-expressing cells in the developing brain, this mutation can be used as a genetic tool to examine the requirement for *hh* function in eye development. Liatta, *et al.*; Hatta, *et al.*, *Proc. Natl. Acad. Sci. USA*, 91:2061-2065, 1994), recently demonstrated that *pax-6* expression is fused at the midline due to loss of ventral midline cells that normally do not express *pax-6* and, in addition, *pax-2*  
10 expression in the fused eye of *eye* mutant embryos is reduced. We extended these observations to an earlier stage when the optic vesicles first form and found that *pax-2* expression is weak and fails to extend within the vesicles in *eye* mutants. In conjunction with the results of ectopic *hh* expression, these observations suggest that *hh* signaling that activity promotes and is required for the induction of proxima fates within the eye  
15 vesicle. In this model, we propose that the protuberance acts as a proximal patterning center for the developing zebrafish eye by providing a localized source of *hh* activity.

#### EXAMPLE 15

##### *hh* ACTIVITY VENTRALIZES THE DEVELOPING BRAIN

- Previous work has established an important role of signals from the floor plate and  
20 notochord in ventral patterning of the neural tube (Jessell, T.M., & Dodd, J., *Cell*, 69:95-110, 1992). For example, Goulding, *et al.*, *Development*, 117:1001-1016, 1993, recently demonstrated that notochord and floor plate grafts can repress the normal lateral expression of *pax-6* in the neural tube. Other recent work has implicated *hh* activity in at least some aspects of ventral neural tube patterning (Echelard, *et al.*, *Cell*, 75:1417-  
25 1430, 1993; Krauss, *et al.*, *supra*; Roelink, *et al.*, *supra*); consequently, we examined *hh*-injected embryos for effects on *pax-6* expression in the brain.

- 103 -

In the zebrafish at 22 hours of development, *pax-6* is expressed in dorso-lateral regions of the diencephalon and in a ventro-lateral domain of the hindbrain and spinal cord that excludes the floor plate and adjacent cells (Krauss, *et al.*, *supra*; Puschel, *et al.*, *supra*). This pattern of expression is reciprocal to that of both *twhh* and *shh* in the diencephalon  
5 (compare FIGURES 14q and 14i) and in the hindbrain. *hh* RNA injection caused repression of *pax-6* in the more ventral domain in the diencephalon, while more dorsal expression persisted. In addition, *pax-6* expression was significantly reduced ventrally in rhombomeres 1, 2, and 4 and, in some cases, was completely abolished in these rhombomeres. The repressing effect of ectopically expressed *hh* and *pax-6* in normal  
10 embryos are due to repression of *pax-6* by nearby *hh* expressing cells.

Since absence of *pax-6* expression is a feature of the ventral midline, repression of *pax-6* in lateral positions suggests ventralization. Consequently, *twhh* was injected into embryos for analysis of induction of a floor plate marker, *F-spondin* (Riddle, *et al.*, *supra*). As described above, ectopic *twhh* induces *F-spondin* expression at more dorsal  
15 levels in the midbrain and anterior hindbrain. The effects of *hh* upon expression of both *pax-6* and *F-spondin* indicate a ventralization of the brain. Adoption of ventral cell identity by lateral cells might explain their failure to form ventricles (FIGURE 15a-f).

The ventralizing activities of *twhh* confirm and extend those previously reported for *shh/vhh-1* class genes of chicken, zebrafish, and rat (Echelard, *et al.*, *supra*; Krauss, *et al.*, *supra*; Roelink *et al.*, *supra*). The early restriction of *twhh* to midline neural progenitors, however, suggests that it may play a specific role in the homeogenic mechanisms of floor plate maintenance and expansion (Placzek, *et al.*, *Dev.*, 117:205-218, 1993). In the zebrafish, wild type cells in *cyclops* hosts can contribute to and induce adjacent cells to form floor plate, but only when the transplanted cells populate the neural  
25 plate and not the notochord (Hatta, *et al.*, *Nature*, 350:339-341, 1991). We have demonstrated that, in *cyclops* mutants, midline expression of *twhh* is lost while *shh* expression is maintained in the notochord (FIGURE 18; Krauss, *et al.*, *supra* for *shh*); taken together, these results suggest that the homeogenic floor plate signal lost in the

- 104 -

*cyclops* mutant may be encoded by the *twhh* gene. In the chick and rat, the floor plate retains auto-inductive potential long after the loss of floor plate inducing properties by the notochord, despite continued expression of *shh/vhh1* in the notochord (Roelink, *et al.*, *supra*; Placzek, *et al.*, *supra*; Yamada, *et al.*, *Cell*, 73:673-686, 1993). Although no  
 5 homologues of the *twhh* class have been reported in other vertebrates, expression of other *hh* homologues in patterns more like those of *twhh* might help explain these discrepancies.

#### EXAMPLE 16

#### TWO DISTINCT SIGNALING PROTEINS DERIVE FROM 10 THE *twhh*-ENCODED PRECURSOR

Endogenous *hh* protein in *Drosophila* is found predominantly as an amino- and a carboxy-terminal fragment (N and C, respectively) derived by an internal auto-proteolytic cleavage of a larger precursor (U for uncleaved), which also occurs *in vivo* but at lower levels (Lee, *et al.*, *supra*). Determinants within the amino-terminal domain appear not  
 15 to be required for auto-proteolytic activity, whereas mutations affecting the carboxy-terminal domain can block auto-proteolysis and reduce activity *in vivo* (Lee, *et al.*, *supra*). The auto-proteolysis is blocked by a substitution of alanine for the histidine normally present at position 329. This histidine is absolutely invariant in alignments of all known *hh* genes, and its sequence context suggests a catalytic role in auto-proteolysis  
 20 (Lee, *et al.*, *supra*).

FIGURE 17 shows zebrafish *twiggy-winkle hedgehog* derivatives. 17(a) Cartoons of various *twhh* open reading frames. SS (shaded) is the predicted N-terminal signal sequence for secretion of these proteins and encompasses the first 27 amino acids of each open reading frame. The arrow indicates the predicted internal site of auto-proteolytic  
 25 cleavage. Amino acid residue numbers are according to Figure 13b. The filled triangle denotes the normal termination codon for the *twhh* open reading frame. Construct U<sub>HA</sub> contains a mutation that blocks auto-proteolysis (the histidine at residue 273 is changed to an alanine; see Lee, J.J., *et al.*, *supra*). Construct U356<sub>HA</sub> contains a stop codon in

- 105 -

place of amino acid residue 357 as well as the H273A mutation in  $U_{HA}$ . Construct N encodes just the first 200 amino acids of *twhh*. Construct C has had the codons for residues 31-197 deleted. 17(b) shows *in vitro* translation of the expression constructs shown schematically in part a. Constructs were translated *in vitro* in the presence of  $^{35}S$  methionine and analyzed by autoradiography after SDS-PAGE. The protein products are shown schematically to the left. Lanes 1 and 6: Auto-proteolysis of the full-length ( $U_{SS}$ ) protein creates two fragments, an N-terminal fragment ( $N_{SS}$ ) and a C-terminal fragment (C). Lane 2: Construct  $U_{HA}$  only makes an uncleaved form of *twhh* protein that comigrates with  $U_{SS}$  *twhh* via auto-cleavage. Lane 5: Construct C encodes processed and unprocessed forms which are visible as two bands migrating closely together. The bottom band is the C protein made from auto-proteolysis of the  $U_{SS}$  ( $\Delta 31-197$ ). All constructs were made by *in vitro* mutagenesis of expression construct T7TStw $hh$  (see FIGURE 15) using the method of RPCR. The sequence of all

constructs were confirmed by dideoxy sequencing. *In vitro* translations were performed according to manufacturer's instructions (Promega).

The vertebrate *hh* proteins encoded by *shh*, *twhh* and mouse-*shh/Hhg-1* also undergo auto-proteolysis to yield two smaller species from a single larger precursor (Lee, *et al.*, *supra*; Chang, *et al.*, *supra*; see lanes 1 and 6 in FIGURE 17b). The invariant histidine to alanine mutation to generate a construct encoding a form of the *twhh* protein that is not auto-proteolytically cleaved ( $U_{HA}$ ). We have also introduced a nonsense codon and deleted a segment of coding sequence to generate constructs that produce either the amino- or the carboxy-terminal domains of *twhh* (N and C, respectively; see lanes 4 and 5 in FIGURE 17b); constructs are schematically diagrammed in FIGURE 17a). To target these proteins to the secretory pathway, all constructs retained the normal *twhh* signal sequence.

Synthetic mRNAs transcribed from these constructs were injected to examine the role of processing and to assay the activities of individual protein fragments; the results are

- 106 -

summarized in Table I and are based on the activities presented in FIGURE 15. The most striking conclusion from these experiments is that N and C both exhibit activity, and that these activities are distinguishable. Thus, although both N and C are capable of ectopically activating *pax-2* in the developing eye, thereby providing an internal  
 5 injection control, only N was capable of efficiently repressing *pax-6* (FIGURE 16). Later effects on lens development were also more extreme for N, consistent with the role of *pax-6* in lens development suggested by its mutant phenotypes in mice. (See Ton, C.C., *et al.*, *Cell* 67:1059-1074, 1991; Glaser, T., *et al.*, *Nat. Genetics* 2:232-239, 1992; Hill, R.E., *et al.*, *Nature* 354:522-525, 1991; Hogan, B.L., *et al.*, *J. Embryol. Exp. Morph.*,  
 10 97:95-110, 1986; and Hogan, B.L., *et al.*, *Development*, 103Suppl.:115-119, 1988.)

In considering the activity of delta N-C, it is important to recognize the activity of endogenous *hh* genes in these experiments, which are inhibited by delta N-C and fragments thereof. (see Example 18 and FIGURE 18 for further discussion)

The uncleaved U<sub>HA</sub> protein is only somewhat less active than C in inducing *pax-2*, but  
 15 it also was not able to repress *pax6* efficiently (FIGURE 16). The latter is particularly notable since the U<sub>HA</sub> protein (U35<sub>HA</sub> ; see FIGURE 17a, b) has activities not significantly different from N (FIGURE 16). Thus, in addition to carrying determinants important for auto-proteolysis and *pax-2* induction, the C-terminus also contains a domain inhibitory to N-terminal function when in the context of the uncleaved *hh* protein. The  
 20 C-terminus can also inhibit N action by an intermolecular mechanism (Lai, *et al.*, *supra*). The existence of such an inhibitory domain in C suggests that if autoproteolysis can be modulated, such modulation might regulate the activity of *hh* *in vivo*. This possibility highlights the importance of ascertaining the processed state of *hh* proteins expressed in any particular patterning center to understand the potential *hh* activities generated.

- 107 -

### EXAMPLE 17

#### DUAL ROLES OF *hh* SIGNALING PROTEINS IN EARLY EYE AND BRAIN PATTERNING

In understanding the normal roles of N and C in eye and brain patterning, the N and C  
5 derivatives of the *Drosophila hh* gene may offer some insight. The *Drosophila* N  
derivative is retained close to its embryonic site of synthesis in a segmentally striped  
pattern (Tabata and Kornberg, *Cell*, 76:89-102, 1994; Taylor, *et al.*, *Mech. Dev.*, 42 89-  
96, 1993), is cell-associated when expressed in cultured cells, and is effectively bound  
by heparin agarose *in vitro*, suggesting the possibility of extracellular matrix association.  
10 The C-terminal fragment, in contrast, is not bound effectively by heparin agarose, is  
almost quantitatively released into the culture supernatant of expressing cultured cells,  
and is only diffusely localized in embryos. Although the activities of individual  
fragments have not been assayed, the biochemical differences and tissue distributions of  
*Drosophila* N and C may account for the short and long range nature of the functions  
15 associated with *hh* during *Drosophila* development.

Although the tissue distributions of zebrafish N and C are not known, their activities in  
ectopic expression assays are also suggestive of short- and long-range functions when  
considered in the context of normal expression patterns of *hh*, *pax-2* and *pax-6*. The  
normal gradient of *pax-2* expression in the optic vesicle extends a substantial distance  
20 from its maximum adjacent to the site of *hh* expression in the protuberance; the ability  
of ectopic C to activate *pax-2* therefore suggests that, consistent with the distribution of  
C in *Drosophila*, zebrafish C may carry out a long-range function. Repression of  
endogenous *pax-6* expression, in contrast, appears to be a short-range function since *pax-6*  
expression occurs close to endogenous *hh* expression. Efficient repression of *pax-6* is  
25 an attribute of constructs producing N, and a short-range function for N would be  
consistent with the distribution of N in *Drosophila*.

- 108 -

Two types of *hh*-dependent activity have been reported for *hh*-transfected cultured cells. One is the apparent contact-dependent induction of floor plate markers (Roelink, H., *et al.*, *Cell* 76:761-775, 1994); the second induction of sclerotome markers in presomitic mesoderm, is diffusible and acts at long-range.

5

### EXAMPLE 18

#### CHARACTERIZATION OF XENOPUS *hh*

##### 1. Materials and Methods

cDNAs encoding full-length *Xenopus* hedgehogs, or encoding amino terminal or carboxy  
10 terminal domains linked to secretory leader sequences were transcribed *in vitro* to yield  
translatable messenger RNA. The synthetic messenger RNAs, and control mRNAs, were  
microinjected into the animal poles of cleavage stage *Xenopus* embryos, which were  
allowed to develop to the blastula stage, at which time the animal cap explants were  
prepared from the upper one fourth of the embryo. These blastula cap explants were then  
15 cultured *in vitro* in physiological saline in the presence or absence of the transforming  
growth factor beta family member, recombinant human activin A. All explants were  
allowed to develop until control embryos had grown to neurula stage, or to tadpole stage.  
Importantly, blastula caps left untreated differentiate from ectoderm into atypical  
epidermis. Blastula caps treated with activin differentiate into mesodermal and neural  
20 cell types. Thus, the question was whether hedgehog, or its proteolytic derivatives,  
would change the differentiation of cells away from becoming epidermis, and into  
another cell type. A second question was whether hedgehog can work with activin to  
alter the normal response of the tissue to either factor by itself.

Explants were then extracted to yield mRNA by methods commonly used by those of  
25 skill in the art, which was used as template with reverse transcriptase to yield cDNA.  
The cDNA was then used as template with various sets of primers for PCR for specific  
genes, reverse-transcriptase-polymerase chain reaction, or RT-PCR. This results in

- 109 -

specific amplification of radioactive products which are diagnostic for the presence and level of the messenger RNAs which were present in the explants. Samples were separated on polyacrylamide gels, which were exposed to X-ray film to yield the bands shown in the figures. Thus, the darker bands correspond to a greater level of the specific mRNA.

FIGURE 18A and B demonstrate that hedgehog induces pituitary and anterior brain genes, and can cooperate with activin or with neural inducers such as noggin and follistatin which are induced by activin to elevate expression of these genes in explanted embryonic tissue. All odd numbered lanes lack reverse transcriptase in the RT-PCR reaction and are negative controls. All even numbered lanes have this enzyme, and thus give specific bands to mRNA. In Panel A, Lanes 1-2 are control blastula caps, lanes 3-4 are *Xenopus* hedgehog-expressing blastula caps, lanes 5-6 are control blastula caps treated with activin, lanes 7-8 are hedgehog-expressing blastula caps treated with activin, and 9-10 are prolactin-expressing blastula caps treated with activin to serve as a control for simply expressing a secreted protein in the blastula cap. The primers used for the assay are shown to the left of each panel, *i.e.*, XAG 1 is a cement gland marker, XANF1B is a pituitary marker, otx-A is an anterior brain marker, en-2 is a midbrain-hindbrain boundary marker, krox 20 is a rhombomere-specific hindbrain marker, *HIHbox* 6 is a posterior hindbrain marker, NCAM is a general neural marker, activin is a control for mesoderm induction, and elongation factor is a positive control to shown that all even numbered lanes did in fact have cDNA present.

The panel labelled XANF1B detects a pituitary gene. Lane 4 (panel A) shows that hedgehog induces this pituitary marker, and thus likely pituitary cell types, in blastula cap explants (see also FIGURE 20, lane 6, for a stronger signal showing this), when compared to control explants in the absence of hedgehog (lane 2), which do not express this gene. Lane 6 shows that explants treated with activin, in the absence of hedgehog, also express the pituitary gene. Lane 8 shows that explants treated with both hedgehog, and with activin, give highest levels of the pituitary gene. Lane 10 proves that this effect

- 110 -

of hedgehog is specific, since prolactin, another secreted protein, does not lead to this elevated level of pituitary gene.

The panel labelled OTX-A detects this anterior brain gene. Lane 4 (and 6 in Figure 20) shows that hedgehog can induce this neural-specific gene. Lane 8 shows that the level of this neural gene is highest in tissue treated with both activin and hedgehog, relative to hedgehog alone (lane 4), or activin alone (lane 6), and control explants do not express this gene (lane 2). Again, this effect is specific to hedgehog, since prolactin (lane 10) did not lead to elevated expression of this gene. The panel labelled XAG-1 detects a cement gland-specific gene, and lane 4 shows that hedgehog induces this gene at high level.

10 In panel 18B, embryos were injected with N or  $\Delta$ N-C, and some animal cap explants were treated with activin before culturing until sibling embryos reached tailbud stage. Lanes 1, 2: control animal caps from uninjected embryos. Lanes 3, 4: control animal caps from uninjected embryos, treated with activin. Lanes 5, 6: animal caps from embryos injected with N and treated with activin. Lanes 7, 8: animal caps from embryos injected with  $\Delta$ N-C and treated with activin. Whereas N displays activities in activin-treated explants similar to those of *X-bhh* (see B)  $\Delta$ N-C produces the opposite effect, decreasing anterior and increasing posterior neural marker expression. As shown in Figure 18B, N behaves like *X-bhh* in that it induces elevated levels of XANF-2 and Otx-A (lane 6) relative to control activin-treated animal caps (lane 4). Moreover, N also leads to a decrease in the expression of more posterior markers, such as *krox-20* and *Xlhbox-6*, as observed following injection of *X-bhh*. In contrast to the activity of N (Fig. 4C, lane 6),  $\Delta$ N-C decreases the expression of the anterior neural genes XANF-2 or Otx-A (Fig. 4C, lane 8) in activin-treated animal caps when compared to uninjected controls (lane 4). Moreover,  $\Delta$ N-C also leads to an increase in the expression of more posterior markers, such as *En-2* and *Xlhbox-6*.

FIGURE 19 shows *X-bhh* modifies the anteroposterior pattern of neural gene expression in explants under the influence of endogenous neural inducers. (A) Isolation of dorsal

- 111 -

explants from injected embryos for the preparation of Keller sandwiches (Keller and Danilchik, 1988; Doniach, *et al.*, 1992; redrawn from Doniach, 1993). (B) Keller sandwiches were made from uninjected (lanes 1 and 2) and *X-bhh*-injected (lanes 3 and 4) embryos, total RNA was isolated when control embryos reached stage 20, and RT-PCR was used to analyze the expression of XAG-1 and neural markers. XAG-1 is a cement gland marker, XANF-2 is an anterior pituitary marker, Otx-A is a forebrain marker, *En-2* demarcates the midbrain-hindbrain boundary, Krox-20 marks rhombomeres 3 and 5 of the hindbrain and *XlHbox-6* is a spinal cord marker. N-CAM is a general neural marker whose expression is not restricted along the anteroposterior axis. The EF-1 $\alpha$  control demonstrates that a comparable amount of RNA was assayed in each set. Note that expression of XAG-1 and anterior neural markers is stimulated by *X-bhh* treatment, whereas expression of posterior neural markers is suppressed.

FIGURE 20 demonstration of differential activities of N and C domains of hedgehog proteins. As in FIGURE 18 above, odd numbered lanes are negative control lanes, and positive numbered lanes show specific gene expression for the markers described above. The N domain of hedgehog is encoded in the construct called Xhh1208 (lane 8), and the C domain is encoded in the construct called Xhh1delta 27-208 (lane 10). The construct Xhh11-1270A (lane 12) is specifically mutated so that it is unable to undergo self-processing. The ability of the N and C domains to induce the genes described above is compared to control blastula cap explants (lane 4), entire embryos as a positive control (lane 2), blastula cap explants expressing a mutated hedgehog as a negative control (lane 14), blastula caps expressing the entire hedgehog 1 (lane 6), and blastula cap explants treated with an independent neural inducer, noggin (lane 16) (discovered by Richard Harland at University of California at Berkeley).

Examining the first panel for the cement gland marker XAG-1 clearly shows that intact hedgehog (lane 6) and the N domain (lane 8) and the processing defective hedgehog (lane 12) are much better than inducing the cement gland than is the C domain (lane 1). Examining the second panel demonstrates that the C domain (lane 10) is better at

- 112 -

inducing the pituitary gene XANF1B than is the N domain (lane 8). Since the N domain induces the XAG-1 marker better, described in point A above, the two results together clearly demonstrate that the N and C domains have distinguishable activities. Examination of the remaining panels shows that all described activities of the normal  
5 hedgehog (lane 6 ) can be defined in terms of the activities of the N and C domain.

Examining the third panel, for the forebrain gene *otx-A*, shows that both the N domain (lane 8) and C domain (lane 10) induce similar levels of this gene, but the processing defective hedgehog (lane 12) is better than either at inducing this gene.

Examining the fourth panel of this figure (NCAM), (as well as the FIGURE 18 panels  
10 EN-2, *krox20*, *XIHbox6*, and NCAM), shows that hedgehog does not induces these more posterior neural genes. Notably, *noggin* (lane 16) is able to induce pituitary gene and forebrain gene, but it also induces the general neural gene, NCAM, which hedgehog does not. This clearly shows that hedgehog is a distinct activity from the neural inducer *noggin*, and has a more restricted ability to induce neural genes.

15 Experiments in the *Xenopus* embryo were conducted by injecting full-length hedgehog RNA, and immunoprecipitating with a C-domain specific antibody, which proves that full length hedgehog does in fact get processed *in vivo* in vertebrates, consistent with the data shown in earlier Examples in *Drosophila*. Thus, the ideas for the utility of detecting hedgehog N and C domains is based on knowledge that such domains do appear through  
20 hedgehog processing in vertebrates. Moreover, the knowledge that hedgehog processing does occur *in vivo* naturally raised the question of whether the resulting N and C domains have independent activity.

The results in FIGURE 18 are novel insofar as they establish that the activity of hedgehog in inducing a pituitary gene, and an anterior brain gene, may be enhanced by  
25 the TGF $\beta$  family of growth factors. This enhancement likely applies to the N and C

- 113 -

domains described in FIGURE 20, since the genes analyzed are the same. This enhancement is due

to *hh* synergizing with neural inducing factors which are themselves induced by TGF- $\beta$  family members, including but not limited to such molecules as noggin and follistatin.

- 5 The data in FIGURE 20 makes several important points. First, the data show that the N and C domains have different though somewhat overlapping activities, and that the N and C activities added together account for all of the observed activity of the intact hedgehog protein. Thus, any clinical or diagnostic uses of hedgehog might be improved by use of the N or C domain, as one generally wishes to use the smallest protein which has an
- 10 activity for clinical work, as it is less likely to evoke adverse immune responses, or other adverse side effects. Second, the data show that the C domain is better than the N domain in inducing pituitary gene expression and, since it has less induction of cement gland genes that intact hedgehog, or N domain, it suggests that the C domain might be useful in clinical situations where one wishes to enhance the development or expression
- 15 of the pituitary as specifically as possible. As the pituitary is the source of a number of hormones, any treatment for enhancing pituitary cell growth and activity would ideally have as few side effects as possible, and the C domain is thus a viable candidate for therapies with enhanced pituitary cell growth and function in mind. Third, relating to studies regarding noggin, FIGURE 20 shows clearly that while both hedgehog and
- 20 noggin can induce pituitary gene expression, hedgehog is more specific, since hedgehog does not induce the general neural marker NCAM, whereas noggin induces NCAM as well as pituitary. Fourth, the hedgehog which was mutated to prevent processing (lane 12) is as active as full-length and wild-type hedgehog (lane 6) in inducing pituitary gene expression, but the processing defective hedgehog is better at inducing the forebrain
- 25 marker *otx-A*. Thus, for some clinical applications of hedgehog in inducing specific cell types, it is possible that the processing-defective hedgehog will be superior compared to normal hedgehog.

- 114 -

FIGURE 21 shows  $\Delta N$ -C interferes with X-*bhh* and N activity in animal cap explants. Embryos were injected with various RNAs, animal cap explants were cultured until sibling embryos reached tailbud (stage 25), at which time RT-PCR was used to analyze the expression of the cement gland marker XAG-1 and the control RNA, EF-1 $\alpha$ . Lanes 1, 2: control animal caps from uninjected embryos. Lanes 3, 4: animal caps from embryos injected with both X-*bhh* and prolactin RNAs. Lanes 5, 6: animal caps from embryos injected with both X-*bhh* and  $\Delta N$ -C. Lanes 7, 8: animal caps from embryos injected with both N and prolactin RNAs. Lanes 9, 10: animal caps from embryos injected with both N and  $\Delta N$ -C. The N and X-*bhh* experiments were conducted independently and thus absolute levels in lanes 3-6 should not be compared to those in lanes 7-10. Note that the induction of XAG-1 expression by X-*bhh* or N is reduced by co-injection of  $\Delta N$ -C.

An internal deletion of X-*bhh* ( $\Delta N$ -C) blocked the activity of X-*bhh* and N in explants and reduced dorsoanterior structures in embryos. As elevated *hh* activity increases the expression of anterior neural genes, and as  $\Delta N$ -C reduces dorsoanterior structures, these complementary data support a role for *hh* in neural induction and anteroposterior patterning.

$\Delta N$ -C deletes amino acids 28-194 of X-*bhh*. The primary translation product is predicted to undergo signal sequence cleavage removing amino acids 1-23, and to undergo autoproteolysis. Based on the cleavage site in *Drosophila hh* (Porter, *et al.*, *Nature*, 374:363, 1995) autoproteolysis would generate a C domain of X-*bhh* amino acids 198-409, as well as a predicted seven amino acid polypeptide, representing amino acids 24-27, and 195-197 (Lai, *et al.*, *Development* 121:2349, 1995). Analysis of the effect of  $\Delta N$ -C on neural markers was by standard methods including Northern blot analysis and in situ hybridization (Lai, *et al.*, *supra*, incorporated herein by reference).

Although  $\Delta N$ -C does not induce the cement gland marker XAG-1, it decreases the expression of anterior ectodermal and neural markers in activin-treated animal caps.

- 115 -

Thus,  $\Delta$ N-C has the capacity to affect neural patterning.  $\Delta$ N-C also promotes an increase in posterior neural markers in activin-treated animal caps. Mixing  $\Delta$ N-C with N or full length X-*bhh* at a 1:1 ratio led to a dramatic inhibition of the induction of cement gland in animal cap assays, supporting the hypothesis that  $\Delta$ N-C interfered with X-*hh*.

5

**EXAMPLE 19****CHOLESTEROL MODIFICATION OF HEDGEHOG POLYPEPTIDE**

In addition to peptide bond cleavage, Hh autoprocessing causes the covalent attachment of a lipophilic adduct to the COOH-terminus of Hh-N<sub>p</sub> (J.A.Porter et al., *Cell* 86, 21, 1996). This modification is critical for the spatially restricted tissue localization of the  
10 Hh signal; in its absence, the signaling domain exerts an inappropriate influence beyond its site of expression (J.A.Porter et al., *Cell* 86, 21, 1996). Physical and biochemical characterization of this lipophilic adduct indicates that it is not the glycosyl phosphatidyl inositol (GPI) anchor, the only other known lipophilic modification associated with secreted cell surface proteins in eukaryotes (S. Udenfriend and K. Kodukula, *A*  
15 *nnu.Rev.Biochem.* 64, 563, 1995; and P.J.Casey, *Science* 268, 221, 1995).

*In vitro* studies of Hh autoprocessing were performed using a bacterially expressed derivative of the Drosophila protein, His<sub>6</sub>Hh-C, in which the majority of the NH - terminal signaling domain and the signal sequence are replaced by a hexa-histidine tag. Cleavage of this protein occurs between residues corresponding to Gly 257 and Cys 258  
20 (J.A. Porter et al., *Nature* 374, 363, 1995) and likely proceeds through a labile thioester intermediate formed by the cysteine thiol and the glycine carbonyl carbon. In the presence of high concentrations of thiols or other small molecules with strongly nucleophilic properties at neutral pH, cleavage of the peptide results from nucleophilic attack upon the thioester carbonyl, causing displacement of the thiol group and formation  
25 of an adduct to Gly 257 by the attacking nucleophilic (Fig 22A). Thus, in reactions with 50 mM dithiothreitol, *in vitro* cleavage of His<sub>6</sub>Hh-C proceeded to greater than 50%

- 116 -

completion within three hours at 30°C (Fig. 22B). At 1mM dithiothreitol, however, the reaction yielded no visible cleavage product (Fig 22B).

Figure 22 shows lipid stimulation of Hh autoprocessing *in vitro*. Panel A illustrates the mechanism of Hh processing. The reaction is initiated by formation of a thioester  
5 between the thiol side chain of cysteine 258 and the carbonyl carbon of glycine 257, and N to S shift. This activated intermediate then undergoes a nucleophilic attack by DTT *in vitro* or by a lipophilic nucleophilic *in vivo* resulting in cleavage as well as a formation of a covalent adduct at the carboxy-terminus of the amino-terminal product, X denotes the attacking nucleophilic. Panel B shows a coomassie blue stained SDS-polyacrylamide  
10 gel showing *in vitro* autocleavage reactions of the bacterially expressed His6Hh-C protein (~29kD) incubated for 3 hours at 30°C with no additions (lane 1), 50 mM DTT (lane 2), 1 mM DTT (lane 3), or 1 mM DTT plus bulk S2 cell lipids (lane 4). The Hh-C product of the autoprocessing reaction migrates as an ~25kD species (lanes 2 and 4); the ~5kD NH<sub>2</sub>-terminal product is not resolved in this gel.

15 The *in vivo* reaction resulted in lipophilic modification of the NH<sub>2</sub>-terminal signaling domain. The most direct mechanism by which this could occur, by analogy to the *in vitro* mechanism (Fig 22A), would be for a lipid to function as the displacing nucleophilic in attack of the thioester. To explore this possibility, bulk lipids extracted from *Drosophila* S2 cultured cells (I.Schneider, *J Embryol Exp Morph* 27, 353 (1972); and F.M. Ausubel  
20 et al., *Current protocols in molecular biology* (Greene Publishing Associates and Wiley-Interscience, New York, 1995) were added to the *in vitro* processing reaction in the presence of 1 mM dithiothreitol. Cleavage was observed and the reaction proceeded to 20% completion in a three hour period (Fig 22B). The reaction continues beyond this time and reaches ~50% completion by 18 hours.

25 To identify the components active in the reaction, the bulk S2 lipids were separated into two classes, neutral and complex, by silicic acid column chromatography (W.W. Christie, *Lipid analysis* (Pergamon, Oxford, ed.2nd, 1982). Figure 23A is a thin layer chromatog-

- 117 -

raphy (TLC) plate coated with silica gel G (Merck) showing the fractionation of bulk S2 cell lipids using a heptane:ether:formic acid solvent (80:20:2). Six major spots are visualized by acid charring and are indicated by letters A-F. Figure 23B is a Coomassie blue-stained SDS-polyacrylamide gel showing *in vitro* autocleavage reactions of the bacterial expressed His<sub>6</sub>Hh-C protein incubated with 1 mM DTT plus either unfractionated S2 cell lipids (lane 1), or spots A through F (lanes 2-7, respectively). Addition of lipid spot B but no other resulted in processing of His<sub>6</sub>Hh-C protein. Figure 23C is TLC of S2 cell lipids (lane 1) along with selected lipid standards: phosphatidylcholine (lane 2), a diacylglycerol (lane 3), cholesterol (lane 4), stearic acid (lane 5), a triacylglycerol (lane 6), and cholesteryl ester (lane 7). Lipid spot B comigrates with cholesterol, as also demonstrated by mixing radio-labeled cholesterol with S2 lipids before TLC fractionation. Figure 23D is a Coomassie blue stained SDS-polyacrylamide gel showing that relative to 1 mM DTT alone (lane 1) cholesterol (0.35 mM) + 1 mM DTT (lane 2) stimulates His<sub>2</sub>Hh-C autocleavage *in vitro*. Figure 23E is an autoradiogram of electrophoretically-resolved products of His<sub>6</sub>Hh-C autocleavage reactions driven by 20 mM DTT (lane 1) or 1 mM DTT+0.35 mM cholesterol (lane 2). For lane 1 [<sup>3</sup>H]cholesterol (3 μCi) was added at the end of the incubation period just prior to electrophoresis; for lane 2 [<sup>3</sup>H]cholesterol was present throughout the incubation period and is incorporated into the amino-terminal product of the reaction. To resolve the ~5 kD product of His<sub>6</sub>Hh-C autocleavage, reaction products were separated in 17% SDS-polyacrylamide gels.

The activity was found exclusively in the neutral class, so the lipids were subjected to preparative thin layer chromatography (TLC) using a solvent system that resolved neutral lipids (W.W. Christie, *Lipid analysis* (Pergamon, Oxford, ed.2nd, 1982) (Fig 23A). Lipid spots were visualized with iodine vapor or acid charring, and adsorbent at the corresponding positions of identical uncharred plates was excised and extracted with chloroform/methanol/water. Only lipids extracted from spot B displayed stimulatory activity in the *in vitro* cleavage reaction (Fig 23B).

- 118 -

With the use of various lipid standards, it was found that spot B comigrated with cholesterol (Fig 23C). In addition, the active S2 cell-derived lipid displayed the same mobility as cholesterol in two other solvent systems and gave a positive color test when sprayed with a specific reagent that reacts with sterols; W.W. Christie, *Lipid analysis* (Pergamon, Oxford, ed.2nd, 1982); and R.R.Lowry, *Journal of Lipid Research* **9**, 397, 1968). Taken together these results imply that the active lipid component is in the sterol fraction of the S2 lipids. Indeed, it was found that cholesterol, which is the principal sterol in eukaryotic cell membranes (W.W. Christie, *Lipid analysis* (Pergamon, Oxford, ed.2nd, 1982)), displayed stimulatory activity similar to that observed with lipids extracted from spot B when added in pure form to the *in vitro* processing reaction (Fig 23D). To establish that the stimulatory activity of cholesterol is a result of its participation as a modifying group, it was shown that <sup>3</sup>H-labeled cholesterol added to the 1 mM dithiothreitol reaction was incorporated into the NH<sub>2</sub>-terminal product (Fig 23E). No incorporation was seen, however, when [<sup>3</sup>H]cholesterol was added just prior to electrophoresis to a reaction incubated for 3 hours with 20 mM dithiothreitol (Fig 23E). Also consistent with covalent cholesterol addition, the NH<sub>2</sub>-terminal fragment of His<sub>6</sub>Hh-C generated by the cholesterol-driven reaction migrated just beneath the 6 kD marker, whereas the product of the reaction driven by 20 mM dithiothreitol migrated just above this marker (Fig 24A). Such a shift in mobility, thought to result from an increase capacity for SDS binding to the covalently linked lipid (M.L.Cardoso de Almeida and M.J. Turner, *Nature* **302**, 349, 1983), was also noted for Hh-N<sub>p</sub> as compared to the precisely truncated NH<sub>2</sub>-terminal fragment (Hh-N, truncated following Gly 257).

The part of the sterol most likely to act as attacking is the 3β hydroxyl. Such an attack would leave cholesterol as a covalent adduct in ester linkage to the carboxylate of the terminal residue of the NH<sub>2</sub>-terminal fragment (GLY 257).

Figure 24A shows Coomassie stained gels of His<sub>6</sub>Hh-C autocleavage reactions carried out in the presence of 20 mM DTT (lane 1), or 1 mM DTT+0.35 mM cholesterol (lane 2). Lane 3 contains a mixture of the samples loaded in lanes 1 and 2. The amino-terminal

- 119 -

product of the cholesterol driven reaction migrates approximately 2 kD faster than the DTT-driven reaction fragment. Figure 24B is Coomassie stained gels showing protein products of His<sub>6</sub>Hh-C autocleavage reactions carried out in the presence of 1 mM DTT+0.35 mM cholesterol (lanes 1 and 2) or with 20 mM DTT (lane 3). Prior to loading  
5 the gel, samples in lane 2 and 3 were incubated for 60 minutes with 50 mM KOH in 90% methanol (M.C. Field and A.K. Menon, in *Lipid modification of proteins* N.M. Hooper, A.J. Turner, Eds. (Oxford University Press, New York 1992) pp.155). Base treatment causes the cholesterol-driven amino-terminal reaction product to comigrate with the corresponding DTT-driven reaction product. Figure 24C is an autoradiogram of  
10 immunoblotted Hh amino-terminal domains purified from cultured S2 cells. Amino-terminal domains were derived either from a construct truncated after glycine 257 (Hh-N lanes 1,3,4,8, and 9) or from a construct encoding wild-type Hh that produces the amino-terminal domain via the processing reaction (Hh-N<sub>p</sub>, lane 2,3,5,6,7,8, and 9). Proteins were either directly loaded (lanes 1 and 2) or base-treated (M.C. Field and A.K. Menon,  
15 in *Lipid modification of proteins* N.M. Hooper, A.J. Turner, Eds. (Oxford University Press, New York 1992) pp.155) for 5 minutes (lane 5), 20 minutes (lane 6) or 1 hour (lanes 7 and 4) prior to electrophoresis. Lane 3 contains a mixture of the samples loaded in lanes 1 and 2, lane 8 contains a mixture of the samples loaded in lanes 7 and 4, and lane 9 contains a mixture of the samples loaded in lanes 7 and 2. Upon base treatment,  
20 Hh-N<sub>p</sub> undergoes a shift in mobility from 18.5 kD to 19.5 kD, the mobility of the unmodified Hh-N protein.

Ester bonds are subject to hydrolysis in alkaline conditions and base treatment prior to electrophoresis indeed reduced the migration of the cholesterol-driven reaction product to a position coinciding with that of the dithiothreitol-driven reaction product. These  
25 results are consistent with stimulation of the *in vitro* processing reaction by direct nucleophilic attack of cholesterol on the thioester intermediate to form an ester-linked adduct. If processing of Hh also results in formation of an ester-linked cholesterol adduct *in vivo*, then the protein-lipid linkage should be subject to base hydrolysis with a concomitant shift in electrophoretic mobility of the protein (normally 18.5 kD). The

- 120 -

immunoblot in Fig 24C shows the base-induced appearance of a species of reduced mobility (19.5 kD), which increased in abundance from ~1/3 of the total after five minutes of treatment to most of the immunoreactive protein after one hour. This novel species comigrated with truncated, unprocessed Hh-N, which is not affected by base treatment. These data are consistent with an ester bond as the protein-lipid linkage in Hh-N<sub>p</sub>.

To confirm the involvement of cholesterol in formation of the Hh-N<sub>p</sub> adduct *in vivo*, S2 cells containing an inducible wild-type Hh construct were metabolically labeled with [<sup>3</sup>H]cholesterol. Figure 25A is an autoradiogram of a gel loaded with total cell proteins from S2 cells containing a stably integrated Cu<sup>++</sup>-inducible hedgehog gene. Prior to harvesting, these cells were grown in media supplemented with [<sup>3</sup>H]cholesterol in the absence (lane 1) or presence (lane 2) of 1 mM CuSO<sub>4</sub>. [<sup>3</sup>H]cholesterol incorporation is dependent upon Cu<sup>++</sup> induction (lane 2) and is restricted to a single protein species migrating at a position corresponding to Hh-N<sub>p</sub>. Figure 25B is an HPLC profile of sterols separated on a C18 column by isocratic elution with a solvent containing methanol:ethanol:water (86:10:4) (R.J. Rodriguez and L.W. Parks, *Methods of Enzymology* 111, 37, 1985). ~5 μg of each sterol was mixed, loaded, and elution monitored by absorbance at 210 nM. The structure of cholesterol is shown above cholesterol peak. Other sterols include: 1) 10 desmosterol, which contains one additional double bond between carbon 24 and 25; 2) 20 7-dehydrocholesterol, which contains one additional double bond between carbon 7 and 8; 3) campesterol which contains an additional methyl group on carbon 24; and 4) sitosterol, which contains an additional ethyl group on carbon 24. Figure 25C shows HPLC analysis as in (B) of the adduct released by base treatment of Hh-N<sub>p</sub> metabolically labeled with [<sup>3</sup>H]cholesterol (A). The radioactive species recovered from the metabolically labeled protein collates with cholesterol. Figure 25D shows metabolic labeling of vertebrate *Sonic hedgehog* protein with [<sup>3</sup>H]cholesterol. Autoradiogram of a gel loaded with total cell proteins from COS-7 cells transfected with a wild-type *Sonic hedgehog* expression construct (*Shh*, lane 1) or a construct that generates an unprocessed amino-terminal protein truncated after the conserved glycine

- 121 -

at the site of autocleavage (*Shh-N*, lane 2). The COS-7 cells were incubated in culture medium supplemented with [ $^3$ H]cholesterol for 24 hours prior to and 36 hours after transfection (COS-7 cells grown at 37°C in DMEM supplemented with 10% fetal calf serum were plated at ~35% confluence onto two 35 mm dishes in 1 ml of Optimem media (Gibco) containing 1.5% fetal bovine sera and 25  $\mu$ Ci of [ $^3$ H]cholesterol, giving  
5 ~40  $\mu$ g/ml as the final concentration of cholesterol with a specific activity of 2 Ci/mmol (labeling medium). After 24 hours the labeling medium was removed and the cells were transfected for 6 hours with *Shh* or *Shh-N* expression constructs using lipofectamine (Gibco) and serum-free DMEM media. After transfection, 1 ml of fresh labeling medium  
10 was added to each dish and the cells were incubated for 36 hours at 37°C. The cells were then harvested without washing, lysed on the plate with Tris buffered saline plus 1% Triton X-100 and the total cell proteins were precipitated with acetone, washed and analyzed as described above for the S2 cell proteins). A strongly labeled species with the *Shh* but not *Shh-N* construct. Several other less heavily labeled species are apparent  
15 in both lanes, and may represent other cholesterol-modified proteins.

After 48 hours of growth in the presence of [ $^3$ H]cholesterol, induced and uninduced cultured cells were detergent extracted and total cell proteins were subjected to SDS-PAGE followed by fluorography (Metabolic labeling of S2 cultured cells with [ $^3$ H]cholesterol was performed essentially as described (Silberkang, *et al.*, *J Biol. Chem.*  
20 258:8503, 1983). Briefly, cells containing a stably integrated Cu $^{++}$ -inducible *hedgehog* gene were grown at 23°C for two weeks in Schneider cell media (Gibco) containing a 5% fetal bovine serum depleted of lipoprotein (low cholesterol media, ~20  $\mu$ g/ml cholesterol). These cells were then plated at 40% confluence onto two 35 mm tissue culture dishes (Nunc) in 1 ml of low cholesterol media supplemented with 300  $\mu$ Ci of  
25 labeled cholesterol, [1.2.6.7- $^3$ H (N)] 65 Ci/mM (NEN) giving a specific activity for cholesterol in this medium of ~5 Ci/mmol. After 24 hours (1 doubling time) one plate of cells was induced to express Hh protein by the addition of CuSO $_4$  (1 mM final concentration). After an additional 24 hours the cells from both dishes were harvested, lysed in Tris buffered saline containing 1% Triton X-100, and total cell protein was

- 122 -

precipitated with 5 volumes of cold acetone. The protein pellet was resuspended in 2% SDS in H<sub>2</sub>O and reprecipitated with acetone several times to remove unincorporated radioactivity prior to loading onto SDS polyacrylamide gels for analysis. Initial labeling experiments in which 25  $\mu$ Ci of cholesterol was added resulted in ~10 fold decrease in extent of label incorporated into the inducible Hh-N<sub>p</sub> protein). Whereas uninduced cells showed no incorporation of [<sup>3</sup>H]cholesterol into cellular proteins, cells induced to express Hh showed a single strong band with a mobility corresponding to that of Hh-N<sub>p</sub> (Fig 25A). Given the hydrophobic character of Hh-N<sub>p</sub>, these results suggest that either cholesterol itself or a sterol derivative constitutes the lipophilic adduct of Hh-N<sub>p</sub>. To determine whether cholesterol is the final form of the adduct, radio-labeled Hh-N<sub>p</sub> protein excised from a gel was base-treated to release the adduct, which was then isolated by either extraction (HPLC analysis of the Hh-N<sub>p</sub> adduct involved gel isolation of the radioactive band, KOH/methanol treatment of the band to break the ester linkage as described, followed by neutralization of the solution with acetic acid, drying in a speedvac, resuspension in H<sub>2</sub>O and extraction of the hydrophobic radioactivity with ether. After evaporation of the ether the sample was resuspended in isopropanol and applied to the C18 column for analysis. Radio-labeled adduct was then subjected to analysis by HPLC with a method specifically designed to resolve various sterols (R.J. Rodriguez and L.W. Parks, *Methods of Enzymology* 111, 37, 1985) (Fig 25B). The radioactive adduct released from Hh-N<sub>p</sub> eluted at the same position as the cholesterol standard, and no radioactivity was detected in any other fraction (Fig 25C).

The amount of radioactive cholesterol incorporated is consistent with that expected if all of the Hh-N<sub>p</sub> synthesized upon induction received a cholesterol adduct (The specific activity of [<sup>3</sup>H]cholesterol in the S2 cell labeling medium was ~5 Ci/mmol. Assuming after a 24 hour doubling time that this concentration approximately represents that within the S2 cell membrane, then any protein subsequently expressed and receiving cholesterol as an adduct would also be labeled at the same specific activity. As determined by standardized coomassie blue staining, ~50-100 ng or 2.5 to 5 picomoles of Hh-N<sub>p</sub> is produced by one 35 mm dish of S2 cells containing the Cu<sup>++</sup>-inducible Hh construct

- 123 -

during 24 hours of induction with 1mM CuSO<sub>4</sub> (13). This predicts ~12.5 to 25 nCi or 2.75 x 10<sup>4</sup> to 5.5 x 10<sup>4</sup> dpm of radioactivity would be incorporated into Hh-N<sub>p</sub> protein produced in our labeling experiment assuming it is cholesterol modified. Total incorporation of radioactivity into Hh-N<sub>p</sub> during the *in vivo* labeling experiment  
5 described above was measured at ~5 x 10<sup>4</sup> dpm by excision and scintillation counting of an Hh-N<sub>p</sub> gel band), suggesting that other cellular components do not compete effectively as nucleophilic adducts in the *in vivo* autoprocessing reaction. Also consistent with a homogenous adduct, the mass of cholesterol is consistent with the mass previously measured by mass spectrometry of processed protein purified from cultured  
10 cells. A recent MALDI mass spectral analysis gave a mass of ~430 daltons for the Hh-N<sub>p</sub> adduct, ~9% larger than the mass of cholesterol (386.6). Detection of this modification required that Hh-N<sub>p</sub> be treated with CNBr/70% formic acid, i.e. full length Hh-N<sub>p</sub> could not be detected. The mass discrepancy noted above could be accounted for by the net addition of formic acid (45 daltons) during CNBr digestion. This reaction  
15 could involve the addition of H<sub>2</sub>O across the 5,6 double bond of cholesterol, a common reaction of secondary alkenes in strong acids [R.T. Morrison, R.N. Boyd, *Organic Chemistry* (Allyn and Bacon, Boston, ed.3rd, 1973)], followed by esterification of formate via this newly formed alcohol [B.I. Cohen, G.S. Tint, T.Kuramoto, E.H. Mosbach, *Steroids* 25, 365-378, 1975. To test whether the sterol backbone could be  
20 modified by the CNBr treatment, a positively charged cholesterol derivative (3β-(N-(N',N'-dimethylamino) ethanecarbamoyl)-cholesterol, Sigma) detectable by MALDI was examined. It was found that incubation of this sterol derivative in 70% formic acid alone resulted in the addition of 45 mass units to the sterol (13), a mass consistent with the net addition of a formic acid molecule). These *in vitro* and *in vivo* results show that the Hh-C  
25 processing domain functions as a cholesterol transferase; as a result of this activity, a cholesterol adduct is attached via an ester linkage to the COOH-terminus of the NH<sub>2</sub>-terminal signaling domain of the Hh protein.

To test whether processing of vertebrate *hedgehog* proteins results in the incorporation of cholesterol as a covalent adduct to the signaling domain, cultured green monkey

- 124 -

kidney cells (COS-7) were metabolically labeled with [<sup>3</sup>H]cholesterol and transfected with expression constructs containing (i) the full length murine *Sonic hedgehog* (*Shh*) open reading frame, leading to production of an autocatalytically processed signaling domain (*Shh-N<sub>p</sub>*) or (ii) *Shh* coding sequences precisely truncated at the site of cleavage, thus producing an unprocessed amino terminal signaling domain (*Shh-N*) (COS-7 cells grown at 37°C in DMEM supplemented with 10% fetal calf serum were plated at ~35% confluence onto two 35 mm dishes in 1 ml of Optimem media (Gibco) containing 1.5% fetal bovine sera and 25 μCi of [<sup>3</sup>H]cholesterol, giving ~40 μg/ml as the final concentration of cholesterol with a specific activity of 2 Ci/mmol (labeling medium). After 24 hours the labeling medium was removed and the cells were transfected for 6 hours with *Shh* or *Shh-N* expression constructs using lipofectamine (Gibco) and serum-free DMEM media. After transfection, 1 ml of fresh labeling medium was added to each dish and the cells were incubated for 36 hours at 37°C. The cells were then harvested without washing, lysed on the plate with Tris buffered saline plus 1% Triton X-100 and the total cell proteins were precipitated with acetone, washed and analyzed as described above for the S2 cell proteins). Cells expressing the full length construct contained a prominent radio-labeled species migrating at ~19 kD, suggesting that cholesterol is covalently added to *Shh-N<sub>p</sub>* (Fig. 25D). This band was not present in cultures expressing the truncated *Shh-N* protein (Fig. 25D), indicating that the incorporation of [<sup>3</sup>H]cholesterol is dependent on the presence of the *Shh* processing domain. These data strongly suggest that the ability to attach cholesterol as a covalent adduct during autocatalytic processing and cleavage is a universal property of Hh proteins. Several other protein species in addition to the *Shh* amino terminal domain also appeared to incorporate cholesterol in cells transfected with either construct, suggesting that covalent modification by cholesterol extends to proteins beyond the Hh family. This possibility is consistent with the recently reported occurrence of several sequences homologous to the Hh processing domain in association with amino terminal sequences distinct from hedgehog.

- 125 -

**EXAMPLE 20**

An experimental model for holoprosencephaly derives from the occurrence of epidemics of congenital craniofacial malformations among newborn lambs on sheep ranches in several National Forests of the western United States. The most dramatically affected lambs showed severe holoprosencephaly, including true cyclopia and other craniofacial malformations characteristic of holoprosencephaly. The occurrence of these defects was traced to grazing by pregnant ewes on the range plant *Veratrum californicum*. The compounds responsible were identified as a family of steroidal alkaloids; the structures of two of these, cyclopamine and jervine, are shown as compared to cholesterol in Figure 33. In Figure 33, sterols were extracted and analyzed by HPLC from COS7 cells metabolically labelled with [<sup>3</sup>H]-mevalonic acid in the presence or absence of jervine, a teratogenic plant steroidal alkaloid. In the presence of 28mM jervine, radiolabelled cholesterol levels were reduced and another radiolabelled sterol was found to accumulate. On the basis of its retention time in this reverse phase HPLC method, this abnormal sterol is tentatively identified as zymosterol, an intermediate in the cholesterol biosynthetic pathway.

Given the structural similarities of these compounds to cholesterol and the similar teratogenic effects of cholesterol synthesis inhibitors upon the offspring of pregnant rats, a reasonable mechanism to consider for the effects of these plant sterol derivatives was the inhibition of cholesterol biosynthesis. Accordingly, COS7 cultured cells treated with jervine were tested for defects in cholesterol biosynthesis by labelling with [<sup>3</sup>H]-mevalonic acid and then extracting and analyzing radiolabelled, non-saponifiable lipids.

Metabolic labeling and sterol analysis was essentially as described (Popjak et al. *J. Biol. Chem.* 264: 630-6238.1989; Rilling et al. 1993 *Arch. Biochem. Biophys.* 301: 210-215.), with minor modifications. Briefly, COS-7 cells were plated at ~35% confluence into two 60 mm dishes at 37°C in 4 ml each of Dulbecco's modified Eagle's medium (DMEM) supplemented with 10% fetal bovine serum (FBS). After 24 hr of growth the medium in

- 126 -

each dish was replaced with 2 ml fresh medium with 10% FBS; [ $^3\text{H}$ ]-mevalonic acid (NEN #NET 176) brought to a specific activity of 0.8 Ci/mmol in a 1% solution of bovine serum albumin was added to this medium to a final concentration of 20mM. At this time, one dish received 6ml of a 4 mg/ml solution of jervine in ethanol (final  
5 concentration 28 mM jervine), and the other received 6 ml of ethanol. After 24 hr further incubation, cells were washed in PBS, extracted with methanol, and 1 M potassium hydroxide (KOH) added to 10%. Following a three hour incubation at 60°C, the methanol/KOH mixture was extracted with diethyl ether, the extract dried down, resuspended in isopropanol, and subjected to reverse phase HPLC analysis by the method  
10 of Rodriguez and Parks (*Methods in Enzymology* 111: 37-511985).

Treated cells synthesized reduced levels of cholesterol and accumulated increased levels of another sterol that we have provisionally identified as the cholesterol precursor, zymosterol. The natural product jervine at these concentrations thus inhibits cholesterol biosynthesis in cultured cells in much the same manner as the synthetic drugs discussed  
15 above, although the specific enzyme(s) affected appear to differ. Given the similarities in their teratogenic effects, this inhibition seems likely to underlie the teratogenic effects of both the synthetic and natural compounds.

## EXAMPLE

Protein expression and purification: *Drosophila melanogaster* Hh protein in which most of the amino-terminal signaling domain and signal sequence have been replaced by a hexa-histidine tag (His<sub>6</sub>Hh-C<sub>25</sub>) was expressed as previously described (Porter et al., 1995). SeMet His<sub>6</sub>Hh-C<sub>25</sub> was prepared by expression in *E. coli* strain B834 (DE3) pLysS, a methionine auxotroph, and growth in minimal media as previously described (Leahy et al., 1994). This His<sub>6</sub>-tagged protein was purified on a Ni<sup>++</sup>-NTA agarose column and autocleavage stimulated by addition of 50 mM DTT. After removal of the DTT by dialysis, the cleaved protein was passed over a Ni<sup>++</sup>-NTA agarose column and the Hh carboxy-terminal domain, Hh-C<sub>25</sub>, collected in the column run through. Hh-C<sub>25</sub> was subjected to limited proteolysis by overnight incubation with 1:500 (w:w) subtilisin (Boehringer Mannheim) at 4°C. A protease-stable fragment of approximately 17 kDa, Hh-C<sub>17</sub>, was identified by SDS-PAGE and purified by anion-exchange chromatography utilizing a Mono-Q column (Pharmacia). The amino- and carboxy-terminal residues of Hh-C<sub>17</sub> were determined to be Cys-258 and Ser-408, respectively, by mass spectral analysis of cyanogen bromide-cleaved fragments. Mass spectral analysis was performed as previously described (Porter et al., 1996a).

Crystallization: Crystals were grown from hanging drops by the method of vapor diffusion (Wlodawer et al., 1975). 6 µl of a 1.4 mg/ml solution of Hh-C<sub>17</sub> in 1.4 mM β-mercaptoethanol were mixed with 2 µl of a 1:1 dilution of reservoir solution (20% PEG 3350, 80 mM ammonium sulfate, and 10 mM sodium cacodylate, pH 5.8) with distilled water and equilibrated over the reservoir solution. Crystals typically grew to a final size of 0.2 mm x 0.2 mm x 0.1 mm over 3-7 days. Crystals are in space group I2<sub>1</sub>3 with unit cell dimension a=b=c=101.54 Å.

Data collection and processing: All data were collected from crystals soaked in mother liquor made 10% (w/v) ethylene glycol and flash frozen in a gaseous nitrogen stream at -180°C. MAD data were collected at four wavelengths from a single SeMet crystal at beamline X-4A of the National Synchrotron Light Source at Brookhaven National Laboratory. Data were collected using Fuji HR-V phosphor-imaging plates and digitized using a Fuji BA-3000 scanner. 2° oscillations at φ and φ+180° were collected with no overlap for each oscillation range at each wavelength. All diffraction images were processed using the program DENZO and scaled with the program SCALEPACK (Otwinowski and Minor, 1997). <I+> and <I-> were used for MAD phase determination and partially recorded reflections were used in all cases. Diffraction data from different wavelengths were scaled with WVLSCAL and values for F<sub>A</sub> and optimal Γ and Γ' were calculated with MADLSQ (Hendrickson, 1991). Data collection statistics are shown in Table I.

Structure determination: Three selenium sites were deduced from  $F_A$  amplitudes using both the program SHELXS (Sheldrick, 1991) and Patterson methods. MAD phase determinations were made with the program MLPHARE (Collaborative Computational Project, 1994; Ramakrishnan and Biou, 1997), and solvent-flattening and histogram-matching were performed with the program DM (Collaborative Computational Project, 1994). An atomic model consisting of Cys-258 to Tyr-401 was readily built into electron density maps computed with MAD-derived phases for reflections in the range 20.0-2.0 Å using the program "O" (Jones et al., 1991). One round of simulated annealing and several rounds of Powell minimization using X-PLOR (Brünger, 1992) alternated with model building with "O" yielded the current model of Hh-C<sub>17</sub> consisting of 145 residues, Cys-258 to Ala-402, and 125 water molecules. The model was refined using the data collected at 0.9919 Å. One molecule is present in the asymmetric unit, and the solvent content is approximately 59%. All backbone torsion angles are within energetically acceptable regions. No electron density was observed for residues 403 to 408, but additional electron density was observed near the thiol group of Cys-258. As the crystallization buffer contained cacodylic acid, both AsO(CF<sub>3</sub>)<sub>2</sub> or an As atom were modeled in this density, but neither the crystallographic R-factor nor the free R-factor improved with these atoms added to the refinement and no atoms have been included in this region in the final atomic model.

Site-directed mutagenesis and in vitro autocleavage assays: His-329, Thr-326, and Asp-303 were each mutated to alanine (H329A, T326A, and D303A, respectively) and Leu-409 was mutated to a stop codon (His<sub>6</sub>Hh-C<sub>17</sub>) by the method of recombinant circle PCR (Jones and Winistorfer, 1992). His<sub>6</sub>-tagged proteins containing residues 83-471 of *Drosophila* Hh protein with residues 89-254 deleted and with the mutated residues were expressed in *E. coli* and purified to near homogeneity as previously described (Porter et al., 1995). Autocleavage activity of the mutant proteins was assessed in 15 µl reactions by incubating 1 µg of protein in 150 mM NaCl, 100 mM Tris-HCl (pH 7.4), 0.05% Triton X-100, 1.25 mM β-mercaptoethanol, and 2.5% glycerol with either 50 mM DTT or 350 µM cholesterol/1 mM DTT for 6 hours at 30°C. The cleavage products were then fractionated by SDS-PAGE and detected by Coomassie Brilliant Blue staining. The activity of D303A and His<sub>6</sub>Hh-C<sub>17</sub> were also assessed by incubating 1 µg of protein with 46 µM [<sup>3</sup>H]cholesterol (11.6 Ci/mmol)/1 mM DTT for 6 hours at 30°C. The proteins were then subjected to SDS-PAGE and labeled proteins detected by autoradiography.

Database searching and sequence alignment: Screening of the non-redundant protein sequence database at the National Center for Biotechnology Information (NIH) was performed using the BLASTPGP program, which is an enhanced version of BLAST that produces gapped alignments

(Altschul and Gish, 1996). Additional searches were performed using the PSI-BLAST (Position-Specific Iterative BLAST) program, which constructs position-specific weight matrices from the BLASTPGP output and employs them for subsequent iterations of database screening using a modification of the BLAST statistics (Altschul et al., in press). Alignments of multiple protein sequences were constructed using the CLUSTALW program (Thompson et al., 1994) or the MACAW program (Schuler et al., 1991).

### Domain Identification and Structure Determination

*Drosophila melanogaster* Hh in which the signal sequence and most of the amino-terminal signaling domain have been replaced by a hexahistidine tag was expressed in *E. coli* as previously described (Porter et al., 1995). Following purification with Ni<sup>++</sup>-NTA agarose, this protein cleaves itself in vitro in the presence of either DTT or cholesterol to liberate the 25 kDa Hh-C fragment (Hh-C<sub>25</sub>, residues Cys-258 to Asp-471). Hh-C<sub>25</sub> prepared by this method was found to be poorly soluble in the absence of detergents and susceptible to further proteolytic breakdown when concentrated to 1 mg/ml or greater. Treatment of Hh-C<sub>25</sub> with subtilisin, however, resulted in a protease-stable fragment of ~17 kDa molecular weight (Hh-C<sub>17</sub>) with improved solubility. Mass spectrometric analysis of cyanogen bromide cleavage fragments of Hh-C<sub>17</sub> showed it to consist of residues Cys-258 to Ser-408 (data not shown). All residues absolutely conserved in Hh-C homologues (Porter et al., 1996a), including the nematode sequences, are contained in Hh-C<sub>17</sub>. To determine if Hh-C<sub>17</sub> retained autoprocessing activity, a mutant version of His<sub>6</sub>-tagged Hh-C containing a termination codon at residue position 409 (His<sub>6</sub>Hh-C<sub>17</sub>) was expressed and assayed for autocleavage in the presence of DTT and cholesterol. As shown in Figure 2, His<sub>6</sub>Hh-C<sub>17</sub> is capable of cleaving itself in the presence of DTT but not cholesterol, indicating that His<sub>6</sub>Hh-C<sub>17</sub> is able to form the thioester intermediate (see Figure 1A) but that some portion of the carboxy-terminal 63 residues of Hh-C<sub>25</sub> (Leu-409 to Asp-471) is required for cholesterol transfer.

Crystals of Hh-C<sub>17</sub> that diffracted to at least 1.9 Å Bragg spacings were readily produced from both native and selenomethionyl-substituted (SeMet) protein. The crystal structure of Hh-C<sub>17</sub> was determined by the method of multiwavelength anomalous diffraction (MAD) using SeMet crystals (Hendrickson et al., 1990; Hendrickson, 1991). High quality experimental electron density maps allowed construction of an atomic model for Hh-C<sub>17</sub> residues Cys-258 to Ala-402 that readily refined to low R-factor with good stereochemistry. Final refinement and stereochemical statistics are summarized in Table 1.

### Description of Hh-C<sub>17</sub> Structure

Hh-C<sub>17</sub> possesses an all-β structure that is roughly disk-shaped with a diameter of ~35 Å and width of ~20 Å. The amino and carboxy termini emerge from the same surface of Hh-C<sub>17</sub> ~6 Å apart. A ribbon drawing and topology diagram of the Hh-C<sub>17</sub> structure are shown in Figure 3. An unexpected feature of the Hh-C<sub>17</sub> structure is the presence of two homologous subdomains related by a pseudo-twofold axis of symmetry (Figures 4A and 4B). The subdomains adopt an

irregular fold characterized by three extended  $\beta$ -hairpin loops and are intimately associated, burying 1372 Å<sup>2</sup> of surface area at a hydrophobic interface such that a single hydrophobic core exists for the entire Hh-C<sub>17</sub> molecule. The topology of the Hh-C<sub>17</sub> subdomains matches that of snake toxins such as cardiotoxin VII4 (Rees et al., 1990) and  $\alpha$ -bungarotoxin (Love and Stroud, 1986), but the toxin and Hh-C<sub>17</sub> structures do not superimpose well and these structures do not seem otherwise related. As discussed below, the full Hh-C<sub>17</sub> fold can be detected in the self-splicing region of inteins (Duan et al., 1997), and the evidence for a divergent evolutionary relationship in this case is strong.

Despite a low level of sequence conservation, the two *Drosophila* Hh-C<sub>17</sub> subdomains are superimposable with an r.m.s. deviation in  $\alpha$ -carbon positions of 1.38 Å, and several notable structural features, including  $\beta$ -bulges and specific  $\beta$ -turn types, are conserved between the subdomains (Figure 4C). A structure-based alignment of the *Drosophila* Hh-C<sub>17</sub> subdomain sequences is shown in Figure 4D. While 8 out of 50 amino-acid residues (16%) in this alignment are conserved, none of these 8 residues is absolutely conserved in both subdomains of all Hh-C homologues. A characteristic pattern of conserved amino-acid types, mostly hydrophobic residues, is discernible in an alignment of these homologues, however.

The level of structural similarity between the two Hh-C<sub>17</sub> subdomains suggests that Hh-C<sub>17</sub> could have arisen by tandem duplication of a primordial gene. The duplicated sequences do not, however, correspond directly to the compact subdomains observed in the Hh-C<sub>17</sub> structure. As can be seen in Figures 4B and 4C, the Hh-C<sub>17</sub> subdomains have exchanged homologous loop regions. Examination of Figure 4B shows how the loop exchange in Hh-C<sub>17</sub> could be achieved by a simple pivot of the loops about a single flex point. The structurally cohesive subdomains of Hh-C<sub>17</sub> are thus mosaics composed of elements from both units of the tandem sequence duplication. To illustrate, if the three successive loops in each Hh-C<sub>17</sub> subdomain are labeled 1-2-3 and A1-A2-A3-B1-B2-B3 in the duplicated molecule prior to loop swapping, then the exchange of the third loop between subdomains can be represented as A1-A2-(A3-B1-B2)-B3 where the structurally distinct subdomains are composed of loops either inside or outside of the parentheses (see Figure 4B). We note that duplication coupled with an interdomain structural exchange such as appears to have occurred in Hh-C<sub>17</sub> provides a mechanism to generate permutations in the order in which specific structural elements occur in the amino-acid sequence. Such permutations have been noted in other systems including saposin homologues (Ponting and Russell, 1995) and bacterial glucanases (Heinemann and Hahn, 1995).

The exchange of domains or elements of secondary structure has been observed in several proteins and is believed to result in a more stable association of subunits in multidomain proteins (Bennett et al., 1995). Exchange of structural regions has principally been observed between independent polypeptide chains within homodimers, but the lac operon repressor and homologues

also appear to represent a case of exchange between duplicated domains within a single polypeptide chain (Schumacher et al., 1994; Lewis et al., 1996).

### Active Site Residues

The amino-terminal residue of Hh-C<sub>17</sub>, Cys-258, is involved in both the thioester formation and cholesterol transfer steps of Hh autoprocessing (see Figure 1A). Amino-acid side chains participating directly in Hh autoprocessing chemistry will most likely possess polar groups, and the only such residues near Cys-258 in the Hh-C<sub>17</sub> structure are His-329, Thr-326, and Asp-303. The arrangement of these three amino acids in relation to Cys-258 is shown in Figures 5A and 5B. His-329 and Thr-326 are absolutely conserved in all Hh-C homologues, and the side chains of both of these residues are within hydrogen bonding distance of the  $\alpha$ -amino group of Cys-258 in the Hh-C<sub>17</sub> structure. Asp-303 is invariably aspartic acid or histidine in Hh-C domains, and the side chain of Asp-303 is exposed to solvent 4.2-4.5 Å away from the Cys-258 thiol group. Significant structural rearrangements would appear necessary for additional residues in Hh-C<sub>17</sub> to participate directly in Hh autoprocessing. Cys-258, His-329, and Asp-282 do not form a serine protease-like catalytic triad as had been proposed (Lee et al., 1994; Porter et al., 1996a).

To assess the involvement of His-329, Thr-326, and Asp-303 in Hh autoprocessing, each of these residues was mutated to alanine within the context of the full-length His<sub>6</sub>Hh-C<sub>25</sub> protein, and the mutant proteins were expressed and assayed for Hh autoprocessing activity. The autocleaving activity of the mutant proteins in the presence of high concentrations of DTT was used as an assay for thioester formation, the first step in the Hh autoprocessing reaction, while the autocleaving activity in the presence of cholesterol was used to assay for cholesterol transfer, the second step in the autoprocessing reaction. The results of these assays are shown in Figure 5C. His-329 is known from earlier experiments to be essential for Hh autoprocessing activity (Lee et al., 1994), and the His-329 to alanine mutant (H329A) was inactive in both the DTT- and cholesterol-stimulated reactions. The Thr-326 to alanine mutant (T326A) also showed greatly reduced activity in both assays. By contrast, the Asp-303 to alanine mutant (D303A) was active in the DTT-stimulated reaction but inactive in the cholesterol-stimulated reaction.

The loss or dramatic reduction of autocleaving activity in the presence of both DTT and cholesterol for H329A and T326A implicates both His-329 and Thr-326 in formation of the internal thioester during Hh autoprocessing. The interaction of the side chains of both of these residues with the  $\alpha$ -amino group of Cys-258, a component of the cleaved peptide bond, strongly implies a direct role for these residues in thioester formation. Possible roles for His-329 during thioester formation include stabilization of negative charge on the carbonyl oxygen of Gly-257.

donation of a proton to the free  $\alpha$ -amino group of Cys-258, and maintenance of an appropriate orientation of reaction components through polar interactions. His-329 may also deprotonate the thiol group of Cys-258 prior to thioester formation, but if this is the case some rearrangement of Cys-258 relative to its position in the Hh-C<sub>17</sub> crystal structure would be required to bring the thiol group of Cys-258 into proximity with His-329. As the  $pK_a$  of the thiol group in free cysteine is 8.3, a base may not be needed to catalyze thiol deprotonation. Possible roles for Thr-326 in thioester formation seem more limited. The high  $pK_a$  of a threonine hydroxyl group (>15) makes Thr-326 an unlikely candidate for proton transfers, suggesting that this residue is needed to form polar interactions that stabilize reactive conformations within the Hh protein.

The activity of the D303A mutant in DTT- but not cholesterol-stimulated autoproducting shows that Asp-303 is not needed for thioester formation but is required for cholesterol transfer. The negatively-charged aspartic acid residue seems unlikely to be involved in binding a hydrophobic cholesterol molecule. A role in activating the cholesterol molecule for nucleophilic attack of the thioester appears more plausible. For cholesterol to become an effective nucleophile, the  $3\beta$ -hydroxyl group must become deprotonated, and Asp-303 is a good candidate for the general base that catalyzes this deprotonation. Substitution of Asp-303 with histidine in Hh-C homologues is consistent with this hypothesis as histidine is also capable of functioning as a general base.

As indicated by the inactivity of Hh-C<sub>17</sub> in cholesterol transfer assays, residues in the 63 amino acids removed from the Hh-C<sub>25</sub> carboxy terminus are also involved in cholesterol transfer. The proximity of the carboxy terminus of Hh-C<sub>17</sub> to the active site implies a direct role for these residues in cholesterol binding or activation. The decreased solubility of Hh-C<sub>25</sub> relative to Hh-C<sub>17</sub> suggests that the carboxy-terminal 63 residues of Hh-C<sub>25</sub> may possess an exposed hydrophobic region that could serve as a cholesterol binding site.

### Relationship between Hh-C<sub>17</sub> and Self-Splicing Proteins

An earlier analysis identified a 36 amino acid conserved motif in the amino-terminal regions of Hh-C homologues and inteins (Koonin, 1995). A greatly expanded database of Hh-C and intein sequences coupled with recent enhancements of the BLAST method for database searching enabled extension of the detectable region of sequence similarity to the amino-terminal ~100 amino acids of Hh-C and intein sequences ( $p \sim 10^{-3}$ - $10^{-4}$ ). The improved methods for database searching include statistical analysis of gapped alignments and iterative database scanning with position-specific matrices derived from previous BLAST outputs (Altschul et al., in press). When a database search was initiated with any of the Hh-C sequences or with most of the intein sequences, members of the respective second protein family were the only additional sequences retrieved from the database at a statistically significant level.

Solution of the Hh-C<sub>17</sub> crystal structure showed the expanded region of Hh-C/intein sequence homology to terminate halfway through one of the subdomains in the turn region of an exposed loop between  $\beta$  strands 3b and 4b (see Figure 3A). This observation, coupled with the presence of characteristic endonuclease motifs in intein sequences shortly after the end of the detectable Hh-C/intein homology suggested that the intein endonuclease domain had been inserted into the  $\beta$ 3b- $\beta$ 4b loop of an Hh-C<sub>17</sub>-like structure. This hypothesis focused the search for resumption of the Hh-C/intein sequence similarity in intein sequences likely to follow the endonuclease region. The recently determined crystal structure of the PI-SceI intein indeed shows the insertion of the endonuclease region of the intein in the  $\beta$ 3b- $\beta$ 4b loop of an Hh-C<sub>17</sub>-like structure and indicates that the region of the intein sequence in which the similarity to Hh-C<sub>17</sub> must resume is immediately amino-terminal to the second extein (Duan et al., 1997). An alignment of Hh-C<sub>17</sub> and intein sequences is shown in Figure 6A. A fully structure-based alignment of the Hh-C<sub>17</sub> and intein sequences awaits direct comparison of the atomic coordinates of Hh-C<sub>17</sub> and PI-SceI.

As can be seen in Figure 6A, aside from sites with conserved hydrophobic character the only residues absolutely or nearly absolutely conserved between Hh-C homologues and inteins are those identified in the active site of Hh-C<sub>17</sub> and shown to be important for thioester formation by site-directed mutagenesis. The amino-terminal cysteine residue directly involved in thioester formation in Hh-C homologues is replaced by serine in some inteins, and these inteins form an ester rather than a thioester intermediate. The yeast HO endonuclease, which lacks an amino-terminal serine or cysteine residue, does not have self-splicing activity (Perlier et al., 1997), and the only intein homologue in which this residue is replaced by alanine (KjBA protein homologue from *Methanococcus jannaschii*) is suspected to be inactive as well.

The only residue absolutely conserved between Hh-C homologues and inteins is a histidine corresponding to His-329 in *Drosophila* Hh-C. The presence of His-329 in the active site of *Drosophila* Hh-C and the loss of thioester formation activity when His-329 is mutated strongly imply that this histidine is conserved because it performs a vital role in thioester formation and that it functions similarly in inteins and Hh-C homologues. The only other residue conserved in the active site of Hh-C homologues and shown by mutagenesis to be required for efficient thioester formation, Thr-326, is also extremely conserved in intein sequences. Of the 39 intein sequences in the database at the time of our comparison, 34 sequences contain a threonine at a homologous position to Thr-326, while three inteins have serine, and one each have asparagine or glutamic acid at this position. The high level of conservation of threonine at this active site position and its substitution with similar amino acids suggests a conserved role for this threonine in inteins and Hh-C homologues. A conserved residue homologous to Asp-303, also found in the Hh-C<sub>17</sub> active

site, is not found in intein sequences, consistent with its role in cholesterol activation rather than thioester formation.

As expected from the sequence homology, the structures of the self-splicing region of the PI-SceI intein (Duan et al., 1997) and Hh-C<sub>17</sub> are clearly homologous. Although not previously noted, the self-splicing region of PI-SceI contains homologous subdomains related by pseudosymmetry. The PI-SceI subdomains are homologous to the Hh-C<sub>17</sub> subdomains and possess the same loop exchange observed in Hh-C<sub>17</sub>. However, these features are obscured by insertion of endonuclease-associated sequences. In addition to insertion of the core endonuclease domain in the region homologous to the  $\beta 3b$ - $\beta 4b$  loop, the PI-SceI intein contains an additional insertion of amino acids relative to the Hh-C<sub>17</sub> structure. The site of this insertion occurs in the turn between  $\beta$  strands 1b and 2b in the Hh-C<sub>17</sub> structure (see Figure 3A), and this inserted region is believed to be involved in aiding DNA recognition by the PI-SceI intein (Duan et al., 1997). Figure 6B shows a stereodiagram of the Hh-C<sub>17</sub> structure depicted in the same orientation as the PI-SceI intein structure in Duan, et al. (1997) with the sites of the endonuclease-associated insertions indicated.

The conservation of structure, sequence, and cleavage mechanism between Hh-C homologues and the intein regions of self-splicing proteins firmly establishes the divergence of these two protein families from a common precursor. Figure 7 shows a plausible evolutionary scenario for the development of the Hh-C and intein protein families from a primordial domain of unknown function. The Hh-C<sub>17</sub> module is sufficient only for the initial replacement of a peptide bond with a thioester or ester in both the Hh autoprocessing and self-splicing reactions. In both protein families, residues carboxy terminal to the Hh-C<sub>17</sub> module are needed for selecting or contributing the second nucleophile that resolves the initial ester/thioester and determines the products of the overall reaction. The loss of detectable sequence similarity in the region of the *C. elegans* Hh-C homologues following the Hh-C<sub>17</sub> module (R. Mann, personal communication) raises the possibility that these residues may transfer a molecule other than cholesterol. The ongoing expansion of sequence databases provides the prospect of additional Hh-C<sub>17</sub> modules being discovered that initiate novel splicing or transfer reactions by formation of ester or thioester intermediates.

## Table Legend

Table I. Statistics for data collection, phase determination and refinement

(A)  $R_{sym}$  and completeness values were calculated considering Bijvoets equivalent. Values in parentheses for  $\langle I/\sigma I \rangle$  are for the highest resolution shell (1.98-1.9 Å).  $R_{sym} = 100 \times \sum_h \sum_i |I_i(h) - \langle I(h) \rangle| / \sum_h \sum_i I_i(h)$ . (B) r.m.s.  $(\Delta I/I)$  / r.m.s.  $(I/I)$  where  $\Delta F$  is the Bijvoet difference at one wavelength (values on the diagonal) or the dispersive difference between two wavelengths (values off the diagonal). Also shown are the anomalous components of the Se scattering factors as a function of wavelength as determined by MADLSQ (Hendrickson, 1991). (C) All data for which  $|F| > 2\sigma$  were used in the refinement. A subset of the data (10%) was excluded from the refinement and used to calculate the free R-value (Brünger, 1992). A final round of refinement including this data was performed to produce the final set of coordinates and crystallographic R-value.  $R\text{-value} = \sum ||F_o| - |F_c|| / \sum |F_o|$ .

Table I Statistics for data collection, phase determination and refinement

## (A) Data Collection Statistics (30.0 to 1.9 Å)

Wavelength (Å)	Reflections (N)	Redundancy	Completeness (%)	Signal ( $\langle I/\sigma I \rangle$ )	$R_{\text{sym}}$ (%)
0.9919	26,790	10.3	100.0	19.9 (4.2)	9.2
0.9793	26,791	10.6	100.0	19.4 (3.8)	9.9
0.9791	26,792	10.4	100.0	18.8 (3.6)	10.4
0.9686	26,792	10.5	100.0	18.7 (3.5)	10.3

## (B) MAD Structure Factor Ratios and Anomalous Scattering Factors

Wavelength (Å)	0.9919	0.9793	0.9791	0.9686	$f'$ (e)	$f''$ (e)
0.9919	0.041	0.064	0.059	0.053	-3.94	0.51
0.9793		0.055	0.049	0.062	-9.45	3.28
0.9791			0.076	0.058	-8.05	6.03
0.9686				0.063	-4.15	4.12

## (C) Refinement and stereochemical statistics

R-value	0.218 ( $F > 2\sigma$ , 6.0-1.9Å)	0.222 (all $F$ , 6.0-1.9Å)
free R-value	0.275 ( $F > 2\sigma$ , 6.0-1.9Å)	0.283 (all $F$ , 6.0-1.9Å)
Average B (Å <sup>2</sup> )	21.5 for protein, 39.6 for solvent	
Rms deviations		
Bonds (Å)	0.008	
Angles (°)	1.97	
B-values (Å <sup>2</sup> )	1.30/1.45 bonds/angles of main chain	
	2.83/3.20 bonds/angles of side chains	

## References

- Altschul, S. F. and Gish, W. (1996). Local alignment statistics. *Meth. Enzymol.* 266, 460-481.
- Altschul, S. F., Madden, T. L., Schaffer, A. A., Zhang, J., Zhang, Z., Miller, W. and Lipman, D. J. Gapped BLAST and PSI-BLAST - a new generation of protein database search programs. *Nucleic Acids Res.*, in press.
- Bennett, M. J., Schlunegger, M. P. and Eisenberg, D. (1995). 3D domain swapping: A mechanism for oligomer assembly. *Prot. Sci.* 4, 2455-2468.
- Brannigan, J. A., Dodson, G., Duggleby, H. J., Moody, P. C. E., Smith, J. L., Temchick, D. R. and Murzin, A. G. (1995). A protein catalytic framework with an N-terminal nucleophile is capable of self-activation. *Nature* 378, 416-419.
- Brünger, A. T. (1992). X-PLOR, Version 3.1 A system for x-ray crystallography and NMR. New Haven, CT, Yale University.
- Bumcrot, D. A., Takada, R. and McMahon, A. P. (1995). Proteolytic processing yields two secreted forms of *sonic hedgehog*. *Mol. Cell. Biol.* 15, 2294-2303.
- Burglin, T. R. (1996). Warthog and Groundhog, novel families related to Hedgehog. *Curr. Biol.* 6, 1047-1050.
- Collaborative Computational Project. N. 4. (1994). The CCP4 Suite: Programs for protein crystallography. *Acta Crystallogr. D50*, 763-763.
- Cooper, A. A. and Stevens, T. H. (1995). Protein splicing: Self-splicing of genetically mobile elements at the protein level. *Trends Biochem. Sci.* 20, 351-356.
- Duan, X., Gimble, F. S. and Quirocho, F. A. (1997). Crystal Structure of PI-SceI, a Homing Endonuclease with Protein Splicing Activity. *Cell* 89, 555-564.
- Ekker, S. C., McGrew, L. L., Lai, C.-J., Lee, J. J., von Kessler, D. P., Moon, R. T. and Beachy, P. A. (1995). Distinct expression and shared activities of members of the *hedgehog* gene family of *Xenopus laevis*. *Development* 121, 2337-2347.
- Ekker, S. C., Ungar, A. R., Greenstein, P., von Kessler, D. P., Porter, J. A., Moon, R. T. and Beachy, P. A. (1995). Patterning activities of vertebrate *hedgehog* proteins in the developing eye and brain. *Curr. Biol.* 5, 944-955.
- Fan, C.-M., Porter, J. A., Chiang, C., Chang, D. T., Beachy, P. A. and Tessier-Lavigne, M. (1995). Long-range sclerotome induction by *sonic hedgehog*: Direct role of the amino-terminal cleavage product and modulation by the cyclic AMP signaling pathway. *Cell* 81, 457-465.
- Fierz, M. J., Jacinto, A., Taylor, A. M., Alexandre, C. and Ingham, P. W. (1995). Secretion of the amino-terminal fragment of the Hedgehog protein is necessary and sufficient for *hedgehog* signalling in *Drosophila*. *Curr. Biol.* 5, 643-650.
- Hammerschmidt, M., Brook, A. and McMahon, A. P. (1997). The world according to hedgehog. *Trends Genet.* 13, 14-21.

- Heinemann, U. and Hahn, M. (1995). Circular permutations of protein sequence: Not so rare? *Trends in Biochemical Sciences* 20, 349-350.
- Hendrickson, W. A. (1991). Determination of macromolecular structures from anomalous diffraction of synchrotron radiation. *Science* 254, 51-58.
- Hendrickson, W. A., Horton, J. R. and LeMaster, D. M. (1990). Selenomethionyl proteins produced for analysis by multiwavelength anomalous diffraction (MAD): a vehicle for direct determination of three-dimensional structure. *EMBO J.* 9, 1665-1672.
- Hutchinson, E. G. and Thornton, J. M. (1996). PROMOTIF--a program to identify and analyze structural motifs in proteins. *Prot. Sci.* 5, 212-220.
- Hynes, M., Porter, J. A., Chiang, C., Chang, D., Tessier-Lavigne, M., Beachy, P. A. and Rosenthal, A. (1995). Induction of midbrain dopaminergic neurons by Sonic hedgehog. *Neuron* 15, 35-44.
- Jones, D. H. and Winistorfer, S. C. (1992). Recombinant circle PCR and recombination PCR for site-specific mutagenesis without PCR product purification. *Biotechniques* 12, 528-530.
- Jones, T. A., Zou, J. Y., Cowan, S. W. and Kjeldgaard, M. (1991). Improved methods for the building of protein methods in electron density maps and the location of errors in these models. *Acta Crystallographica, A* 47, 110-119.
- Koenin, E. V. (1995). A protein splice-junction motif in hedgehog family proteins. *Trends Biochem. Sci.* 20, 141-142.
- Kraulis, P. J. (1991). MOLSCRIPT: a program to produce both detailed and schematic plots of protein structures. *J. Appl. Cryst.* 24, 946-950.
- Lai, C.-J., Ekker, S. C., Beachy, P. A. and Moon, R. T. (1995). Patterning of the neural ectoderm of *Xenopus laevis* by the amino-terminal product of hedgehog autoproteolytic cleavage. *Development* 121, 2349-2360.
- Leahy, D. J., Erickson, H. P., Aukhil, I., Joshi, P. and Hendrickson, W. A. (1994). Crystallization of a fragment of human fibronectin: Introduction of methionine by site-directed mutagenesis to allow phasing by selenomethionine. *Proteins* 19, 48-54.
- Lee, J. J., Ekker, S. C., von Kessler, D. P., Porter, J. A., Sun, B. I. and Beachy, P. A. (1994). Auto-proteolysis in *hedgehog* protein biogenesis. *Science* 266, 1528-1537.
- Lewis, M., Chang, G., Horton, N. C., Kercher, M. A., Pace, H. C., Schumacher, M. A., Brennan, R. G. and Lu, P. (1996). Crystal structure of the lactose operon repressor and its complexes with DNA and inducer. *Science* 271, 1247-1254.
- Lopez-Martinez, A., Chang, D. T., Chiang, C., Porter, J. A., Ros, M. A., Simandl, B. K., Beachy, P. A. and Fallon, J. F. (1995). Limb-patterning activity and restricted posterior localization of the amino-terminal product of Sonic hedgehog cleavage. *Curr. Biol.* 5(791-796).
- Love, R. A. and Stroud, R. M. (1986). The crystal structure of alpha-bungarotoxin at 2.5 Å resolution: relation to solution structure and binding to acetylcholine receptor. *Prot. Eng.* 1, 37-46.

- Marti, E., Bumcrot, D. A., Takada, R. and McMahon, A. P. (1995). Requirement of 19K form of sonic hedgehog for induction of distinct ventral cell types in CNS explants. *Nature* 375, 322-325.
- Murzin, A. G. (1996). Structural classification of proteins: new superfamilies. *Curr. Opin. Struct. Biol.* 6, 386-394.
- Otwinowski, Z. and Minor, V. (1997). Processing of x-ray diffraction data collected in oscillation mode. *Meth. Enzymol.* 276, 307-326.
- Perler, F. B., Olsen, G. J. and Adam, E. (1997). Compilation and analysis of intein sequences. *Nucleic Acids Res.* 25, 1087-1093.
- Petrokovski, S. (1994). Conserved sequence features of inteins (protein introns) and their use in identifying new inteins and related proteins. *Prot. Sci.* 3, 2340-2350.
- Ponting, C. P. and Russell, R. B. (1995). Swaposins: Circular permutations within genes encoding saposin homologues. *Trends Biochem. Sci.* 20, 179-180.
- Porter, J. A., Ekker, S. C., Park, W.-J., von Kessler, D. P., Young, K. E., Chen, C.-H., Ma, Y., Woods, A. S., Cotter, R. J., Koonin, E. V. and Beachy, P. A. (1996a). Hedgehog patterning activity: Role of a lipophilic modification mediated by the carboxy-terminal autoprocessing domain. *Cell* 86, 21-34.
- Porter, J. A., von Kessler, D. P., Ekker, S. C., Young, K. E., Lee, J. J., Moses, K. and Beachy, P. A. (1995). The product of *hedgehog* autoproteolytic cleavage active in local and long-range signalling. *Nature* 374, 365-366.
- Porter, J. A., Young, K. E. and Beachy, P. A. (1996b). Cholesterol modification of Hedgehog signaling proteins in animal development. *Science* 274, 255-259.
- Ramakrishnan, V. and Bicu, V. (1997). Treatment of multiwavelength anomalous diffraction data as a special case of multiple isomorphous replacement. *Meth. Enzymol.* 276, 538-557.
- Rees, B., Bilwes, A., Samama, J. P. and Moras, D. (1990). Cardiotoxin VII4 from *Naja mssambica mssambica*. The refined crystal structure. *J. Mol. Biol.* 214, 281-297.
- Roelink, H., Porter, J. A., Chiang, C., Tanabe, Y., Chang, D. T., Beachy, P. A. and Jessell, T. M. (1995). Floor plate and motor neuron induction by different concentrations of the amino-terminal cleavage product of *sonic hedgehog* autoproteolysis. *Cell* 81, 445-455.
- Schuler, G. D., Altschul, S. F. and Lipman, D. J. (1991). A workbook for multiple alignment construction and analysis. *Proteins* 9, 180-190.
- Schumacher, M. A., Choi, K. Y., Zalkin, H. and Brennan, R. G. (1994). Crystal structure of LacI member, PurR, bound to DNA: Minor groove binding by  $\alpha$  helices. *Science* 266, 763-770.
- Sheidrick, G. (1991). Patterson Interpretation and the use of macromolecular delta-F data. Daresbury, UK.
- Thompson, J. D., Higgins, D. G. and Gibson, T. J. (1994). CLUSTAL W: Improving the sensitivity of progressive multiple sequence alignment through sequence weighting, position-specific gap penalties and weight matrix choice. *Nucleic Acids Res.* 22, 4673-4680.

Wlodawer, A., Hodgson, K. O. and Shooter, E. M. (1975). Crystallization of nerve growth factor from mouse submaxillary glands. *Proc. Natl. Acad. Sci. USA* 72, 777-779.

Xu, M.-Q. and Perler, F. B. (1996). The mechanism of protein splicing and its modulation by mutation. *EMBO J.* 15, 5146-5153.

- 142 -

The above disclosure generally describes the present invention. A more complete understanding can be obtained by reference to the following specific examples which are provided herein for purposes of illustration only and are not intended to limit the scope of the invention.

- 143 -

## SEQUENCE LISTING

## (1) GENERAL INFORMATION:

- (i) APPLICANT: The Johns Hopkins University School of Medicine et al.
- (ii) TITLE OF INVENTION: NOVEL HEDGEHOG-DERIVED POLYPEPTIDES
- (iii) NUMBER OF SEQUENCES: 20
- (iv) CORRESPONDENCE ADDRESS:
  - (A) ADDRESSEE: Fish & Richardson P.C.
  - (B) STREET: 4225 Executive Square, Suite 1400
  - (C) CITY: La Jolla
  - (D) STATE: CA
  - (E) COUNTRY: U.S.A.
  - (F) ZIP: 92037
- (v) COMPUTER READABLE FORM:
  - (A) MEDIUM TYPE: Floppy disk
  - (B) COMPUTER: IBM PC compatible
  - (C) OPERATING SYSTEM: PC-DOS/MS-DOS
  - (D) SOFTWARE: PatentIn Release #1.0, Version #1.30
- (vi) CURRENT APPLICATION DATA:
  - (A) APPLICATION NUMBER:
  - (B) FILING DATE: 07-OCT-1997
  - (C) CLASSIFICATION:
- (vii) PRIOR APPLICATION DATA:
  - (A) APPLICATION NUMBER: 08/729,743
  - (B) FILING DATE: 07-OCT-1996
  - (C) CLASSIFICATION:
- (vii) PRIOR APPLICATION DATA:
  - (A) APPLICATION NUMBER: 60/---,---
  - (B) FILING DATE: 02-OCT-1997
  - (C) CLASSIFICATION:
- (viii) ATTORNEY/AGENT INFORMATION:
  - (A) NAME: Haile, Lisa A.
  - (B) REGISTRATION NUMBER: 38,347
  - (C) REFERENCE/DOCKET NUMBER: 07265/099WO1
- (ix) TELECOMMUNICATION INFORMATION:
  - (A) TELEPHONE: 619/678-5070
  - (B) TELEFAX: 619/678-5099

## (2) INFORMATION FOR SEQ ID NO:1:

- (i) SEQUENCE CHARACTERISTICS:
  - (A) LENGTH: 144 base pairs
  - (B) TYPE: nucleic acid
  - (C) STRANDEDNESS: both
  - (D) TOPOLOGY: both
- (ii) MOLECULE TYPE: cDNA
- (ix) FEATURE:
  - (A) NAME/KEY: CDS

- 144 -

(B) LOCATION: 1..142

(xi) SEQUENCE DESCRIPTION: SEQ ID NO:1:

GTG AAA CTG CGG GTG ACC GAG CCC TGG GAC GAA GAT GGC CAC CAC TCA	48
Val Lys Leu Arg Val Thr Glu Pro Trp Asp Glu Asp Gly His His Ser	
1 5 10 15	
CAG GAG TCT CTG CAC TAC GAG GGC CGC GCA GTG GAC ATC ACC ACG TCT	96
Gln Glu Ser Leu His Tyr Glu Gly Arg Ala Val Asp Ile Thr Thr Ser	
20 25 30	
GAC CGC GAC CGC AGC AAG TAC GGC ATG CTG GCC CGC CTG GCG GTG G	142
Asp Arg Asp Arg Ser Lys Tyr Gly Met Leu Ala Arg Leu Ala Val	
35 40 45	
AG	144

(2) INFORMATION FOR SEQ ID NO:2:

- (i) SEQUENCE CHARACTERISTICS:
- (A) LENGTH: 144 base pairs
  - (B) TYPE: nucleic acid
  - (C) STRANDEDNESS: both
  - (D) TOPOLOGY: both

(ii) MOLECULE TYPE: cDNA

- (ix) FEATURE:
- (A) NAME/KEY: CDS
  - (B) LOCATION: 1..142

(xi) SEQUENCE DESCRIPTION: SEQ ID NO:2:

GTG AAG CTG CGG GTG ACC GAG GGC TGG GAC GAG GAC GGC CAC CAC TCA	48
Val Lys Leu Arg Val Thr Glu Gly Trp Asp Glu Asp Gly His His Ser	
50 55 60	
GAG GAG TCC CTG CAT TAT GAG GGC CGC GCG GTG GAC ATC ACC ACA TCA	96
Glu Glu Ser Leu His Tyr Glu Gly Arg Ala Val Asp Ile Thr Thr Ser	
65 70 75	
GAC CGC GAC CGC AAT AAG TAT GGA CTG CTG GCG CGC TTG GCA GTG G	142
Asp Arg Asp Arg Asn Lys Tyr Gly Leu Leu Ala Arg Leu Ala Val	
80 85 90	
AG	144

(2) INFORMATION FOR SEQ ID NO:3:

- (i) SEQUENCE CHARACTERISTICS:
- (A) LENGTH: 14 amino acids
  - (B) TYPE: amino acid
  - (C) STRANDEDNESS: not relevant
  - (D) TOPOLOGY: both

(ii) MOLECULE TYPE: protein

- 145 -

(xi) SEQUENCE DESCRIPTION: SEQ ID NO:3:

Ile	Ser	Ser	His	Val	His	Gly	Cys	Phe	Thr	Pro	Glu	Ser	Thr
1				5					10				

(2) INFORMATION FOR SEQ ID NO:4:

(i) SEQUENCE CHARACTERISTICS:

- (A) LENGTH: 14 amino acids
- (B) TYPE: amino acid
- (C) STRANDEDNESS: not relevant
- (D) TOPOLOGY: both

(ii) MOLECULE TYPE: protein

(xi) SEQUENCE DESCRIPTION: SEQ ID NO:4:

Ser	Ile	Ser	His	Met	His	Gly	Cys	Phe	Thr	Pro	Glu	Ser	Thr
1				5					10				

(2) INFORMATION FOR SEQ ID NO:5:

(i) SEQUENCE CHARACTERISTICS:

- (A) LENGTH: 14 amino acids
- (B) TYPE: amino acid
- (C) STRANDEDNESS: not relevant
- (D) TOPOLOGY: both

(ii) MOLECULE TYPE: protein

(xi) SEQUENCE DESCRIPTION: SEQ ID NO:5:

Val	Ala	Ala	Lys	Ser	Gly	Gly	Cys	Phe	Pro	Gly	Ser	Ala	Thr
1				5					10				

(2) INFORMATION FOR SEQ ID NO:6:

(i) SEQUENCE CHARACTERISTICS:

- (A) LENGTH: 14 amino acids
- (B) TYPE: amino acid
- (C) STRANDEDNESS: not relevant
- (D) TOPOLOGY: both

(ii) MOLECULE TYPE: protein

(xi) SEQUENCE DESCRIPTION: SEQ ID NO:6:

Val	Ala	Ala	Lys	Ser	Asp	Gly	Cys	Phe	Pro	Gly	Ser	Ala	Thr
1				5					10				

(2) INFORMATION FOR SEQ ID NO:7:

(i) SEQUENCE CHARACTERISTICS:

- (A) LENGTH: 14 amino acids
- (B) TYPE: amino acid

- 146 -

- (C) STRANDEDNESS: not relevant
- (D) TOPOLOGY: both

(ii) MOLECULE TYPE: protein

(xi) SEQUENCE DESCRIPTION: SEQ ID NO:7:

Val	Ala	Ala	Lys	Ser	Gly	Gly	Cys	Phe	Pro	Gly	Ser	Ala	Leu
1				5					10				

(2) INFORMATION FOR SEQ ID NO:8:

- (i) SEQUENCE CHARACTERISTICS:
  - (A) LENGTH: 14 amino acids
  - (B) TYPE: amino acid
  - (C) STRANDEDNESS: not relevant
  - (D) TOPOLOGY: both

(ii) MOLECULE TYPE: protein

(xi) SEQUENCE DESCRIPTION: SEQ ID NO:8:

Val	Ala	Ala	Lys	Ser	Gly	Gly	Cys	Phe	Pro	Gly	Ser	Gly	Thr
1				5					10				

(2) INFORMATION FOR SEQ ID NO:9:

- (i) SEQUENCE CHARACTERISTICS:
  - (A) LENGTH: 15 amino acids
  - (B) TYPE: amino acid
  - (C) STRANDEDNESS: not relevant
  - (D) TOPOLOGY: both

(ii) MOLECULE TYPE: protein

(xi) SEQUENCE DESCRIPTION: SEQ ID NO:9:

Val	Ala	Ala	Lys	Ser	Gly	Gly	Cys	Phe	Pro	Ala	Gly	Ala	Arg	Thr
1				5					10				15	

(2) INFORMATION FOR SEQ ID NO:10:

- (i) SEQUENCE CHARACTERISTICS:
  - (A) LENGTH: 14 amino acids
  - (B) TYPE: amino acid
  - (C) STRANDEDNESS: not relevant
  - (D) TOPOLOGY: both

(ii) MOLECULE TYPE: protein

(xi) SEQUENCE DESCRIPTION: SEQ ID NO:10:

- 147 -

Val Ala Ala Lys Thr Gly Gly Cys Phe Pro Ala Gly Ala Gln  
1 5 10

## (2) INFORMATION FOR SEQ ID NO:11:

## (i) SEQUENCE CHARACTERISTICS:

- (A) LENGTH: 14 amino acids
- (B) TYPE: amino acid
- (C) STRANDEDNESS: not relevant
- (D) TOPOLOGY: both

(ii) MOLECULE TYPE: protein

## (xi) SEQUENCE DESCRIPTION: SEQ ID NO:11:

Val Ala Ala Lys Thr Gly Gly Cys Phe Pro Gly Glu Ala Leu  
1 5 10

## (2) INFORMATION FOR SEQ ID NO:12:

## (i) SEQUENCE CHARACTERISTICS:

- (A) LENGTH: 14 amino acids
- (B) TYPE: amino acid
- (C) STRANDEDNESS: not relevant
- (D) TOPOLOGY: both

(ii) MOLECULE TYPE: protein

## (xi) SEQUENCE DESCRIPTION: SEQ ID NO:12:

Leu Gly Val Arg Ser Gly Gly Cys Phe Pro Gly Thr Ala Met  
1 5 10

## (2) INFORMATION FOR SEQ ID NO:13:

## (i) SEQUENCE CHARACTERISTICS:

- (A) LENGTH: 14 amino acids
- (B) TYPE: amino acid
- (C) STRANDEDNESS: not relevant
- (D) TOPOLOGY: both

(ii) MOLECULE TYPE: protein

## (xi) SEQUENCE DESCRIPTION: SEQ ID NO:13:

Leu Ala Val Arg Ala Gly Gly Cys Phe Pro Gly Asn Ala Thr  
1 5 10

## (2) INFORMATION FOR SEQ ID NO:14:

## (i) SEQUENCE CHARACTERISTICS:

- (A) LENGTH: 8 amino acids
- (B) TYPE: amino acid
- (C) STRANDEDNESS: not relevant

- 148 -

(D) TOPOLOGY: both

(ii) MOLECULE TYPE: protein

(xi) SEQUENCE DESCRIPTION: SEQ ID NO:14:

His	Gly	His	Gly	Cys	Phe	Thr	Pro
1				5			

(2) INFORMATION FOR SEQ ID NO:15:

(i) SEQUENCE CHARACTERISTICS:

- (A) LENGTH: 8 amino acids
- (B) TYPE: amino acid
- (C) STRANDEDNESS: not relevant
- (D) TOPOLOGY: both

(ii) MOLECULE TYPE: protein

(xi) SEQUENCE DESCRIPTION: SEQ ID NO:15:

His	Gly	His	Gly	Cys	Phe	Thr	Pro
1				5			

(2) INFORMATION FOR SEQ ID NO:16:

(i) SEQUENCE CHARACTERISTICS:

- (A) LENGTH: 8 amino acids
- (B) TYPE: amino acid
- (C) STRANDEDNESS: not relevant
- (D) TOPOLOGY: both

(ii) MOLECULE TYPE: protein

(xi) SEQUENCE DESCRIPTION: SEQ ID NO:16:

Lys	Ser	Gly	Gly	Cys	Phe	Pro	Gly
1				5			

(2) INFORMATION FOR SEQ ID NO:17:

(i) SEQUENCE CHARACTERISTICS:

- (A) LENGTH: 416 amino acids
- (B) TYPE: amino acid
- (D) TOPOLOGY: linear

(ii) MOLECULE TYPE: protein

(xi) SEQUENCE DESCRIPTION: SEQ ID NO:17:

Met	Asp	Val	Arg	Leu	His	Leu	Lys	Gln	Phe	Ala	Leu	Leu	Cys	Phe	Ile
1				5				10						15	

- 149 -

Ser Leu Leu Leu Thr Pro Cys Gly Leu Ala Cys Gly Pro Gly Arg Gly  
                   20                  25                  30  
 Tyr Gly Lys Arg Arg His Pro Lys Lys Leu Thr Pro Leu Ala Tyr Lys  
                   35                  40                  45  
 Gln Phe Ile Pro Asn Val Ala Glu Lys Thr Leu Gly Ala Ser Gly Lys  
                   50                  55                  60  
 Tyr Glu Gly Lys Ile Thr Arg Asn Ser Glu Arg Phe Lys Glu Leu Ile  
                   65                  70                  75                  80  
 Pro Asn Tyr Asn Pro Asp Ile Ile Phe Lys Asp Glu Glu Asn Thr Asn  
                   85                  90                  95  
 Ala Asp Arg Leu Met Thr Lys Arg Cys Lys Asp Lys Leu Asn Ser Leu  
                   100                  105                  110  
 Ala Ile Ser Val Met Asn His Trp Pro Gly Val Lys Leu Arg Val Thr  
                   115                  120                  125  
 Glu Gly Trp Asp Glu Asp Gly His His Leu Glu Glu Ser Leu His Tyr  
                   130                  135                  140  
 Glu Gly Arg Ala Val Asp Ile Thr Thr Ser Asp Arg Asp Lys Ser Lys  
                   145                  150                  155                  160  
 Tyr Gly Met Leu Ser Arg Leu Ala Val Glu Ala Gly Phe Asp Trp Val  
                   165                  170                  175  
 Tyr Tyr Glu Ser Lys Ala His Ile His Cys Ser Val Lys Ala Glu Asn  
                   180                  185                  190  
 Ser Val Ala Ala Lys Ser Gly Gly Cys Phe Pro Gly Ser Gly Thr Val  
                   195                  200                  205  
 Thr Leu Gly Asp Gly Thr Arg Lys Pro Ile Lys Asp Leu Lys Val Gly  
                   210                  215                  220  
 Asp Arg Val Leu Ala Ala Asp Glu Lys Gly Asn Val Leu Ile Ser Asp  
                   225                  230                  235                  240  
 Phe Ile Met Phe Ile Asp His Asp Pro Thr Thr Arg Arg Gln Phe Ile  
                   245                  250                  255  
 Val Ile Glu Thr Ser Glu Pro Phe Thr Lys Leu Thr Leu Thr Ala Ala  
                   260                  265                  270  
 His Leu Val Phe Val Gly Asn Ser Ser Ala Ala Ser Gly Ile Thr Ala  
                   275                  280                  285  
 Thr Phe Ala Ser Asn Val Lys Pro Gly Asp Thr Val Leu Val Trp Glu  
                   290                  295                  300  
 Asp Thr Cys Glu Ser Leu Lys Ser Val Thr Val Lys Arg Ile Tyr Thr  
                   305                  310                  315                  320  
 Glu Glu His Glu Gly Ser Phe Ala Pro Val Thr Ala His Gly Thr Ile  
                   325                  330                  335  
 Ile Val Asp Gln Val Leu Ala Ser Cys Tyr Ala Val Ile Glu Asn His  
                   340                  345                  350

- 150 -

Lys Trp Ala His Trp Ala Phe Ala Pro Val Arg Leu Cys His Lys Leu  
           355                                  360                                  365

Met Thr Trp Leu Phe Pro Ala Arg Glu Ser Asn Val Asn Phe Gln Glu  
           370                                  375                                  380

Asp Gly Ile His Trp Tyr Ser Asn Met Leu Phe His Ile Gly Ser Trp  
   385                                  390                                  395                                  400

Leu Leu Asp Arg Asp Ser Phe His Pro Leu Gly Ile Leu His Leu Ser  
                                   405                                  410                                  415

## (2) INFORMATION FOR SEQ ID NO:18:

## (i) SEQUENCE CHARACTERISTICS:

- (A) LENGTH: 418 amino acids  
 (B) TYPE: amino acid  
 (D) TOPOLOGY: linear

## (ii) MOLECULE TYPE: protein

## (xi) SEQUENCE DESCRIPTION: SEQ ID NO:18:

Met Arg Leu Leu Thr Arg Val Leu Leu Val Ser Leu Leu Thr Leu Ser  
   1                                  5                                  10                                  15

Leu Val Val Ser Gly Leu Ala Cys Gly Pro Gly Arg Gly Tyr Gly Arg  
                                   20                                  25                                  30

Arg Arg His Pro Lys Lys Leu Thr Pro Leu Ala Tyr Lys Gln Phe Ile  
                                   35                                  40                                  45

Pro Asn Val Ala Glu Lys Thr Leu Gly Ala Ser Gly Arg Tyr Glu Gly  
                                   50                                  55                                  60

Lys Ile Thr Arg Asn Ser Glu Arg Phe Lys Glu Leu Thr Pro Asn Tyr  
   65                                  70                                  75                                  80

Asn Pro Asp Ile Ile Phe Lys Asp Glu Glu Asn Thr Gly Ala Asp Arg  
                                   85                                  90                                  95

Leu Met Thr Gln Arg Cys Lys Asp Lys Leu Asn Ser Leu Ala Ile Ser  
                                   100                                  105                                  110

Val Met Asn His Trp Pro Gly Val Lys Leu Arg Val Thr Glu Gly Trp  
                                   115                                  120                                  125

Asp Glu Asp Gly His His Phe Glu Glu Ser Leu His Tyr Glu Gly Arg  
   130                                  135                                  140

Ala Val Asp Ile Thr Thr Ser Asp Arg Asp Lys Ser Lys Tyr Gly Thr  
   145                                  150                                  155                                  160

Leu Ser Arg Leu Ala Val Glu Ala Gly Phe Asp Trp Val Tyr Tyr Glu  
                                   165                                  170                                  175

Ser Lys Ala His Ile His Cys Ser Val Lys Ala Glu Asn Ser Val Ala  
                                   180                                  185                                  190

Ala Lys Ser Gly Gly Cys Phe Pro Gly Ser Ala Leu Val Ser Leu Gln  
   195                                  200                                  205

- 151 -

Asp Gly Gly Gln Lys Ala Val Lys Asp Leu Asn Pro Gly Asp Lys Val  
 210 215 220  
 Leu Ala Ala Asp Ser Ala Gly Asn Leu Val Phe Ser Asp Phe Ile Met  
 225 230 235 240  
 Phe Thr Asp Arg Asp Ser Thr Thr Arg Arg Val Phe Tyr Val Ile Glu  
 245 250 255  
 Thr Gln Glu Pro Val Glu Lys Ile Thr Leu Thr Ala Ala His Leu Leu  
 260 265 270  
 Phe Val Leu Asp Asn Ser Thr Glu Asp Leu His Thr Met Thr Ala Ala  
 275 280 285  
 Tyr Ala Ser Ser Val Arg Ala Gly Gln Lys Val Met Val Val Asp Asp  
 290 295 300  
 Ser Gly Gln Leu Lys Ser Val Ile Val Gln Arg Ile Tyr Thr Glu Glu  
 305 310 315 320  
 Gln Arg Gly Ser Phe Ala Pro Val Thr Ala His Gly Thr Ile Val Val  
 325 330 335  
 Asp Arg Ile Leu Ala Ser Cys Tyr Ala Val Ile Glu Asp Gln Gly Leu  
 340 345 350  
 Ala His Leu Ala Phe Ala Pro Ala Arg Leu Tyr Tyr Tyr Val Ser Ser  
 355 360 365  
 Phe Leu Phe Pro Gln Asn Ser Ser Arg Ser Asn Ala Thr Leu Gln  
 370 375 380  
 Gln Glu Gly Val His Trp Tyr Ser Arg Leu Leu Tyr Gln Met Gly Thr  
 385 390 395 400  
 Trp Leu Leu Asp Ser Asn Met Leu His Pro Leu Gly Met Ser Val Asn  
 405 410 415  
 Ser Ser

## (2) INFORMATION FOR SEQ ID NO:19:

- (i) SEQUENCE CHARACTERISTICS:
- (A) LENGTH: 425 amino acids
  - (B) TYPE: amino acid
  - (C) STRANDEDNESS: not relevant
  - (D) TOPOLOGY: both

(ii) MOLECULE TYPE: protein

## (xi) SEQUENCE DESCRIPTION: SEQ ID NO:19:

Met Val Glu Met Leu Leu Leu Thr Arg Ile Leu Leu Val Gly Phe Ile  
 1 5 10 15  
 Cys Ala Leu Leu Val Ser Ser Gly Leu Thr Cys Gly Pro Gly Arg Gly  
 20 25 30

Ile	Gly	His	Arg	Arg	His	Pro	Lys	Lys	Leu	Thr	Pro	Leu	Ala	Tyr	Lys
		35					40						45		
Gln	Phe	Ile	Pro	Asn	Val	Ala	Glu	Lys	Thr	Leu	Gly	Ala	Ser	Gly	Arg
	50					55					60				
Tyr	Glu	Gly	Lys	Ile	Thr	Arg	Asn	Ser	Glu	Arg	Phe	Lys	Glu	Leu	Ile
65					70					75					80
Pro	Asn	Tyr	Asn	Pro	Asp	Ile	Ile	Phe	Lys	Asp	Glu	Glu	Asn	Thr	Gly
				85					90					95	
Ala	Asp	Arg	Leu	Met	Thr	Cys	Arg	Cys	Lys	Asp	Lys	Leu	Asn	Ala	Leu
			100					105					110		
Ala	Ile	Ser	Val	Met	Asn	Cys	Trp	Pro	Gly	Val	Met	Leu	Arg	Val	Thr
		115					120					125			
Glu	Gly	Trp	Asp	Glu	Asp	Gly	His	His	Ser	Lys	Glu	Ser	Leu	His	Tyr
	130					135					140				
Glu	Gly	Arg	Ala	Val	Asp	Ile	Thr	Thr	Ser	Asp	Arg	Asp	Arg	Ser	Lys
145					150					155					160
Tyr	Gly	Met	Leu	Ala	Arg	Leu	Ala	Val	Glu	Ala	Gly	Phe	Asp	Trp	Val
				165					170					175	
Tyr	Tyr	Glu	Ser	Lys	Ala	His	Ile	Cys	Ser	Val	Lys	Ala	Glu	Asn	Ser
			180					185					190		
Val	Ala	Ala	Lys	Ser	Gly	Gly	Cys	Phe	Pro	Gly	Ser	Ala	Thr	Val	His
		195					200					205			
Leu	Glu	His	Gly	Gly	Thr	Lys	Leu	Val	Lys	Asp	Leu	Ser	His	Gly	Asp
	210					215					220				
Arg	Val	Leu	Ala	Ala	Asp	Ala	Asp	Gly	Arg	Leu	Leu	Val	Ser	Asp	Phe
225					230					235					240
Leu	Leu	Thr	Phe	Leu	Asp	Arg	Met	Asp	Ser	Ser	Arg	Lys	Leu	Phe	Tyr
				245					250					255	
Val	Ile	Glu	Thr	Arg	Gln	Pro	Arg	Ala	Arg	Leu	Leu	Leu	Thr	Ala	Ala
			260					265					270		
His	Leu	Leu	Phe	Val	Ala	Pro	Gln	His	Asn	Gln	Ser	Glu	Ala	Thr	Gly
		275					280					285			
Ser	Thr	Ser	Gly	Gln	Ala	Leu	Phe	Ala	Ser	Asn	Val	Lys	Pro	Gly	Gln
		290				295					300				
Pro	Val	Val	Val	Leu	Gly	Glu	Gly	Gly	Gln	Gln	Leu	Leu	Pro	Ala	Ser
305					310					315					320
Val	His	Ser	Val	Ser	Leu	Arg	Glu	Glu	Ala	Ser	Gly	Ala	Tyr	Ala	Pro
				325					330				335		
Thr	Thr	Ala	Cys	Gly	Thr	Ile	Leu	Ile	Asn	Arg	Val	Leu	Ala	Ser	Cys
			340					345					350		
Tyr	Ala	Val	Ile	Glu	Glu	His	Ser	Trp	Ala	His	Ala	Ala	Phe	Ala	Pro
		355					360					365			

- 153 -

His Arg Leu Ala Gln Gly Leu Leu Ala Ala Leu Cys Pro Asp Gly Ala  
 370 375 380

Ile Pro Thr Ala Ala Thr Thr Thr Thr Gly Ile His Trp Tyr Ser Arg  
 385 390 395 400

Leu Leu Tyr Arg Ile Gly Ser Trp Val Leu Asp Gly Asp Ala Leu His  
 405 410 415

Pro Leu Gly Met Val Ala Pro Ala Ser  
 420 425

## (2) INFORMATION FOR SEQ ID NO:20:

## (i) SEQUENCE CHARACTERISTICS:

- (A) LENGTH: 437 amino acids
- (B) TYPE: amino acid
- (D) TOPOLOGY: linear

## (ii) MOLECULE TYPE: protein

## (xi) SEQUENCE DESCRIPTION: SEQ ID NO:20:

Met Leu Leu Leu Leu Ala Arg Cys Phe Leu Val Ile Leu Ala Ser Ser  
 1 5 10 15

Leu Leu Val Cys Pro Gly Leu Ala Cys Gly Pro Gly Arg Gly Phe Gly  
 20 25 30

Lys Arg Arg His Pro Lys Lys Leu Thr Pro Leu Ala Tyr Lys Gln Phe  
 35 40 45

Ile Pro Asn Val Ala Glu Lys Thr Leu Gly Ala Ser Gly Arg Tyr Glu  
 50 55 60

Gly Lys Ile Thr Arg Asn Ser Glu Arg Phe Lys Glu Leu Thr Pro Asn  
 65 70 75 80

Tyr Asn Pro Asp Ile Ile Phe Lys Asp Glu Glu Asn Thr Gly Ala Asp  
 85 90 95

Arg Leu Met Thr Gln Arg Cys Lys Asp Lys Leu Asn Ala Leu Ala Ile  
 100 105 110

Ser Val Met Asn Gln Trp Pro Gly Val Lys Leu Arg Val Thr Glu Gly  
 115 120 125

Trp Asp Glu Asp Gly His His Ser Glu Glu Ser Leu His Tyr Glu Gly  
 130 135 140

Arg Ala Val Asp Ile Thr Thr Ser Asp Arg Asp Arg Ser Lys Tyr Gly  
 145 150 155 160

Met Leu Ala Arg Leu Ala Val Glu Ala Gly Phe Asp Trp Val Tyr Tyr  
 165 170 175

Glu Ser Lys Ala His Ile His Cys Ser Val Lys Ala Glu Asn Ser Val  
 180 185 190

Ala Ala Lys Ser Gly Gly Cys Phe Pro Gly Ser Ala Thr Val His Leu  
 195 200 205

- 154 -

Glu Gln Gly Gly Thr Lys Leu Val Lys Asp Leu Arg Pro Gly Asp Arg  
 210 215 220  
 Val Leu Ala Ala Asp Asp Gln Gly Arg Leu Leu Tyr Ser Asp Phe Leu  
 225 230 235 240  
 Thr Phe Leu Asp Arg Asp Glu Gly Ala Lys Lys Val Phe Tyr Val Ile  
 245 250 255  
 Glu Thr Leu Glu Pro Arg Glu Arg Leu Leu Leu Thr Ala Ala His Leu  
 260 265 270  
 Leu Phe Val Ala Pro His Asn Asp Ser Gly Pro Thr Pro Gly Pro Ser  
 275 280 285  
 Ala Leu Phe Ala Ser Arg Val Arg Pro Gly Gln Arg Val Tyr Val Val  
 290 295 300  
 Ala Glu Arg Gly Gly Asp Arg Arg Leu Leu Pro Ala Ala Val His Ser  
 305 310 315 320  
 Val Thr Leu Arg Glu Glu Glu Ala Gly Ala Tyr Ala Pro Leu Thr Ala  
 325 330 335  
 His Gly Thr Ile Leu Ile Asn Arg Val Leu Ala Ser Cys Tyr Ala Val  
 340 345 350  
 Ile Glu Glu His Ser Trp Ala His Arg Ala Phe Ala Pro Phe Arg Leu  
 355 360 365  
 Ala His Ala Leu Leu Ala Ala Leu Ala Pro Ala Arg Thr Asp Gly Gly  
 370 375 380  
 Gly Gly Gly Ser Ile Pro Ala Ala Gln Ser Ala Thr Glu Ala Arg Gly  
 385 390 395 400  
 Ala Glu Pro Thr Ala Gly Ile His Trp Tyr Ser Gln Leu Leu Tyr His  
 405 410 415  
 Ile Gly Thr Trp Leu Leu Asp Ser Glu Thr Met His Pro Leu Gly Met  
 420 425 430  
 Ala Val Lys Ser Ser  
 435

- 155 -

## CLAIMS

1. A substantially pure polypeptide characterized by having an amino acid sequence of a hedgehog polypeptide or a fragment derived from amino terminal amino acids of a hedgehog polypeptide, wherein the polypeptide or fragment thereof comprises a sterol moiety.  
5
2. The polypeptide of claim 1, wherein the fragment is an extracellular hedgehog polypeptide fragment.
3. The polypeptide of claim 2, wherein the fragment has at its carboxy terminus, a G↓CF cleavage site specifically recognized by a proteolytic activity of the carboxy terminal fragment of a native hedgehog polypeptide.  
10
4. The polypeptide of claim 1, wherein the sterol is cholesterol.
5. The polypeptide of claim 1, wherein the hedgehog polypeptide is selected from the group consisting of Drosophila, Zebrafish, Xenopus, chicken, murine and human hedgehog.  
15
6. The polypeptide of claim 1, wherein the hedgehog fragment is about 30 to 450 amino acids in length.
7. The polypeptide of claim 1, wherein the hedgehog fragment is about 50 to 300 amino acids in length.
- 20 8. The polypeptide of claim 1, wherein the hedgehog fragment is about 75 to 250 amino acids in length.

- 156 -

9. The polypeptide of claim 1, wherein the hedgehog fragment is about 100 to 200 amino acids in length.
10. A method for affecting cholesterol biosynthesis or transport in a cell comprising contacting a cell with an effective amount of a compound that affects hedgehog, thereby affecting cholesterol biosynthesis or transport.
11. The method of claim 10, wherein the effect is inhibition.
12. The method of claim 10, wherein the effect is stimulation.
13. A method for inhibiting the neural inducing activity of a hedgehog polypeptide in cells, comprising
- 10 introducing into the cells a polypeptide selected from the group consisting of:
- a) SEQ ID NO:17, beginning at amino acid residue 257 to the final carboxy amino acid;
- b) SEQ ID NO:18, beginning at amino acid residue 257 to the final carboxy amino acid;
- 15 c) SEQ ID NO:19, beginning at amino acid residue 257 to the final carboxy amino acid; and
- d) SEQ ID NO:20, beginning at amino acid residue 257 to the final carboxy amino acid, and having at its carboxy terminus, a Gly<sup>1</sup>Cys Phe cleavage site specifically recognized by a proteolytic activity of the
- 20 carboxy terminal fragment of the native hedgehog polypeptide, wherein the introduced polypeptide interferes with neural inducing activity of a hedgehog polypeptide in the cells, wherein the hedgehog peptide is selected from the group consisting of
- e) the amino acid sequence of SEQ ID NO:1;
- 25 f) the amino acid sequence of SEQ ID NO:2;

- 157 -

- g) SEQ ID NO:17, from amino acid residue 1 to amino acid residue 259;
- h) SEQ ID NO:18, from amino acid residue 1 to amino acid residue 259;
- i) SEQ ID NO:19, from amino acid residue 1 to amino acid residue 259;

and

5

- j) SEQ ID NO:20, from amino acid residue 1 to amino acid residue 259, and having at its carboxy terminus, a Gly↓Cys Phe cleavage site specifically recognized by a proteolytic activity of the carboxy terminal fragment of the native hedgehog polypeptide.

14. The method of claim 13, wherein the introduced polypeptide induces the development of dorsal anatomical structures.

10

15. The method of claim 13, wherein the introduced polypeptide increases the expression of en-2 and krox20.

16. A method of inducing pituitary gland gene expression comprising introducing to cells of the pituitary gland, a polypeptide selected from the group consisting of

15

a) SEQ ID NO:17, beginning at amino acid residue 257 to the final carboxy amino acid;

b) SEQ ID NO:18, beginning at amino acid residue 257 to the final carboxy amino acid;

20

c) SEQ ID NO:19, beginning at amino acid residue 257 to the final carboxy amino acid; and

25

d) SEQ ID NO:20, beginning at amino acid residue 257 to the final carboxy amino acid, and having at its carboxy terminus, a Gly↓Cys Phe cleavage site specifically recognized by a proteolytic activity of the carboxy terminal fragment of the native hedgehog polypeptide, wherein the introduced polypeptide induces the expression of pituitary gland-specific genes.

1148

FIG. 1A

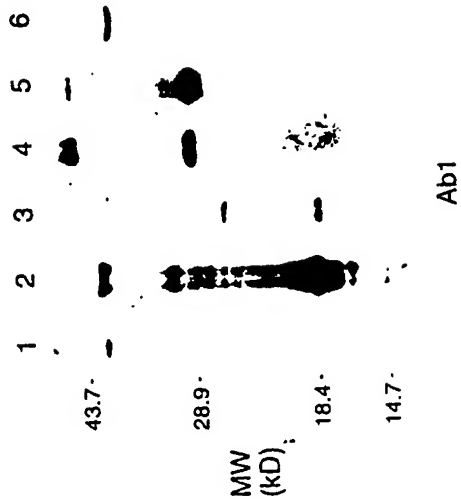


FIG. 1B

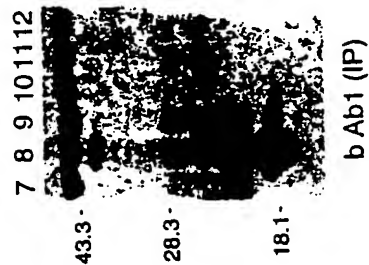


FIG. 1C

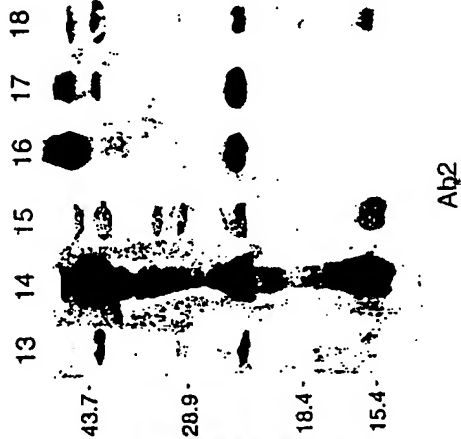
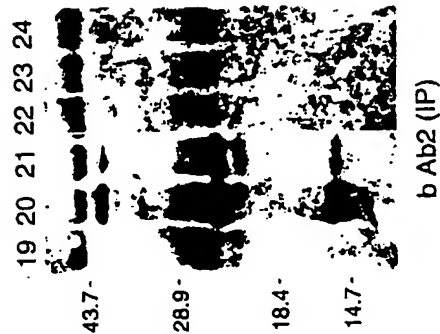


FIG. 1D



## Hh-C Cleavage Mechanism

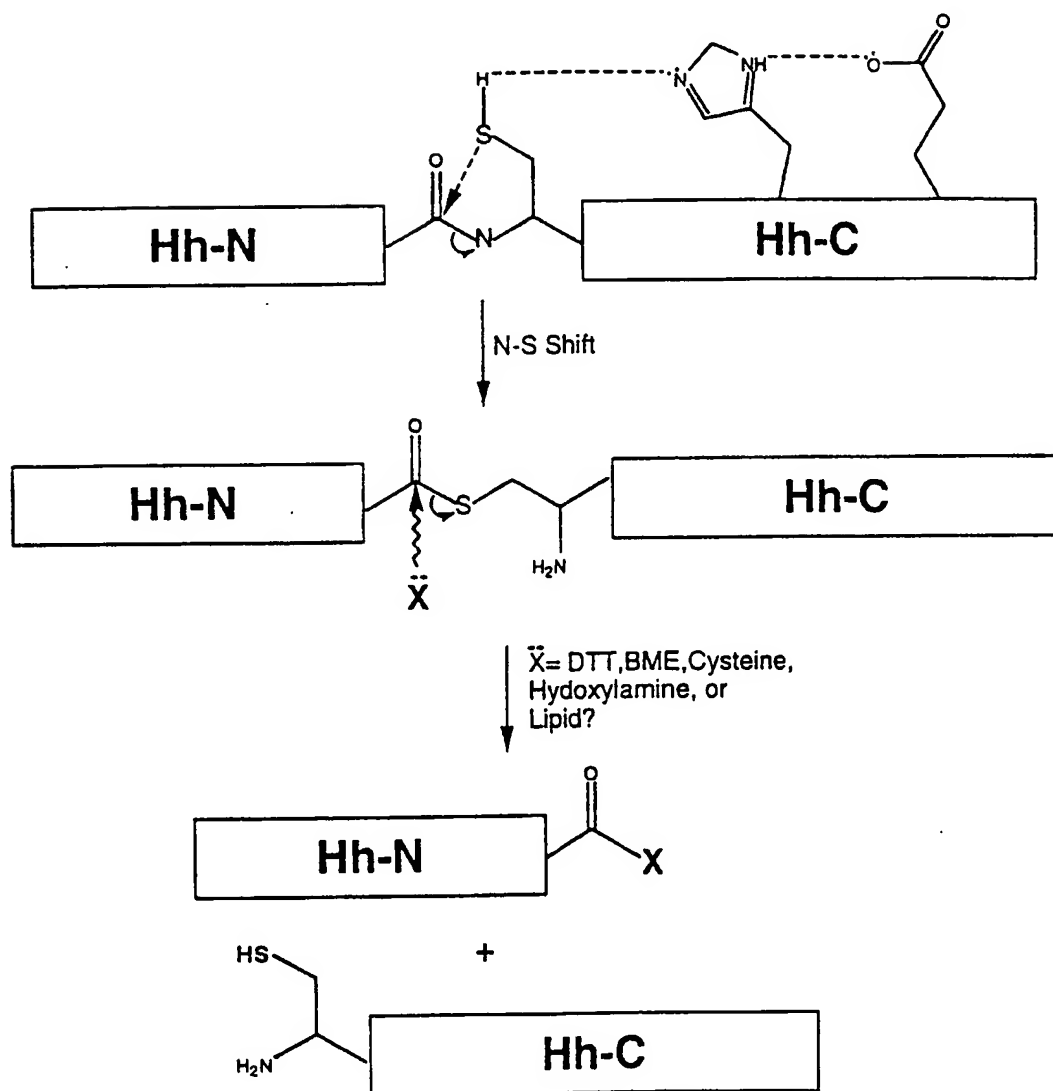


FIG. 1E

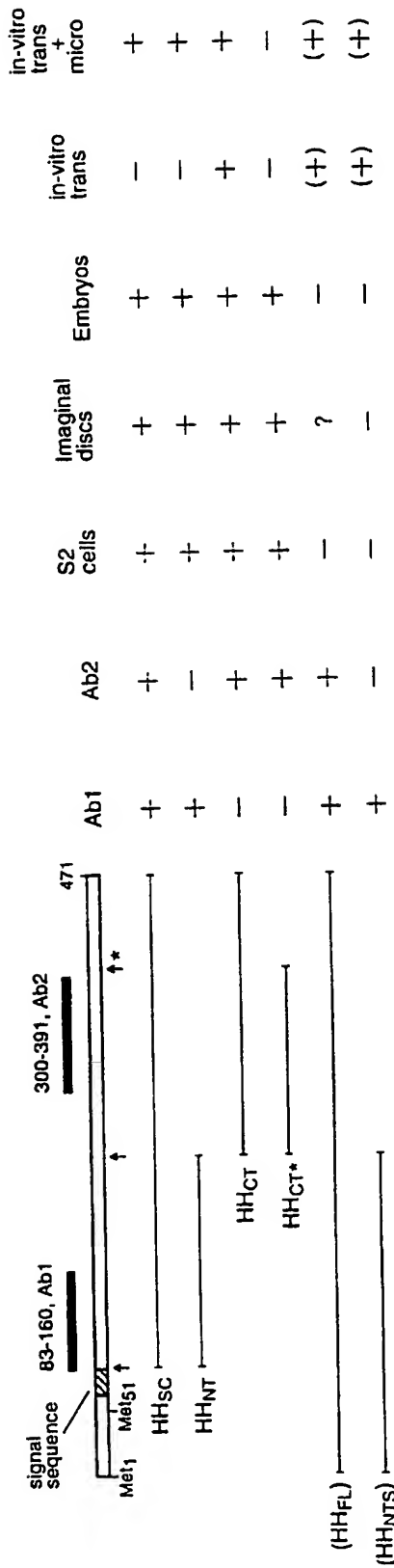


FIG. 1F

	1	2	3	4	5	6	7
D. mel. hh	L	T	V	T	P	A	H
D. hydei hh	L	T	V	T	P	A	H
C-Shh	L	L	L	T	A	A	H
M-Shh/Hhg-1	L	L	L	T	A	A	H
R vhh-1	L	L	L	T	A	A	H
Z-Shh/Zf vhh-1	I	T	L	T	A	A	H
twhh	L	T	L	T	A	A	H
M-Dhh	L	L	L	T	P	W	H
M-lhh	L	A	L	T	P	A	H

**FIG. 2A**

CHT	W	V	V	T	A	A	H
TRP	W	V	V	S	A	A	H
ELA	W	V	M	T	A	A	H
UKH	W	V	I	S	A	T	H
C1R	W	I	L	T	A	A	H
C1S	W	V	L	T	A	A	H
MCP	F	V	L	T	A	A	H
FAX	Y	V	L	T	A	A	H
TPA	W	I	L	S	A	A	H

**FIG. 2B**

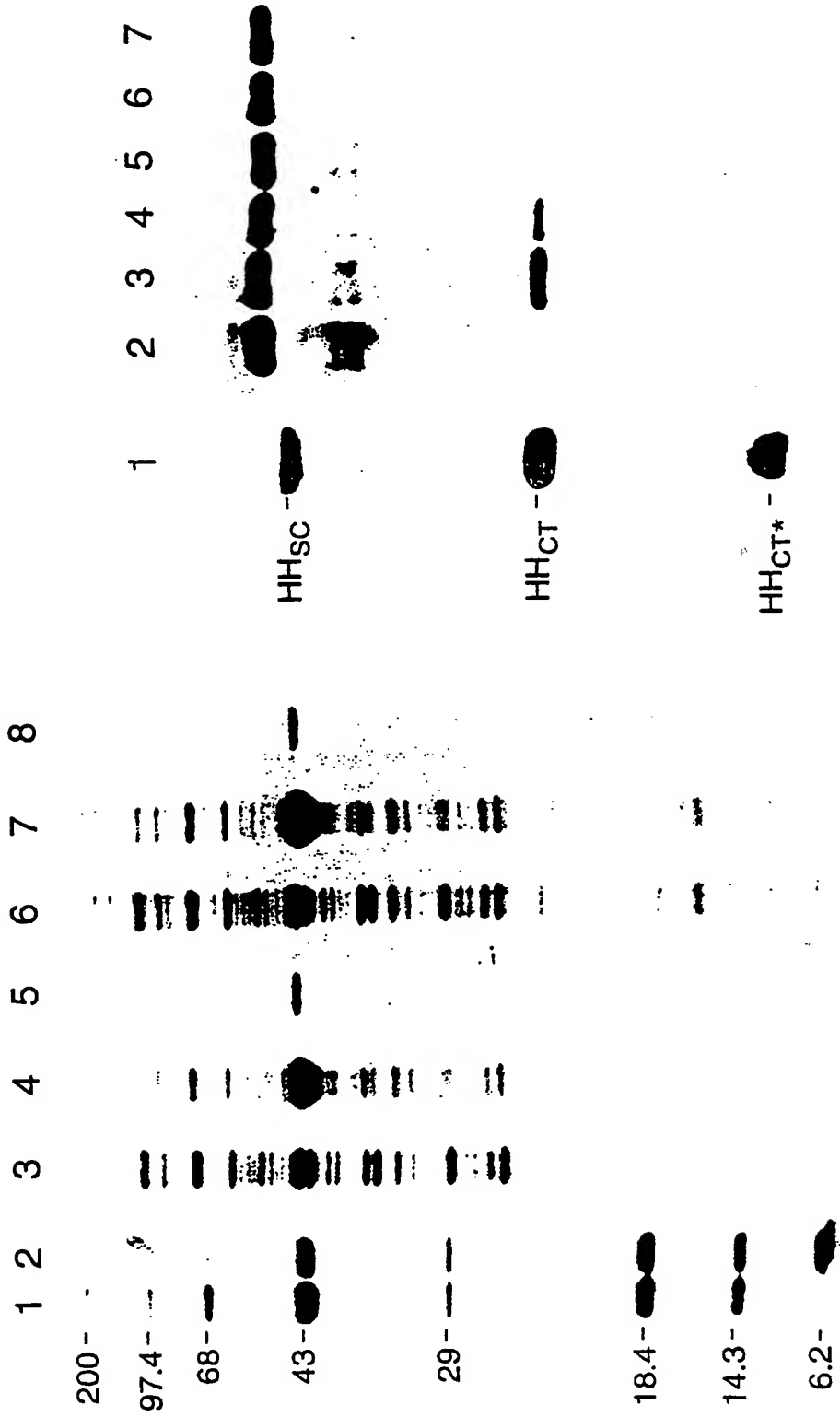
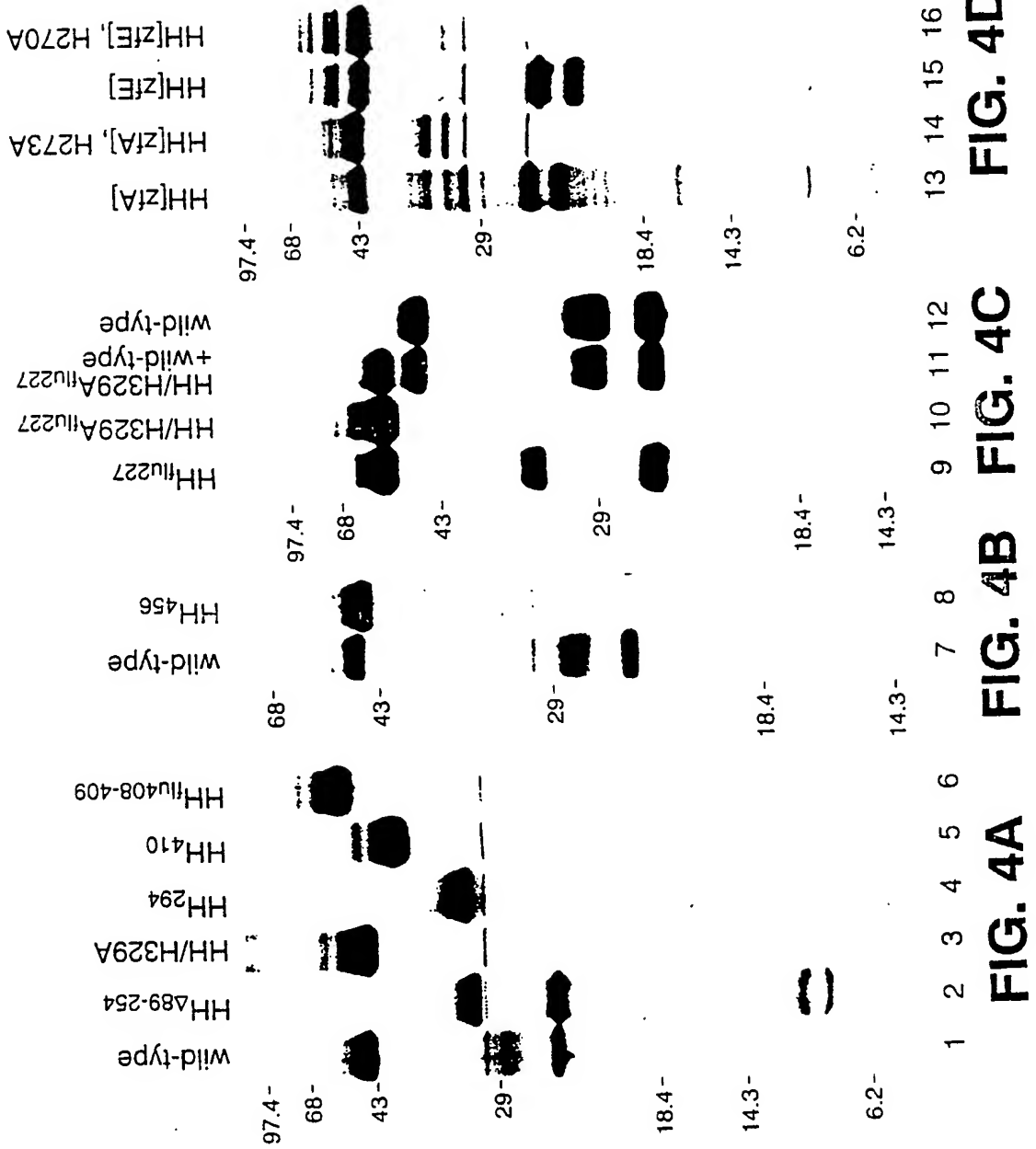


FIG. 3B

FIG. 3A



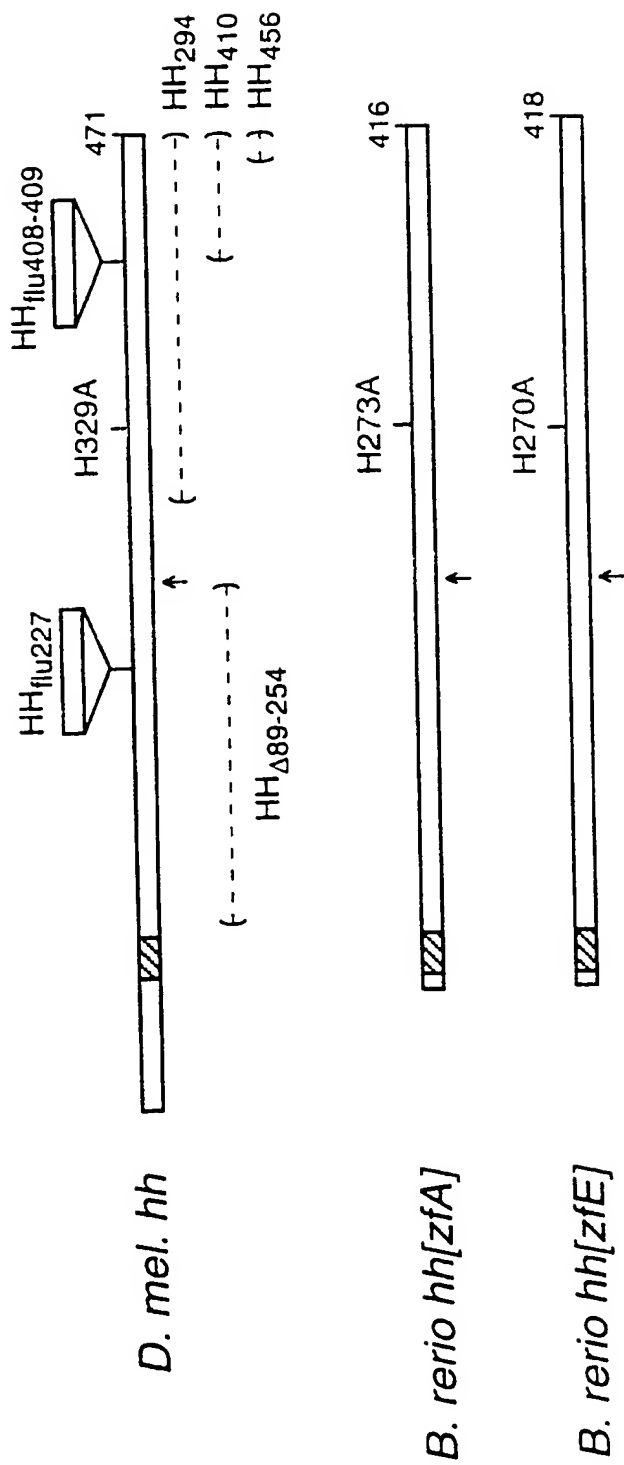
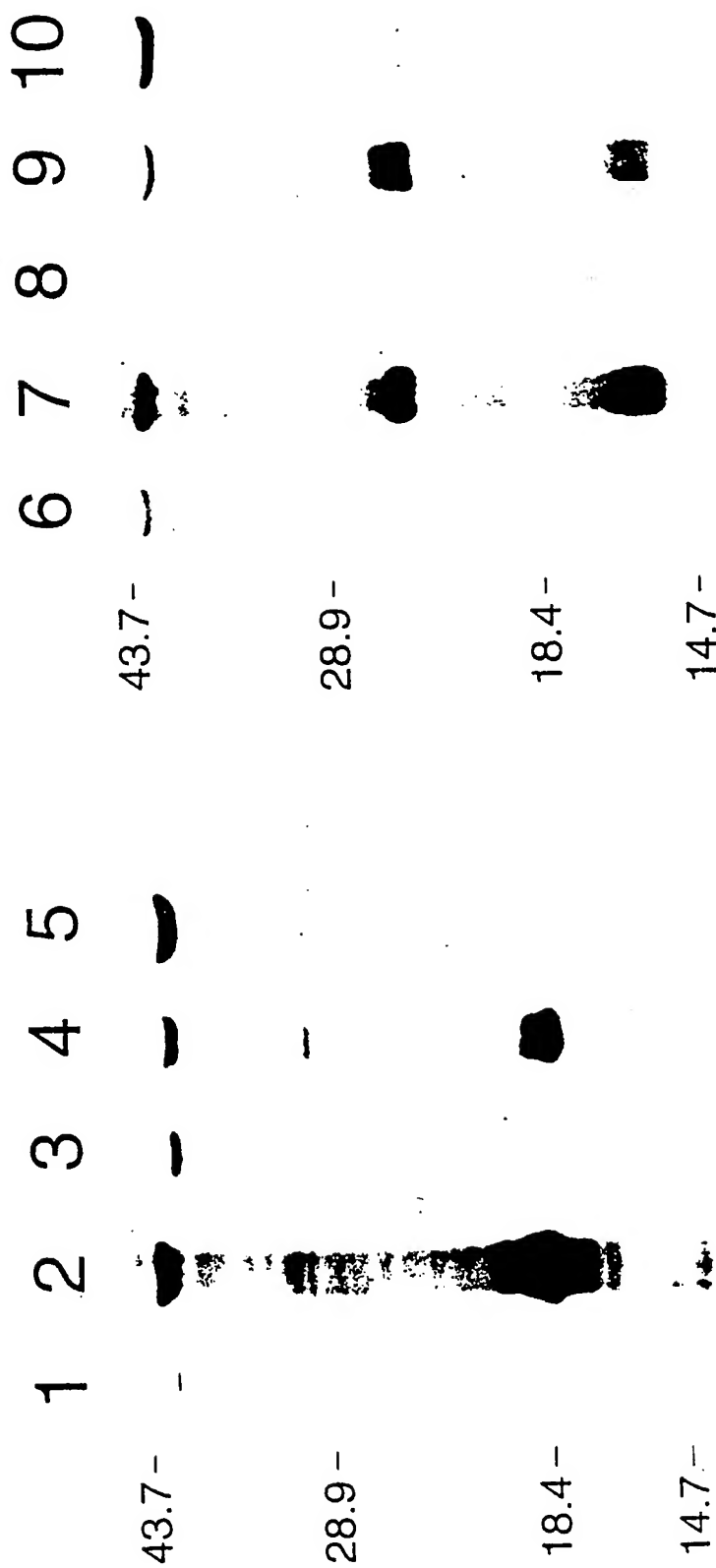


FIG. 4E



Ab1

Ab2

FIG. 5A

FIG. 5B



FIG. 6C

FIG. 6B

FIG. 6A

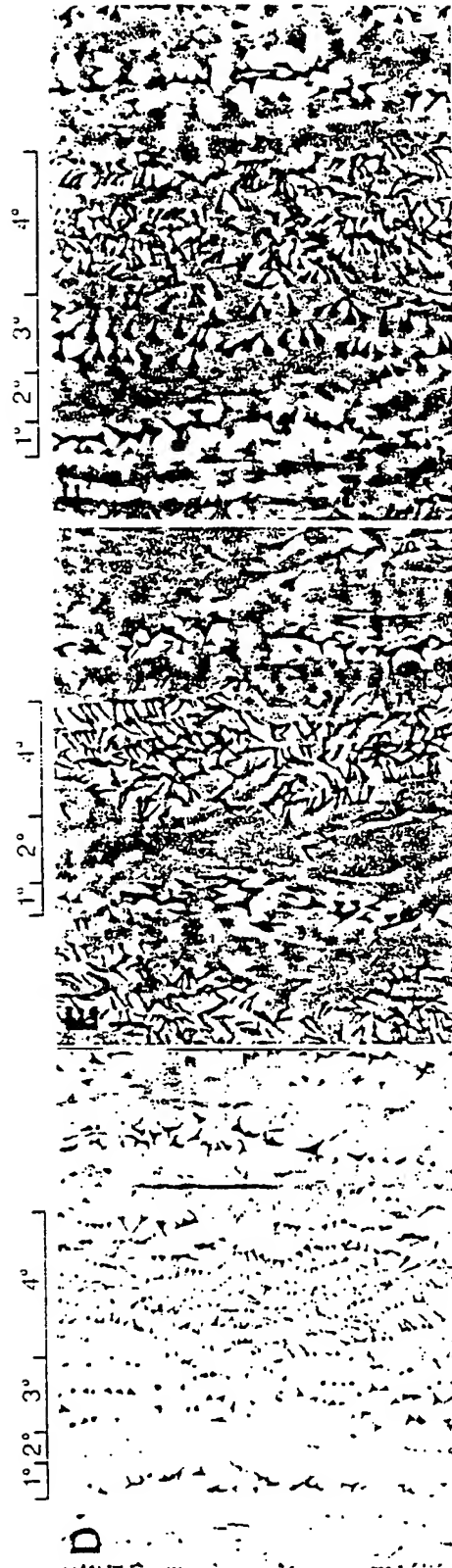


FIG. 6F

FIG. 6E

FIG. 6D

70/48

A



FIG. 7A

B



FIG. 7B

C



FIG. 7C

D



FIG. 7D

E



FIG. 7E

F



FIG. 7F

G



FIG. 7G

H



FIG. 7H

I



FIG. 7I

J



FIG. 7J

K



FIG. 7K

L



FIG. 7L

M



FIG. 7M

N



FIG. 7N

O



FIG. 7O

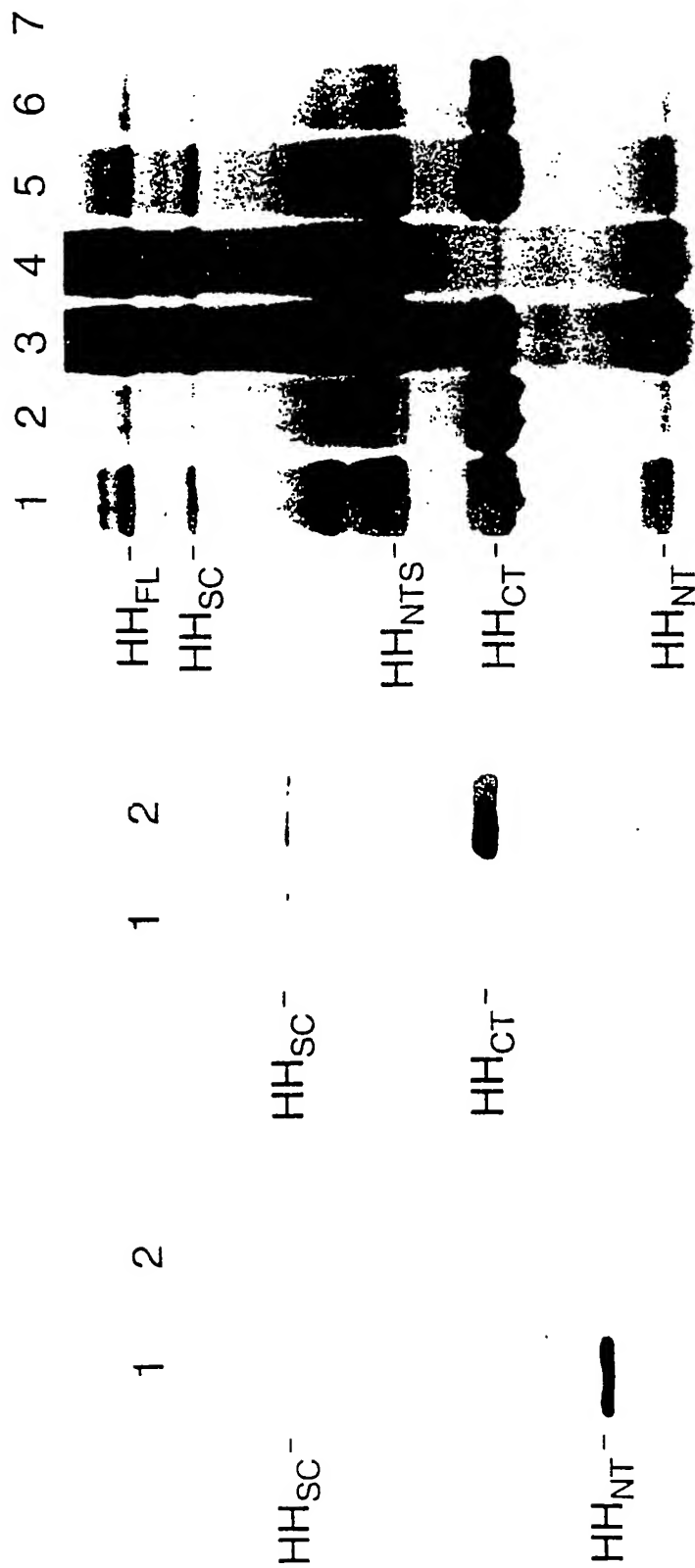


FIG. 8C

FIG. 8B

FIG. 8A

FIG. 9A



FIG. 9B



FIG. 9C



FIG. 9D

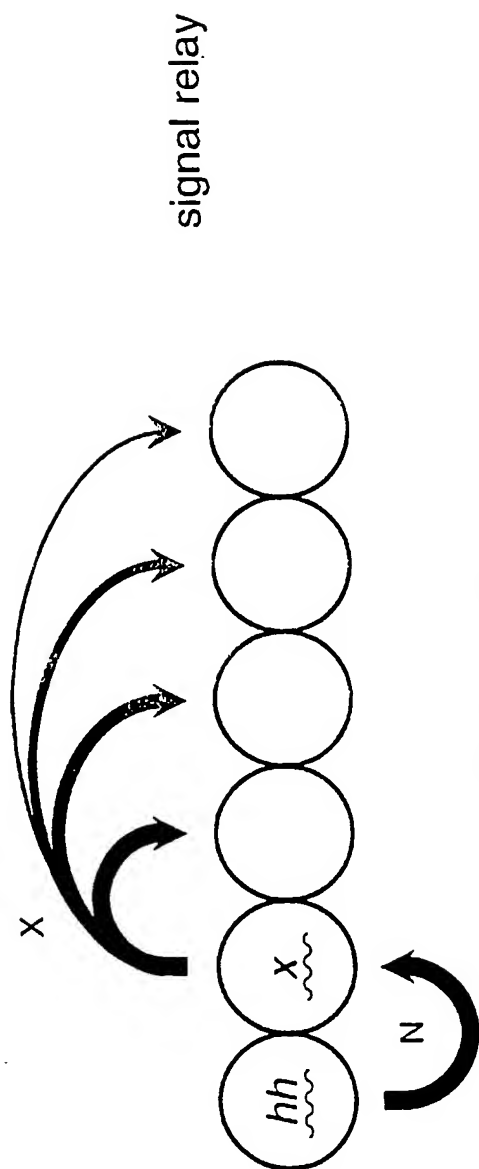


FIG. 10A

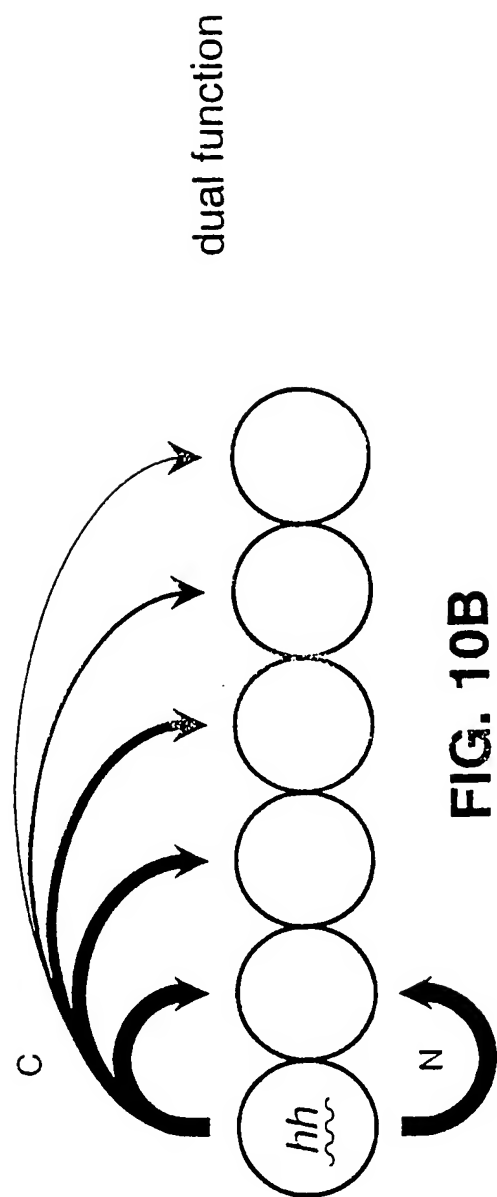


FIG. 10B

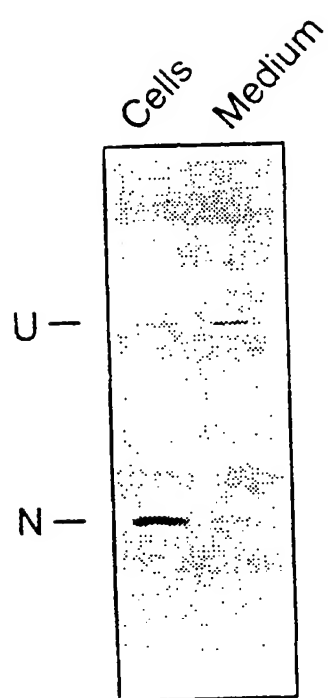


FIG. 10C

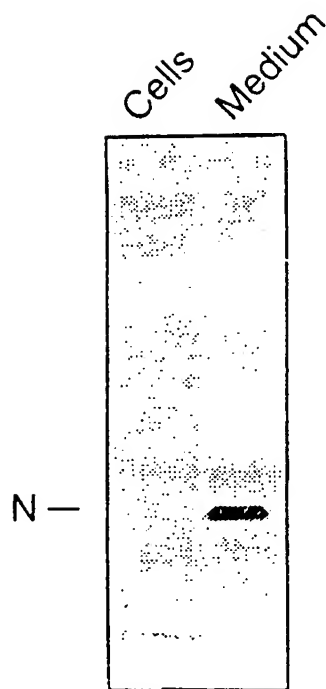


FIG. 10D

1/1 GTG AAA CTG CGG GTG ACC GAG CCC TGG GAC GAA GAT GGC CAC CAC TCA CAG GAG TCT CTG  
 V K L R V T E G W D E D E D G H E S E S L  
 61/21 CAC TAC GAG GGC CGC GCA GTG GAC ATC ACC ACG TCT GAC CGC GAC CGC AGC AAG TAC GGC  
 H Y E G R A V D I T S D R S K Y G  
 121/41 ATG CTG GCC CGC CTG GCG GTG GAG  
 M L A R L A V E

FIG. 11A

1/1 GTG AAG CTG CGG GTG ACC GAG GGC TGG GAC GAG GAC GGC CAC CAC TCA GAG GAG TCC CTG  
 V K L R V T E G W D E D E D G H E S E S L  
 61/21 CAT TAT GAG GGC CGC GCG GTG GAC ATC ACC ACA TCA GAC CGC GAC CGC AAT AAG TAT GGA  
 H Y E G R A V D I T S D R D R N K Y G  
 121/41 CTG CTG GCG TGG GCA GTG GAG  
 L L A R L A V E

FIG. 11B

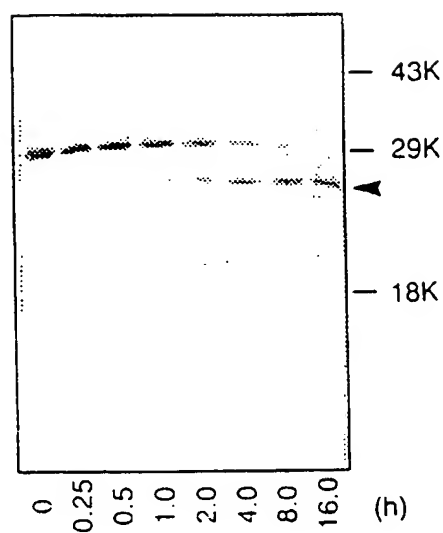


FIG. 12A

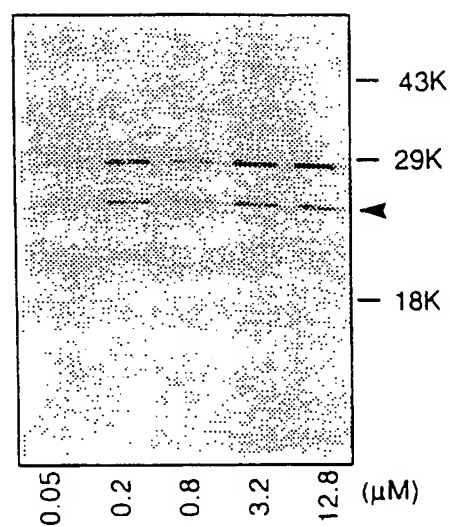


FIG. 12B

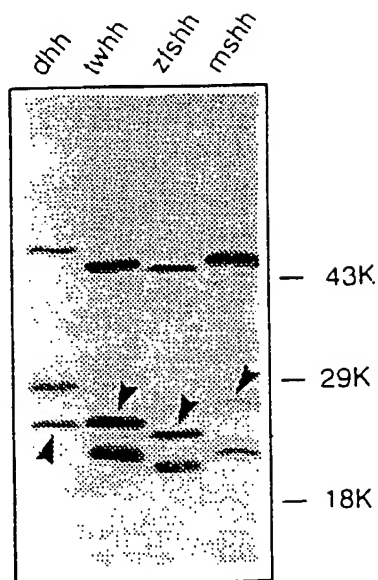


FIG. 12D

## Cleavage Site Sequence



D. melanogaster hh	ISSHVHGCFTPEST
D. hydei hh	SISHMHGCFTPEST
m-sonic hh	VAAKSGGCFFGSAT
r-sonic hh	VAAKSDGCFFGSAT
c-sonic hh	VAAKSGGCFFGSAL
z-sonic hh	VAAKSGGCFFPGSGT
z-twhh	VAAKSGGCFFPAGAR
x-sonic hh	VAAKTGGCFFPAGAQ
m-indian hh	VAAKTGGCFFPGEAL
x-bhh	LGVRSGGCFFPGTAM
x-hh4	LGVRSGGCFFPGTAM
x-hh3	LGVRSGGCFFPGTAM
m-desert hh	LAVRAGGCFFGNAT

FIG. 12C

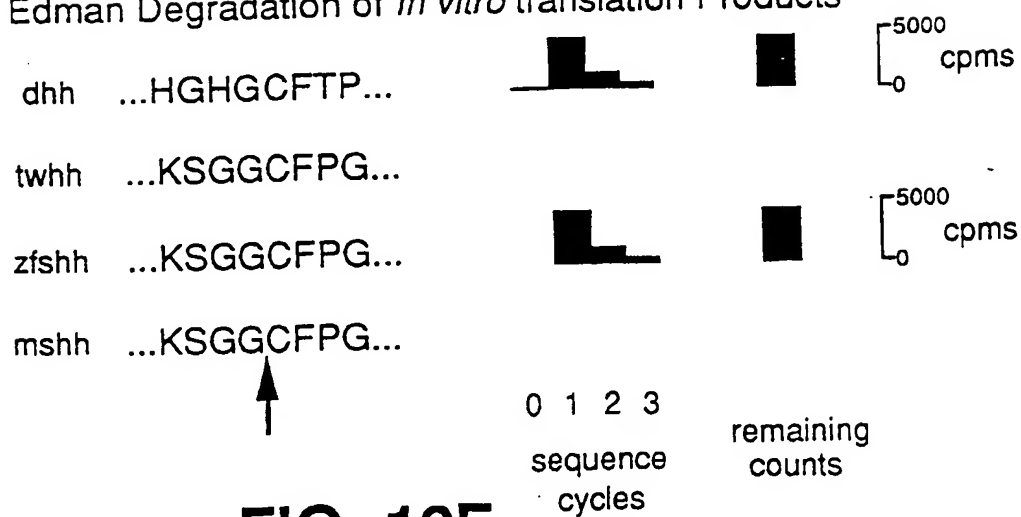
Edman Degradation of *In vitro* translation Products

FIG. 12E

zebrafish twhh	MDVRLHLKQFALLCFISLILTPCGLACGPGRGYCHRRHPKKLTPLAYKQFI PNVAEKTILGASCHYEKGKITRNSER	75
zebrafish shh	M--RL-LTRVLLVSLTLTSLVVSGLACGPGRGYCHRRHPKKLTPLAYKQFI PNVAEKTILGASCHYEKGKITRNSER	72
Chicken shh	MVEMLLLTRILLVGFICALLVSSGLTCGPGRGYCHRRHPKKLTPLAYKQFI PNVAEKTILGASCHYEKGKITRNSER	75
Mouse shh	M--LLLARCFLVILASSLLVCPGLACGPGRGYCHRRHPKKLTPLAYKQFI PNVAEKTILGASCHYEKGKITRNSER	73
zebrafish twhh	FKELIPNYPNDIIFKDEENTNADRLMTNCRCKDKLNLAIISVMNFWPGVNLRVTEGWDEDDGHHEESLHYEGRAVD	150
zebrafish shh	FKELIPNYPNDIIFKDEENTNADRLMTNCRCKDKLNLAIISVMNFWPGVNLRVTEGWDEDDGHHEESLHYEGRAVD	147
Chicken shh	FKELIPNYPNDIIFKDEENTNADRLMTNCRCKDKLNLAIISVMNFWPGVNLRVTEGWDEDDGHHEESLHYEGRAVD	150
Mouse shh	FKELIPNYPNDIIFKDEENTNADRLMTNCRCKDKLNLAIISVMNFWPGVNLRVTEGWDEDDGHHEESLHYEGRAVD	148
zebrafish twhh	ITTSDDRDKSKYGMISRLAVEAGFDWVYYESKAHIHCSVKAENSVAAKSGGCGPFGSGTIVILGLGTHKPIKDKLVGD	225
zebrafish shh	ITTSDDRDKSKYGMISRLAVEAGFDWVYYESKAHIHCSVKAENSVAAKSGGCGPFGSGTIVILGLGTHKPIKDKLVGD	222
Chicken shh	ITTSDDRDKSKYGMISRLAVEAGFDWVYYESKAHIHCSVKAENSVAAKSGGCGPFGSGTIVILGLGTHKPIKDKLVGD	225
Mouse shh	ITTSDDRDKSKYGMISRLAVEAGFDWVYYESKAHIHCSVKAENSVAAKSGGCGPFGSGTIVILGLGTHKPIKDKLVGD	223
zebrafish twhh	RVLAADEKGNVLLISDFIMFIDHDPTTRRQFIVVETSEPFKTLTLTAAHLFVFNSSAAS--GITAT---FASNV	294
zebrafish shh	RVLAADEKGNVLLISDFIMFIDHDPTTRRQFIVVETSEPFKTLTLTAAHLFVFNSSAAS--GITAT---FASNV	293
Chicken shh	RVLAADEKGNVLLISDFIMFIDHDPTTRRQFIVVETSEPFKTLTLTAAHLFVFNSSAAS--GITAT---FASNV	300
Mouse shh	RVLAADEKGNVLLISDFIMFIDHDPTTRRQFIVVETSEPFKTLTLTAAHLFVFNSSAAS--GITAT---FASNV	295
zebrafish twhh	KFGDTVLVWEDTCESLKS--TVKRI-YTIEEHEGSHAPMTAGTILVDQVLASCYAVTIEHHKWAHAFAPVRLCH	366
zebrafish shh	KFGDTVLVWEDTCESLKS--TVKRI-YTIEEHEGSHAPMTAGTILVDQVLASCYAVTIEHHKWAHAFAPVRLCH	364
Chicken shh	KFGDTVLVWEDTCESLKS--TVKRI-YTIEEHEGSHAPMTAGTILVDQVLASCYAVTIEHHKWAHAFAPVRLCH	373
Mouse shh	KFGDTVLVWEDTCESLKS--TVKRI-YTIEEHEGSHAPMTAGTILVDQVLASCYAVTIEHHKWAHAFAPVRLCH	370
zebrafish twhh	KLMTWDLFP-----ARESNNVFQED-----GTHWYSNMLFHJGSMILIRDSFHPILGI-LIHS	416
zebrafish shh	KLMTWDLFP-----ARESNNVFQED-----GTHWYSNMLFHJGSMILIRDSFHPILGI-LIHS	418
Chicken shh	KLMTWDLFP-----ARESNNVFQED-----GTHWYSNMLFHJGSMILIRDSFHPILGI-LIHS	425
Mouse shh	KLMTWDLFP-----ARESNNVFQED-----GTHWYSNMLFHJGSMILIRDSFHPILGI-LIHS	437

FIG. 13

19/48

FIG. 14A FIG. 14B FIG. 14C FIG. 14D

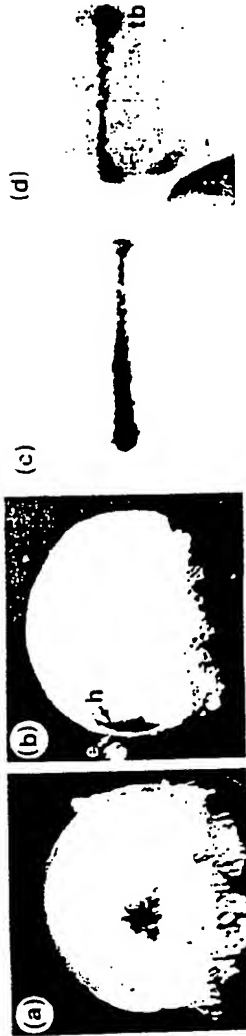


FIG. 14E FIG. 14F FIG. 14G



FIG. 14H

(h)



FIG. 14I

(i)



FIG. 14J

(j)



FIG. 14M

(m)



FIG. 14L

(l)



FIG. 14K

(k)



FIG. 14N

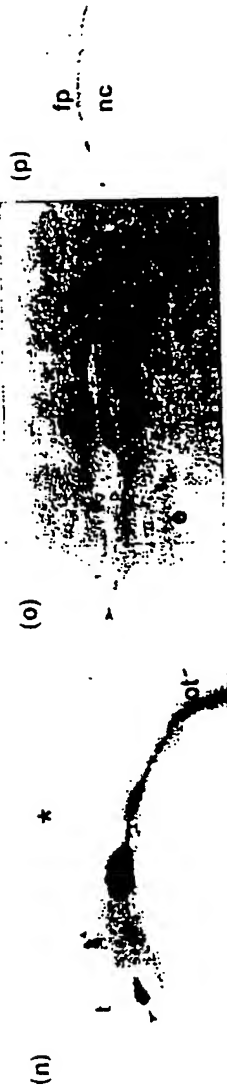


FIG. 14O



FIG. 14P



FIG. 14S



FIG. 14R



FIG. 14Q





FIG. 15A

FIG. 15B

FIG. 15C



FIG. 15D

FIG. 15E

FIG. 15F

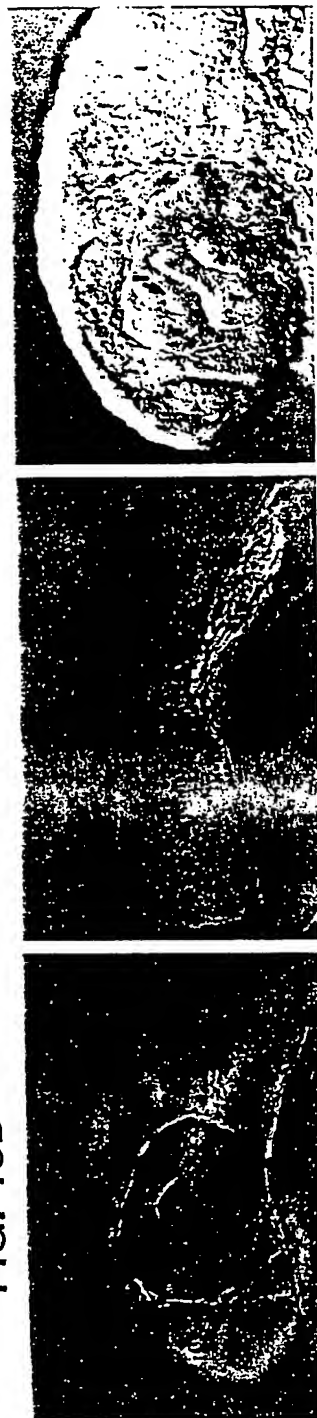


FIG. 15G

FIG. 15H

FIG. 15I

23/48

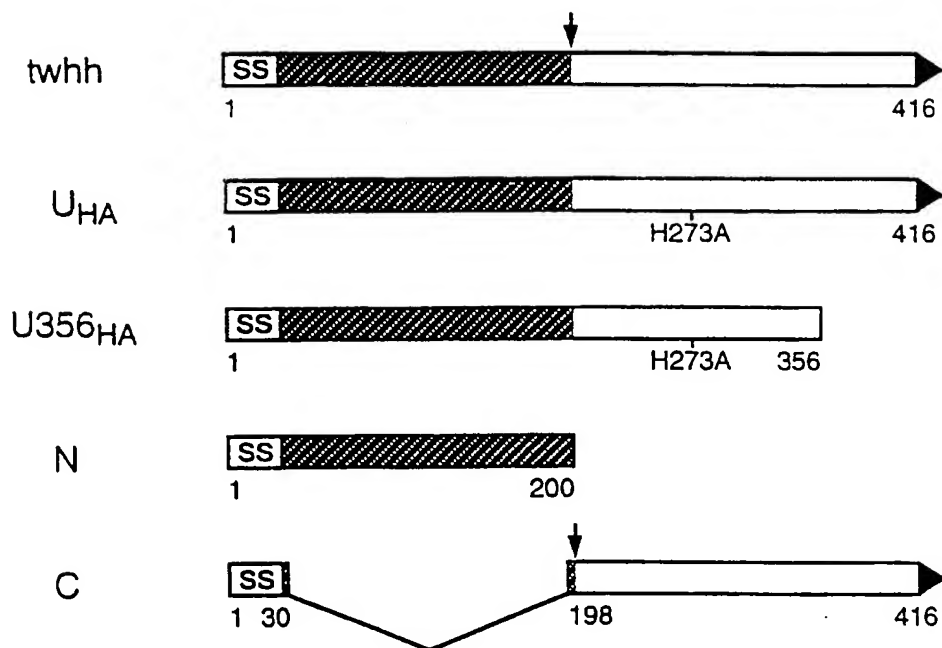
Table 1. Effects of ectopic expression of *ssh*, *twhh*, *twhh-N*, *twhh-UHA* and *lacZ* on zebrafish embryonic development.

Injected mRNA	<i>ssh</i>	<i>twhh</i>	<i>twhh-N</i>	<i>twhh-UHA</i>	<i>lacZ</i>
<b>12.5 h</b>					
Ectopic pax-2 in eye	89% (35)	82% (22)	92% (26)	90% (30)	0% (31)
<b>22 h</b>					
Ectopic pax-2 in eye	22% (54)	62% (50)	76% (42)	21% (39)	0% (34)
Reduced pax-6 in eye	20%	68%	54%	1%	0%
Reduced pax-6 in ventral forebrain	0%	43%	79%	0%	0%
Reduced pax-6 in hindbrain	0% (35)	18% (40)	61% (28)	0% (68)	0% (14)
<b>28 h</b>					
Lens absent	16%	86%	100%	9%	0%
Lens smaller	48%	9%	0%	36%	0%
Reduced eye pigment	80%	91%	100%	64%	0%
No midbrain-hindbrain constriction	48% (25)	77% (44)	100% (16)	22% (45)	3% (37)

The percentages of affected embryos are shown; the numbers of embryos assayed are given in parentheses. Embryos are analyzed at the indicated time-points after injection of synthetic mRNA, as described in the text Figs. 3-5. These results represent a set of assays performed together for direct comparison of activities; repetitions yielded similar results. See text Fig. 7 for description of transcription constructs.

FIG. 16

24/48

**FIG. 17A**

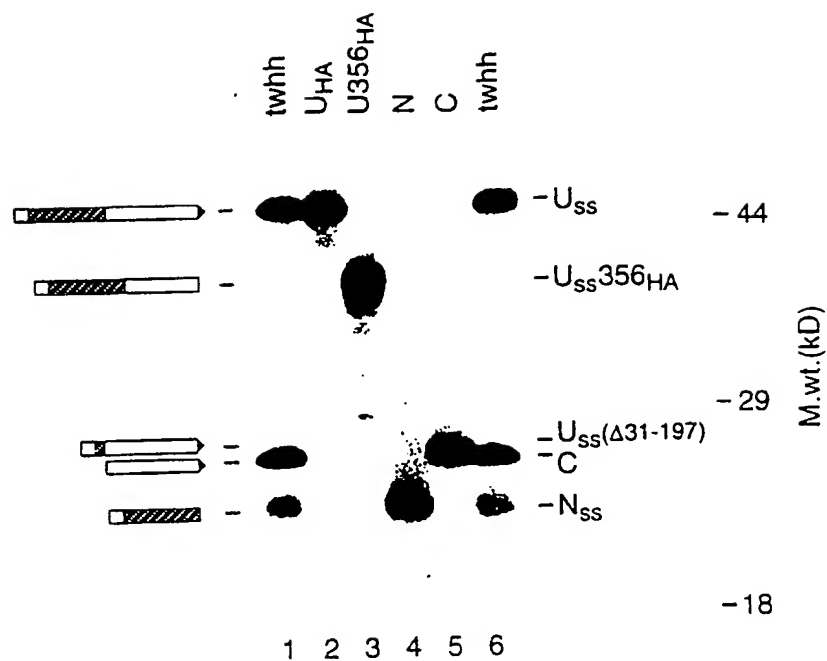


FIG. 17B

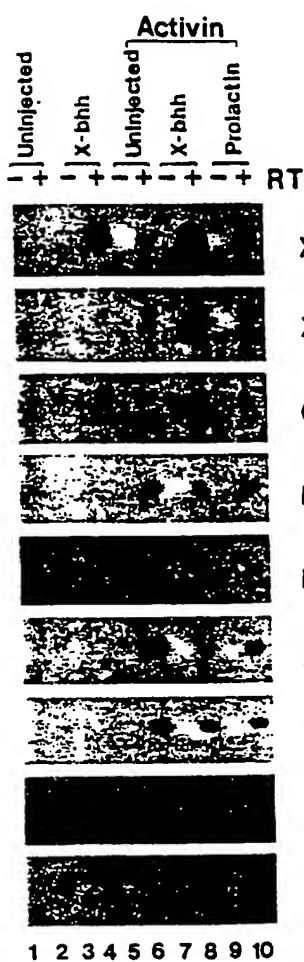


FIG. 18A

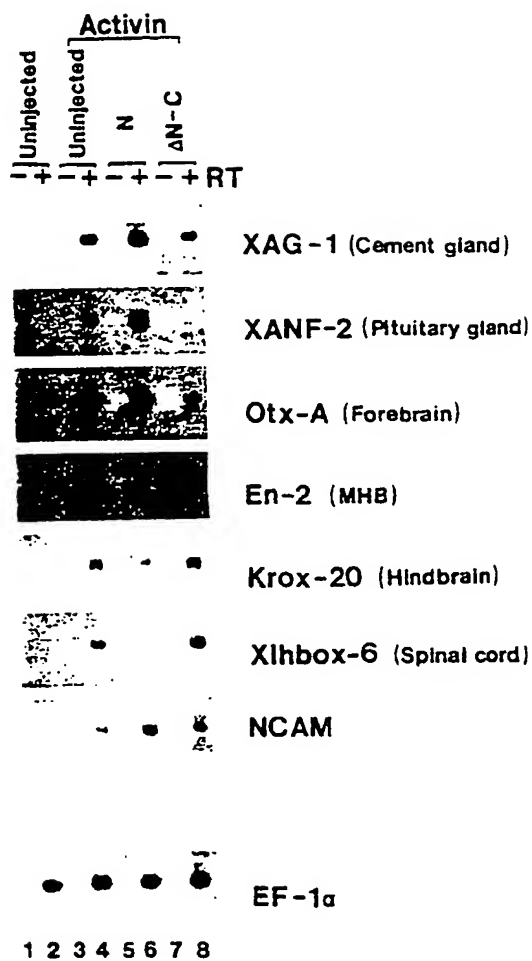


FIG. 18B

Uninjected      X-bhh

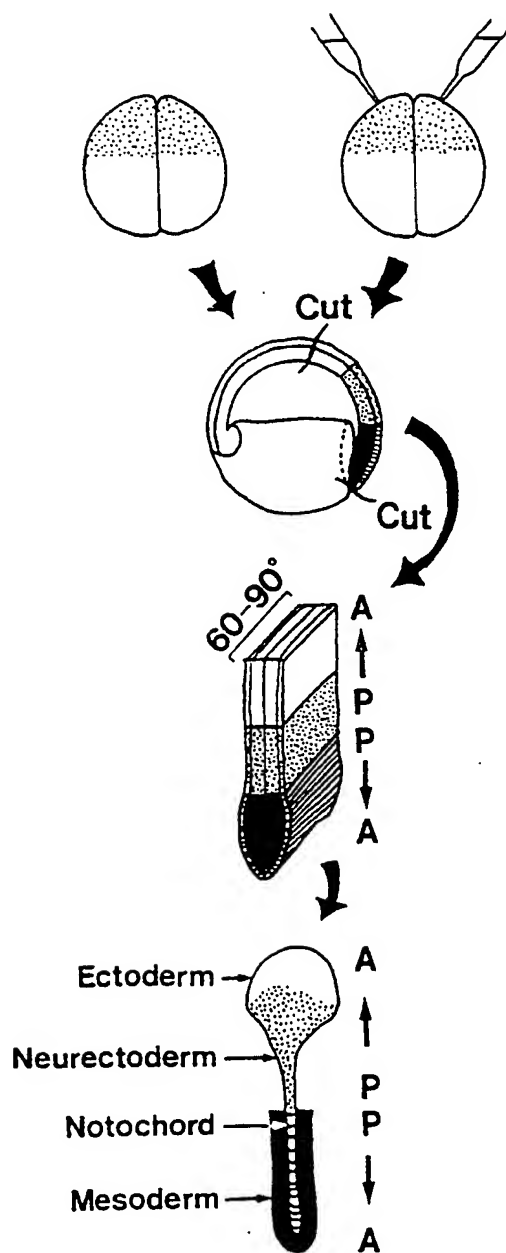


FIG. 19A



100

4



**1 2 3 4**

FIG. 19B

29/48

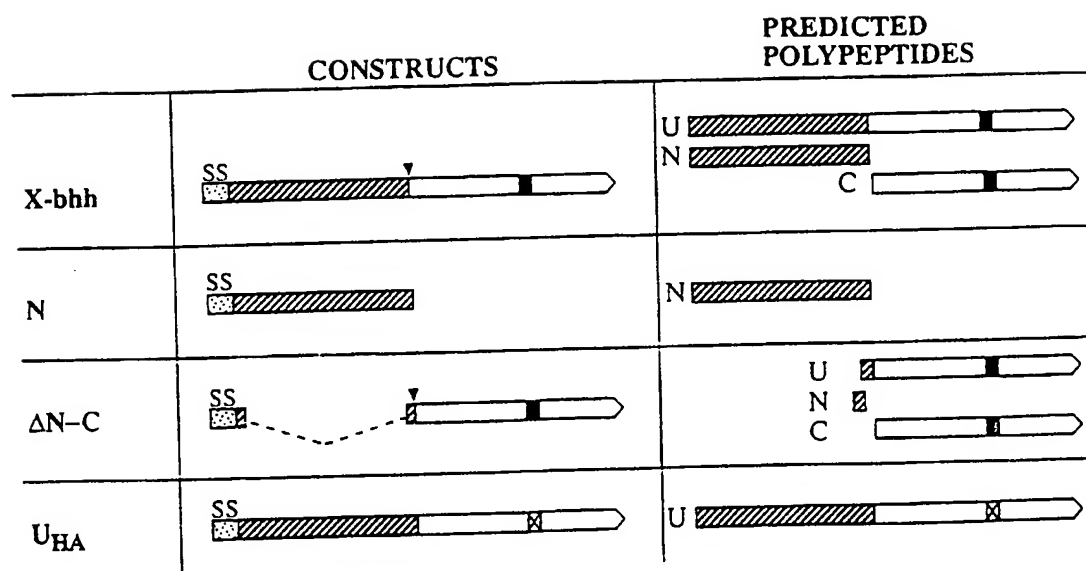


FIG. 20A

30/48

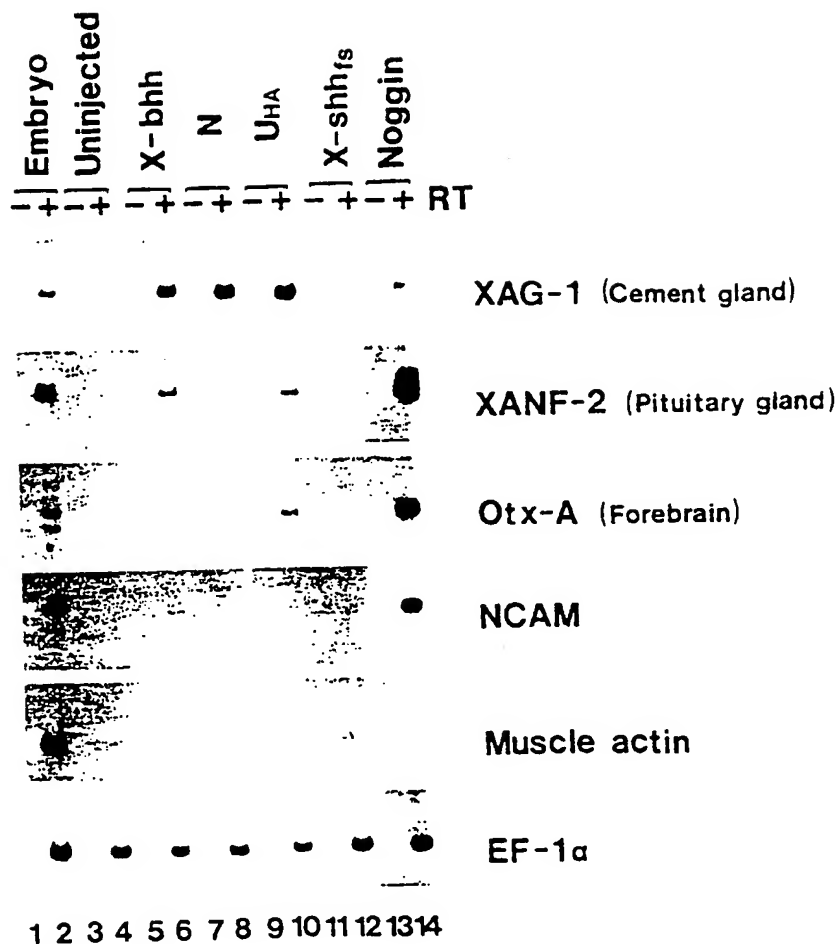


FIG. 20B

31/48

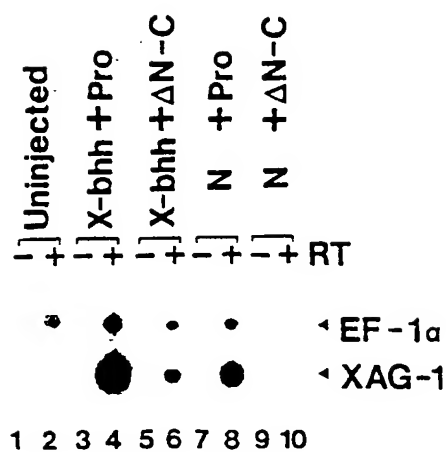


FIG. 21

32/48

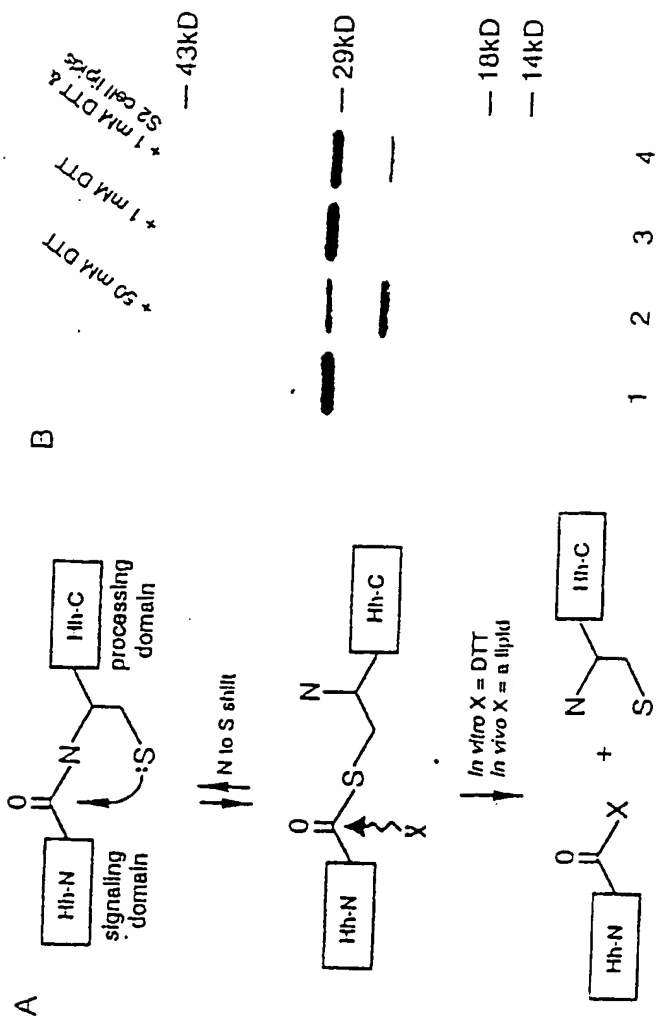


Figure 22

33/48

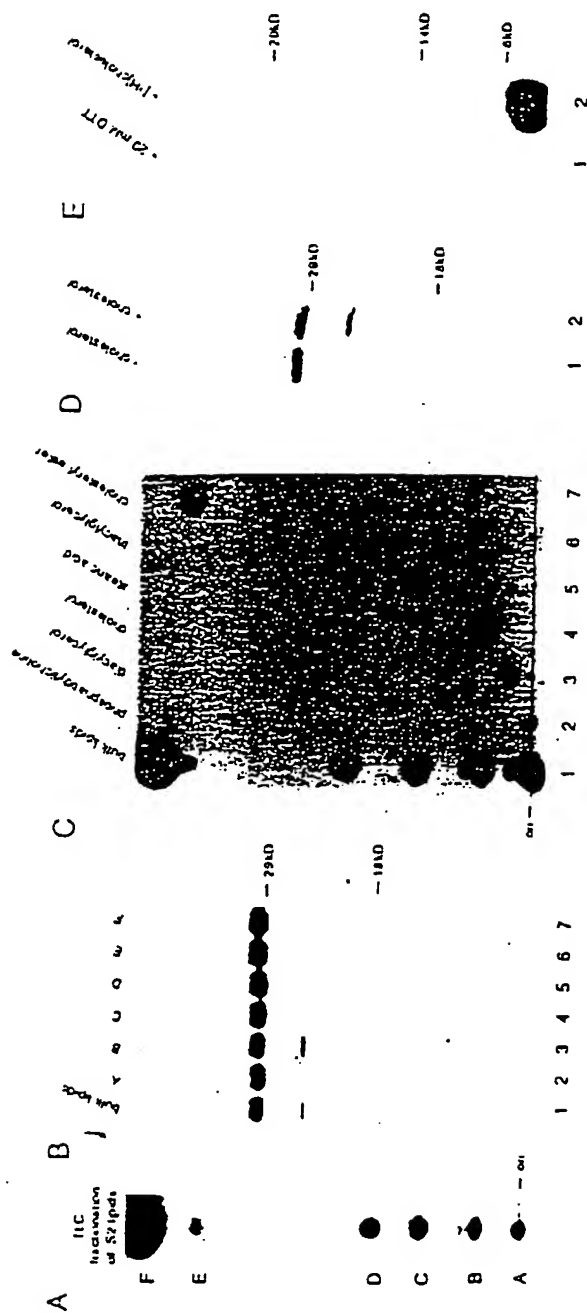


Figure 23

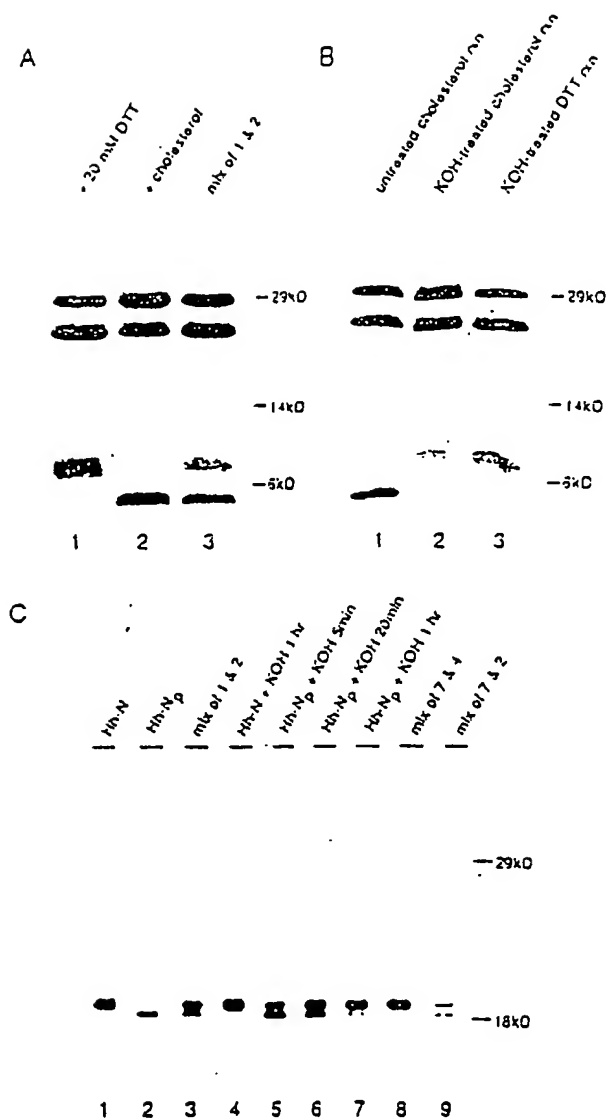


Figure 24

35  $\mu$ l

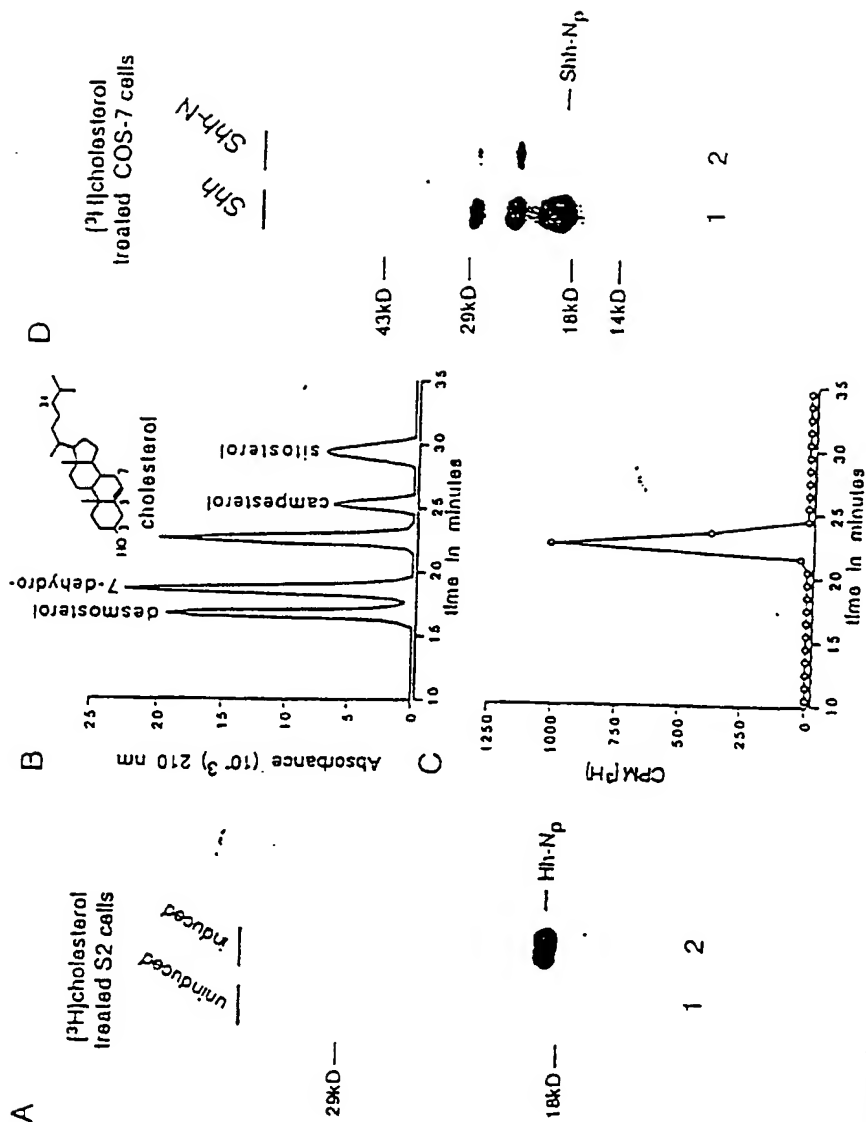


Figure 4:25

36/48

Figure 26

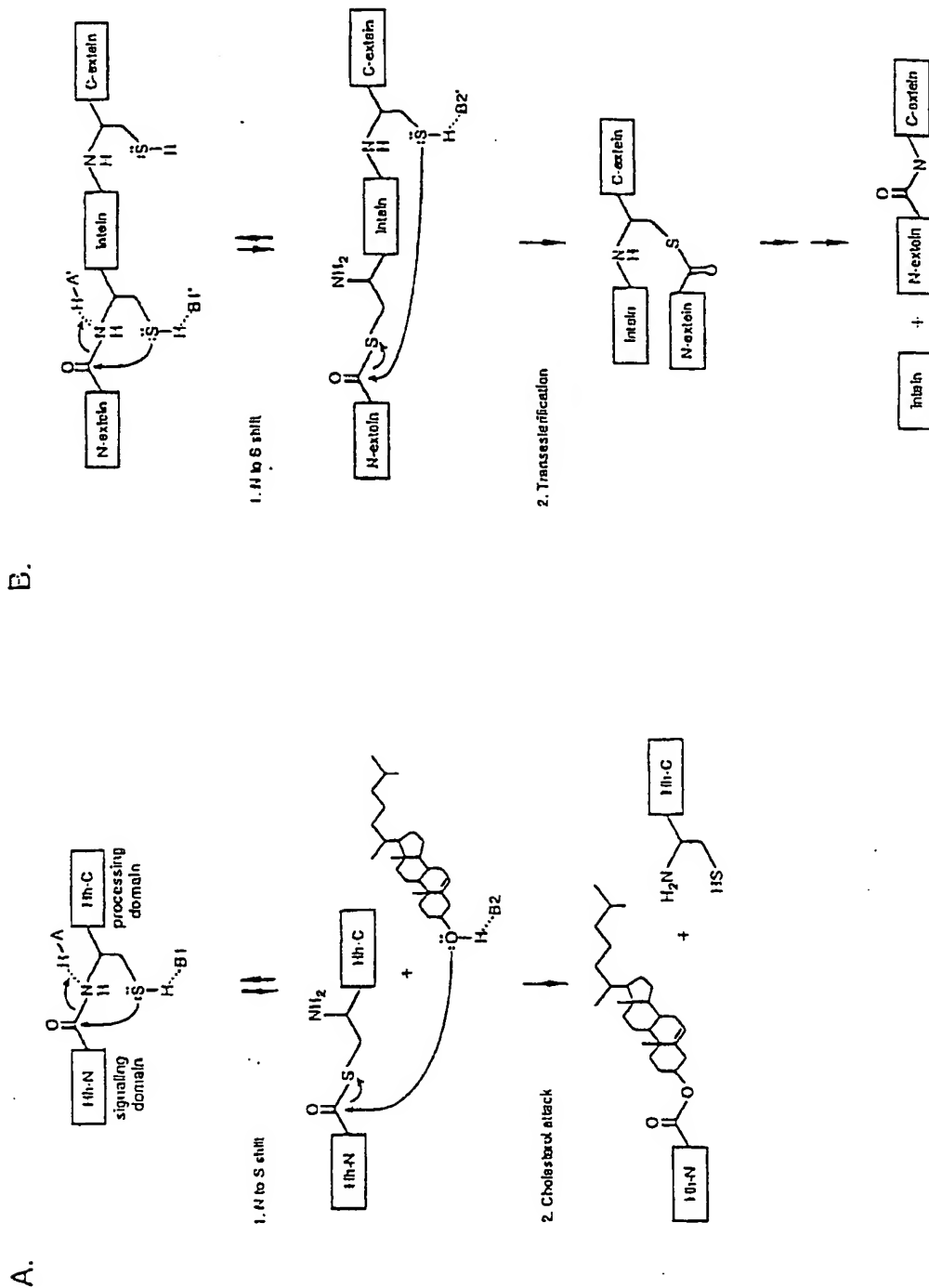
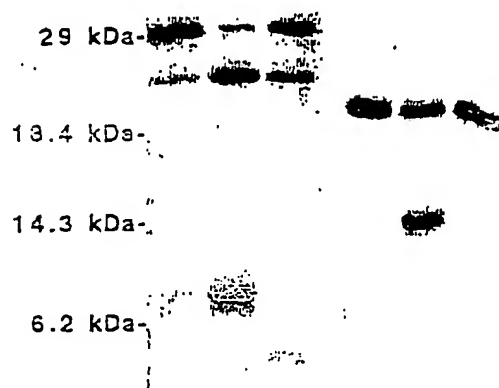


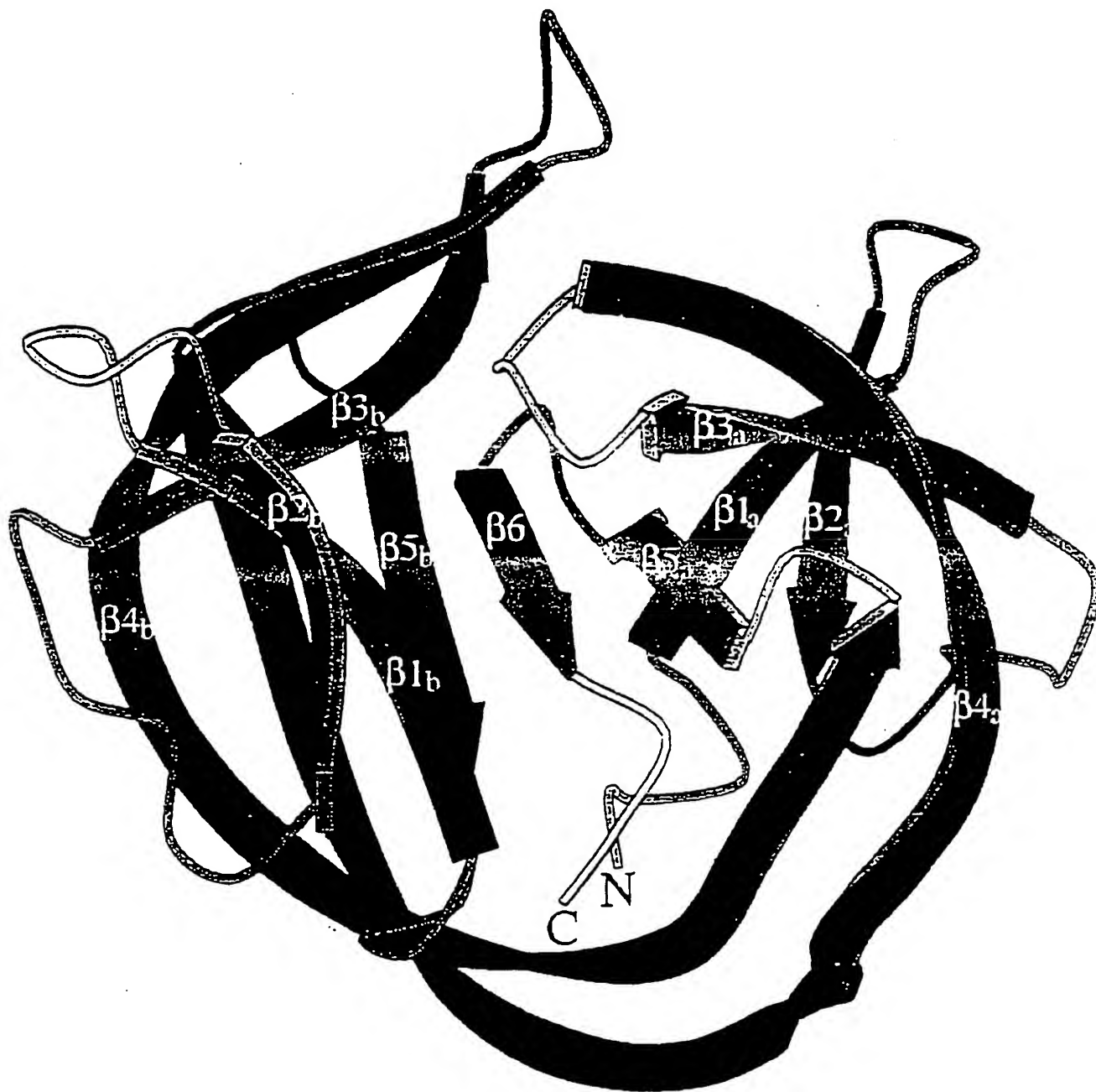
Figure 27

	His <sub>6</sub> Hh-C <sub>25</sub>			His <sub>6</sub> Hh-C <sub>17</sub>		
350 $\mu$ M chol	-	-	+	-	-	+
50 mM DTT	-	+	-	-	+	-
1 mM DTT	+	-	+	+	-	+



38/48

Figure<sup>28</sup> A



3g/ud

Figure 28

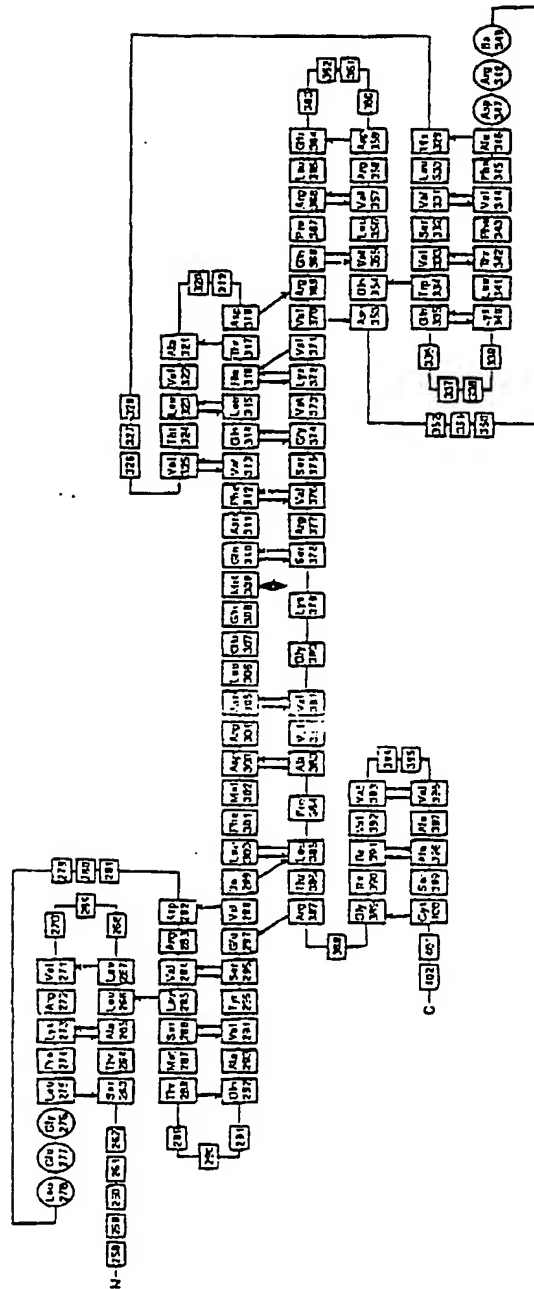
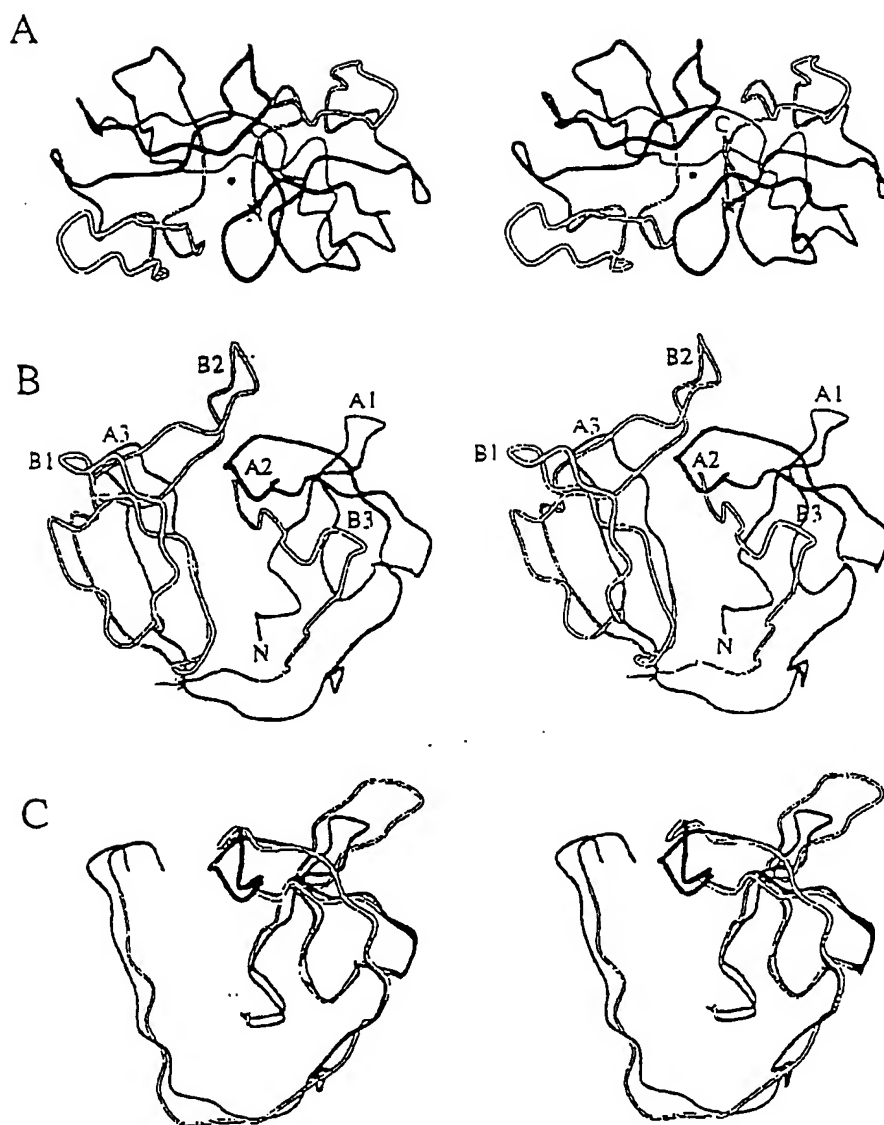
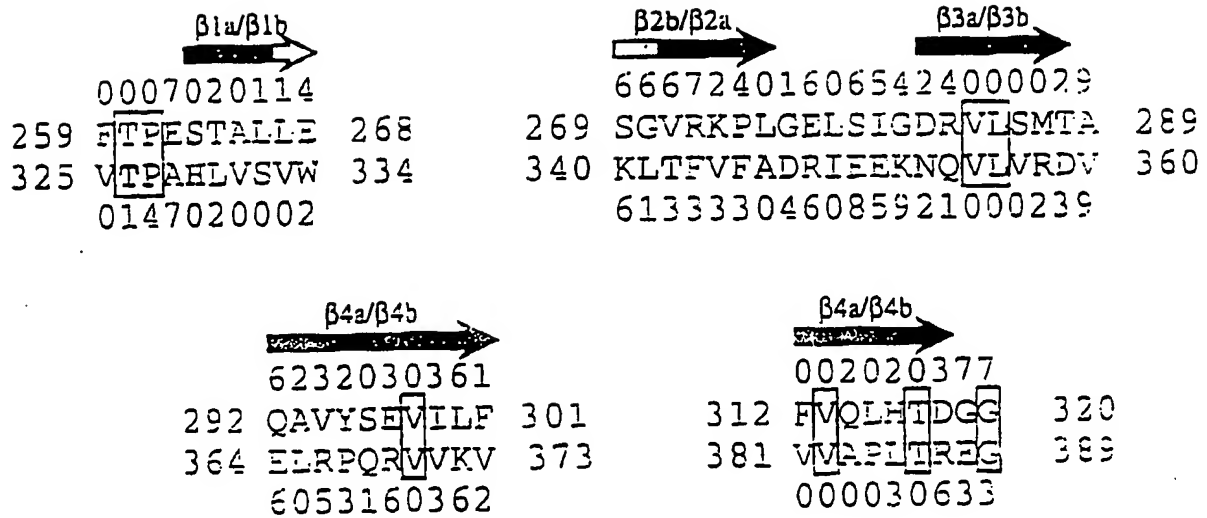


Figure 29



41/48

Figure 29D



42/48

Figure 39A

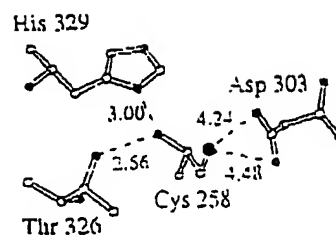
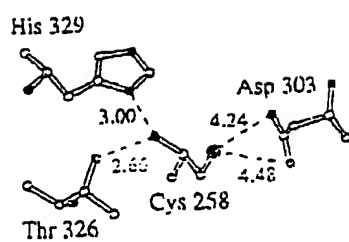
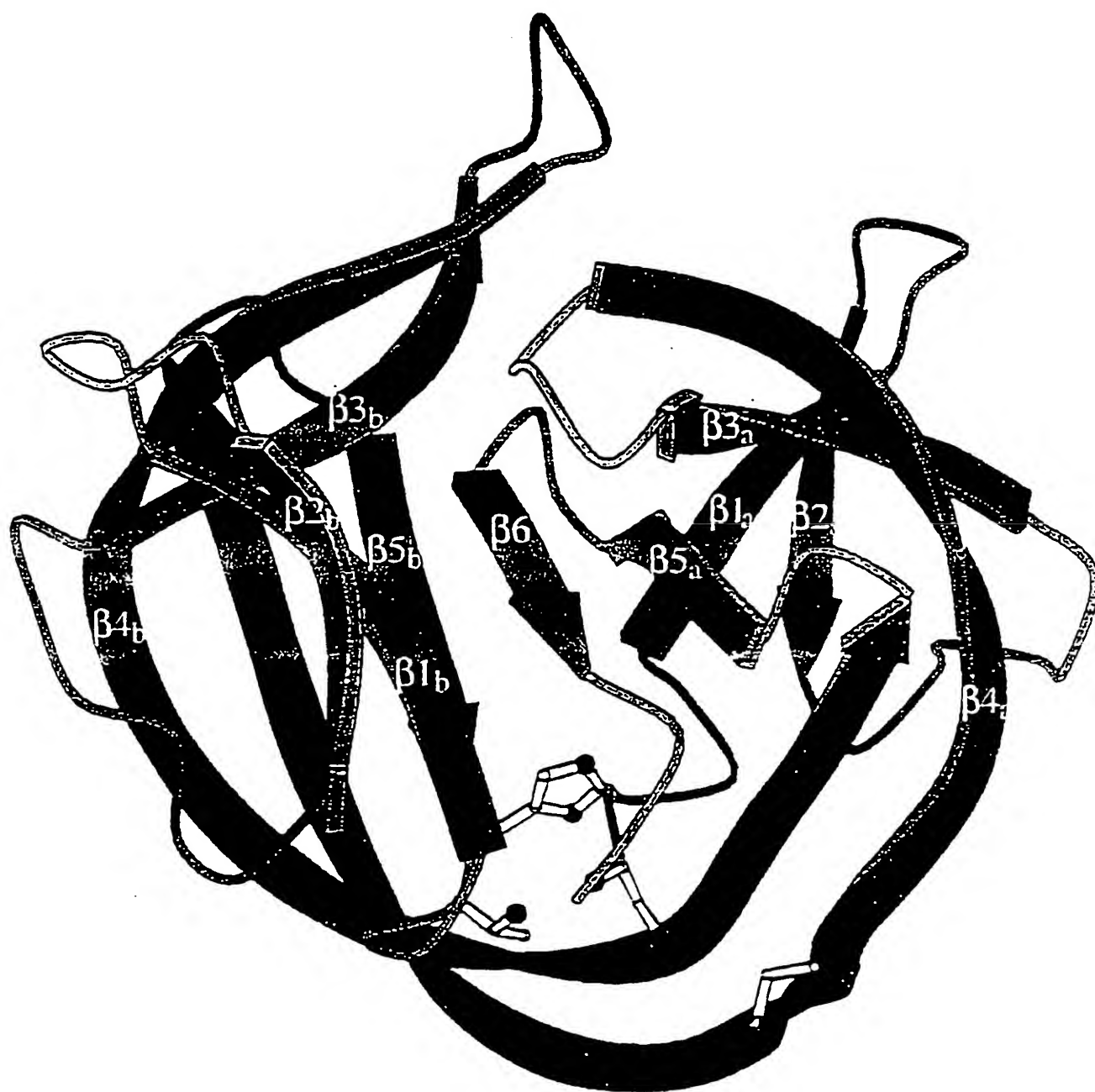
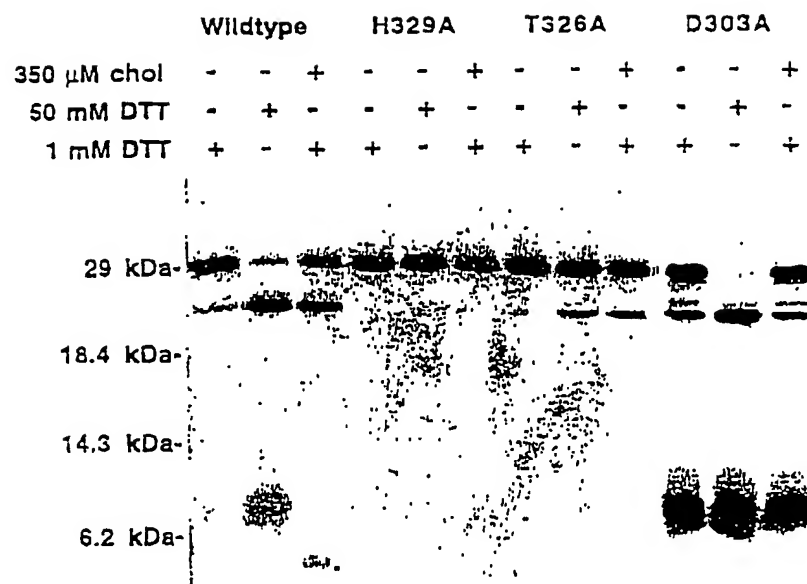


Figure 30B



44/48

Figure 30C



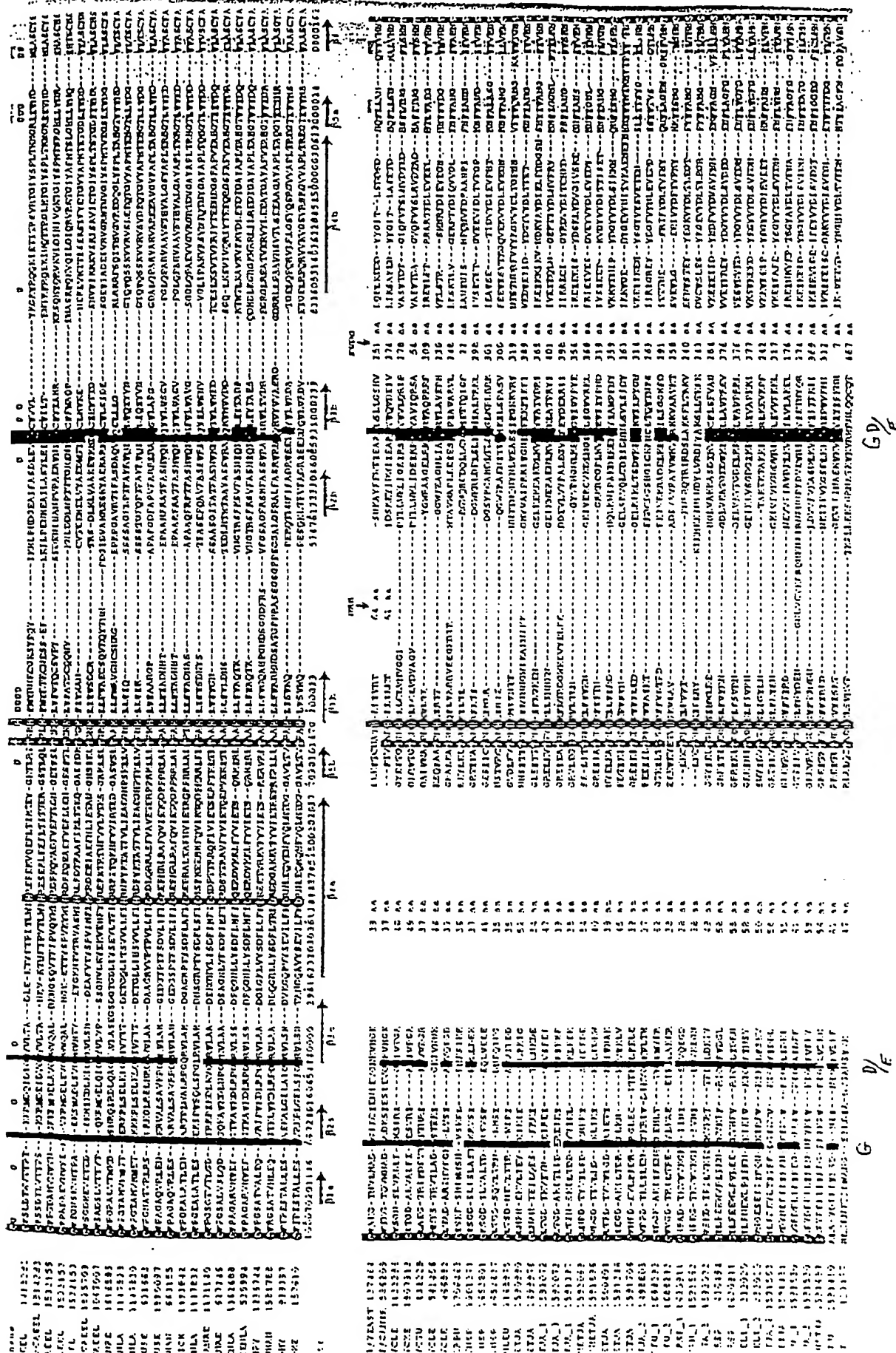
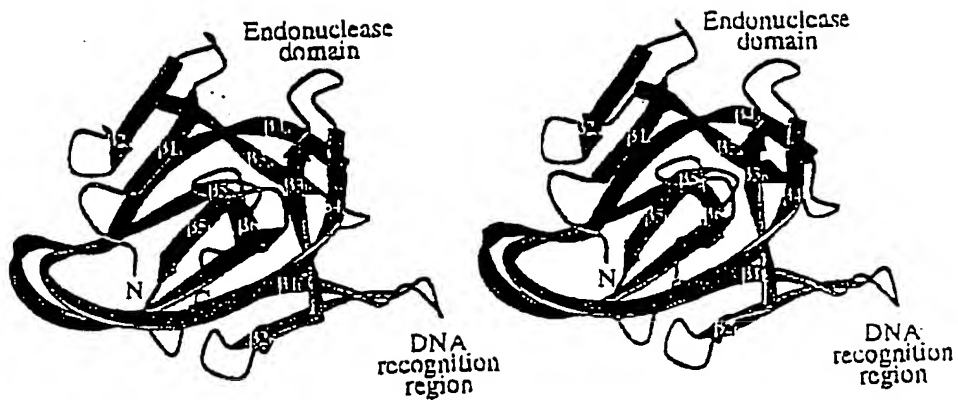


FIGURE 31A

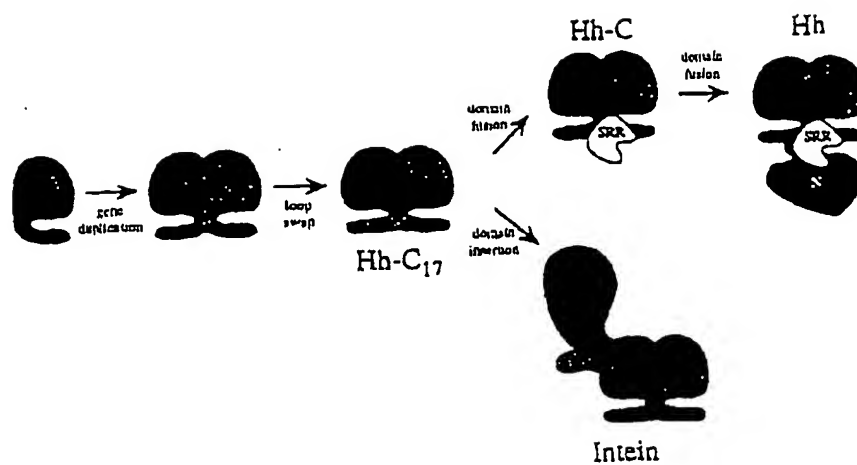
46/48

Figure 3B



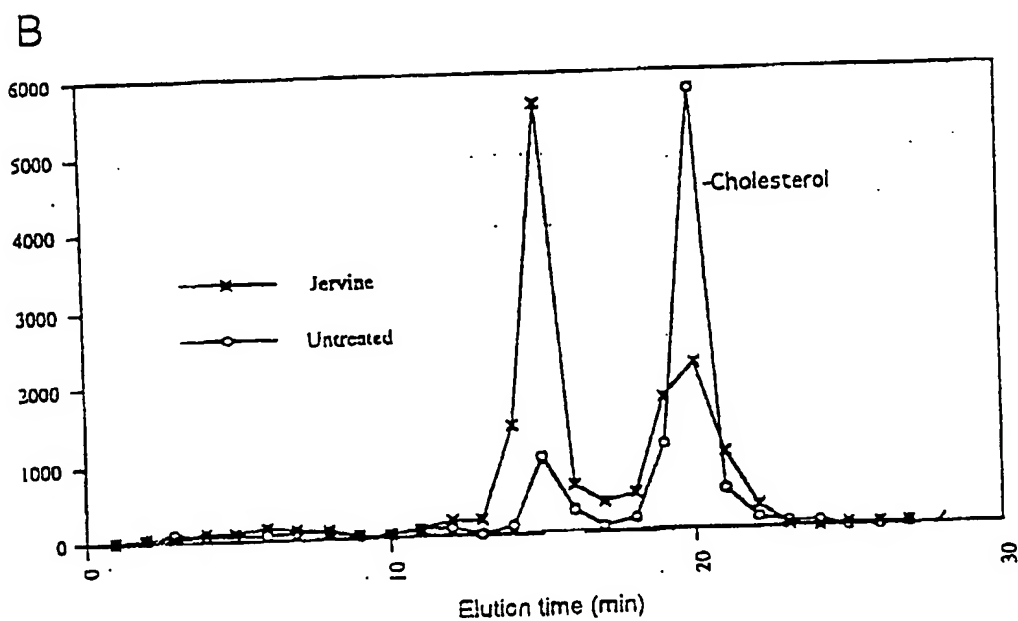
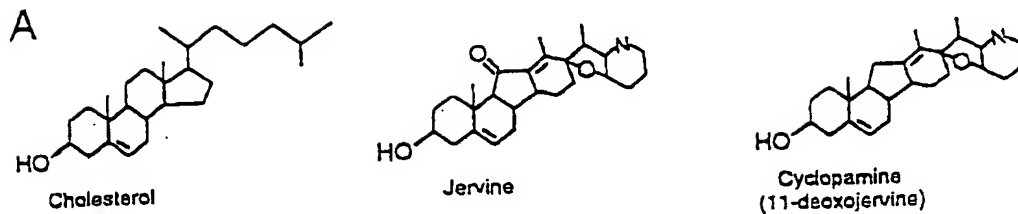
47/48

Figure 32



48/48

Fig. 33



## INTERNATIONAL SEARCH REPORT

International application No.  
PCT/US97/15753

**A. CLASSIFICATION OF SUBJECT MATTER**

IPC(6) : C07K 1/00, 14/00; G01N 33/53, 33/567

US CL : 530/300, 350; 435/7.1, 7.21

According to International Patent Classification (IPC) or to both national classification and IPC

**B. FIELDS SEARCHED**

Minimum documentation searched (classification system followed by classification symbols)

U.S. : 530/300, 350; 435/7.1, 7.21

Documentation searched other than minimum documentation to the extent that such documents are included in the fields searched

Electronic data base consulted during the international search (name of data base and, where practicable, search terms used)

Please See Extra Sheet.

**C. DOCUMENTS CONSIDERED TO BE RELEVANT**

Category*	Citation of document, with indication, where appropriate, of the relevant passages	Relevant to claim No.
Y	MOHLER et al. Molecular organization and embryonic expression of the hedgehog gene involved in cell-cell communication in segmental patterning of Drosophila. Development. 1992, Vol 115, pages 957-971, especially pages 958-968.	1-9
Y	LEE et al. Secretion and localized transcription suggest a role in positional signalling for products of the segmentation gene hedgehog. Cell. 02 October 1992, Vol. 71, pages 33-50, especially pages 34-44.	1-9

☒ Further documents are listed in the continuation of Box C. ☐ See patent family annex.

* Special categories of cited documents:	*T* later document published after the international filing date or priority date and not in conflict with the application but cited to understand the principle or theory underlying the invention
*A* document defining the general state of the art which is not considered to be of particular relevance	*X* document of particular relevance; the claimed invention cannot be considered novel or cannot be considered to involve an inventive step when the document is taken alone
*B* earlier document published on or after the international filing date	*Y* document of particular relevance; the claimed invention cannot be considered to involve an inventive step when the document is combined with one or more other such documents, such combination being obvious to a person skilled in the art
*L* document which may throw doubts on priority claim(s) or which is cited to establish the publication date of another citation or other special reason (as specified)	*A* document member of the same patent family
*O* document referring to an oral disclosure, use, exhibition or other means	
*P* document published prior to the international filing date but later than the priority date claimed	

Date of the actual completion of the international search 19 NOVEMBER 1997	Date of mailing of the international search report 30 JAN 1998
Name and mailing address of the ISA/US Commissioner of Patents and Trademarks Box PCT Washington, D.C. 20231 Facsimile No. (703) 305-3230	Authorized officer KENNETH A. SORENSEN Telephone No. (703) 308-0196

## INTERNATIONAL SEARCH REPORT

International application No.  
PCT/US97/15753

## C (Continuation). DOCUMENTS CONSIDERED TO BE RELEVANT

Category*	Citation of document, with indication, where appropriate, of the relevant passages	Relevant to claim No.
Y	CLARKE et al. Cellular lipid binding proteins: expression, function, and nutritional regulation. FASEB J. November 1989, Vol. 3, pages 2480-2487, especially pages 2481-2485.	1-9
A	INGHAM, P.W. Signalling by hedgehog family proteins in Drosophila and vertebrate development. Cur. Opin. Gen. Dev. 1995, Vol. 5, pages 492-498, entire document.	1-9

## INTERNATIONAL SEARCH REPORT

International application No.  
PCT/US97/15753

### B. FIELDS SEARCHED

Electronic data bases consulted (Name of data base and where practicable terms used):

APS, MEDLINE, CAPLUS

search terms: hedgehog - polypeptide/protein/fragment, cholesterol biosynthesis, neural induction, neural inducing activity of hedgehog, induction/pituitary gene expression

### BOX II. OBSERVATIONS WHERE UNITY OF INVENTION WAS LACKING

This ISA found multiple inventions as follows:

This application contains the following inventions or groups of inventions which are not so linked as to form a single inventive concept under PCT Rule 13.1.

Group I. Claims 1-9, drawn to a substantially pure polypeptide having an amino acid sequence of a hedgehog polypeptide, and a method for inhibiting the neural inducing activity of hedgehog polypeptide in cells, and a method for inducing pituitary gland gene expression comprising introducing to cells of the pituitary, hedgehog polypeptide.

Group II. Claims 10-12, drawn to a method for affecting cholesterol biosynthesis or transport comprising contacting a cell with an effective amount of a compound that affects hedgehog.

The inventions listed as Groups I-II do not relate to a single inventive concept under PCT Rule 13.1 because, under PCT Rule 13.2, they lack the same or corresponding special technical features for the following reasons: The claims of Group I are drawn to an invention whose special technical feature is the hedgehog polypeptide, whereas Group II is drawn to: a method for affecting cholesterol biosynthesis or transport with chemical compounds that are unrelated and materially different from the hedgehog polypeptide. The protein and methods of Group I and the method of Group II each have materially different chemical structures and materially different functional properties. These chemical structures and functional properties are the special technical features that identify each invention and distinguish each invention from the others, because none of the special technical features is shared by the separate groups. The claims are not so linked by a special technical feature within the meaning of PCT Rule 13.2 so as to form a single inventive concept.

**This Page is Inserted by IFW Indexing and Scanning  
Operations and is not part of the Official Record**

**BEST AVAILABLE IMAGES**

Defective images within this document are accurate representations of the original documents submitted by the applicant.

Defects in the images include but are not limited to the items checked:

☒ **BLACK BORDERS**

☐ **IMAGE CUT OFF AT TOP, BOTTOM OR SIDES**

☐ **FADED TEXT OR DRAWING**

☐ **BLURRED OR ILLEGIBLE TEXT OR DRAWING**

☐ **SKEWED/SLANTED IMAGES**

☒ **COLOR OR BLACK AND WHITE PHOTOGRAPHS**

☐ **GRAY SCALE DOCUMENTS**

☐ **LINES OR MARKS ON ORIGINAL DOCUMENT**

☐ **REFERENCE(S) OR EXHIBIT(S) SUBMITTED ARE POOR QUALITY**

☐ **OTHER: \_\_\_\_\_**

**IMAGES ARE BEST AVAILABLE COPY.**

**As rescanning these documents will not correct the image problems checked, please do not report these problems to the IFW Image Problem Mailbox.**